

Research Reports from the Communications Research Laboratory
at Ilmenau University of Technology

Jianshu Zhang

**Advanced Signal Processing Techniques
for Two-Way Relaying Networks
and Full-Duplex Communication Systems**



ILMENAU UNIVERSITY OF TECHNOLOGY



Fakultät für Elektrotechnik und Informationstechnik
der Technischen Universität Ilmenau

ADVANCED SIGNAL PROCESSING TECHNIQUES
FOR TWO-WAY RELAYING NETWORKS
AND FULL-DUPLEX COMMUNICATION SYSTEMS

Jianshu Zhang

Dissertation zur Erlangung des
akademischen Grades Doktor-Ingenieur (Dr.-Ing)

Anfertigung im: Fachgebiet Nachrichtentechnik
Institut für Informationstechnik
Fakultät für Elektrotechnik und Informationstechnik

Gutachter: Univ.-Prof. Dr.-Ing. Martin Haardt
Univ.-Prof. Dr.-Ing. Eduard Jorswieck
Prof. Dr. Sergiy A. Vorobyov

Vorgelegt am: 04.07.2014

Verteidigt am: 19.12.2014

urn:nbn:de:gbv:ilm1-2014000439

Abstract

To enable ultra-high data rate and ubiquitous coverage in future wireless networks, new physical layer techniques are desired. Relaying is a promising technique for future wireless networks since it can boost the coverage and can provide low cost wireless backhauling solutions, as compared to traditional wired backhauling solutions via fiber and copper. Traditional one-way relaying (OWR) techniques suffer from the spectral loss due to the half-duplex (HD) operation at the relay. On one hand, two-way relaying (TWR) allows the communication partners to transmit to and/or receive from the relay simultaneously and thus uses the spectrum more efficiently than OWR. Therefore, we study two-way relays and more specifically multi-pair/multi-user TWR systems with amplify-and-forward (AF) relays. These scenarios suffer from inter-pair or inter-user interference. To deal with the interference, advanced signal processing algorithms, in other words, spatial division multiple access (SDMA) techniques, are desired. On the other hand, if the relay is a full-duplex (FD) relay, the spectral loss due to a HD operation can also be compensated. However, in practice, a FD device is hard to realize due to the strong loop-back self-interference and the limited dynamic range at the transceiver. Thus, advanced self-interference suppression techniques should be developed. This thesis contributes to the two goals by developing optimal and/or efficient algebraic solutions for different scenarios subject to different utility functions of the system, e.g., sum rate maximization and transmit power minimization.

In the first part of this thesis, we first study a multi-pair TWR network with a multi-antenna AF relay. This scenario can be also treated as the sharing of the relay and the spectrum among multiple operators assuming that different pairs of users belong to different operators. Existing approaches focus on interference suppression. We propose a projection based separation of multiple operators (ProBaSeMO) scheme, which can be easily extended when each user has multiple antennas or when different system design criteria are applied. To benchmark the ProBaSeMO scheme, we develop optimal relay transmit strategies to maximize the system sum rate, minimize the required transmit power at the relay, or maximize the minimum signal to interference plus noise ratio (SINR) of the users. Specifically for the sum rate maximization problem, gradient based methods are developed regardless whether each user has a single antenna or multiple antennas. To guarantee a worst-case polynomial time solution, we also develop a polynomial time algorithm which has been inspired by the polynomial time difference of convex functions (POTDC) method. Finally, we analyze the conditions for obtaining the

sharing gain in terms of the sum rate. Then we study the sum rate maximization problem of a multi-pair TWR network with multiple single antenna AF relays and single antenna users. The resulting sum rate maximization problem, subject to a total transmit power constraint of the relays in the network, yields a similar problem structure as in the previous scenario. Therefore the optimal solution for one scenario can be used for the other. Moreover, a global optimal solution, which is based on the polyblock approach, and several suboptimal solutions, which are more computationally efficient and approximate the optimal solution, are developed when there is a total transmit power constraint of the relays in the network or each relay has its own transmit power constraint. We then shift our focus to a multi-pair TWR network with multiple multi-antenna AF relays and multiple dumb repeaters. This scenario is more general because the previous two scenarios can be seen as special realizations of this scenario. The interference management in this scenario is more challenging due to the existence of the repeaters. Interference neutralization (IN) is a solution for dealing with this kind of interference. Thereby, necessary and sufficient conditions for neutralizing the interference are derived. Moreover, a general framework to optimize different system utility functions in this network with or without IN is developed regardless whether the AF relays in the network have a total transmit power limit or individual transmit power limits. Finally, we develop the relay transmit strategy as well as base station (BS) precoding and decoding schemes for a TWR assisted multi-user MIMO (MU-MIMO) downlink channel. Compared to the multi-pair TWR network, this scenario suffers from the co-channel interference. We develop three suboptimal algorithms which are based on channel inversion, ProBaSeMO and zero-forcing dirty paper coding (ZFDPC), which has a low computational complexity, provides a balance between the performance and the complexity, and suffers only a little when the system is heavily loaded, respectively.

In the second part of this thesis, we investigate self-interference (SI) suppression techniques to exploit the FD gain for a point-to-point MIMO system. We first develop SI aware transmit strategies, which provide a balance between the SI suppression and the multiplexing gain of the system. To get the best performance, perfect channel state information (CSI) is needed, which is imperfect in practice. Thus, worst case transmit strategies to combat the imperfect CSI are developed, where the CSI errors are modeled deterministically and bounded by ellipsoids. In real word applications, the RF chain is imperfect. This affects the performance of the SI suppression techniques and thus results in residual SI. We develop efficient transmit beamforming techniques, which are based on the signal to leakage plus noise ratio (SLNR) criterion, to deal with the imperfections in the RF chain. All the proposed design concepts can be extended to FD OWR systems.

Zusammenfassung

Sehr hohe Datenraten und eine ständige Netzabdeckung in zukünftigen drahtlosen Netzwerken erfordern die Entwicklung neuer Algorithmen auf der physikalischen Schicht. Die Nutzung von Relais stellt dabei ein vielversprechendes Verfahren dar, um die Netzabdeckung zu vergrößern. Zusätzlich steht hierdurch im Vergleich zu Kupfer- oder Glasfaserleitungen eine preiswerte Lösung zur Anbindung an die Netzinfrastruktur zur Verfügung. Traditionelle Einwege-Relais-Techniken (One-Way Relaying [OWR]) nutzen Halbduplex-Verfahren (HD-Verfahren), welche das Übertragungssystem ausbremsen und zu spektralen Verlusten führen. Einerseits erlauben es Zweiwege-Relais-Techniken (Two-Way Relaying [TWR]), simultan sowohl das Senden als auch das Empfangen am Relais, wodurch im Vergleich zu OWR das Spektrum effizienter genutzt wird. Aus diesem Grunde untersuchen wir Zweiwege-Relais und im Speziellen TWR-Systeme für den Mehrpaar-/Mehrnutzer-Betrieb unter Nutzung von Amplify-and-forward-Relais (AF-Relais). Derartige Szenarien leiden unter Interferenz zwischen Paaren bzw. zwischen Nutzern. Um diesen Interferenz zu vermeiden, werden hochentwickelte Signalverarbeitungsalgorithmen – oder in anderen Worten räumliche Mehrfachzugriffsverfahren (Spatial Division Multiple Access [SDMA]) – benötigt. Andererseits kann der spektrale Verlust durch den HD-Betrieb auch kompensiert werden, wenn das Relais im Vollduplexbetrieb arbeitet. Nichtsdestotrotz ist ein FD-Gerät in der Praxis aufgrund starker interner Selbstinterferenz (SI) und begrenztem Dynamikumumfang des Transceivers schwer zu realisieren. Aus diesem Grunde sollten fortschrittliche Verfahren zur SI-Unterdrückung entwickelt werden. Diese Dissertation trägt diesen beiden Zielen Rechnung, indem optimale und/oder effiziente algebraische Lösungen entwickelt werden, welche verschiedene Nutzenfunktionen, wie Summenrate und minimale Sendeleistung, optimieren.

Im ersten Teil der Arbeit studieren wir zunächst Mehrpaar-TWR-Netzwerke mit einem einzelnen Mehrantennen-AF-Relais. Dieser Anwendungsfall kann auch so betrachtet werden, dass sich mehrere verschiedene Dienstoperatoren das Relais und das Spektrum teilen, wobei verschiedene Nutzerpaare zu verschiedenen Dienstoperatoren gehören. Aktuelle Ansätze zielen auf die Interferenzunterdrückung ab. Wir schlagen ein auf Projektion basiertes Verfahren zur Trennung mehrerer Dienstoperatoren (projection based separation of multiple operators [ProBaSeMO]) vor. ProBaSeMO ist leicht anpassbar für den Fall, dass jeder Nutzer mehrere Antennen besitzt oder unterschiedliche Systemdesignkriterien angewendet werden müssen. Als Bewertungsmaßstab für ProBaSeMO entwickeln wir optimale Algorithmen zur Maximierung

der Summenrate, zur Minimierung der Sendeleistung am Relais oder zur Maximierung des minimalen Signal-zu-Interferenz-und-Rausch-Verhältnisses (Signal to Interference plus Noise Ratio [SINR]) am Nutzer. Zur Maximierung der Summenrate wurden spezifische gradientenbasierte Methoden entwickelt, die unabhängig von den Anzahl der Antennen am Nutzer sind. Um im Falle eines „Worst-Case“ immer noch eine geringe Rechenkomplexität zu garantieren, entwickelten wir einen Algorithmus mit polynomieller Laufzeit. Dieser ist inspiriert von der „Polynomial Time Difference of Convex Functions“-Methode (POTDC-Methode). Bezüglich der Summenrate des Systems untersuchen wir schließlich, welche Bedingungen erfüllt sein müssen, um einen Gewinn durch gemeinsames Nutzen zu erhalten. Hiernach untersuchen wir die Maximierung der Summenrate eines Mehrpaar-TWR-Netzwerkes mit mehreren Einantennen-AF-Relais und Einantennen-Nutzern. Das daraus resultierende Problem der Summenraten-Maximierung, gebunden an eine bestimmte Gesamtsendeleistung aller Relais im Netzwerk, ist ähnlich dem des vorangegangenen Szenarios. Dementsprechend kann eine optimale Lösung für das eine Szenario auch für das jeweils andere Szenario genutzt werden. Weiterhin werden basierend auf dem Polynomialzeitalgorithmus global optimale Lösungen entwickelt. Diese Lösungen sind entweder an eine maximale Gesamtsendeleistung aller Relais oder an eine maximale Sendeleistung jedes einzelnen Relais gebunden. Zusätzlich entwickeln wir suboptimale Lösungen, die effizient in ihrer Laufzeit sind und eine Approximation der optimalen Lösung darstellen. Anschließend legen wir unser Augenmerk auf ein Mehrpaar-TWR-Netzwerk mit mehreren Mehrantennen-AF-Relais und mehreren Repeatern. Solch ein Szenario ist allgemeiner, da die vorherigen beiden Szenarien als spezielle Realisierungen dieses Szenarios aufgefasst werden können. Das Interferenz-Management in diesem Szenario ist herausfordernder aufgrund der vorhandenen Repeater. Eine Interferenzneutralisierung (IN) stellt eine Lösung dar, um diese entstehende Interferenz zu handhaben. Im Zuge dessen werden notwendige und ausreichende Bedingungen zur Aufhebung der Interferenz hergeleitet. Weiterhin wird ein Framework entwickelt, dass verschiedene Systemnutzenfunktionen optimiert, wobei IN im jeweiligen Netzwerk vorhanden sein kann oder auch nicht. Dies ist unabhängig davon, ob die Relais einer maximalen Gesamtsendeleistung oder einer individuellen maximalen Sendeleistung unterliegen. Letztendlich entwickeln wir ein Übertragungsverfahren sowie ein Vorkodier- und Dekodierverfahren für Basisstationen (BS) in einem TWR-assistierten Mehrbenutzer-MIMO-Downlink-Kanal. Im Vergleich mit dem Mehrpaar-TWR-Netzwerk leidet dieses Szenario unter Interferenzen zwischen den Kanälen. Wir entwickeln drei suboptimale Algorithmen, welche auf die Kanalinverson, ProBaSeMO und „Zero-Forcing Dirty Paper Coding“ (ZFDPC) beruhen. Diese weisen eine geringe Zeitkomplexität auf und schaffen eine Balance zwischen Leistungsfähigkeit und Komplexität. Zusätzlich gibt es jeweils nur geringe Einbrüche in stark beanspruchten Kom-

munikationssystemen.

Im zweiten Teil untersuchen wir Techniken zur SI-Unterdrückung, um den FD-Gewinn in einem Punkt-zu-Punkt-System auszunutzen. Zunächst entwickeln wir ein Übertragungsverfahren, das auf SI Rücksicht nimmt und die SI-Unterdrückung gegen den Multiplexgewinn abwägt. Die besten Ergebnisse werden durch die perfekte Kenntnis des Kanals erzielt, was praktisch kaum der Fall ist. Aus diesem Grund werden Übertragungstechniken für den „Worst Case“ entwickelt, die den Kanalschätzfehlern Rechnung tragen. Diese Fehler werden deterministisch modelliert und durch Ellipsoide beschränkt. In praktischen Szenarien sind außerdem die HF-Schaltkreise nicht perfekt. Dies hat Einfluss auf die Verfahren zur SI-Unterdrückung und führt zu einer Restselbstinterferenz. Wir entwickeln effiziente Übertragungstechniken mittels Beamforming, welche auf dem Signal-zu-Verlust-und-Rausch-Verhältnis (signal to leakage plus noise ratio [SLNR]) aufbauen, um Unvollkommenheiten der HF-Schaltkreise auszugleichen. Zusätzlich können alle Designkonzepte auf FD-OWR-Systeme erweitert werden.

Contents

Abstract	v
Zusammenfassung	vii
Contents	xi
List of Figures	xv
List of Tables	xx
List of Algorithms	xxi
1 Introduction and scope of the thesis	1
1.1 Summary of contributions	3
1.1.1 Part I: Two-Way Relaying Networks	4
1.1.2 Part II: Full-Duplex Wireless Communication Systems	11
1.1.3 Other contributions	13
1.2 Organization of the thesis	14
I Two-Way Relaying Networks	16
2 Introduction to two-way relaying networks	19
2.1 Relaying protocols and relaying strategies	20
2.2 Standardization activities	24
2.3 System assumption, transmission protocols, and mathematical notation	26
3 Multi-operator relaying networks with a MIMO relay	29
3.1 Problem description and state of the art	29
3.2 Data model and transmission protocol	32
3.3 Projection based separation of multiple operators (ProBaSeMO) concept	35
3.4 Sum rate maximization via gradient-based methods	44
3.5 Sum rate maximization via POTDC	49
3.6 Relay transmit power minimization	54

3.7	SINR balancing	56
3.8	Widely linear relay amplification matrix design	57
3.9	Simulation results	65
3.10	Discussion of the sharing gain	70
3.11	Summary	71
4	Multi-pair relaying networks with multiple single antenna relays	84
4.1	Problem description and state of the art	84
4.2	System model	85
4.3	Sum rate maximization under a total relay transmit power constraint	87
4.4	Sum rate maximization under individual relay transmit power constraints	91
4.5	Simulation results	97
4.6	Summary	99
5	Multi-pair relaying networks with non-cooperative repeaters	104
5.1	State of the art	104
5.2	Our contributions	106
5.3	Preliminaries	108
5.4	Interference neutralization	112
5.5	Relay power minimization	118
5.6	SINR balancing	119
5.7	Weighted sum rate maximization	124
5.8	Simulation results	127
5.9	Summary	130
6	Relay broadcasting channel	136
6.1	Problem description and state of the art	136
6.2	Data model	137
6.3	Transmit strategies design for the BS and the relay	140
6.4	Summary	144
7	Summary of the two-way relaying networks	146
7.1	Summary of contributions	146
7.2	Future work	148
II	Full-duplex wireless communication systems	151

8 Self-interference aware transmit strategies for full-duplex point-to-point MIMO systems	153
8.1 Motivation and state of the art	153
8.2 System model	155
8.3 Optimal linear transmit strategies for sum rate maximization	157
8.4 Worst-case design for transmit power minimization	162
8.5 Simulation results	168
8.6 Summary	170
9 Transmit strategies for full-duplex systems with imperfect RF chain	176
9.1 Problem description and our contributions	176
9.2 System model	178
9.3 Signal to leakage plus noise ratio (SLNR) based precoder design	179
9.4 Power adjustment for performance improvement	183
9.5 Simulation results	188
9.6 Summary	190
10 Summary of full-duplex wireless communication systems	193
10.1 Summary of contributions	193
10.2 Future work	194
III Conclusions and Outlook	196
11 Conclusions	197
12 Future work	200
IV Appendices	202
Appendix A Glossary of Acronyms, Symbols and Notation	203
A.1 Acronyms	203
A.2 Symbols and Notation	205
Appendix B Convex optimization background	208
B.1 Convex sets and convex functions	208
B.2 Convex optimization and duality theory	211

B.3	Convex optimization problems	213
Appendix C Proofs and derivations for Part I		218
C.1	Derivation of RBD in the MAC Phase	218
C.2	Calculation of the precoding and decoding matrices in the presence of colored noise	219
C.3	Derivation of quadratic terms when each UT has a single antenna	220
C.4	Proof for Section 5.4.1 (feasibility of interference neutralization)	220
C.5	Proof to Lemma C.4.2	228
C.6	Proof to Lemma 5.6.1	229
C.7	Monotonic optimization and the polyblock algorithm	231
Appendix D Proofs and derivations for Part II		235
D.1	Proof of Proposition 8.3.1	235
D.2	Proof of Corollary 8.3.2	236
D.3	Proof of Proposition 8.3.4	237
Bibliography		241
Erklärung		257

List of Figures

1.1	Cisco's forecasts of the global mobile devices growth and the mobile data traffic by 2018. [Cis14]	2
1.2	Cisco's forecasts of the global M2M growth and mitigation from 2G to 4G, and the growth of global connected wearable devices by 2018. [Cis14].	3
2.1	A traditional one-way relaying protocol where the communication is completed in 4 phases. The communication partner S_1 has a message x_1 for S_2 . The communication partner S_2 has a message x_2 for S_1 .	20
2.2	Different types of two-way relaying. x_1 and x_2 represent the messages from the two communication partners S_1 and S_2 while x_{12} represent the forwarded signal from the relay, which is a coded version of x_1 and x_2 .	20
2.3	An example of multi-way relaying with three communication partners S_1 , S_2 , and S_3 . The messages x_1 , x_2 , and x_3 are messages from one partner to the other two partners. The three-phase protocol in the figure is the same as in [AK10b].	21
2.4	A Type-1, Type-1a, or Type-1b relay defined in LTE. These types of relays have their own cell identities.	25
2.5	A Type-2 relay defined in LTE. A Type-2 relay does not has its own cell identity.	26
3.1	A typical metropolitan scenario where two operators share the spectrum and a multi-antenna relay. The arrows show the data flow in two phases, i.e., in the first time slot, all the UTs transmit to the multi-antenna relay and the relay amplifies and sends the signal to all the UTs in the second time slot.	30
3.2	L -operator two-way relaying system model. The k -th terminal belonging to the ℓ -th operator has $M_k^{(\ell)}$ antennas and the relay station is equipped with M_R antennas.	33
3.3	The average interference level at the UTs when RBD is applied and $L = 2$. (2,16) stands for (M_U, M_R) . The SNR is defined in equation (3.100) of Section 3.9.	38
3.4	Fractional sharing gain as a function of SNR for $M_U = 1$ and $L = 2$.	71
3.5	Fractional sharing gain as a function of M_R for $M_U = 1$ and $L = 2$.	72
3.6	Fractional sharing gain as a function of L for $M_U = 1$ and $M_R = 4L$.	72

3.7	Sum rate comparison of time-shared approach and ProBaSeMO approach for $M_U = 1$ and $L = 2$	75
3.8	Relay transmit power vs. SINR constraint, SNR = 15 dB, 1000 channel realizations	75
3.9	SINR balancing, $P_R = 1$ W	76
3.10	Achievable average minimum SINR by using WL design and linear design for different pairs and various number of antennas at the relay.	76
3.11	Average minimum transmit power at the relay by using WL design and linear design for different pairs and various number of antennas at the relay. SNR = 20 dB. 1000 channel realizations	77
3.12	Sum rate comparison of ProBaSeMO ({BA, RR}) and POTDC approaches for $L = 2$	77
3.13	Sum rate comparison of different multi-operator TWR approaches for $M_U = 1$ and $L = 2$	78
3.14	Sum rate comparison of different multi-operator TWR approaches for $M_U = 1$, SNR= 25 dB and $L = 2$	78
3.15	Sum rate comparison of different multi-operator TWR approaches for $M_U = 1$, SNR= 25 dB, and $M_R = 20$	79
3.16	Effects of path loss of different multi-operator TWR approaches for $M_R = 8$, $M_U = 1$ and $L = 2$ in a symmetric scenario, i.e., N/F ratio = $d_2^{(\ell)}/d_1^{(\ell)} = d_2/d_1, \forall \ell$	79
3.17	Effects of path loss of ProBaSeMO ({BA, RR}), MMSE, and POTDC approaches for $M_R = 4$ and $L = 2$ in an asymmetric scenario, i.e., N/F ratio = $d_2^{(1)}/d_1^{(1)} = d_1^{(2)}/d_2^{(2)}$	80
3.18	Effects of path loss of ProBaSeMO ({BA, RR}), MMSE, and POTDC approaches for $M_R = 8$ and $L = 2$ in an asymmetric scenario, i.e., N/F ratio = $d_2^{(1)}/d_1^{(1)} = d_1^{(2)}/d_2^{(2)}$	80
3.19	Uncoded system BER comparison of different multi-operator TWR approaches for QPSK modulation, $M_U = 1$, $M_R = 4$ and $L = 2$	81
3.20	Sum rate comparison of different multi-operator TWR transmit strategies for $M_U = 2$, $M_R = 8$ and $L = 2$	81
3.21	Sum rate comparison of different multi-operator TWR approaches for $M_U = 2$, SNR= 25 dB and $L = 2$	82
3.22	Sum rate comparison of different approaches for $M_U = 2$, $M_R = 8$, and $L = 2$ when $\rho_R = 0.9$	82

3.23	System spectral efficiency comparison of different approaches for QPSK modulation, $M_U = 2$, $M_R = 8$ and $L = 2$	83
4.1	Multi-pair two-way relaying with multiple single antenna amplify and forward relays.	85
4.2	Sum rate comparison of the proposed algorithms under a total transmit power constraint.	101
4.3	Convergence property of the POTDC inspired method with different N and SNRs. Averaged over 100 channel realizations.	101
4.4	Convergence property of GPM with different N and SNRs. Averaged over 100 channel realizations.	102
4.5	Convergence property of the polyblock approach with different N and SNRs. Averaged over 100 channel realizations.	102
4.6	Sum rate comparison of the polyblock algorithm and the POTDC algorithm under individual relay transmit power constraints.	103
4.7	Sum rate comparison of the POTDC algorithm, the total SINR eigen-beamformer (low SNR approximation), and the interference neutralization based design (high SNR approximation) under individual relay transmit power constraints.	103
5.1	Multi-pair two-way relaying with multiple repeaters and amplify-and-forward relays where each relay has M_R antennas.	109
5.2	An illustration of condition (5.12) in Theorem 5.4.1. Given the number of user pairs K , the feasible region of interference neutralization consists of all pairs (M_R, N) which are on or above the plotted curve.	131
5.3	An illustration of the asymptotic analysis of (5.12) in Theorem 5.4.1. Let $K, M_R \rightarrow \infty$ and the ratio $\frac{K}{M_R}$ be a constant.	132
5.4	An illustration of the average minimum required total transmit power as a function of M_R . Given K and M_R , N is the minimum integer value which satisfies (5.12). In other words, N is the corresponding value on the curves of Figure 5.2. $\sigma_n^{-2} = 15$ dB.	132
5.5	The cumulative distribution function (CDF) of the minimum required total transmit power under different pairs of (M_R, N) for $K = 2$ and $\sigma_n^{-2} = 15$ dB. M_R and N are calculated in the same way as in Figure 5.4.	133
5.6	An illustration of the average minimum required total transmit power as a function of σ_n^{-2} . We have $K = 2$. M_R and N are calculated in the same way as in Figure 5.4.	133

5.7	A comparison of the minimum required transmit power with and without interference neutralization.	134
5.8	A demonstration of the convergence speed of the bisection search method (“BiSec”), the DT-1 algorithm (“DT-1”), and the DT-2 algorithm (“DT-2”) without IN. $N = 2$ and $M_R = 4$	134
5.9	A comparison of the achievable minimum SINR using the state of art algorithm and the proposed algorithm.	135
5.10	Maximum achievable sum rate with and without interference neutralization. . .	135
6.1	Multi-user two-way relaying with a MIMO amplify and forward relay.	137
6.2	Sum rate comparison for $M_R = 8$ and $K = 2$	145
6.3	Sum rate comparison for $M_R = 20$ and SNR = 25 dB.	145
8.1	The sketch of a symmetric full-duplex point-to-point MIMO system.	156
8.2	A symmetric FD point-to-point system with deterministic channel errors.	162
8.3	Achievable sum rate as a function of SNR for a FD system with a MIMO setup, $\epsilon = \eta = 1$	171
8.4	Achievable sum rate as a function of ϵ for a FD system with a MIMO setup, $M_r = M_t = 4$, $\eta = 1$	172
8.5	Achievable sum rate as a function of η for a FD system with a MIMO setup, $M_r = M_t = 4$, $\epsilon = 1$	173
8.6	Achievable sum rate as a function of SNR for a FD system with a MISO setup, $\epsilon = \eta = 1$	173
8.7	Achievable sum rate as a function of ϵ for a FD system with a MISO setup, $M_t = 4$, $\eta = 1$	174
8.8	Achievable sum rate as a function of η for a FD system with a MISO setup, $M_t = 4$, $\epsilon = 1$	174
8.9	Average minimum required power vs. SINR constraint $\eta = \eta_i, \forall i$, $M_t = M_r = 2$, $P_i^{(\text{ref})} = 60$ dBW, $\forall i$	175
8.10	Average minimum required power vs. $v_1, v_2 = 0.01$, $\eta_i = 5$ dB, $\forall i$, $P_i^{(\text{ref})} = 40$ dBW, $\forall i$	175
9.1	A MIMO point-to-point full-duplex system with insuppressible interference [DMBS12].	179

9.2	Average consumed power in a SISO FD system using power adjustment schemes in 9.4.1 and $P_{\max} = 1$ W. Max PT: full power transmission. MI: medium interference environment in Section 9.5. HI: high interference environment in Section 9.5.	186
9.3	The proposed beamforming and power adjustment schemes selection procedure for achieving a higher sum rate.	188
9.4	Comparison of different algorithms in a SISO setup. Max PT: full power transmission. MI: medium interference. HI: high interference.	189
9.5	Comparison of different algorithms in a MISO setup where $M_t = 4$. ZF: zero forcing technique	191
9.6	Comparison of different algorithms in a MIMO setup where $M_r = M_t = 2$	192
C.1	An illustration of a normal set $\bar{\mathbb{G}} \in \mathbb{R}_+^2$ and a reverse normal set $\bar{\mathbb{H}} \in \mathbb{R}_+^2$	231
C.2	An illustration of the polyblock approach for a feasible region of $\bar{\mathbb{D}} = \bar{\mathbb{G}} \cap \bar{\mathbb{H}} \in \mathbb{R}_+^2$. The initial vertex set is $\mathbb{T}^{(1)} = \{\mathbf{z}_0\}$	234

List of Tables

3.1	Comparison of Relay Amplification Schemes	42
8.1	A summary of the existing SI cancellation techniques.	154

List of Algorithms

1	Iterative power control at the relay in case of multi-stream transmission	42
2	Generalized power method (GPM) for sum rate maximization	47
3	Steepest descent method for sum rate maximization	49
4	Iterative algorithm for solving the optimization problem (3.49)	52
5	Iterative algorithm for approximately solving the problem (3.44)	53
6	(ϵ, η) -optimal polyblock algorithm for solving (4.7)	89
7	POTDC approach for solving problem (4.23)	94
8	The generalized Dinkelbach algorithm	124
9	(ϵ, ν) -optimal polyblock algorithm for weighted sum rate maximization given fixed weighting factor α_m	127
10	Gaussian randomization procedure	217

1 Introduction and scope of the thesis

The successful deployment of new applications in wireless communications, e.g., short message services (SMS) in the second generation (2G) of cellular communications, mobile Internet services and wireless data services in the third generation (3G), etc., has allowed its rapid development from the first generation (1G) to the fourth generation (4G) [5GN13]. The popularity of the smart phone and its associated mobile data services, e.g., video streaming, set up a strong demand on high data rate and real-time communications everywhere and every time. This is the current challenge for the 4G. As reported in [Cis14] and shown in Figure 1.1, the smart phone will occupy the largest portion of wireless devices in 2018. This makes it still the focus of the service architecture for future mobile networks. Meanwhile, the mobile data traffic by 2018 is estimated to be nearly 11 times more than in 2013. As also reported in [4G 14], the data traffic on mobile Internet doubles per year. Moreover, the growth of the machine-to-machine (M2M) connections, e.g., home and office security and automation, smart metering and utilities, and wearable devices, e.g., smart watches, heads-up displays, health and fitness trackers, etc., which bring together people, processes and things to make networked connections more relevant and valuable, will have a tangible impact on mobile traffic, as shown in Figure 1.2. The next generation of mobile broadband, say, the fifth generation (5G), should be fully prepared for forthcoming challenges and be able to support different service requirements [Eri13]. First of all, the requirement on higher data rate, which will be accelerated by video streaming, data sharing, and cloud devices, should be fulfilled. Moreover, new applications such as augmented reality and ultra-high-resolution video require not only reliable Gbps data rates but also lower latency down to a few milliseconds. In addition, the large-scale M2M communications are not human centric any more. Instead, they should operate without the monitoring of human beings [TK12]. They will also bring requirements on new levels of services, e.g., for sensor networks low energy consumption is extremely important; for applications like e-health and traffic surveillance very high levels of network reliability are required, etc..

To enable ultra-high traffic capacity and data rate, the key solution is to have ultra-dense small-cell deployments, as foreseen by Ericsson [Eri13]. That is, low-power access nodes, which operate with a very wide bandwidth and in higher frequency band, i.e., 10 - 100 GHz, are deployed with much higher density than the networks of today. The motivation of using higher frequency bands is because they can provide a contiguous large bandwidth, which

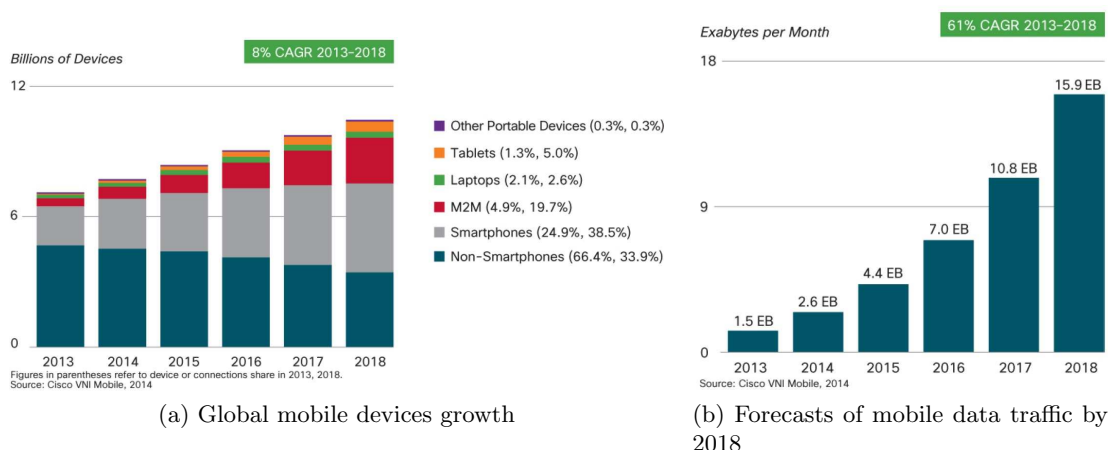


Figure 1.1: Cisco’s forecasts of the global mobile devices growth and the mobile data traffic by 2018. [Cis14]

is the direct enabler of a high data rate. Moreover, the millimeter-wave technology, which provides radio communications over the band 30 - 300 GHz, becomes more mature after years of development [PK11]. A drawback of using ultra-dense networks is the associated overwhelming task of installing and configuring backhaul network nodes, where the conventional backhauling solutions, e.g., via optic fibers, becomes cost and operation inefficient. New backhauling technology, i.e., wireless backhauling via relays (also called self-backhauling [ITN10]), becomes promising for this purpose. Relaying means that the communications between partners are accomplished via the help of multiple intermediate nodes, i.e., relays. Transmit strategies, which can enhance the performance of a relaying network, will be investigated in Part I of this thesis. One major drawback of the relaying technology is the latency introduced by multiple hops and the half-duplex (HD) operation, i.e., a device can only transmit or receive in one time slot (time-division duplex (TDD)) or on a single frequency (frequency-division duplex (FDD)). Full-duplex (FD) communications allow simultaneous transmission and reception at the same time and on the same frequency, which in theory can reduce the round-trip time by half. Therefore, it can be used to alleviate or even overcome the disadvantage of the HD operation [CJLK10]. But in practice there are still obstacles, which prevent us from fully exploiting the gain of a FD system. One of these obstacles is the strong loop-back interference. In Part II of this thesis, we will introduce transmit strategies which can help to suppress the self-interference such that a simultaneous transmission and reception is guaranteed.

In summary, our thesis is motivated but not restricted by the possible 5G application of relaying technologies and FD communications. To enhance the overall structure of the thesis,

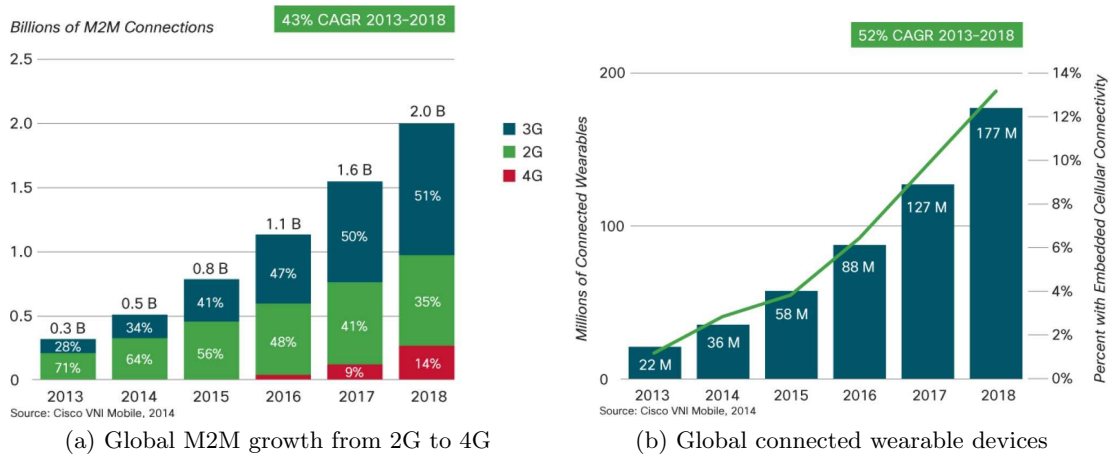


Figure 1.2: Cisco’s forecasts of the global M2M growth and mitigation from 2G to 4G, and the growth of global connected wearable devices by 2018. [Cis14].

the two different technologies are presented in a separate part of the thesis which can be read independently of each other. The following sections provide a brief introduction of different research problems, outlining the possible applications, summarizing the major contributions, and sketching the overall structure of the thesis.

1.1 Summary of contributions

In this thesis we provide a general framework to optimize different system utility functions in a multi-pair or multi-user non-regenerative two-way relaying network and a general framework to improve the performance of a FD system with limited dynamic range based on spatial division multiple access (SDMA) techniques.

Before we discuss the detailed contributions, it is worth introducing some common assumptions of our research. First, all the system models are valid under a narrow band assumption, or considering a frequency flat subcarrier of a broadband multi-carrier system, e.g., this can be achieved by considering a subcarrier of an orthogonal frequency division multiplexing (OFDM) system with cyclic prefix (CP). Second, the considered transmit power constraints are average power constraints, i.e., the power of the transmitted data (assuming a zero mean) is set to its variance. Lastly, the sum rate maximization problem refers to the maximization of the mutual information using complex circularly symmetric Gaussian inputs. Note that Gaussian inputs are optimal from a mutual information point of view and they cannot be realized in practice. Discrete modulations/constellations, e.g., quadrature amplitude modulation (QAM), are used

in practice, which can significantly depart from the Gaussian idealization. To maximize the mutual information subject to arbitrary input constellations, one may consider the so called mercury/waterfilling technique in [LTV06].

Furthermore, convex optimization theory is the one of the major mathematical tools, which is used to solve the formulated optimization problems in this thesis. If the formulated problems are convex, they can be solved using a unified approach, i.e., the interior-point algorithm in [BV04]. Many software programs are available for solving standard convex optimization problems, e.g., the CVX toolbox [CVX12] and the MOSEK toolbox [MOS12]. A short introduction to convex optimization theory is found in Appendix B. Nevertheless, it is worth stressing two major enablers, which make it possible to solve our problems using convex optimization theory. First, in general convex optimization theory is more suitable/developed for vector or scalar optimization variables. However, in most of our problems, e.g., the relay amplification matrix design in Part I, the optimization variable is a matrix. In this case, the properties of the Kronecker product, e.g., in Chapter 3, and the Hadamard product, e.g., in Chapter 4, enable the transformation from matrix variables to vector variables. Second, most of our formulated optimization problems are non-convex quadratically constrained quadratic programming (QCQP) problems. Convex reformulations are required such that the non-convex problems can be reformulated, e.g., via the S-procedure in Chapter 8, or relaxed, e.g., using the semidefinite relaxation (SDR) technique or the second-order cone programming (SOCP) method in Chapter 3, to convex problems.

1.1.1 Part I: Two-Way Relaying Networks

Relays have a good potential in reducing the deployment cost, enhancing the network capacity, mitigating shadowing effects, and providing reliable communications for different applications. When placed at the cell edge, relays can also boost the coverage. Earlier works focus on one-way relaying (OWR) [CT91]. In one-way relaying the communication between two nodes is completed in four phases since the channels are accessed by the two nodes in an orthogonal manner and a HD relay is considered. By allowing non-orthogonal channel access, i.e., both nodes transmit to or receive from the relay at the same time, the communication can be completed in two phases. This is the so-called two-way relaying (TWR) or bidirectional relaying technique. It can compensate the spectral efficiency loss in one-way relaying due to the HD constraint of the relay and therefore uses the radio resources in a particular efficient manner [RW07]. Moreover, it can be combined with the amplify-and-forward (AF) relaying strategy, which simply amplifies the received data and retransmits it to the destination. In contrast to the decode-and-forward (DF) relaying strategy, which decodes the received data

and re-encodes and retransmits it to the destination, the AF strategy has a reduced processing delay and a reduced hardware complexity [ZLCC09]. Hence, AF TWR is also considered in our work. Single-pair AF TWR systems are well studied especially for the case where two nodes communicate with the help of a multiple-antenna relay [UK08, ZLCC09] or multiple cooperative single antenna relays [DS10]. The fundamental problem associated with the TWR systems is the design of the relay transmit strategy based on the available channel state information (CSI). For a scenario with a MIMO¹ relay, this refers to the design of a relay amplification matrix. For a scenario with multiple single antenna relays, this refers to the design of a complex weighting factor per relay. Nevertheless, in practice single pair TWR scenarios are not sufficient to cover all network structures. For instance, the optimal transmit strategies for single-pair TWR systems are in general suboptimal when they are applied to multi-user TWR scenarios. By multi-user TWR scenarios, we mean multi-pair multi-user TWR scenarios and the relay-assisted multi-user downlink scenario. These scenarios have important practical applications. For example, if different pairs of users belong to different operators, then we will have a multi-operator TWR scenario [ZRH12b]. Typically, in such a scenario the physical resources, i.e., the spectrum and the relays, are used by different operators in an orthogonal manner, e.g., users of different operators can access the spectrum and the relay in different time slots. However, the orthogonal manner is spectrally inefficient compared to the case that users of different operators access the spectrum and the relay at the same time, i.e., the non-orthogonal manner. Such a non-orthogonal resource access scheme is termed as the physical resource sharing and it is a potential candidate for improving the spectral efficiency of future networks. However, in the aforementioned application interference from users of the other operators is introduced due to the co-channel transmissions. When the noise is weak, the performance of the inter-operator/inter-pair TWR system will be dominated by the interference. In other words, the system is interference limited. Since the inter-operator/inter-pair interference does not exist in a single-pair system, the optimal single-pair relay transmit strategies are naturally suboptimal for the multi-operator/multi-pair TWR system with a non-orthogonal resource access. Thus, this motivates us to develop advanced relay transmit strategies, which are more suitable for the multi-operator/multi-pair TWR system. A similar motivation holds for our study of the relay-assisted multi-user MIMO (MU-MIMO) downlink scenario, where the difference is that the interference is caused by the dedicated signal to the other users of the same operator or the same base station (BS).

¹Multiple-input and multiple output (MIMO) relay here means that the relay has multiple transmit and receive antennas and it receives and transmits the signal using MIMO techniques, e.g., spatial multiplexing schemes or diversity schemes.

Relay transmit strategy design for the multi-operator/multi-pair TWR system

The relay transmit strategy is usually designed such that a specific performance criterion is optimized under constraints on the available resources or quality of service (QoS) requirements. This can be done by setting up a constrained optimization problem and then solving it using optimization theory, e.g., maximizing the sum rate under the power constraint at the relay. However, this methodology might result in a non-linear problem which is in general non-deterministic polynomial time hard (NP-hard) to solve [GJ79]. Moreover, the obtained optimal strategy might not be simply adapted for other performance criteria or other system settings. Therefore, it is also attractive to have low-complexity (e.g., closed-form) efficient (e.g., close to optimal performance) solutions which are flexible to be used under different system setups or for different performance criteria.

The first scenario we investigate is the multi-operator TWR scenario with a MIMO AF relay, where the users of different operators can have single or multiple antennas. In previous works the relay amplification matrix has been designed based on zero-forcing (ZF) and minimum mean-squared-error (MMSE) criteria [JS10], or only single antenna users are considered [YZGK10]. Inspired by the transmit strategy for the MU-MIMO downlink channel [SSH04], i.e., linear precoding techniques are designed to first suppress the inter-user interference and then to optimize each user's performance separately, we propose to design the relay amplification matrix in the way that first the inter-operator interference is suppressed and then each operator can design their relay transmit strategies independently. The proposed scheme is called the projection based separation of multiple operators (ProBaSeMO) scheme [ZRH12b]. It provides an interference-free communication environment for different operators. The relay amplification matrix is obtained as a closed-form solution. It can also be easily adapted to different utility functions such as sum rate maximization, relay transmit power minimization, or minimum signal to interference plus noise ratio (SINR) maximization. When each user has multiple antennas, the ProBaSeMO strategy can be easily extended. Since it allows each operator to design its own relay transmit strategy, it protects the privacy of each operator. This is especially important in the context of physical resource sharing. Nevertheless, the proposed ProBaSeMO strategy is a suboptimal solution. It is worth to know its performance loss compared to the optimal solution. Hence, we study optimal relay transmit strategies to maximize the system sum rate subject to the transmit power constraint at the relay [ZRH12b], [ZVKH13], minimize the required transmit power at the relay subject to SINR constraints at each user [ZBR⁺12], and maximize the minimum achievable SINR at the users subject to the transmit power constraint at the relay (also known as SINR balancing) [ZBR⁺12]. It is worth mentioning that we are the first to study these optimization problems. We reformulate the

sum rate maximization problem into an unconstrained optimization problem. This optimization problem is non-linear and in general NP-hard to solve regardless of whether each user has single or multiple antennas. We then adopt the gradient based solutions. More specifically, when each user has a single antenna, we show that, by taking the first-order derivative of the cost function and setting it to zero, the obtained equation is similar to a dominant eigenvector problem. Thus, we apply the power method, which is an iterative algorithm for calculating the dominant eigenvalue and the corresponding dominant eigenvector of a square matrix [GL96]. When each user has multiple antennas, we apply the steepest descent method from [Ber95]. Interestingly, the power method shows fast convergence in numerical simulations. However, in general we do not have analytic evidences that either the power method or the steepest descent method have a guaranteed polynomial time convergence. Moreover, they might only converge to local optima. Therefore, it is worth further investigating the sum rate maximization problem in the direction of reducing the computational complexity or finding a global optimum. To this end, we study this optimization problem from the aspect of the optimization theory. Moreover, to avoid intractable optimization problems, we consider only single antenna users from now on. We first show that the corresponding sum rate maximization problem corresponds to the difference of convex functions (DC) programming problem which is non-convex and NP-hard in general. Afterwards, we derive an efficient polynomial time convex optimization based algorithm to solve the problem approximately. The derived algorithm can be viewed as an extension of the polynomial time DC (POTDC) method which has been recently proposed in [KRVH12] to maximize the sum rate of a single pair TWR system. For the latter problem, the POTDC algorithm, one step of which is based on SDR, is exact, while in the case of multiple operators, the randomization procedure has to be used that makes it approximate ². Numerical results show that the POTDC inspired algorithm converges much faster than the power method. Then we derive the optimal relay amplification matrix to minimize the required transmit power at the relay or to solve the SINR balancing problem. Both optimization problems are non-convex QCQP problems, which are in general NP-hard to solve [LMS⁺10]. We show that they can be solved using the SDR technique. More specifically, the transmit power minimization problem can be solved using the SDR technique together with the randomization procedure while for solving the SINR balancing problem an additional bisection search is required. Additionally, we show that the transmit power mini-

²The SDR technique first transforms the quadratic terms into the traces of a matrix product and then drops the non-convex rank-1 constraint on the new matrix variable. The goal is to relax a non-convex QCQP problem into a convex semidefinite programming (SDP) problem [LMS⁺10]. After solving the relaxed problem, rank-1 extraction has to be performed to obtain a rank-1 approximation for the original problem. The randomization technique is one of the rank-1 extraction techniques. More details are discussed in Appendix B.3.5.

mization problem can be also reformulated into a SOCP problem. One advantage of the SOCP approach is that it has less computational complexity compared to the SDP approach [BPG12]. Simulation results show that the obtained solutions for both problems are almost always optimal. We compare the proposed ProBaSeMO approach to optimal solutions by adapting it to different utility functions. Numerical results show that the proposed ProBaSeMO approach has close to optimal performance especially when there are many antennas at the relay. The last research we carry on for the multi-operator TWR scenario is the derivation of an optimal widely linear relay amplification matrix. The motivation behind this is that if the transmitted complex-valued signal is non-circular, i.e., the real part and the imaginary part of the signal are correlated, also known as non-circularity, widely linear signal processing techniques can be used to exploit this non-circularity such that additional gain is obtained compared to purely linear processing [Ste07]. The key idea of a widely linear design is to perform linear processing to the real and imaginary parts of the signal separately. Again, we study both optimal and suboptimal widely linear relay amplification matrix designs. For optimal designs we use relay transmit power minimization and SINR balancing as the design criteria. After some reformulation we obtain optimization problems which have same problem structure but doubled parameter size compared to their linear counterparts. For a suboptimal widely linear design we consider a single pair TWR system. We propose the widely linear dual channel matching (DCM) scheme [VRWH11] and derive the gain of using widely linear signal processing over linear signal processing analytically [ZH13].

The second scenario we investigate is a multi-pair TWR network with multiple single antenna AF relays and single antenna users. Here relay transmit strategy design means that the relays cooperate with each other to design their amplification coefficients, i.e., a complex-valued coefficient is applied to each relay. Due to the change of the parameter structure, it is not possible to apply the ProBaSeMO scheme. The optimization problem also needs to be reformulated. Among previous works, reference [LXDL10] deals with the adaptive power allocation problem while assuming different pairs of users access the network using different subcarriers, i.e., no inter-pair interference is created during the data transmission. Reference [WCY⁺11] proposes suboptimal beamforming techniques for networks with inter-pair interference, where the proposed strategy is to first null the inter-pair interference using a ZF method and then optimize the interference-free system using a relay transmit power minimization criterion (under a linear constraint). In summary, both [LXDL10] and [WCY⁺11] resort to ZF based transmission. Moreover, none of them deals with the case that each relay has its own transmit power constraint. In other words, previous works consider only a total transmit power constraint for all relays in the network. In contrast, we study the sum rate maximization problem for such a

network with either a total transmit power constraint or individual transmit power constraints [ZRH⁺12c, ZRH12a]. We first show that the objective function of the optimization problem can be represented as a product of quadratic ratios, which is a non-convex QCQP optimization problem. Then we prove that regardless of the considered power constraints the optimization problem satisfies the monotonic optimization framework [Tuy00]. Thus, a polyblock approach, which is a unified approach to solve the monotonic optimization problem [Tuy00], can be applied to solve our problem. Although theoretically the polyblock approach provides globally optimal solutions, its computational cost is high and thus low complexity algorithms are required. It is worth mentioning that when the total transmit power is considered the sum rate maximization problem has the same problem structure as the sum rate maximization problem of the previous multi-operator TWR scenario with single antenna users. This implies that the optimal algorithm designed for one scenario can be used for the other scenario and vice versa. Therefore, we can apply the power method and the POTDC algorithm to the sum rate maximization problem in this scenario, which yield a lower computational complexity compared to the polyblock approach. When each relay has its own transmit power constraint, we show that a low complexity solution can be also obtained by extending the POTDC algorithm. To further reduce the computational complexity, we propose a heuristic approach, i.e., the total SINR eigen-beamformer. The total SINR eigen-beamformer maximizes the ratio between the sum of the signal powers of all the users and the sum of the interference plus noise powers of all the users. It provides a closed-form solution when a total transmit power constraint is considered while it does not require iterations when individual transmit power constraints are considered. Numerical results demonstrate the superiority of the proposed methods over the previously developed methods.

The third scenario under investigation is a multi-pair TWR network with single antenna users and two types of AF relays, namely, the smart relays and the dummy repeaters. Smart relays mean that the relays have multiple antennas and they perform linear processing over the signal as in the scenarios before. By dummy repeaters we refer to the relays which do not require CSI and only amplify the power of the received signal. Dummy repeaters do not cooperate with each other so that cooperative transmission is not possible. Assume that the dummy repeaters can be shut off. Then the considered scenario simplifies to the multi-operator TWR scenario if the smart relays in the network are grouped together to form a big MIMO relay. The considered scenario degenerates to the multi-pair TWR scenario with single antenna relays if the antennas are distributed in the network such that each relay only has a single antenna. Therefore, the third scenario generalizes the first and the second scenario. Interference management in this kind of scenario is more challenging due to the existence of

the dummy repeaters [HJG13b]. Interference neutralization (IN) is a technique, which tunes the interfering signals such that they neutralize each other at the destination node, is proven to be a powerful tool to handle interference in a multi-pair OWR network with both smart relays and repeaters [HJ12], and in deterministic channels [MDFT08a, MDT09]. Therefore, we study the IN feasibility and derive necessary and sufficient IN conditions for our scenario [ZHJH14c, ZHJH14a]. The derived conditions provide an interesting result on how the total number of antennas in the network, which are required to realize IN, decreases when clusters of relays can be formed. Afterwards, we develop relay amplification matrices to optimize different system utility functions with or without IN [ZHJH14b]. The utility functions include minimizing the required transmit power at the relays subject to minimum SINR constraints, maximizing the minimum SINR of the users subject to relay transmit power constraint(s) (i.e., the SINR balancing problem), and maximize the weighted sum rate subject to relay transmit power constraint(s), regardless whether the smart relays in the network have a total transmit power limit or individual transmit power limits. We solve the relay power minimization problem and the sum rate maximization problem using the SDR technique and the monotonic optimization framework, respectively. For the SINR balancing problem, we propose a generalized Dinkelbach-type algorithm, which has a better convergence speed compared to the traditional solution using bisection search [GSS⁺10]. Simulation results show that the IN based solution has close to optimal performance but has a much lower computational complexity compared to optimal solutions without IN.

Joint relay transmit strategy design and BS precoder and decoder design for relay-assisted MU-MIMO downlink channel

The last scenario we study is the relay-assisted MU-MIMO downlink channel (or relay broadcasting channel) with a MIMO AF relay. Here the BS has individual messages for each single antenna user and it communicates with its users via the help a MIMO AF relay. The problem is that the transmit strategy design includes not only the relay transmit strategy but also the transmit and receive strategy (precoding and decoding strategy) for the BS. Before our work [ZRH11], only [TS09] and [DKTL11] discuss the transmit strategy design problem for a MIMO AF relay broadcasting channel and they consider only the channel inversion based techniques. Finding the sum rate optimal transmit strategy for our scenario might result in an intractable optimization problem. To avoid this issue, we resort to a suboptimal transmit strategy design. We propose three suboptimal algorithms for computing the transmit and receive beamforming matrices at the BS as well as the amplification matrix at the relay [ZRH11]. They are based on conventional channel inversion (CI), the ProBaSeMO approach, and ZF dirty paper cod-

ing (ZFDPC), which is a non-linear precoding technique [YH10]. Numerical results show the superiority of the proposed methods over the previously developed methods in [TS09].

1.1.2 Part II: Full-Duplex Wireless Communication Systems

FD technologies enable simultaneous transmission and reception at the same time on the same frequency and thus they have the potential to improve the spectral efficiency. For example, if the relay node can operate in a FD mode, then the spectral efficiency loss of a OWR system due to the HD limitation of the relay can be compensated. This will make a FD OWR system competitive when compared to a TWR system. Moreover, if both the users and the relays can operate in FD modes and a TWR protocol is deployed, then the spectral efficiency of the relaying system can be further improved. The latter scenario, i.e., a FD TWR system, is more ambitious and thus can be considered as a future research topic. The major challenge of enabling a FD operation is that the loop-back self-interference (SI) is much stronger than the received desired signal [JCK⁺11]. Theoretically, the loop-back SI is known at the receiver and hence it can be successfully subtracted from the received signal if we have a sufficiently large dynamic range at the receiver and the SI channel is perfectly known. In practice these two requirements cannot be satisfied especially in an outdoor scenario³. To suppress the SI as much as possible, most of the current SI cancellation techniques suggests a combining of RF cancellation techniques and digital baseband cancellation techniques at the receiver. First, a sufficient isolation between the transmit and the receive chain has to be achieved via geometrical separation of the transmit and the receive antennas or via exploiting the antenna diversity [EDDS11]. This kind of techniques can be seen as an artificial injection of path loss for the SI channel. Then one can consider utilizing specific physical phenomena [CJLK10], [JCK⁺11], [SPS11], e.g., an antenna cancellation approach using two transmit antennas is proposed [CJLK10]. By properly adjusting the position of the two antennas, the signals of both transmit antennas overlap destructively at the receiver antenna. All the aforementioned technique are performed in the RF domain and thus they are RF cancellation techniques. The amount of SI suppression provided by most of the RF cancellation techniques is limited by the hardware capabilities. Therefore, other SI cancellation techniques, i.e., digital baseband cancellation techniques [RWW11], have to be used to further reduce the SI. Digital baseband cancellation can be achieved via the subtraction of the estimated SI signal at the receiver or via spatial suppression schemes by jointly designing the precoder at the transmitter and the decoder at the receiver [RWW11]. There are several disadvantages of the current SI

³In an outdoor scenario the path loss and the user mobility is more severe and thus requires a even larger dynamic range compared to an indoor scenario for an idealistic FD implementation.

cancellation schemes. First, they only guarantee a SI suppression in a specific scenario under a specific system configuration, i.e., their extendability to a different scenario and to a general system setup, e.g., MIMO settings, are unknown. Second, most of the cancellation techniques focus only on the SI minimization but are not aware of the resulting system performance, e.g., the achievable sum rate.

Hence, we propose a SI aware transmit beamforming solution for realizing a FD point-to-point (P2P) MIMO system. Our concept here is to first define a SI threshold (which is known a priori). This threshold guarantees that with or without using RF cancellation techniques the received SI should be within the limited dynamic range of the receiver chain. Then the residual SI can be estimated and then be subtracted at the digital baseband of the receiver. Since this threshold can be formulated as a constraint, this allows us to develop transmit beamformers to optimize different system utility functions by setting up constrained optimization problems. Clearly, this approach provides more flexibilities in SI cancellation, which can be very useful for critical scenarios such as wide-area deployments. The other advantage of this approach is that it allows two transceivers to design their transmit strategies independently compared to the joint design in [DMBS12]. We develop optimal SI aware precoders to maximize the sum rate of the FD system [ZTLH12]. By analyzing active constraints at the optimality, i.e., the constraints are satisfied with equality at the optimality, we show that closed-form solutions can be obtained when each FD device has multiple transmit antennas and a single receive antenna, i.e., a multiple-input single-output (MISO) setup, or when each FD device has 2 transmit antennas and 2 receive antennas, i.e., a 2-by-2 MIMO setup. To achieve the best performance, perfect CSI is desired, which is difficult to obtain practice. Thus, robust design approaches which take into account the imperfections of the CSI such as [WP09] are important for a realistic system implementation. Therefore, we also develop a worst-case optimal transmit strategy by applying a deterministic channel error model in case of imperfect CSI [ZTH13b]. The system utility function is to minimize the total transmit power subject to total SINR constraints at each user. Simulation results demonstrate the robustness of the developed algorithm.

Due to the imperfect RF chain, even after subtracting the known SI, the residual SI can still affect the achievable sum rate of a FD P2P system [DMBS12]. The resulting sum rate maximization problem is non-convex and thus a gradient projection (GP) algorithm is applied in [DMBS12]. Moreover, to guarantee that the achievable FD sum rate is never below the achievable sum rate of a HD baseline scenario, reference [DMBS12] proposes to jointly optimize the transmit covariance matrices of the two terminals for every two time slots. Thereby, when the achievable FD rate is smaller than its HD counterpart, a FD operation is switched to a

HD operation by the proposed algorithm. To avoid a prohibitive computational complexity, we develop sub-optimal transmit strategies which can be calculated during each time slot [ZTH13c]. First, we exploit the statistics of the residual interference and develop signal to leakage plus noise ratio (SLNR) based precoders which have closed-form solutions for both the MISO and the MIMO setup [HMVS01]. The proposed precoders allow the devices to always operate in a FD mode (such that simultaneous transmission and reception is always available). A FD gain is obtained especially in the low to medium SNR regime. Second, noticing that properly controlling the transmit power can also improve the performance of a FD system, we design optimal power adjustment schemes while the precoder is fixed. Power adjustment schemes which maximize the achievable sum rate are developed for the single-input single-output (SISO) and MISO setup while a power adjustment scheme which maximizes the sum SINRs are found for the MIMO setup. Considering the fairness in the system, we also develop power adjustment schemes which maximize the minimum total SINR per user in the system. The proposed power adjustment algorithms can be further combined with the proposed precoding algorithms to enhance the performance. Simulation results demonstrate that the proposed transmit strategies achieve a significant gain over traditional HD transmit strategies when applied to FD systems.

1.1.3 Other contributions

In this section we provide a list of contributions which are not directly related to the two major contributions before. These contributions are worth mentioning because either they are side products of our major contributions or the knowledge we have learned from the major contributions can be applied here. They are not part of the thesis.

The first contribution is a tensor-based channel estimation algorithm for single-pair TWR systems with multiple multi-antenna AF relays and multi-antenna users [ZNH14]. The motivation behind this is that advanced transmit strategy designs (especially the precoder and decoder design at the users) require instantaneous CSI at the transmitter and/or at the receiver. To estimate the channel for relaying networks, tensor-based channel estimation methods, e.g., [RH10b] and [RKX12], can provide a better estimation accuracy, require less training and lead to less ambiguities compared to the traditional matrix-based methods, e.g., [LV08].

The second contribution deals with an optimal transmit strategy for the single-pair TWR scenario with a DF relay [GZV⁺12, GVJ⁺13a, GVJ⁺13b]. In these works we consider only a single carrier flat fading system but each node has multiple antennas and the superposition coding in [OWB09] is applied at the relay. Our task is to characterize the achievable rate region by optimizing the transmit strategies at the relay as well as at the users. By analyzing

active constraints at the optimality, we obtain analytical solutions at the end.

Another contribution is about the joint source and relay precoding design for FD MIMO OWR systems with a MIMO AF relay. Specifically, we study the sum rate maximization problem subject to a SI power constraint and the transmit power constraints at the source and the relay [ZTH13a, TZH14]. Moreover, the sum rate maximization problem for a FD P2P MIMO system with multiple linear constraints is studied in [CZHH14].

The last part of the contributions we would like to mention are the works related to the transmit strategy for MU-MIMO downlink scenarios [CLZ⁺12, LCZ⁺12, CLZ⁺13, ZRH13]. The works in [CLZ⁺12, LCZ⁺12, CLZ⁺13] are devoted to the development of practical low-complexity transmit strategies for OFDM based MU-MIMO downlink systems. The results of these works are successfully patented in [DCL⁺13a], [DCL⁺13c], and [DCL⁺13b]. In [ZRH13], we study the analytic performance of the block diagonalization (BD) scheme under imperfect CSI.

1.2 Organization of the thesis

The thesis is organized as follows. In Part I we first provide a detailed introduction and motivation of TWR in Chapter 2. Then we present the multi-operator TWR scenario with a MIMO AF relay in Chapter 3. Here we propose the ProBaSeMO scheme and derive optimal relay amplification matrices subject to different system utility functions. We also develop optimal and suboptimal widely linear relay transmit strategies for TWR systems with non-circular signals. Then in Chapter 4 we study the sum rate maximization problem for a multi-pair TWR scenario with multiple single antenna AF relays. We develop optimal and suboptimal transmit strategies under a total transmit power constraint of the relays in the network or under individual relay transmit power constraints. In Chapter 5 we study a multi-pair TWR network with multiple MIMO AF relays and dumb repeaters. The necessary and sufficient conditions for interference-free transmission via IN are derived. A general framework for optimizing different utility functions is also developed. In Chapter 6 we develop suboptimal solutions for the joint design of the precoder and the decoder at the BS as well as the relay amplification matrix in a relay-assisted MU-MIMO downlink channel with a two-way MIMO AF relay. Chapter 7 provides a summary and outlines possible future research directions related to TWR. Proofs and derivations are found in Appendix C.

In Part II of this thesis we discuss the possibilities of using digital transmit strategies to suppress the SI in a FD point to point system. In Chapter 8 we develop SI aware transmit strategies to maximize the sum rate of the system. To combat the imperfect CSI at the

transmitter, we also develop a robust transmit strategy, i.e., worst-case beamforming to minimize the required transmit power. In Chapter 9 we develop transmit strategies to combat the residual interference in a FD system due to imperfect RF chains. To this end, SLNR based beamformers and power adjustment algorithms are designed. A complete summary of Part II and possible future research topics are given in Chapter 10. The related proofs of this part are provided in Appendix D.

The final Chapters 11 and 12 collect all the contributions from the thesis again and summarize the future research directions. There are four appendices to the thesis. Appendix A summarizes the list of acronyms and the mathematical notation used throughout the thesis. Appendix B provides background knowledge of convex optimization. Appendices C and D contain proofs and derivations of Part I and Part II, respectively. The bibliography is split into two parts: one part with the own publications and the other part with all other references.

Part I

Two-Way Relaying Networks

The first part of the thesis is devoted to the development of suboptimal or optimal linear relay transmit strategies for relay-assisted communications with two-way amplify-and-forward (AF) relays. More specifically, we focus on multi-pair/multi-user two-way relaying (TWR) networks. Here the network is interference limited especially in the high signal to noise ratio (SNR) regime. In other words, we allow non-orthogonal physical resource access, in contrast to the orthogonal physical resource access schemes, e.g., time-division multiple access (TDMA). The physical resources include the spectrum and the infrastructure, e.g., the relay. By a non-orthogonal physical resource access, we mean the simultaneous access of the spectrum and the relay, i.e., spatial-division multiple access (SDMA) schemes. One of the applications of this scenario is the spectrum and the relay sharing among multiple operators. Non-orthogonal physical resource access suffers from the co-channel interference, which is caused by the non-orthogonal use of the channels at the same time and on the same frequency. If the interference is not dealt with carefully, the network might fail to provide sufficient quality of services (QoS) to the users. The QoS measures include the total throughput, the achievable SINR per user, etc..

In Chapter 2 we give a thorough introduction into commonly used relaying protocols, strategies, and its standardization activities. At the end of this chapter we provide the assumption on the relay model and the system model, which are used in the rest of this part. In Chapter 3 we introduce a multi-operator TWR network with a MIMO AF relay, where multiple operators share the spectrum and the relay. This scenario motivates our study of interference limited relay networks. In this chapter we first present a low complexity close to optimal performance relay amplification matrix design, which is called the projection based separation of multiple operators (ProBaSeMO) scheme. The ProBaSeMO scheme nulls the inter-operator interference and thus allow an interference-free transmission of each operator's signals via the relay. It is flexible in the sense that it can be extended to different system utility functions, i.e., maximizing the system sum rate, minimizing the transmit power at the relay, and maximizing the minimum SINR per user, and that the users can have multiple antennas. Concerning the sum rate maximization problem of the considered scenario, we develop gradient based solutions which are suitable for both single and multiple antenna terminals. Furthermore, when each user has only a single antenna, we derive optimal relay amplification matrices, which can be used for maximizing the achievable sum rate, minimizing the transmit power at the relay, or maximizing the minimum SINR at each user. At the end of this chapter, we also study widely linear relay transmit strategies for single/multiple pair AF TWR systems, which can exploit the non-circularity (as defined in Section 3.8) of the source signals. In Chapter 4, we study the sum rate maximization problem of a multi-pair TWR network with multiple single

antenna AF relays. This scenario can be seen as a counterpart of the scenario in Chapter 3, i.e., instead of using a multi-antenna relay we use multiple relays each with a single antenna. The relays cooperate with each other to calculate the optimal beamforming vectors for a centralized network. A globally optimal solution has been found using the monotonic optimization framework. In Chapter 5 we study interference neutralization, which is a technique that creates positive and negative copies of the interference at the receiver such that they cancel each other, for more general multi-pair TWR networks. It is general because this scenario considers multiple multi-antenna relays as well as repeaters, which simply scale the received signals and forward them. The scenarios in Chapter 3 and Chapter 4 can be seen as special cases of this scenario. Necessary and sufficient conditions for interference neutralization are derived and optimal relay amplification matrices are developed with or without interference neutralization. The last TWR scenario we introduce is the relay broadcast channel in Chapter 6, which is a common scenario in a cellular network. Here we develop suboptimal linear and non-linear relay transmit strategies as well as precoders and decoders at the base station to provide a better system throughput. Finally, a conclusion and a future perspective are given in Chapter 7.

2 Introduction to two-way relaying networks

The increasing demand on high data rates and better user experiences have significantly influenced the development of next generation wireless communications systems. It is a common view that larger bandwidths, densified network structures using small cells, and high spectrum efficiency are key solutions to satisfy the demand. On the one hand, a larger bandwidth requires the shift from the current low frequency bands, i.e., 300 MHz - 3 GHz to much higher frequency bands, e.g., the millimeter-wave band from 30 - 300 GHz [PK11], in addition to the lower frequency. A drawback of the frequency shift is that the path loss will increase exponentially such that the cell size has to be decreased. Thus, a coverage extension is required. Instead of building new network facilities, i.e., sites, base stations (BSs), and backhauls etc., one economic solution for coverage extension is to use intermediate nodes to forward the signal from the BSs to user terminals (UTs). The intermediate node which performs the relaying functionality is called a *relay*. On the other hand, small cells can be used to connect both perspective UTs in the vicinity and massive devices, e.g., smart home devices. However, unless the terminals within the small cell only communicate with each other, backhaul solutions are required for an access to the mobile Internet. Compared to the wired backhauls via fibers, relays can provide wireless backhauling solutions with much lower costs [WIN06]. Therefore, relays will become essential elements of future wireless networks. For more motivations or practical scenarios we refer to [SAP10] and the references therein.

Unlike the typical single-hop communication scenarios, e.g., point-to-point, point-to-multi-point, multi-point-to-multi-point, multi-hop communications have more variations depending on the transmission protocols, e.g., one-way, two-way, or the transmit strategies, e.g., amplify-and-forward or decode-and-forward, at the intermediate nodes (relays), and whether a direct link between the source and the destination is available. Thereby, even though the capacity region of some relaying scenarios has been derived [EK11], the optimal relay transmit strategies are in general unknown. To be focused, we limit ourselves to *two-hop* relaying and *half-duplex* relays. Moreover, we assume that the direct link between the source and the destination is poor and thus it can be ignored. In the rest of this chapter, we first introduce popular relay transmit strategies of two-hop relaying in Section 2.1. Then we summarize the current standardization activities in the area of two-hop relaying in the long term evolution advanced (LTE-A) standard by the 3rd Generation Partnership Project (3GPP). Finally, we discuss the relaying model considered in the rest of Part I.

2.1 Relaying protocols and relaying strategies

Relaying protocols

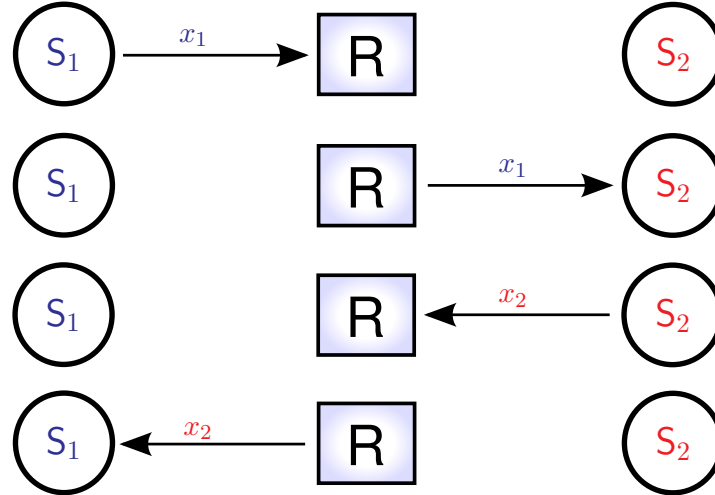


Figure 2.1: A traditional one-way relaying protocol where the communication is completed in 4 phases. The communication partner S_1 has a message x_1 for S_2 . The communication partner S_2 has a message x_2 for S_1 .

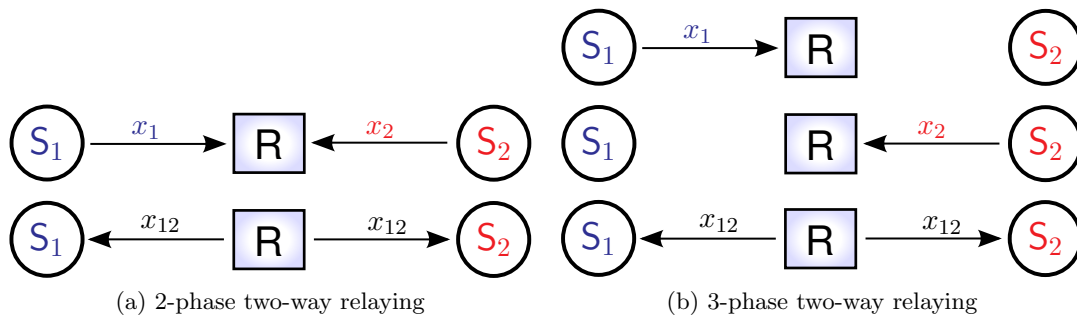


Figure 2.2: Different types of two-way relaying. x_1 and x_2 represent the messages from the two communication partners S_1 and S_2 while x_{12} represent the forwarded signal from the relay, which is a coded version of x_1 and x_2 .

The simplest relaying protocol is *one-way relaying* (OWR) in Figure 2.1. Here one-way means that the information flows in a unidirectional way, i.e., from one specific source via one relay or multiple relays to a specific destination. One-way relaying is also the earliest relaying protocol which was investigated [CT91]. Therefore, it has been comparably well studied. However, the main drawback of one-way relaying is that for a bidirectional exchange

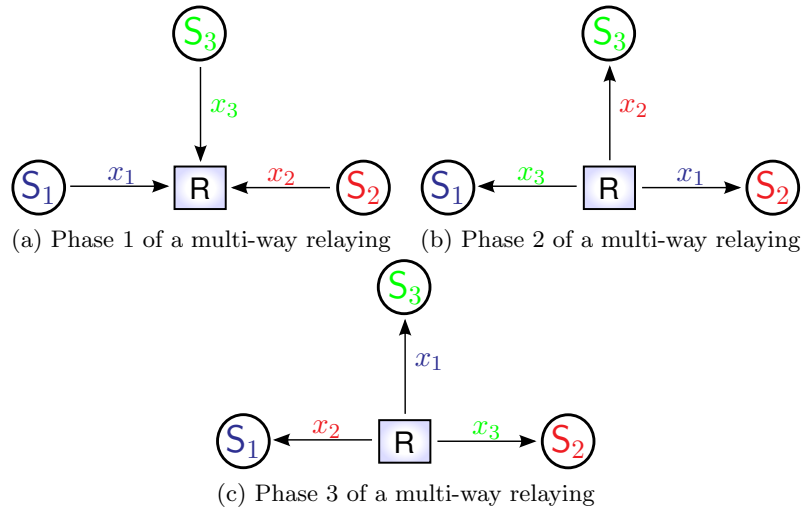


Figure 2.3: An example of multi-way relaying with three communication partners S_1 , S_2 , and S_3 . The messages x_1 , x_2 , and x_3 are messages from one partner to the other two partners. The three-phase protocol in the figure is the same as in [AK10b].

of information, at least four time slots are needed if the relay operates in the half-duplex mode. This causes a fundamental loss in spectral efficiency.

To compensate this drawback, *two-way relaying* (TWR), where two communication partners exchange data bidirectionally with the assistance of one relay node as shown in Figure 2.2, has been proposed [RW07]. Each of these communication partners could be a mobile user as well as a fixed BS. Moreover, the information exchange between two partners takes only two time slots instead of four time slots of the OWR protocol, i.e., in the first time slot all the communication partners transmit simultaneously to the relay and in the second time slot the relay processes the received data, and forwards it to all the nodes. Thereby, the spectral efficiency loss of one-way relaying is compensated and the two-way relaying protocol has been popularized especially via [RW07] and [UK08]. Not surprisingly, two-way relaying has its own drawbacks. The most obvious one is the interference introduced into the two phases: the multi-user uplink interference is created in the first time slot; the multi-user downlink interference and the self-interference are created in the second time slot. Although each communication partner knows its own transmitted symbols and thus the self-interference can be subtracted given the channel knowledge at the receiver, additional coding and signal processing are required, which is much more complex compared to one-way relaying. It is worth mentioning that there also exists a three-phase version of two-way relaying, where in the first phase the communication partners transmit to the relay sequentially [SGS11]. The original purpose of this three-phase two-way

relaying is to apply network coding schemes [LK10].

Recently, another relaying protocol, namely, *multi-way relaying* (MWR), has drawn more and more research interest [GYGP09]. Here multi-way means that there are more than two communication partners, at least three, that communicate with the help of a relay, where each partner has a message and wants to decode messages from all the other partners. Multi-way relaying has its applications such as video conferencing and multi-player gaming. In such applications, multiple nodes communicate with each other. Multi-way relaying can be treated as an extension of one-way or two-way relaying [AK10b]. But it is more difficult to deal with because more co-channel interferences from the other users are introduced. An example of a multi-way relaying scenario is demonstrated in Figure 2.3. In the first phase, the sources S_1 , S_2 , and S_3 send messages x_1 , x_2 , and x_3 to a multi-antenna relay. The relay uses beamforming to spatially separate the data streams and forwards them to the destinations. In the second phase, the relay forwards x_1 to S_2 , x_2 to S_3 , and x_3 to S_1 . In the third phase, the relay forwards x_1 to S_3 , x_2 to S_1 , and x_3 to S_2 . After three phases, each node has received the messages from the other nodes [AK10b].

Relaying strategies

Relaying strategies specify what kind of processing is applied to the received data at the relay. One of the relaying strategies is *decode-and-forward* (DF) relaying. DF relays decode the original message from the received signal via base band signal processing, similarly as what the receiver does in a single-hop communication. Afterwards, it encodes the decoded information using dedicated modulation and coding schemes (MCSs) and then transmit the re-encoded information to the destination, similarly as a general transmitter does. Therefore, DF relays are closely related to single-hop communications. Signal processing techniques from single-hop communications can be easily adopted. Moreover, if there are no decoding errors, the information will be forwarded in a noise-free manner. The drawback of a DF relay is that it performs the functions of the transmitter and the receiver in a sequential way, and thus an additional delay is introduced. When combined with the TWR protocol, additional coding schemes have to be applied to remove the self-interference at the destination. Commonly used codes are superposition codes and network codes, e.g., XOR codes [OWB09]. The superposition code can be easily implemented but it is power inefficient. The XOR code can achieve a rectangular rate region in the second phase (also called the broadcast channel (BC) phase) but it is not suitable if two communication partners experience asymmetric data traffic. In other words, the existing coding schemes do not achieve the capacity of a DF relay channel. But the optimal coding scheme is unknown. Furthermore, one should be aware that

in a DF channel the rate from one communication partner to the other communication partner is dominated by the weakest link, i.e., the weaker one of the link from the source to the relay and the link from the relay to the destination. In a two-way relaying channel, this restriction is extended such that the rate region is limited by the minimum achievable rate in the first phase (also called the multiple access channel (MAC) phase) and in the second phase.

Another well-known relaying strategy is the so called *amplify-and-forward* (AF) relaying strategy. The AF relays simply amplify the received data and retransmit it to the destination. Thereby, the received noise at the relay is also amplified and forwarded, which will affect the performance at the destination. However, compared to the DF relay, it does not decode and re-encode the data and thus it requires less computational complexity and has a smaller delay. Moreover, since it does not require detailed modulation and coding information, it protects the privacy of the communication partners, which is important especially in a relay sharing scenario, e.g., the multi-operator relay sharing scenario in Chapter 3. The simplest implementation of the AF relaying strategy is to amplify the received data directly in the radio frequency (RF) band, i.e., without going to base band. This version of AF relays is also known as *repeaters* [3GP08], which we will call *analog AF*. From the signal processing point of view, only powers are tuned or trivial complex coefficients are adopted at each RF chain. Moreover, this implies that the signal cannot be stored and hence the relay must operate in full-duplex mode. A full-duplex mode operation will result in the problem of a strong loop-back interference, i.e., the transmitted signal of the relay is much stronger than its received signal. Thus, additional loop-back interference cancellation techniques are required [RWW11]. One way to avoid the loop-back interference is to use different bands for the source-to-relay link and the relay-to-destination link. Obviously, such an operation mode is spectrally inefficient. Another operation mode of AF relays is to process the received signal at the base band, i.e., the received signal is converted to the base band and then its weighted linear combination is amplified and transmitted. This processing happens in the digital domain and thus we call it *digital AF*. Compared to repeaters, digital AF relay can tune both the powers and the phases and thus it has more flexibilities in signal processing, e.g., it can be used to realize sophisticated cooperative relaying networks, although this means that channel state information (CSI) has to be available at the relay. When combined with two-way relaying, the estimated self-interference, i.e., the product of the estimated channel and its own transmitted symbols is subtracted at the receiver, which is known as *analog network coding* [ZLCC09].

There are also other relaying strategies, e.g., *compress-and-forward* (CrF) [CE79], [KGG05], [SMMVC10] and *compute-and-forward* (CuF) [NG11]. Both CrF and CuF relaying are proposed from an information theory basis and are more closely related to DF relaying. Consider

a OWR channel, when the capacity of the source to relay link becomes infinitely high, the DF strategy becomes capacity achieving since the relay channel capacity tends to that of a point-to-point channel given that the duration of the first time slot of DF relaying can be shortened as much as possible. Now, thinking about of the second time slot, instead of sending a replica of the received signal, we can quantize it, e.g., using the Wyner-Ziv (WZ) source coding scheme, and send the resulting finite sequence of bits. The destination can then reconstruct the relay observation, and the duration of the second time slot can be made arbitrarily short regardless of the quantization accuracy, provided the relay to destination link capacity is infinite. In this case, this quantized relaying strategy, which is called compress-and-forward, becomes capacity-achieving. Compared to the noisy quantization introduced by the CrF relays, compute and forward relays tend to provide reliable information especially in a multi-user relaying channel, e.g., the TWR channel. That is, if the source transmits coded messages using structured codes, e.g., nested lattice codes, CuF relays can decode linear equations of the transmitted messages using the noisy linear combinations provided by the channel. The destination can decode the desired message if it receives sufficiently many linear combinations [NG11]. The advantage of using structured codes is that a better MAC rate region is obtained compared to traditional DF relaying strategies.

2.2 Standardization activities

Standardization bodies, e.g., 3GPP, IEEE 802.16j, are also active in pushing relays to real-world deployments [YHXM09]. In this section we focus on the relaying operations and terminologies defined in 3GPP LTE-A [HCM⁺12], [ITN10], [SVP⁺13]. Two types of relays have been exactly defined in the 3GPP LTE-Advanced standards, namely, a Type-1 relay and a Type-2 relay [3GP10]. Moreover, relays in the LTE network can also be classified as L1 relays, L2 relays and L3 relays according to the functionality at the relay. Recently, moving relay nodes (MRNs) have also become an active item of the 3GPP standardization group [SVP⁺13].

Type-1 relay vs. Type-2 relay

According to [3GP10], a Type-1 relay station (RS) is non-transparent to the user equipments (UEs). It is in control of cells of its own and has a unique physical-layer cell identity as depicted in Figure 2.4. It is used to help remote UEs, which are located far away from an evolved Node B (eNB, or a BS), to access the eNB. Thus, its main objective is to extend the coverage. A Type-1 RS uses the DF relaying strategy. There are two variants of Type-1 RSs, namely, a *Type-1a* RS and a *Type-1b* RS. A Type-1a RS is *half-duplex* and operates *outband*,

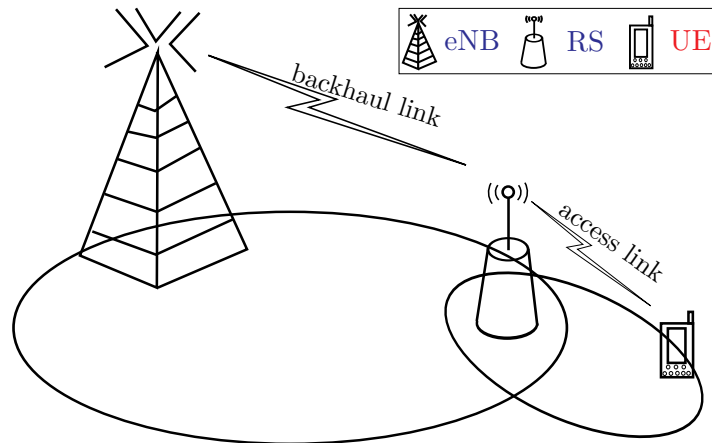


Figure 2.4: A Type-1, Type-1a, or Type-1b relay defined in LTE. These types of relays have their own cell identities.

i.e., the eNB-relay link (also known as the backhaul link) and the relay-UE link (also known as the access link) use different frequencies. A *Type-1b* relay operates *inband*, i.e., the backhaul link and the access link use the same frequency. Since the backhaul link and the access links of a Type-1b RS operate in the same spectrum, an adequate antenna isolation is required to minimize the self-interference between the access link and the backhaul link [DPS14]. Thus, a Type-1b relay is expensive to implement. In contrast, a Type-1 RS is always a *half-duplex inband* relay, where the backhaul link and the access link operate in different time slots and thus the self-interference is avoided. It is said that at least Type 1 and Type-1a relays are part of LTE-Advanced. On the other hand, a Type-2 relay helps a local UE, which is located within the coverage of an eNB and has a direct communication link with the eNB as shown in Figure 2.5, to improve its service quality and link capacity. It is always an inband relay and thus does not have its own cell identity [YHXM09]. The relaying system in this thesis fits to the description of a Type-1 RS except that an AF relaying strategy is used.

L1 relays, L2 relays and L3 relays

According to [ITN10], relays in LTE can be also categorized into *L1 relays*, *L2 relays* and *L3 relays* according to the functionality of the relay. A L1 relay is a smart repeater. In contrast to a dumb repeater (also considered in Chapter 5), which, once installed, continuously forwards the received signal regardless of whether there is a terminal in its coverage area, a smart repeater can be controlled, e.g., activate the repeater only when users are present in the area. However, scheduling and retransmission control is always handled by the eNB. If the RS performs the

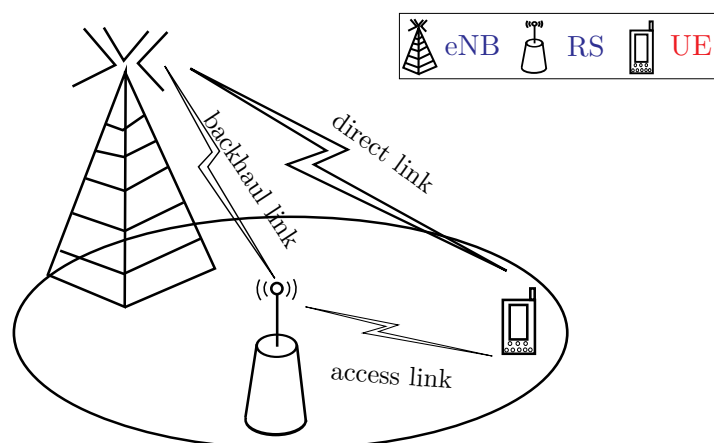


Figure 2.5: A Type-2 relay defined in LTE. A Type-2 relay does not have its own cell identity.

DF strategy, less noise is forwarded by the relay and thus more options can be included on the RS, e.g., rate adaptation. Nevertheless, this kind of relay distinguishes itself based on whether forwarding is performed on Layer 2 (thus denoted as L2 relaying) or on Layer 3 (thus denoted as L3 relaying or self-backhauling).

Moving relay nodes

MRNs or *mobile relays nodes* aim at providing good quality of service to users on high speed vehicles, e.g., trains that operate at 350 km/h [3GP13]. The advantages of using a mobile relay for such scenarios are shown as follows: firstly, group handover can be performed by considering the UEs served by the same MRN as a group. The probability of a group handover failure can be noticeably reduced [SVP⁺13]. Secondly, the MRN is not limited by the size and power compared to the regular UE, and thus it can better exploit MIMO techniques and other advanced signal processing schemes. Lastly, by a proper placement of the indoor and outdoor antennas, an MRN can circumvent the strong vehicular penetration loss [SVP⁺13].

2.3 System assumption, transmission protocols, and mathematical notation

In this section, we describe the general relay and system assumptions used in our study, i.e., in the rest of Part I. We consider TWR with half-duplex AF relays. That is, half-duplex UTs communicate with each other via AF relays and the direct links between UTs are ignored due to their weaknesses. Moreover, in our work one successful communication consists of a

training phase and a data transmission phase. That is, in the training phase each UT only transmits training symbols. These training symbols are used for channel estimation. The estimated channels are used for the calculation of the complex weighting coefficients at each antenna of the relays. The training symbols are also used for channel estimation and the calculation of precoding matrices at the UTs, given multiple receive antennas at the UTs. The algorithms proposed in the rest of Part I are all executed after the training phase. In the data transmission phase, each UT transmits data symbols using the precoding matrices computed from the training phase and a scaled version of the complex weighting coefficients can be applied at each antenna of the relays ¹. Furthermore, the considered systems are narrow band systems. Symbol level synchronization is assumed. The channel is assumed to be frequency flat and quasi-static block fading. Moreover, we assume that the reciprocity holds for the uplink and downlink channel between the UTs and the relay, which is valid in an ideal reciprocal time-division duplex (TDD) system. Note that in an OFDM system the proposed signal processing algorithms can be applied on a per-subcarrier basis. But the resulting performance is suboptimal in general since some problems can only be studied under a multi-carrier setup, e.g., optimal power allocation over different subcarriers [HDL11].

Upper-case and lower-case bold-faced letters denote matrices and vectors, respectively. The expectation, trace of a matrix, transpose, conjugate, Hermitian transpose, and Moore-Penrose pseudo inverse are denoted by $\mathbb{E}\{\cdot\}$, $\text{Tr}\{\cdot\}$, $\{\cdot\}^T$, $\{\cdot\}^*$, $\{\cdot\}^H$, and $\{\cdot\}^+$, respectively. The m -by- m identity matrix is \mathbf{I}_m . The m -by- n matrix with all zero elements is $\mathbf{0}_{m \times n}$. The Euclidean norm of a vector and the Frobenius norm of a matrix are denoted by $\|\cdot\|$ and $\|\cdot\|_F$, respectively. The operator $|\cdot|$ denotes the absolute value or the determinant of a matrix and \equiv stands for identical. The Kronecker product is \otimes and the Hadamard product is \odot . The Khatri-Rao product is denoted by \diamond , which is defined as a column-wise Kronecker product. The $\text{vec}\{\cdot\}$ operator stacks the columns of a matrix into a vector. The $\text{unvec}_{M \times N}\{\cdot\}$ operator stands for the inverse function of $\text{vec}\{\cdot\}$. The operator $\text{diag}\{\mathbf{v}\}$ creates a diagonal matrix by aligning the elements of the vector \mathbf{v} onto its diagonal. A block diagonal matrix is created by the operation $\text{blkdiag}\{\mathbf{A}_n\}_{n=1}^N$ or $\text{blkdiag}\{\mathbf{A}, \mathbf{B}\}$. The rank of a matrix is denoted by $\text{rank}\{\cdot\}$. For vectors \geq and $>$ denote element-wise inequality while for matrices they denote positive semidefinite and positive definite, correspondingly. The ceiling function $\lceil x \rceil$ maps a real number x to the smallest integer that is greater or equal to x . The dimension of a subspace, the image/range of a matrix, and the null space of a matrix are denoted by $\dim\{\cdot\}$, $\mathcal{S}\{\cdot\}$, and $\mathcal{N}\{\cdot\}$, correspondingly. The operator ∂ stands for the partial derivative. The dominant eigenvalue and the dominant eigenvector of a square matrix are denoted as $\lambda_{\max}\{\cdot\}$ and $\mathcal{P}(\cdot)$, respectively. Moreover, \log

¹The reason for the scaling will be elaborated in Section 3.3.5.

and \log_2 stand for the natural logarithm and the logarithm to the base 2, respectively.

3 Multi-operator relaying networks with a MIMO relay

In this chapter, we discuss multi-operator two-way relaying networks, where UTs of multiple operators communicate with each other with a shared MIMO AF relay. Specifically, we develop optimal and suboptimal transmit strategies and verify the sharing gain in terms of the system sum rate of the simultaneous spectrum and relay sharing compared to the time-shared use of the spectrum and the relay by the operators¹. We first propose an efficient relay transmit strategy which is the projection based separation of multiple operators (ProBaSeMO) [RZHJ10, ZRH12b] in Section 3.3. Using ProBaSeMO, the system is firstly decoupled into multiple independent single-operator TWR sub-systems via inter-operator interference suppression techniques at the relay. Then, arbitrary transmit strategies for single-operator two-way AF MIMO relaying are applied to enhance the performance of the sub-systems of each operator. Note that the ProBaSeMO approach also facilitates the use of multiple antennas at the UTs. Therefore, we introduce precoding and decoding strategies for UTs with multiple antennas in Section 3.3.4. Moreover, we introduce a least squares (LS) based channel estimation algorithm for acquiring channel knowledge about the compound channel at both the relay and each UT in Section 3.3.6. Next, to get benchmarks for the ProBaSeMO strategy, we study the sum rate maximization problem subject to a transmit power constraint at the relay [ZRH12b, ZVKH13] in Sections 3.4 and 3.5, the relay transmit power minimization problem [ZRH⁺12c] in Section 3.6, and the SINR balancing problem [ZRH⁺12c] in Section 3.7. Afterwards, we develop widely linear transmit strategies, which can take advantage of the non-circularity of the transmitted complex-valued signals [ZH13] in contrast to the linear transmit strategies, in Section 3.8. Finally, the developed algorithms are compared based on simulations in Section 3.9. Moreover, the sharing gain compared to the time-shared approach is also evaluated and discussed in Section 3.9.

3.1 Problem description and state of the art

In general, the physical resources in wireless communications are spectrum and infrastructure [JBF⁺10]. Traditionally these resources are allocated orthogonally or exclusively in frequency, time, and space inside the network of a single operator or among the networks of different operators. Nevertheless, it is shown in [LJLM09] that spectrum sharing offers the potential

¹In the time-shared approach the operators and the UTs are multiplexed in the time domain.

to improve the network spectral efficiency. It is also reported that infrastructure (including network equipments, sites, etc.) sharing provides advantages like reduced capital expenditures and reduced operating expenditures [GSM08]. However, by sharing physical resources, new types of interference are created on the physical layer. Handling these new types of interference poses a significant and novel challenge to the design of appropriate transmission techniques.

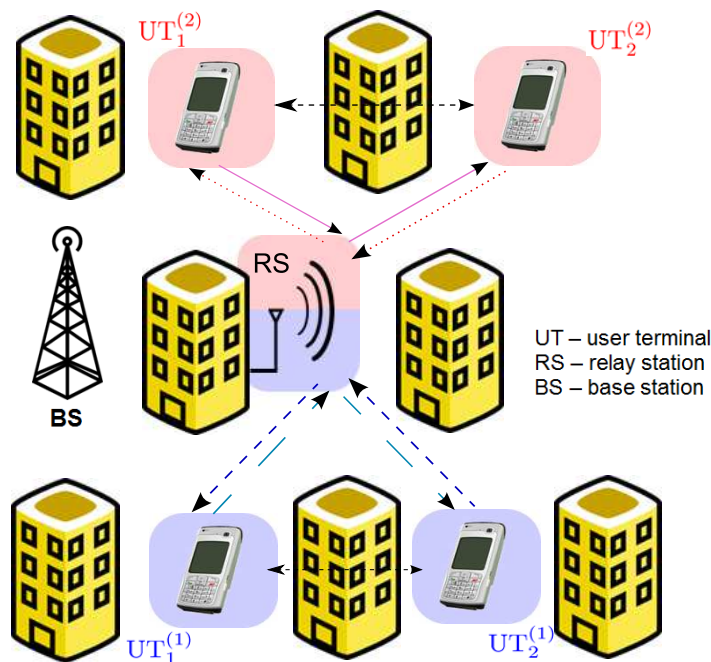


Figure 3.1: A typical metropolitan scenario where two operators share the spectrum and a multi-antenna relay. The arrows show the data flow in two phases, i.e., in the first time slot, all the UTs transmit to the multi-antenna relay and the relay amplifies and sends the signal to all the UTs in the second time slot.

We present a relay-assisted resource sharing scenario in which multiple communication partners (belonging to different operators) use one relay (possibly owned by a third party / virtual operator) to bidirectionally exchange information using the same spectrum. The relay has multiple antennas and operates in a half-duplex mode. Note that this scenario includes spectrum as well as infrastructure (relay) sharing and has attractive practical applications. One concrete application for this kind of relay sharing is the metropolitan scenario as shown in Figure 3.1. Here, strong shadowing effects may cause many coverage holes. Therefore, dense networks are required to guarantee the quality of service (QoS) at the user terminals. Also taking into account that more than one operator or service provider operate in the same area,

if they share the relays as well as the spectrum, this leads to lower capital expenditures and operating expenditures for all the operators. Another application is a disaster scenario where the BS cannot provide services any more. Then the relays can be deployed to temporarily maintain the communication among the local residents. Concerning the privacy and the competitiveness of different operators, in our scenario AF relays are preferable since they avoid complex signaling and data sharing among operators, e.g., an AF relay does not need the knowledge of the modulation and coding formats of different operators as opposed to the regenerative relaying strategies such as DF. Moreover, AF relays significantly reduce the delay and the complexity.

A traditional transmit strategy for our scenario is to assign the physical resources to all the operators in an orthogonal manner, e.g., via different time slots (TDMA manner which is the time-shared approach used in this chapter). Hence, if there is voluntary infrastructure (relay) and spectrum sharing, four important questions arise:

- What are the potential gains (losses) with respect to the chosen performance metric (e.g., the system sum rate, the achievable rate region, etc.) as compared to the orthogonally sharing (e.g., time-shared) approach?
- What are the parameter settings such that a significant gain is achieved?
- What is the order of magnitude of the gain?
- Which transmit strategies, i.e., optimal transmit strategies or suboptimal transmit strategies, are more efficient to achieve the sharing gain?

These are the questions that we will answer in this chapter. For simplicity, we focus on the abstracted system model for L operators shown in Figure 3.2. A multi-antenna AF relay is deployed to assist the communication between pairs of UTs belonging to L different operators. This system model has the same mathematical formulation as the multi-pair TWR scenario with a MIMO AF relay. Thereby, each UT experiences not only the intra-operator interference (the self-interference (SI) caused by its own transmitted signal) but also the inter-operator interference (interference caused by other data signals dedicated to the UTs of other operators). The SI can be subtracted at the UTs if channel knowledge can be acquired. Depending on whether to subtract the SI at the UTs, the SDMA based techniques for our scenario can be categorized into pairing aware methods (in which the SI is subtracted at the UTs, e.g., [RZHJ10], [YZGK10]) and non-pairing aware methods (in which the SI is nulled at the relay, e.g., [JS10]). We will adopt pairing aware methods to design optimal or suboptimal relay transmit strategies.

Let us first provide a brief review of the state of the art in relay transmit strategy design. One-way relaying techniques with MIMO AF relays have been well studied. For example, the optimal beamforming design for single pair one-way relaying systems with single antenna or multiple-antenna UTs are studied in [HNSG10] and [KYA08], respectively. In [FDSG09] it is also implicitly shown that sharing relays between multiple UT pairs outperforms the TDMA scheme. Nevertheless, TWR can compensate the spectral efficiency loss of one-way relaying due to the half-duplex constraint and therefore uses the radio resources more efficiently [RW07]. Previous work on TWR systems with MIMO AF relays includes [JS10], [LLSL09], [RH09], [RH10a], [YZGK10], [ZLCC09]. The optimal beamforming technique [LLSL09], [ZLCC09] as well as several linear preprocessing techniques [RH09], [RH10a], have been proposed for the design of relay amplification matrix in the single pair two-way AF relay channel. Beamforming solutions for the multi-pair two-way MIMO relay channel are shown in [JS10], [YZGK10]. The transmit strategy proposed in [JS10] is based on zero-forcing (ZF) and minimum mean-squared-error (MMSE) criteria. In [YZGK10] the authors consider single antenna UTs and focus on the quantize and forward relaying strategy. In [TW12] the max-min fair relay amplification matrix design for multi-pair two-way MIMO relay channel is presented, which has been published almost at the same time as our work [ZBR⁺12]. In a more recent work [FWY13] optimal relay transmit strategies based on Dinkelbach type I algorithm are also studied, which maximize the sum rate (using the same polyblock approach as in our work [ZRH⁺12c], [ZRH12a]), minimize the transmit power at the relay (less efficient than our proposed algorithm in [ZBR⁺12]), or maximize the minimum SINR per UT. However, to our knowledge, no references deal explicitly with the relay sharing scenario other than our work in [RZHJ10] and [ZRH12b]. Therefore, we consider the transmit strategy design to accomplish this form of spectrum and infrastructure sharing by exploiting the multiple antennas at the relay.

3.2 Data model and transmission protocol

The scenario under investigation is shown in Figure 3.2. Pairs of UTs belonging to L different operators want to communicate with each other. However, due to the poor quality of the direct channel between these pairs of UTs, they can communicate only with the help of the relay. For notational simplicity, the k th UT of the ℓ th operator has $M_k^{(\ell)} = M_U$ antennas $\forall k, \ell$ ($k \in \{1, 2\}$ is the UT index, $\ell \in \{1, \dots, L\}$ denotes the operator index). The relay is equipped with M_R antennas. We assume that the synchronization is perfect ² and the channel is flat fading. The

²In practice, the level of synchronization between UTs of the same operator and UTs of different operators might be different which will have practical impacts on the performance of the proposed algorithms. However, analyzing this issue is out of our scope since detailed mathematical modeling and analysis are required.

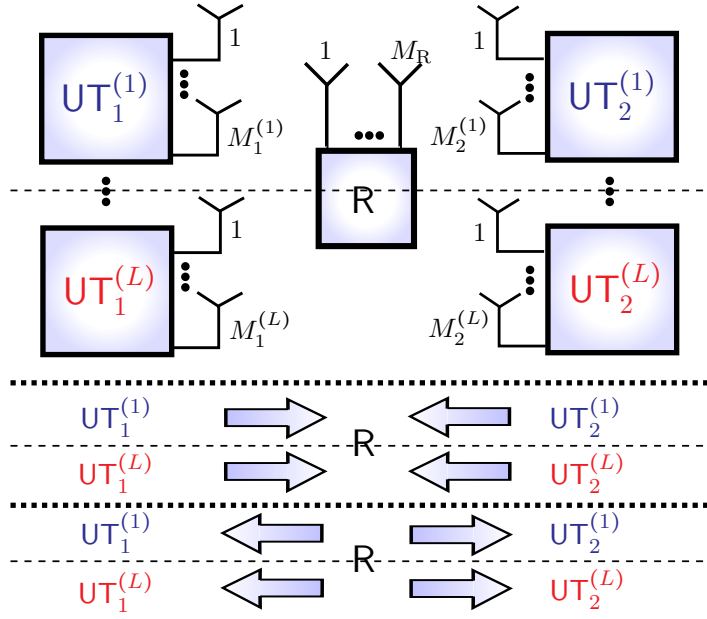


Figure 3.2: L -operator two-way relaying system model. The k -th terminal belonging to the ℓ -th operator has $M_k^{(\ell)}$ antennas and the relay station is equipped with M_R antennas.

channel between the k th UT of the ℓ th operator and the relay is denoted by $\mathbf{H}_k^{(\ell)} \in \mathbb{C}^{M_R \times M_U}$. Furthermore, we assume $\mathbf{H}_k^{(\ell)}$ is a full rank matrix which implies $\text{rank}\{\mathbf{H}_k^{(\ell)}\} = \min\{M_R, M_U\}$.

The two-way AF relaying protocol consists of two transmission phases: in the first phase, which could also be called MAC phase, all the UTs transmit their data simultaneously to the relay. Let the k th UT of the ℓ th operator transmit the data vector $\mathbf{s}_k^{(\ell)} \in \mathbb{C}^{r_k^{(\ell)}}$ with transmit precoding matrix $\mathbf{W}_k^{(\ell)} \in \mathbb{C}^{M_U \times r_k^{(\ell)}}$ ($r_k^{(\ell)}$ is the number of transmitted data streams of the corresponding UT.). Then its transmitted signal vector $\mathbf{x}_k^{(\ell)}$ can be written as

$$\mathbf{x}_k^{(\ell)} = \mathbf{W}_k^{(\ell)} \mathbf{s}_k^{(\ell)}, \quad (3.1)$$

with the transmit power constraint $\mathbb{E}\{\|\mathbf{x}_k^{(\ell)}\|^2\} = P_k^{(\ell)}$. The elements of the input data vectors $\mathbf{s}_k^{(\ell)}$ are independently distributed with zero mean and unit variance.

The received signal vector at the relay is then

$$\mathbf{r} = \sum_{\ell=1}^L \sum_{k=1}^2 \mathbf{H}_k^{(\ell)} \mathbf{x}_k^{(\ell)} + \mathbf{n}_R \in \mathbb{C}^{M_R}, \quad (3.2)$$

where $\mathbf{n}_R \in \mathbb{C}^{M_R}$ denotes the zero-mean circularly symmetric complex Gaussian (ZMCSCG)

noise vector and $\mathbb{E}\{\mathbf{n}_R \mathbf{n}_R^H\} = \sigma_R^2 \mathbf{I}_{M_R}$.

In the second phase, which could also be called BC phase, the relay amplifies the received signal and then forwards it to all the UTs simultaneously. The signal transmitted by the relay can be expressed as

$$\bar{\mathbf{r}} = \mathbf{G} \cdot \mathbf{r}. \quad (3.3)$$

where $\mathbf{G} \in \mathbb{C}^{M_R \times M_R}$ is the relay amplification matrix. The transmit power constraint at the relay should be fulfilled such that $\mathbb{E}\{\|\bar{\mathbf{r}}\|^2\} \leq P_R$, where P_R denotes the total power at the relay.

For notational simplicity, we assume that the reciprocity assumption between the first- and second-phase channels is valid. This assumption is fulfilled in a TDD system if the RF chains are calibrated.³ The received signal vector $\mathbf{y}_k^{(\ell)}$ at the k th UT of the ℓ th operator can be written as

$$\begin{aligned} \mathbf{y}_k^{(\ell)} &= \mathbf{H}_k^{(\ell)\top} \bar{\mathbf{r}} + \mathbf{n}_k^{(\ell)} \\ &= \underbrace{\mathbf{H}_k^{(\ell)\top} \mathbf{G} \mathbf{H}_{3-k}^{(\ell)} \mathbf{x}_{3-k}^{(\ell)}}_{\text{desired signal}} + \underbrace{\mathbf{H}_k^{(\ell)\top} \mathbf{G} \mathbf{H}_k^{(\ell)} \mathbf{x}_k^{(\ell)}}_{\text{self-interference}} \\ &+ \underbrace{\sum_{\substack{\bar{k}=1,2 \\ \bar{\ell} \neq \ell}} \mathbf{H}_k^{(\ell)\top} \mathbf{G} \mathbf{H}_{\bar{k}}^{(\bar{\ell})} \mathbf{x}_{\bar{k}}^{(\bar{\ell})}}_{\text{inter-operator interference}} + \underbrace{\mathbf{H}_k^{(\ell)\top} \mathbf{G} \mathbf{n}_R + \mathbf{n}_k^{(\ell)}}_{\text{effective noise}} \in \mathbb{C}^{M_U}, \end{aligned} \quad (3.4)$$

where $\mathbf{n}_k^{(\ell)} \in \mathbb{C}^{M_U}$ denotes the ZMCSCG noise vector and $\mathbb{E}\{\mathbf{n}_k^{(\ell)} \mathbf{n}_k^{(\ell)H}\} = \sigma_k^{(\ell)^2} \mathbf{I}_{M_U}$. Then the decoding matrix $\mathbf{F}_k^{(\ell)} \in \mathbb{C}^{\bar{r}_k^{(\ell)} \times M_U}$ ($\bar{r}_k^{(\ell)}$ is the number of received data streams of the corresponding UT.) will be used to convert the received signal $\mathbf{y}_k^{(\ell)}$ into an estimate of the transmitted data

$$\hat{\mathbf{s}}_k^{(\ell)} = \mathbf{F}_k^{(\ell)} \mathbf{y}_k^{(\ell)}. \quad (3.5)$$

The overall sum rate of the system is equal to

$$R_{\text{sum}} = \frac{1}{2} \sum_{\ell=1}^L \sum_{k=1}^2 \sum_{i=1}^{\bar{r}_k^{(\ell)}} \log_2(1 + \eta_{k,i}^{(\ell)}) \quad (3.6)$$

where $\eta_{k,i}^{(\ell)}$ is the SINR per stream at each UT and the factor 1/2 is due to the two transmission

³Our method is not limited to the reciprocity assumption.

phases (half duplex).

3.3 Projection based separation of multiple operators (ProBaSeMO) concept

The system in Figure 3.2 is an interference limited system since the UTs of one operator suffer from both the inter-operator interference which is created by the UTs of the other operators and the additional self-interference which is due to the two-way relaying protocol. We need to manage these interferences in an efficient way such that the QoS of all the UTs can be guaranteed. A similar situation occurs in the multi-user MIMO (MU-MIMO) downlink system. There linear precoding techniques like block diagonalization (BD) [SSH04] and regularized block diagonalization (RBD) [SH08] first suppress the inter-user interference and then calculate the precoder for each user separately, which simplifies the system design and significantly improves the system performance. Inspired by this two-step strategy for MU-MIMO systems, we propose to first suppress the inter-operator interference in our system, e.g., by designing the relay amplification matrix such that the UTs of one operator transmit and receive in the null space of the combined channels of all the other UTs. Thereby, the system will be decoupled into L parallel independent single-operator TWR sub-systems. Then, in the second step, arbitrary transmission techniques for single-operator TWR systems can be applied separately on each sub-system. This also facilitates the differentiation among multiple operators. To fulfill the requirement of our proposed projection based separation of multiple operators (ProBaSeMO) approach, we decompose the relay amplification matrix \mathbf{G} into

$$\mathbf{G} = \gamma_0 \cdot \mathbf{G}_0 = \gamma_0 \cdot \mathbf{G}_T \cdot \mathbf{G}_S \cdot \mathbf{G}_R \in \mathbb{C}^{M_R \times M_R} \quad (3.7)$$

where $\mathbf{G}_R \in \mathbb{C}^{LM_R \times M_R}$ and $\mathbf{G}_T \in \mathbb{C}^{M_R \times LM_R}$ are filters designed to suppress the inter-operator interference during the MAC phase and the BC phase, respectively. The parameter $\gamma_0 \in \mathbb{R}_+$ is chosen such that the transmit power constraint at the relay is fulfilled. Moreover, the dimensions of the system increase such that the block diagonal matrix $\mathbf{G}_S \in \mathbb{C}^{LM_R \times LM_R}$ can be written as

$$\mathbf{G}_S = \text{blkdiag}\left\{\mathbf{G}_S^{(\ell)}\right\}_{\ell=1}^L = \begin{bmatrix} \mathbf{G}_S^{(1)} & \cdots & \mathbf{0}_{M_R \times M_R} \\ \vdots & \ddots & \vdots \\ \mathbf{0}_{M_R \times M_R} & \cdots & \mathbf{G}_S^{(L)} \end{bmatrix},$$

where $\mathbf{G}_S^{(1)}, \dots, \mathbf{G}_S^{(L)} \in \mathbb{C}^{M_R \times M_R}$ are the relay amplification matrices for each sub-system. Note that \mathbf{G}_S is block diagonal since it represents the processing performed in the individual sub-

systems.

The overall transmit and receive filter matrices \mathbf{G}_T and \mathbf{G}_R can also be partitioned as

$$\mathbf{G}_T = [\mathbf{G}_T^{(1)}, \dots, \mathbf{G}_T^{(L)}], \quad \mathbf{G}_R = [\mathbf{G}_R^{(1)\top}, \dots, \mathbf{G}_R^{(L)\top}]^\top$$

where $\mathbf{G}_T^{(\ell)} \in \mathbb{C}^{M_R \times M_R}$ and $\mathbf{G}_R^{(\ell)} \in \mathbb{C}^{M_R \times M_R}$. In the following we show how to calculate the matrices $\mathbf{G}_T^{(\ell)}$, $\mathbf{G}_S^{(\ell)}$, and $\mathbf{G}_R^{(\ell)}$ for each operator.

3.3.1 Block-diagonalization at the Relay

As mentioned before, to eliminate only the inter-operator interference but leave the intra-operator interference to the UTs themselves, one choice is to adapt the BD technique for MU-MIMO systems in [SSH04] to design the matrices $\mathbf{G}_T^{(\ell)}$ and $\mathbf{G}_R^{(\ell)}$.

Taking the design of the $\mathbf{G}_R^{(\ell)}$ matrix for the MAC phase as an example, let us define the combined channel matrix $\tilde{\mathbf{H}}^{(\ell)} \in \mathbb{C}^{M_R \times 2(L-1)M_U}$ for all UTs except the UTs of the ℓ th operator as

$$\tilde{\mathbf{H}}^{(\ell)} = [\mathbf{H}^{(1)} \ \dots \ \mathbf{H}^{(\ell-1)} \ \mathbf{H}^{(\ell+1)} \ \dots \ \mathbf{H}^{(L)}], \quad (3.8)$$

where $\mathbf{H}^{(\ell)} = [\mathbf{H}_1^{(\ell)} \ \mathbf{H}_2^{(\ell)}] \in \mathbb{C}^{M_R \times 2M_U}$ is the concatenated channel matrix of the UTs of the ℓ th operator. Then the receive filter matrix $\mathbf{G}_R^{(\ell)}$ should lie in the left null space of $\tilde{\mathbf{H}}^{(\ell)}$ so that the signal of the ℓ th operator will not cause interference to all the other operators. Let $\tilde{L}^{(\ell)} = \text{rank}\{\tilde{\mathbf{H}}^{(\ell)}\}$ and define the singular value decomposition (SVD) of $\tilde{\mathbf{H}}^{(\ell)}$ as

$$\tilde{\mathbf{H}}^{(\ell)} = [\tilde{\mathbf{U}}_s^{(\ell)} \ \tilde{\mathbf{U}}_n^{(\ell)}] \tilde{\mathbf{\Sigma}}^{(\ell)} \tilde{\mathbf{V}}^{(\ell)\text{H}}, \quad (3.9)$$

where $\tilde{\mathbf{U}}_n^{(\ell)}$ contains the last $(M_R - \tilde{L}^{(\ell)})$ left singular vectors. Thus, $\tilde{\mathbf{U}}_n^{(\ell)}$ forms an orthogonal basis for the left null space of $\tilde{\mathbf{H}}^{(\ell)}$ such that $\tilde{\mathbf{U}}_n^{(\ell)\text{H}} \tilde{\mathbf{H}}^{(\ell)} = \mathbf{0}$. Then a linear combination of the rows of $\tilde{\mathbf{U}}_n^{(\ell)\text{H}}$ is the candidate for the receive filter $\mathbf{G}_R^{(\ell)}$. Unlike the work in [YZGK10], we choose

$$\mathbf{G}_R^{(\ell)} = \tilde{\mathbf{U}}_n^{(\ell)} \tilde{\mathbf{U}}_n^{(\ell)\text{H}} \in \mathbb{C}^{M_R \times M_R}. \quad (3.10)$$

It can be easily seen that the $\mathbf{G}_R^{(\ell)}$ in (3.10) is a projection matrix which projects any matrix onto the left null space of $\tilde{\mathbf{H}}^{(\ell)}$.

In the BC phase, due to the reciprocity of the channel and the usage of BD, the transmit filter $\mathbf{G}_T^{(\ell)}$ and receive filter $\mathbf{G}_R^{(\ell)}$ are also reciprocal, so that we get

$$\mathbf{G}_T^{(\ell)} = \mathbf{G}_R^{(\ell)\top}. \quad (3.11)$$

Note that the BD inspired strategy can null the inter-operator interference completely. However, it is restricted by the dimensionality constraint, i.e., the left null space of $\tilde{\mathbf{H}}^{(\ell)}$ cannot be empty. For our system it implies that the condition $M_R > 2(L-1)M_U$ has to be fulfilled.

3.3.2 Regularized Block-diagonalization at the Relay

One algorithm for MU-MIMO systems which is not limited by the dimensionality constraint is the RBD algorithm [SH08]. It allows a residual amount of interference in order to balance it with the noise enhancement. It has been also proved in [SH09] that the performance of RBD converges to BD in the high SNR regime. Now we adopt the RBD design for our scenario.

In the MAC phase, the mean square error (MSE) of the received signal vector can be written as:

$$\mathbb{E} \left\{ \|\mathbf{x} - \mathbf{G}_R \mathbf{r}\|^2 \right\} = \mathbb{E} \left\{ \|\mathbf{x} - \mathbf{G}_R \mathbf{H} \mathbf{x} - \mathbf{G}_R \mathbf{n}_R\|^2 \right\} = \mathbb{E} \left\{ \|\mathbf{x} - \mathbf{G}_R \mathbf{H} \mathbf{x}\|^2 + \|\mathbf{G}_R \mathbf{n}_R\|^2 \right\} \quad (3.12)$$

where $\mathbf{x} = [\mathbf{x}_1^{(1)\text{T}}, \mathbf{x}_2^{(1)\text{T}}, \dots, \mathbf{x}_1^{(L)\text{T}}, \mathbf{x}_2^{(L)\text{T}}]^{\text{T}} \in \mathbb{C}^{2LM_U}$ contains the concatenated transmitted signal vectors of all the UTs and the equivalent combined channel matrix of all the operators $\mathbf{G}_R \mathbf{H}$ is equal to

$$\mathbf{G}_R \mathbf{H} = \begin{bmatrix} \mathbf{G}_R^{(1)} \mathbf{H}^{(1)} & \mathbf{G}_R^{(1)} \mathbf{H}^{(2)} & \dots & \mathbf{G}_R^{(1)} \mathbf{H}^{(L)} \\ \mathbf{G}_R^{(2)} \mathbf{H}^{(1)} & \mathbf{G}_R^{(2)} \mathbf{H}^{(2)} & \dots & \mathbf{G}_R^{(2)} \mathbf{H}^{(L)} \\ \vdots & \vdots & \ddots & \vdots \\ \mathbf{G}_R^{(L)} \mathbf{H}^{(1)} & \mathbf{G}_R^{(L)} \mathbf{H}^{(2)} & \dots & \mathbf{G}_R^{(L)} \mathbf{H}^{(L)} \end{bmatrix}. \quad (3.13)$$

Using the same definition of the interference channel $\tilde{\mathbf{H}}^{(\ell)}$ as in (3.8), the ℓ th operator's effective channel is given by $\mathbf{G}_R^{(\ell)} \mathbf{H}^{(\ell)}$ and the interference caused by the other operators to the ℓ th operator is determined by $\mathbf{G}_R^{(\ell)} \tilde{\mathbf{H}}^{(\ell)}$. Inspired by the RBD algorithm, the matrix \mathbf{G}_R is designed to minimize the interference plus noise power, i.e., the optimization criterion of our RBD inspired strategy is given as

$$\mathbf{G}_R = \arg \min_{\mathbf{G}_R} \mathbb{E} \left\{ \sum_{\ell=1}^L \left\| \mathbf{G}_R^{(\ell)} \tilde{\mathbf{H}}^{(\ell)} \tilde{\mathbf{x}}^{(\ell)} \right\|^2 + \|\mathbf{G}_R \mathbf{n}_R\|^2 \right\}, \quad (3.14)$$

where $\tilde{\mathbf{x}}^{(\ell)} = [\mathbf{x}^{(1)\text{T}} \dots \mathbf{x}^{(\ell-1)\text{T}} \mathbf{x}^{(\ell+1)\text{T}} \dots \mathbf{x}^{(L)\text{T}}]^{\text{T}}$ with $\mathbf{x}^{(\ell)} = [\mathbf{x}_1^{(\ell)\text{T}} \mathbf{x}_2^{(\ell)\text{T}}]^{\text{T}}$.

Let us again compute the SVD of $\tilde{\mathbf{H}}^{(\ell)}$ as

$$\tilde{\mathbf{H}}^{(\ell)} = \tilde{\mathbf{U}}^{(\ell)} \tilde{\Sigma}^{(\ell)} \tilde{\mathbf{V}}^{(\ell)\text{H}}. \quad (3.15)$$

Following a similar procedure as in [SH08], the solution to (3.14) can be obtained as

$$\mathbf{G}_R^{(\ell)} = \left(\frac{P_k^{(\ell)}}{M_U} \tilde{\Sigma}^{(\ell)} \tilde{\Sigma}^{(\ell)H} + \sigma_R^2 \mathbf{I}_{M_R} \right)^{-1/2} \tilde{\mathbf{U}}^{(\ell)H}. \quad (3.16)$$

The complete proof is given in the Appendix C.1.

In the BC phase, the design of the \mathbf{G}_T matrix follows the same way. The interference generated to the other operators is determined by $\tilde{\mathbf{H}}^{(\ell)T} \mathbf{G}_T^{(\ell)}$.⁴ Then, the optimization criterion becomes

$$\mathbf{G}_T = \arg \min_{\mathbf{G}_T} \mathbb{E} \left\{ \sum_{\ell=1}^L \left(\left\| \tilde{\mathbf{H}}^{(\ell)T} \mathbf{G}_T^{(\ell)} \tilde{\mathbf{x}}^{(\ell)} \right\|^2 + \left\| \mathbf{n}^{(\ell)} \right\|^2 \right) \right\}, \quad (3.17)$$

where $\mathbf{n}^{(\ell)} = \left[\mathbf{n}_1^{(\ell)T} \mathbf{n}_2^{(\ell)T} \right]^T$ and we set $\sum_{\ell=1}^L \left\| \mathbf{G}_T^{(\ell)} \right\|_F^2 = P_R$. After following the optimization procedure in [SH08] and utilizing the SVD definition in (3.15), $\mathbf{G}_T^{(\ell)}$ is obtained as

$$\mathbf{G}_T^{(\ell)} = \tilde{\mathbf{U}}^{(\ell)*} \left(\tilde{\Sigma}^{(\ell)*} \tilde{\Sigma}^{(\ell)T} + 2LM_U \sigma_k^{(\ell)2} \mathbf{I}_{M_R} / P_R \right)^{-1/2}. \quad (3.18)$$

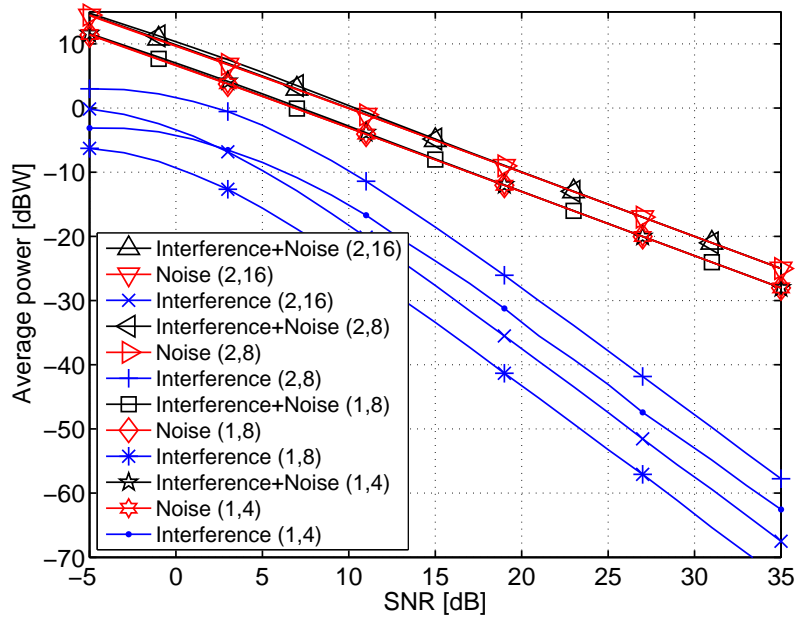


Figure 3.3: The average interference level at the UTs when RBD is applied and $L = 2$. (2,16) stands for (M_U, M_R) . The SNR is defined in equation (3.100) of Section 3.9.

Figure 3.3 demonstrates the relationship between the residual interference power and the

⁴ $\{\cdot\}^T$ comes from the reciprocity assumption.

effective noise power when the RBD inspired strategy is applied. It is obvious that the residual interference decreases significantly as SNR increases. This implies that the RBD inspired design is noise dominated especially in the high SNR regime for our application.

3.3.3 Relay amplification matrix for each sub-system

After applying the receive filter \mathbf{G}_R and the transmit filter \mathbf{G}_T , we get L independent single-operator TWR systems when BD is used which corresponds to RBD in the high SNR regime. Thus, each sub-matrix $\mathbf{G}_S^{(\ell)}$ can be derived separately. In general, any arbitrary design of $\mathbf{G}_S^{(\ell)}$ can be applied. Nevertheless, in our work we use the algebraic norm maximizing (ANOMAX) transmit strategy where the Frobenius norm of the desired signal is maximized [RH09] and its modification rank-restored ANOMAX (RR-ANOMAX) which restores the rank while preserving the same subspace and is thus more suitable for spatial multiplexing [RH10a]. Both algorithms have a good trade-off between performance and computational complexity.

The received signal vectors (3.4) at the UTs of the ℓ th operator can be further expanded as

$$\begin{aligned}\mathbf{y}_1^{(\ell)} &= \mathbf{H}_{1,1}^{(\ell)} \mathbf{x}_1^{(\ell)} + \mathbf{H}_{1,2}^{(\ell)} \mathbf{x}_2^{(\ell)} + \tilde{\mathbf{n}}_1^{(\ell)} \\ \mathbf{y}_2^{(\ell)} &= \mathbf{H}_{2,2}^{(\ell)} \mathbf{x}_2^{(\ell)} + \mathbf{H}_{2,1}^{(\ell)} \mathbf{x}_1^{(\ell)} + \tilde{\mathbf{n}}_2^{(\ell)},\end{aligned}\quad (3.19)$$

where $\tilde{\mathbf{n}}_k^{(\ell)} = \sum_{\bar{k}, \bar{\ell} \neq \ell} \mathbf{H}_k^{(\ell)\top} \mathbf{G} \mathbf{H}_k^{(\bar{\ell})} \mathbf{x}_k^{(\bar{\ell})} + \mathbf{H}_k^{(\ell)\top} \mathbf{G} \mathbf{n}_R + \mathbf{n}_k^{(\ell)}$ denotes the effective noise term which consists of the residual inter-operator interference, the UTs' own noise, and the forwarded relay noise. The effective channel $\mathbf{H}_{k,m}^{(\ell)}$ between the source m and destination k up to γ_0 is defined as

$$\mathbf{H}_{k,m}^{(\ell)} = \mathbf{H}_k^{(\ell)\top} \mathbf{G}_T^{(\ell)} \mathbf{G}_S^{(\ell)} \mathbf{G}_R^{(\ell)} \mathbf{H}_m^{(\ell)}, \quad (3.20)$$

where $m \in \{1, 2\}$. The ANOMAX algorithm solves the following cost function [RH09]

$$\arg \max_{\|\mathbf{G}_S^{(\ell)}\|_F=1} \beta^2 \|\mathbf{H}_{1,2}^{(\ell)}\|_F^2 + (1 - \beta)^2 \|\mathbf{H}_{2,1}^{(\ell)}\|_F^2 \quad (3.21)$$

where $\beta \in [0, 1]$ is a weighting factor. Next we introduce the definitions $\mathbf{g}_S^{(\ell)} = \text{vec}\{\mathbf{G}_S^{(\ell)}\}$ and

$$\mathbf{K}_\beta^{(\ell)} = \left[\beta \left(\left(\mathbf{G}_R^{(\ell)} \mathbf{H}_2^{(\ell)} \right) \otimes \left(\mathbf{G}_T^{(\ell)\top} \mathbf{H}_1^{(\ell)} \right) \right), (1 - \beta) \left(\left(\mathbf{G}_R^{(\ell)} \mathbf{H}_1^{(\ell)} \right) \otimes \left(\mathbf{G}_T^{(\ell)\top} \mathbf{H}_2^{(\ell)} \right) \right) \right]. \quad (3.22)$$

We compute the SVD of $\mathbf{K}_\beta^{(\ell)}$ as $\mathbf{K}_\beta^{(\ell)} = \mathbf{U}_\beta^{(\ell)} \boldsymbol{\Sigma}_\beta^{(\ell)} \mathbf{V}_\beta^{(\ell)\text{H}}$. Then, the optimal $\mathbf{g}_S^{(\ell)}$ is given by $\mathbf{g}_S^{(\ell)} = \mathbf{u}_{\beta,1}^{(\ell)*}$, where $\mathbf{u}_{\beta,1}^{(\ell)}$ is the first column of $\mathbf{U}_\beta^{(\ell)}$ [RH09]. Finally, the optimal matrix $\mathbf{G}_S^{(\ell)}$ is

computed via $\mathbf{G}_S^{(\ell)} = \text{unvec}_{M_R \times M_R} \left\{ \mathbf{u}_{\beta,1}^{(\ell)*} \right\}$.

However, as discussed in [RH10a], the ANOMAX scheme yields a low rank relay amplification matrix and therefore cannot reach the full multiplexing gain for high SNRs especially when multiple antennas are deployed at the UTs. Therefore, one alternative low complexity scheme which is called water-filling rank-restored ANOMAX (WF RR-ANOMAX) is proposed in the same paper. The WF RR-ANOMAX scheme restores the rank of the relay amplification matrix $\mathbf{G}_S^{(\ell)}$ via an optimization inspired by the water filling algorithm over the profile of the singular values of the matrix $\mathbf{G}_S^{(\ell)}$ [RH10a].

3.3.4 Transmit and receive strategies at the UTs

When each UT has multiple antennas, it is beneficial to apply the precoding matrix to either exploit the multiplexing gain or the diversity gain. Beamforming designs have also been addressed in [JS10]. The beamforming schemes used in [JS10] are based on the amount of channel state information (CSI) available at the UTs. Moreover, in [JS10] $\mathbf{H}_k^{(\ell)}$ is required for each UT to generate its beamforming vector. However, it is more natural to design the beamforming vector based on the equivalent channel between the transceiver pair, i.e., the pair of UTs which communicate with each other. It is also easier to obtain the equivalent channel than to obtain $\mathbf{H}_k^{(\ell)}$ at each UT as shown in Section 3.3.6.

Since the transmit and receive strategies of the same UT are based on different equivalent channels, we define two kinds of equivalent channels. The first one, which we refer to as the equivalent forward channel, denotes the effective channel from the source to the destination. The second one, which we refer to as the equivalent backward channel, denotes the effective channel measured at the destination from the source. Taking UTs of the ℓ th operator as an example, the equivalent forward channel of its first UT is $\mathbf{H}_2^{(\ell)\text{T}} \mathbf{G} \mathbf{H}_1^{(\ell)}$ and its corresponding equivalent backward channel is $\mathbf{H}_1^{(\ell)\text{T}} \mathbf{G} \mathbf{H}_2^{(\ell)}$.

Assume that ProBaSeMO is used to determine \mathbf{G} and we fix \mathbf{G}_0 during the training phase and the data transmission phase. The resulting system will comprise $2L$ independent point-to-point MIMO systems.⁵ In our work, the matrices $\mathbf{W}_k^{(\ell)}$ and $\mathbf{F}_k^{(\ell)}$ are designed using two optimal transmit strategies for single stream transmission and multiple stream transmission in the point-to-point MIMO system, respectively.

- **Dominant eigenmode transmission (DET):** The transmit and receive beamforming vectors of the effective channel between the transceiver pair are chosen to be its right and left dominant singular vector, respectively. DET is a single stream transmission scheme

⁵For RBD the residual inter-operator interference is treated as noise.

which maximizes the receive SNR.

- **Spatial multiplexing with water-filling algorithm (WF)**: With perfect CSI at the transmitter the capacity maximizing spatial multiplexing strategy corresponds to the SVD based precoding along with a power allocation based on water-filling [PNG03].

Note that all the point-to-point MIMO systems experience colored noise. Therefore, prewhitening operation is required. The details on the DET and WF schemes are shown in Appendix C.2.

3.3.5 Power control at the relay

In this section, we determine the amplification factor γ_0 which scales \mathbf{G}_0 such that the transmit power constraint at the relay is fulfilled. The amplification factor γ_0 can be obtained via

$$\gamma_0 = \sqrt{\frac{P_R}{\mathbb{E}\{\|\bar{\mathbf{r}}\|^2\}}} = \sqrt{\frac{P_R}{\text{Tr}\left\{\mathbf{G}_0 \left(\sum_{k,\ell} P_k^{(\ell)} \mathbf{Q}_k^{(\ell)} + \sigma_R^2 \mathbf{I}_{M_R}\right) \mathbf{G}_0^H\right\}}}, \quad (3.23)$$

with $\mathbf{Q}_k^{(\ell)} = \mathbf{H}_k^{(\ell)} \mathbf{R}_{x_k^{(\ell)} x_k^{(\ell)}} \mathbf{H}_k^{(\ell)H}$. Here the transmit covariance matrix of the k th UT of the ℓ th operator is defined as $\mathbf{R}_{x_k^{(\ell)} x_k^{(\ell)}} = \mathbf{W}_k^{(\ell)} \mathbf{W}_k^{(\ell)H}$.

However, when the transmit strategies in Section 3.3.4 are used, γ_0 cannot be calculated in a closed-form using (3.23). This is due to the fact that in general the precoding matrices (e.g., WF) of the UTs depend on the the effective SNR which is a function of γ_0 . Vice versa, the power allocation at each UT will affect $\text{Tr}\left\{\mathbf{G}_0 P_k^{(\ell)} \mathbf{Q}_k^{(\ell)} \mathbf{G}_0^H\right\}$ and thus the received power at the relay. Hence, to fulfill the transmit power constraint at the relay a joint design of $\mathbf{R}_{x_k^{(\ell)} x_k^{(\ell)}}$ and γ_0 is required. To avoid a complex joint optimization, we propose an iterative solution which finds the two parameters sequentially. The proposed iterative algorithm is presented in Algorithm 1. It is observed from numerical simulations that in general the proposed algorithm converges in less than 10 iterations.

Remarks

Remark 1. As shown in [RH09], if the weighting factor β is set to 0.5, we will have $\mathbf{G}_S^{(\ell)} = \mathbf{G}_S^{(\ell)T}$. Furthermore, if BD is applied or RBD is applied in the high SNR regime, we get $\mathbf{G} = \mathbf{G}^T$. Such a feature can help to avoid the use of channel feedback or backhauling when channel reciprocity exists. Thus it further reduces the complexity of the system.

Algorithm 1 Iterative power control at the relay in case of multi-stream transmission

- 1: **Initialize:** set $\gamma_0^{(0)} = 1$, $\mathbf{G}_0^{(0)} = \mathbf{G}_0$, maximum iteration number N_{\max} and the threshold value ϵ .
 - 2: **Main step:**
 - 3: **for** $p = 1$ to N_{\max} **do**
 - 4: Insert $\mathbf{G}_0^{(p-1)}$ into the algorithm in Appendix C.2 to calculate $\mathbf{R}_{\mathbf{x}_k^{(\ell)} \mathbf{x}_k^{(\ell)}}^{(p)}$.
 - 5: Insert $\mathbf{R}_{\mathbf{x}_k^{(\ell)} \mathbf{x}_k^{(\ell)}}^{(p)}$ and $\mathbf{G}_0^{(p-1)}$ into equation (3.23) to obtain $\gamma_{\text{update}}^{(p)}$.
 - 6: $\gamma_0^{(p)} = \gamma_0^{(p-1)} \cdot \gamma_{\text{update}}^{(p)}$
 - 7: $\mathbf{G}_0^{(p)} = \gamma_0^{(p)} \mathbf{G}_0$
 - 8: **if** $|\log_{10}(\gamma_{\text{update}}^{(p)})| < \epsilon$ **then**
 - 9: $\mathbf{G} = \gamma_0^{(p)} \cdot \mathbf{G}_0$
 - 10: **break**
 - 11: **end if**
 - 12: **end for**
-

Table 3.1: Comparison of Relay Amplification Schemes

Algorithm	\mathbf{G}_T	\mathbf{G}_S	\mathbf{G}_R
ZF [JS10]	$(\mathbf{F}\mathbf{H}^T)^H ((\mathbf{F}\mathbf{H}^T)(\mathbf{F}\mathbf{H}^T)^H)^{-1}$	$\mathbf{I}_L \otimes (\mathbf{\Pi}_2 \otimes \mathbf{I}_{M_U})$	$((\mathbf{H}\mathbf{W})^H (\mathbf{H}\mathbf{W}))^{-1} (\mathbf{H}\mathbf{W})^H$
MMSE [JS10]	$(\mathbf{H}^H \mathbf{F}^H \mathbf{F} \mathbf{H}^T + 2L\sigma_k^{(\ell)2} \mathbf{I}_{M_R/P_R})^{-1} \mathbf{H}^H \mathbf{F}^H$	$\mathbf{I}_L \otimes (\mathbf{\Pi}_2 \otimes \mathbf{I}_{M_U})$	$\mathbf{W}^H \mathbf{H}^H (\mathbf{H}\mathbf{W}\mathbf{W}^H \mathbf{H}^T + \sigma_R^2 \mathbf{I}_{M_R/P_k^{(\ell)}})^{-1}$
ProBaSeMO (BD)	\mathbf{G}_R^T	Arbitrary block diagonal matrix	$\tilde{\mathbf{U}}_n^{(\ell)} \tilde{\mathbf{U}}_n^{(\ell)H} \forall \ell$
ProBaSeMO (RBD)	$\tilde{\mathbf{U}}^{(\ell)*} (\tilde{\mathbf{\Sigma}}^{(\ell)*} \tilde{\mathbf{\Sigma}}^{(\ell)T} + 2LM_U \sigma_k^{(\ell)2} \mathbf{I}_{M_R/P_R})^{-1/2}, \forall \ell$	Arbitrary block diagonal matrix	$(P_k^{(\ell)} \tilde{\mathbf{\Sigma}}^{(\ell)} \tilde{\mathbf{\Sigma}}^{(\ell)H} / M_U + \sigma_R^2 \mathbf{I}_{M_R})^{-1/2} \tilde{\mathbf{U}}^{(\ell)H}, \forall \ell$

Remark 2. The ZF and MMSE solution in [JS10] can be also obtained using the routine of (3.7), i.e., designing \mathbf{G}_T and \mathbf{G}_R using the ZF and MMSE criteria. Since in these cases all the channels are equalized, the matrix $\mathbf{G}_S^{(\ell)} = \mathbf{\Pi}_2 \otimes \mathbf{I}_{M_U}$ is a permutation matrix where $\mathbf{\Pi}_2 = \begin{bmatrix} 0 & 1 \\ 1 & 0 \end{bmatrix}$ is the exchange matrix which ensures that the user will not receive its own transmitted data. A detailed comparison is shown in Table 3.1. Note that the ZF algorithm requires that $M_R \geq 2LM_U$ if the same transmit strategy is used.

Remark 3. As discussed in Section 3.3.1, to apply BD, there should be at least $M_R > 2(L - 1)M_U$ antennas at the relay. However, this requirement is exact only if M_U data streams per UT have to be transmitted without interference. In other words, given fixed number of M_R and M_U , BD can be still applied by jointly designing the precoder and the decoder at the UTs (also known as coordinated beamforming [SRH13]) once $M_R > 2(L - 1)$, i.e., each UT only transmits a single stream.

Remark 4. The problem of jointly designing \mathbf{G} , $\mathbf{W}_k^{(\ell)}$, and $\mathbf{F}_k^{(\ell)}$ is non-convex. To simplify

the non-convexity, iteratively designing these matrices using the strategy in Section 3.3 can improve the performance. However, this requires an additional overhead in both signaling and computational complexity compared to the proposed scheme.

3.3.6 Acquisition of channel knowledge

The ProBaSeMO strategy requires that the relay and each UT possess channel knowledge. The relay needs to know the channels $\mathbf{H}_k^{(\ell)}$, $\forall k, \ell$. If a single antenna is deployed at each UT, the equivalent backward channel is needed at each UT; if multiple antennas are deployed at each UT, both the equivalent forward and backward channels are needed at each UT. In both cases, knowledge of the self-interference channel should be also obtained at each UT. In general, the equivalent backward channel can be obtained via channel estimation. If $\mathbf{G} = \mathbf{G}^T$, the equivalent forward channel is equal to the transpose of the equivalent backward channel. Otherwise, feedback from the relay is required.

To avoid unnecessary complexity, we propose a simple extension of the LS scheme introduced in [RH10b] to estimate these channels. To this end, all the terminals need to transmit a sequence of $M_U \cdot N_p$ pilot symbols $p_{k,j}^{(\ell)}$ for $j = [1, 2, \dots, N_p]$. The overall training data received at the relay is then

$$\mathbf{B} = \sum_{\ell=1}^L \sum_{k=1}^2 \mathbf{H}_k^{(\ell)} \mathbf{P}_k^{(\ell)} + \mathbf{N}_R \in \mathbb{C}^{M_R \times N_p}, \quad (3.24)$$

where \mathbf{N}_R denotes the ZMCSCG noise matrix and the pilot matrix $\mathbf{P}_k^{(\ell)}$ is defined as

$$\mathbf{P}_k^{(\ell)} = \begin{bmatrix} p_{k,1,1}^{(\ell)} & p_{k,1,2}^{(\ell)} & \cdots & p_{k,1,N_p}^{(\ell)} \\ p_{k,2,1}^{(\ell)} & p_{k,2,2}^{(\ell)} & \cdots & p_{k,2,N_p}^{(\ell)} \\ \vdots & \vdots & \ddots & \vdots \\ p_{k,M_k^{(\ell)},1}^{(\ell)} & p_{k,M_k^{(\ell)},2}^{(\ell)} & \cdots & p_{k,M_k^{(\ell)},N_p}^{(\ell)} \end{bmatrix}. \quad (3.25)$$

Let $\mathbf{P} = [\mathbf{P}_1^{(1)T}, \mathbf{P}_2^{(1)T}, \dots, \mathbf{P}_1^{(L)T}, \mathbf{P}_2^{(L)T}]^T$ be a row-orthogonal matrix. The conventional LS estimate $\hat{\mathbf{H}}$ of the overall channel matrix \mathbf{H} at the relay is obtained via

$$\hat{\mathbf{H}} = \mathbf{B} \cdot \mathbf{P}^+. \quad (3.26)$$

Note that (3.26) requires $N_p \geq 2 \cdot L \cdot M_U$. Let us denote the relay amplification matrix computed from the imperfect channel knowledge as $\tilde{\mathbf{G}}$. The relay can compute $\tilde{\mathbf{G}}$, e.g., using BD, and then transmits $\tilde{\mathbf{G}} \cdot \mathbf{B}$ to all UTs. At the k th UT of the l th operator, the received signal can

be written as

$$\mathbf{Y}_k^{(\ell)} = \tilde{\mathbf{H}}_{k,k}^{(\ell)} \mathbf{P}_k^{(\ell)} + \tilde{\mathbf{H}}_{k,m}^{(\ell)} \mathbf{P}_m^{(\ell)} + \tilde{\mathbf{N}}_k^{(\ell)}, \quad (3.27)$$

with $m \neq k$, $m, k \in \{1, 2\}$ and $\tilde{\mathbf{H}}_{i,j}^{(\ell)} = \mathbf{H}_i^{(\ell)\text{T}} \tilde{\mathbf{G}} \mathbf{H}_j^{(\ell)}$, $\forall i, j, \ell$. The effective noise matrix is denoted by $\tilde{\mathbf{N}}_k^{(\ell)} = \sum_{\bar{k}, \bar{\ell} \neq \ell} \mathbf{H}_{k,\bar{k}}^{(\ell, \bar{\ell})} \mathbf{P}_{\bar{k}}^{(\bar{\ell})} + \tilde{\mathbf{G}} \mathbf{N}_R + \mathbf{N}_k^{(\ell)}$ where $\mathbf{N}_k^{(\ell)}$ denotes the ZMCSCG noise matrix at the UT.

Similarly, the LS estimates of the effective channels for UTs of the l th operator are given by

$$\begin{aligned} \begin{bmatrix} \hat{\mathbf{H}}_{1,1}^{(\ell)} & \hat{\mathbf{H}}_{1,2}^{(\ell)} \end{bmatrix} &= \mathbf{Y}_1^{(\ell)} \cdot \mathbf{P}^{(\ell)+} \text{ for UT1 and} \\ \begin{bmatrix} \hat{\mathbf{H}}_{2,1}^{(\ell)} & \hat{\mathbf{H}}_{2,2}^{(\ell)} \end{bmatrix} &= \mathbf{Y}_2^{(\ell)} \cdot \mathbf{P}^{(\ell)+} \text{ for UT2,} \end{aligned} \quad (3.28)$$

where $\mathbf{P}^{(\ell)}$ is defined as $\mathbf{P}^{(\ell)} = [\mathbf{P}_1^{(\ell)\text{T}}, \mathbf{P}_2^{(\ell)\text{T}}]^\text{T}$. Here we only require that $N_p \geq 2M_U$. It implies that to estimate the channel at the relay requires additional training overhead.

3.4 Sum rate maximization via gradient-based methods

In this section, we derive the optimal matrix \mathbf{G} using the sum rate maximization criterion. Then, the results will be used as the benchmark for our ProBaSeMO scheme.

3.4.1 Single antenna at each UT

The specific case with $M_U = 1$ is considered in the following while the general case is discussed in Section 3.4.2. We compute the optimal \mathbf{G} which maximizes the sum rate of the system subject to a transmit power constraint at the relay, i.e.,

$$\begin{aligned} \max_{\mathbf{G}} \quad & \frac{1}{2} \sum_{\ell=1}^L \sum_{k=1}^2 \log_2 (1 + \eta_k^{(\ell)}) \\ \text{s. t.} \quad & \mathbb{E}\{\|\bar{\mathbf{r}}\|^2\} \leq P_R. \end{aligned} \quad (3.29)$$

Since each UT has only a single antenna, the SINR $\eta_k^{(\ell)}$ of each UT is expressed as

$$\eta_k^{(\ell)} = \frac{\mathbb{E}\left\{\left|\mathbf{h}_k^{(\ell)\text{T}} \mathbf{G} \mathbf{h}_{3-k}^{(\ell)} x_{3-k}^{(\ell)}\right|^2\right\}}{\mathbb{E}\left\{\left|\sum_{\bar{k}, \bar{\ell} \neq \ell} \mathbf{h}_k^{(\ell)\text{T}} \mathbf{G} \mathbf{h}_{\bar{k}}^{(\bar{\ell})} x_{\bar{k}}^{(\bar{\ell})}\right|^2\right\} + \mathbb{E}\left\{\left\|\mathbf{h}_k^{(\ell)\text{T}} \mathbf{G} \mathbf{n}_R\right\|^2\right\} + \sigma_k^{(\ell)2}} \quad (3.30)$$

where all the terms in (3.30) come from the single antenna version of (3.4).

To derive the optimal \mathbf{G} , further algebraic manipulations are required. The transmit power at the relay can be expanded as

$$\begin{aligned}
 \mathbb{E}\{\|\bar{\mathbf{r}}\|^2\} &= \mathbb{E}\{\text{Tr}\{\mathbf{G}\mathbf{r}(\mathbf{G}\mathbf{r})^{\text{H}}\}\} \\
 &= \text{Tr}\left\{\mathbf{G}\left(\sum_{k,\ell} P_k^{(\ell)} \mathbf{h}_k^{(\ell)} \mathbf{h}_k^{(\ell)\text{H}} + \sigma_{\text{R}}^2 \mathbf{I}_{M_{\text{R}}}\right)\mathbf{G}^{\text{H}}\right\} \\
 &= \sum_{k,\ell} \text{Tr}\left\{P_k^{(\ell)} \mathbf{G} \mathbf{h}_k^{(\ell)} \mathbf{h}_k^{(\ell)\text{H}} \mathbf{G}^{\text{H}}\right\} + \text{Tr}\left\{\sigma_{\text{R}}^2 \mathbf{G} \mathbf{G}^{\text{H}}\right\} \\
 &= \sum_{k,\ell} P_k^{(\ell)} \left(\mathbf{G} \mathbf{h}_k^{(\ell)}\right)^{\text{H}} \mathbf{G} \mathbf{h}_k^{(\ell)} + \sigma_{\text{R}}^2 \mathbf{g}^{\text{H}} \mathbf{g} = \mathbf{g}^{\text{H}} \mathbf{C} \mathbf{g}
 \end{aligned} \tag{3.31}$$

where $\mathbf{g} = \text{vec}\{\mathbf{G}\}$. The fact $\text{Tr}\{\mathbf{\Gamma}_1 \mathbf{\Gamma}_2\} = \text{Tr}\{\mathbf{\Gamma}_2 \mathbf{\Gamma}_1\}$ and $\text{vec}\{\mathbf{\Gamma}_1 \mathbf{X} \mathbf{\Gamma}_2\} = (\mathbf{\Gamma}_2^{\text{T}} \otimes \mathbf{\Gamma}_1) \text{vec}\{\mathbf{X}\}$ is used in the derivation. Moreover, \mathbf{C} is a positive definite Hermitian matrix which is defined as

$$\mathbf{C} = \sum_{k,\ell} P_k^{(\ell)} \left(\left(\mathbf{h}_k^{(\ell)} \mathbf{h}_k^{(\ell)\text{H}} \right)^{\text{T}} \otimes \mathbf{I}_{M_{\text{R}}} \right) + \sigma_{\text{R}}^2 \mathbf{I}_{M_{\text{R}}^2}.$$

Following a similar procedure, the SINR $\eta_k^{(\ell)}$ can be rewritten as

$$\eta_k^{(\ell)} = \frac{\mathbf{g}^{\text{H}} \mathbf{D}_k^{(\ell)} \mathbf{g}}{\mathbf{g}^{\text{H}} \mathbf{E}_k^{(\ell)} \mathbf{g} + \sigma_k^{(\ell)^2}} \tag{3.32}$$

where $\mathbf{D}_k^{(\ell)} \geq 0$ and $\mathbf{E}_k^{(\ell)} > 0$ are defined as

$$\begin{aligned}
 \mathbf{D}_k^{(\ell)} &= P_k^{(\ell)} \left(\mathbf{h}_{3-k}^{(\ell)\text{T}} \otimes \mathbf{h}_k^{(\ell)\text{T}} \right)^{\text{H}} \left(\mathbf{h}_{3-k}^{(\ell)\text{T}} \otimes \mathbf{h}_k^{(\ell)\text{T}} \right) \\
 \mathbf{E}_k^{(\ell)} &= \sum_{\bar{k}, \bar{\ell} \neq \ell} P_{\bar{k}}^{(\bar{\ell})} \left(\mathbf{h}_{\bar{k}}^{(\bar{\ell})\text{T}} \otimes \mathbf{h}_k^{(\ell)\text{T}} \right)^{\text{H}} \left(\mathbf{h}_{\bar{k}}^{(\bar{\ell})\text{T}} \otimes \mathbf{h}_k^{(\ell)\text{T}} \right) + \sigma_{\text{R}}^2 \left(\mathbf{I}_{M_{\text{R}}} \otimes \left(\mathbf{h}_k^{(\ell)} \mathbf{h}_k^{(\ell)\text{H}} \right)^{\text{T}} \right).
 \end{aligned}$$

The derivation of (3.32) is found in Appendix C.3.

Inserting (3.32) and (3.31) into (3.29), the original problem can be reformulated as

$$\begin{aligned}
 \max_{\mathbf{g}} \quad & \frac{1}{2} \sum_{\ell=1}^L \sum_{k=1}^2 \log_2 \left(1 + \frac{\mathbf{g}^{\text{H}} \mathbf{D}_k^{(\ell)} \mathbf{g}}{\mathbf{g}^{\text{H}} \mathbf{E}_k^{(\ell)} \mathbf{g} + \sigma_k^{(\ell)^2}} \right) \\
 \text{s. t.} \quad & \mathbf{g}^{\text{H}} \mathbf{C} \mathbf{g} \leq P_{\text{R}}.
 \end{aligned} \tag{3.33}$$

Problem (3.33) is non-convex. To simplify the optimization problem we note that the inequality constraint in (3.33) has to be satisfied with equality at the optimal point. Otherwise, the

optimal \mathbf{g} can be scaled up to satisfy the constraint with equality while increasing the objective function, which contradicts the optimality. Inserting the power constraint into the objective function and dropping the logarithm in the cost function, problem (3.33) can be reformulated as an unconstrained optimization problem

$$\max_{\mathbf{g}} \lambda(\mathbf{g}) = \prod_{\ell=1}^L \prod_{k=1}^2 \frac{\mathbf{g}^H \mathbf{A}_k^{(\ell)} \mathbf{g}}{\mathbf{g}^H \mathbf{B}_k^{(\ell)} \mathbf{g}} \quad (3.34)$$

where $\mathbf{B}_k^{(\ell)} = \mathbf{E}_k^{(\ell)} + \frac{\sigma_k^{(\ell)^2}}{P_R} \mathbf{C}$ and $\mathbf{A}_k^{(\ell)} = \mathbf{B}_k^{(\ell)} + \mathbf{D}_k^{(\ell)}$ are positive definite Hermitian matrices. Since the objective function in (3.34) is homogeneous and any scaling in \mathbf{g} does not change the optimality, the solution to problem (3.34) differs from the solution to (3.29) only in scaling and reshaping, i.e., if $\bar{\mathbf{g}}$ is the solution to (3.34), the optimal solution to (3.29) is given by

$$\mathbf{G} = \text{unvec}_{M_R \times M_R} \left\{ \bar{\mathbf{g}} \sqrt{\frac{P_R}{\bar{\mathbf{g}}^H \mathbf{C} \bar{\mathbf{g}}}} \right\}. \quad (3.35)$$

To solve (3.34), we follow a similar routine as in [RH10b]. We take the necessary condition for optimality of (3.34), i.e.,

$$\frac{\partial \lambda(\mathbf{g})}{\partial \mathbf{g}^*} = 0. \quad (3.36)$$

After some algebraic manipulations [RH10b], we obtain

$$\tilde{\mathbf{K}} \cdot \mathbf{g} = \lambda(\mathbf{g}) \cdot \tilde{\mathbf{J}} \cdot \mathbf{g} \quad (3.37)$$

The matrices $\tilde{\mathbf{K}}$ and $\tilde{\mathbf{J}}$ are defined as

$$\begin{aligned} \tilde{\mathbf{K}} &= \sum_{\ell=1}^L \sum_{k=1}^2 \left(\prod_{\bar{k}, \bar{\ell} \setminus k, \ell} \mathbf{g}^H \mathbf{A}_{\bar{k}}^{(\bar{\ell})} \mathbf{g} \right) \mathbf{A}_k^{(\ell)} \\ \tilde{\mathbf{J}} &= \sum_{\ell=1}^L \sum_{k=1}^2 \left(\prod_{\bar{k}, \bar{\ell} \setminus k, \ell} \mathbf{g}^H \mathbf{B}_{\bar{k}}^{(\bar{\ell})} \mathbf{g} \right) \mathbf{B}_k^{(\ell)}. \end{aligned} \quad (3.38)$$

where $\bar{k}, \bar{\ell} \setminus k, \ell$ stands for the whole set $\{\{\bar{k}, \bar{\ell}\} | \bar{k} \in \{1, 2\}, \bar{\ell} \in \{1, 2, \dots, L\}\}$ excluding the condition $\{\bar{k} = k, \bar{\ell} = \ell\}$. Clearly, equation (3.37) shows that the optimal \mathbf{g} must be a generalized eigenvector of the matrices $\tilde{\mathbf{K}}$ and $\tilde{\mathbf{J}}$. This is similar as in [RH10b]. However, the bisection search of [RH10b] cannot be applied here since an increase in L will increase the number of parameters to search over and thus results in a prohibitive computational complexity. Fortunately, $\tilde{\mathbf{J}}$ is a positive definite matrix and thus it is invertible. Equation (3.37) can be

reformulated into an eigenvalue problem as

$$\tilde{\mathbf{J}}^{-1} \tilde{\mathbf{K}} \cdot \mathbf{g} = \lambda(\mathbf{g}) \cdot \mathbf{g}. \quad (3.39)$$

From (3.39) the dominant eigenvalue of $\tilde{\mathbf{J}}^{-1} \tilde{\mathbf{K}}$ will be the global optimum for (3.34) and the corresponding dominant eigenvector will be the optimal \mathbf{g} . If $\tilde{\mathbf{J}}^{-1} \tilde{\mathbf{K}}$ and $\lambda(\mathbf{g})$ are not functions of \mathbf{g} , the dominant eigenvalue and the dominant eigenvector can be obtained using the power method (PM) in [GL96] (*Section 7.3.1*). In our case, although the matrix $\tilde{\mathbf{J}}^{-1} \tilde{\mathbf{K}}$ and the scalar $\lambda(\mathbf{g})$ are functions of \mathbf{g} , we still propose to compute optimal \mathbf{g} using the iterative power method. Since our problem is more general than the one in [GL96], we call the proposed algorithm as generalized power method (GPM). The details for the GPM are summarized in Algorithm 2. It is worth mentioning that using the PM to solve the maximization problem of the form in (3.34) is also proposed in [LYC08]. Although simulation results show that the GPM algorithm converges, compared to ProBaSeMO it has a significantly higher computational complexity and can only be used as a benchmark.

Algorithm 2 Generalized power method (GPM) for sum rate maximization

- 1: **Initialize:** set a random $\mathbf{g}^{(0)}$, maximum iteration number N_{\max} and the threshold value v .
 - 2: **Main step:**
 - 3: **for** $p = 1$ to N_{\max} **do**
 - 4: Calculate $\Psi^{(p-1)} = (\tilde{\mathbf{J}}^{-1} \tilde{\mathbf{K}})^{(p-1)}$ using $\mathbf{g}^{(p-1)}$.
 - 5: $\mathbf{z}^{(p)} = \Psi^{(p-1)} \mathbf{g}^{(p-1)}$
 - 6: $\mathbf{g}^{(p)} = \mathbf{z}^{(p)} / \|\mathbf{z}^{(p)}\|$
 - 7: **if** $\|\mathbf{g}^{(p)} - \mathbf{g}^{(p-1)}\| < v$ **then**
 - 8: **break**
 - 9: **end if**
 - 10: **end for**
-

3.4.2 Multiple antennas at each UT

In this section, we calculate the optimal relay amplification matrix assuming that $\mathbf{W}_k^{(\ell)} = \sqrt{P_k^{(\ell)}} \mathbf{I}_{M_U} / \sqrt{M_U}$. The achievable rate for the k th UT of the ℓ th operator is

$$R_k^{(\ell)} = \frac{1}{2} \log_2 \left(\left| \mathbf{I}_{M_U} + \frac{P_{3-k}^{(\ell)}}{M_U} \mathbf{H}_k^{(\ell)\text{T}} \mathbf{G} \mathbf{H}_{3-k}^{(\ell)} \mathbf{H}_{3-k}^{(\ell)\text{H}} \mathbf{G}^{\text{H}} \mathbf{H}_k^{(\ell)*} \right| \right)$$

$$\cdot \left(\sum_{\bar{k}, \bar{\ell} \neq \ell} \frac{P_{\bar{k}}^{(\bar{\ell})}}{M_U} \mathbf{H}_k^{(\ell)\top} \mathbf{G} \mathbf{H}_{\bar{k}}^{(\bar{\ell})} \mathbf{H}_{\bar{k}}^{(\bar{\ell})\text{H}} \mathbf{G}^{\text{H}} \mathbf{H}_k^{(\ell)*} + \sigma_{\text{R}}^2 \mathbf{H}_k^{(\ell)\top} \mathbf{G} \mathbf{G}^{\text{H}} \mathbf{H}_k^{(\ell)*} + \sigma_k^{(\ell)2} \mathbf{I}_{M_U} \right)^{-1} \Bigg|.$$

The sum rate maximization problem is then formulated as

$$\begin{aligned} \max_{\mathbf{G}} \quad & R_{\text{sum}} = \sum_{\ell=1}^L \sum_{k=1}^2 R_k^{(\ell)} \\ \text{s. t.} \quad & \mathbb{E}\{\|\bar{\mathbf{r}}\|^2\} \leq P_{\text{R}}. \end{aligned} \quad (3.40)$$

The same argument as in Section 3.4.1 holds, i.e., the constraint has to be satisfied with equality at the optimum. Inserting the constraint into the cost function in (3.40), again we calculate the necessary condition for optimality. Using the fact that $d(\log|\mathbf{\Gamma}|) = \text{tr}\{\mathbf{\Gamma}^{-1}d\mathbf{\Gamma}\}$, $d\{\text{tr}\{\mathbf{\Gamma}\}\} = \text{tr}\{d\mathbf{\Gamma}\}$ [Hj011], the gradient of the sum rate is then obtained as:

$$\begin{aligned} \nabla R_{\text{sum}} &= \frac{\partial R_{\text{sum}}}{\partial \mathbf{G}^*} \\ &= \sum_{k,\ell} \frac{1}{2M_U \log 2} \left[\frac{\sigma_k^{(\ell)2}}{P_{\text{R}}} \text{Tr}\{\mathbf{\Psi}_k^{(\ell)-1} - \mathbf{\Psi}_{3-k}^{(\ell)-1}\} \mathbf{G} \mathbf{\Omega} + \mathbf{H}_k^{(\ell)*} (\mathbf{\Psi}_k^{(\ell)-1} - \mathbf{\Psi}_{3-k}^{(\ell)-1}) \mathbf{H}_k^{(\ell)\top} \right. \\ &\quad \cdot \left. \mathbf{G} (\mathbf{\Omega} - P_k^{(\ell)} \mathbf{H}_k^{(\ell)} \mathbf{H}_k^{(\ell)\text{H}}) + P_{3-k}^{(\ell)} \mathbf{H}_k^{(\ell)*} \mathbf{\Psi}_{3-k}^{(\ell)-1} \mathbf{H}_k^{(\ell)\text{H}} \mathbf{G} \mathbf{H}_{3-k}^{(\ell)} \mathbf{H}_{3-k}^{(\ell)\text{H}} \right] \end{aligned} \quad (3.41)$$

where $\mathbf{\Omega}$, $\mathbf{\Psi}_k^{(\ell)}$, and $\mathbf{\Psi}_{3-k}^{(\ell)}$ are defined as

$$\begin{aligned} \mathbf{\Omega} &= \sum_{k,\ell} P_k^{(\ell)} \mathbf{H}_k^{(\ell)} \mathbf{H}_k^{(\ell)\text{H}} + \sigma_{\text{R}}^2 M_U \mathbf{I}_{M_{\text{R}}} \\ \mathbf{\Psi}_k^{(\ell)} &= \frac{\sigma_k^{(\ell)2} \text{Tr}\{\mathbf{\Omega}\}}{M_U P_{\text{R}}} \mathbf{I}_{M_U} + \frac{1}{M_U} \mathbf{H}_k^{(\ell)\top} \mathbf{G} (\mathbf{\Omega} - P_k^{(\ell)} \mathbf{H}_k^{(\ell)} \mathbf{H}_k^{(\ell)\text{H}}) \mathbf{G}^{\text{H}} \mathbf{H}_k^{(\ell)*} \\ \mathbf{\Psi}_{3-k}^{(\ell)} &= \mathbf{\Psi}_k^{(\ell)} - \frac{P_{3-k}^{(\ell)}}{M_U} \mathbf{H}_k^{(\ell)\top} \mathbf{G} \mathbf{H}_{3-k}^{(\ell)} \mathbf{H}_{3-k}^{(\ell)\text{H}} \mathbf{G}^{\text{H}} \mathbf{H}_k^{(\ell)*} \end{aligned} \quad (3.42)$$

Finally, we apply the steepest descent method as in Algorithm 3 to obtain \mathbf{G} . The step size t is chosen using the Armijo's Rule which provides provable convergence [Ber95]. That is, t is calculated as $t = \beta^n$ where n is the smallest integer such that

$$R_{\text{sum}}(\mathbf{G} + \beta^n \nabla R_{\text{sum}}) - R_{\text{sum}}(\mathbf{G}) \leq \alpha \beta^n \text{Tr}\{\nabla R_{\text{sum}}^{\text{H}} \nabla R_{\text{sum}}\} \quad (3.43)$$

where β and α are fixed scalars between zero and one. Since the cost function in (3.40) is non-convex, this solution here might be merely a local minimum.

Algorithm 3 Steepest descent method for sum rate maximization

-
- 1: **Initialize:** set a random \mathbf{G} and calculate $R_{\text{sum}}^{(0)}$, maximum iteration number N_{max} and the threshold value v .
 - 2: **Main step:**
 - 3: **for** $p = 1$ to N_{max} **do**
 - 4: Calculate the steepest descent direction $\nabla R_{\text{sum}} / \|\nabla R_{\text{sum}}\|_{\text{F}}$.
 - 5: Choose a step size t using Armijo's Rule in (3.43).
 - 6: Update $\mathbf{G} = \mathbf{G} + t \nabla R_{\text{sum}} / \|\nabla R_{\text{sum}}\|_{\text{F}}$.
 - 7: Calculate $R_{\text{sum}}^{(p)}$ with the updated \mathbf{G} .
 - 8: **if** $|R_{\text{sum}}^{(p)} - R_{\text{sum}}^{(p-1)}| < v$ **then**
 - 9: **break**
 - 10: **end if**
 - 11: **end for**
-

3.5 Sum rate maximization via POTDC

The sum rate maximization problem can be also formulated as a difference of convex functions (DC) programming problem, which is non-convex and NP-hard in general. Using the DC structure, in the following we derive an efficient polynomial time convex optimization-based algorithm to solve the problem approximately. This algorithm can be viewed as an extension of the polynomial time DC (POTDC) method which has been recently proposed in [KRVH12] to maximize the sum rate in AF TWR with multiple antennas at the relay and just a single pair of users. For the latter problem, the POTDC algorithm, one step of which is based on semidefinite programming (SDP) relaxation, is exact, while in the case of multiple operators (multiple pairs of users that share the same relay), the randomization procedure has to be used that makes it approximate.

We consider the sum rate maximization problem (3.33), which is

$$\begin{aligned}
 \max_{\mathbf{g}} \quad & \frac{1}{2} \sum_{\ell=1}^L \sum_{k=1}^2 \log_2 \left(1 + \frac{\mathbf{g}^H \mathbf{D}_k^{(\ell)} \mathbf{g}}{\mathbf{g}^H \mathbf{E}_k^{(\ell)} \mathbf{g} + \sigma_k^{(\ell)2}} \right) \\
 \text{s. t.} \quad & \mathbf{g}^H \mathbf{C} \mathbf{g} \leq P_{\text{R}}.
 \end{aligned} \tag{3.44}$$

Using the observation that the relay transmit power constraint in (3.44) can be rewritten as an equality constraint, changing to the natural logarithm, and also omitting the constant $\frac{1}{2}$ in the objective function, the constrained optimization problem (3.44) can be turned into the

following *unconstrained* optimization problem

$$\max_{\mathbf{g}} \sum_{\ell=1}^L \sum_{k=1}^2 \log \left(1 + \frac{\mathbf{g}^H \mathbf{D}_k^{(\ell)} \mathbf{g}}{\mathbf{g}^H \mathbf{E}_k^{(\ell)} \mathbf{g} + \mathbf{g}^H \frac{\sigma_k^{(\ell)2}}{P_R} \mathbf{C} \mathbf{g}} \right). \quad (3.45)$$

Moreover, after some straightforward algebra, the problem (3.45) can be shown to be equivalent to the following optimization problem

$$\max_{\mathbf{g}} \log \left(\prod_{\ell=1}^L \prod_{k=1}^2 \frac{\mathbf{g}^H \mathbf{A}_k^{(\ell)} \mathbf{g}}{\mathbf{g}^H \mathbf{B}_k^{(\ell)} \mathbf{g}} \right). \quad (3.46)$$

The problem (3.46) is a homogeneous quadratically constrained quadratic programming (QCQP) problem which is NP-hard in general.

Introducing the new notation $\mathbf{X} = \mathbf{g}\mathbf{g}^H$ and using the property that $\text{Tr}\{\mathbf{\Gamma}\mathbf{X}\} = \mathbf{g}^H \mathbf{\Gamma} \mathbf{g}$, the problem (3.46) can be equivalently written as

$$\begin{aligned} \max_{\mathbf{X}} \quad & \sum_{\ell=1}^L \sum_{k=1}^2 (\log(\text{Tr}\{\mathbf{A}_k^{(\ell)} \mathbf{X}\}) - \log(\text{Tr}\{\mathbf{B}_k^{(\ell)} \mathbf{X}\})) \\ \text{s. t.} \quad & \text{rank}(\mathbf{X}) = 1 \\ & \mathbf{X} \geq \mathbf{0}. \end{aligned} \quad (3.47)$$

Moreover, using SDP relaxation, i.e., removing the non-convex rank-1 constraint in (3.47), the relaxed problem can be shown to be a DC programming problem, which is still non-convex. Hereafter, for notational simplicity, we define an index m to substitute the indices $\binom{\ell}{k}$ such that $m = 2(\ell - 1) + k, \forall k, \ell$ (i.e., $m \in \{1, 2, \dots, 2L\}$). Then the relaxed problem (3.47) with new simplified indices can be rewritten as

$$\begin{aligned} \max_{\mathbf{X}, \{\alpha_m, \beta_m\}} \quad & \log(\text{Tr}\{\mathbf{A}_1 \mathbf{X}\}) - \log(\text{Tr}\{\mathbf{B}_1 \mathbf{X}\}) + \sum_{m=2}^{2L} \log(\alpha_m) - \sum_{m=2}^{2L} \log(\beta_m) \\ \text{s. t.} \quad & \text{Tr}\{\mathbf{A}_m \mathbf{X}\} = \alpha_m, \quad m = 2, 3, \dots, 2L \\ & \text{Tr}\{\mathbf{B}_m \mathbf{X}\} = \beta_m, \quad m = 2, 3, \dots, 2L \\ & \mathbf{X} \geq \mathbf{0}. \end{aligned} \quad (3.48)$$

Due to the Rayleigh-quotient structure of (3.46), the problem does not change by setting $\mathbf{g}^H \mathbf{B}_1 \mathbf{g} = \text{Tr}\{\mathbf{B}_1 \mathbf{X}\} = 1$. Furthermore, the objective function in (3.48) turns into a convex function by replacing the concave elements, i.e., the elements with the minus signs by scalar

variables. Then the reformulated problem, which is equivalent to (3.48), is written as

$$\begin{aligned}
 & \max_{\mathbf{X}, \{\alpha_m, \beta_m, t_m\}} \quad \log(\text{Tr}\{\mathbf{A}_1 \mathbf{X}\}) + \sum_{m=2}^{2L} \log(\alpha_m) - \sum_{m=2}^{2L} t_m \\
 & \text{s. t.} \quad \text{Tr}\{\mathbf{A}_m \mathbf{X}\} = \alpha_m, \quad m = 2, 3, \dots, 2L \\
 & \quad \quad \text{Tr}\{\mathbf{B}_m \mathbf{X}\} = \beta_m, \quad m = 2, 3, \dots, 2L \\
 & \quad \quad \log(\beta_m) \leq t_m, \quad m = 2, 3, \dots, 2L \\
 & \quad \quad \text{Tr}\{\mathbf{B}_1 \mathbf{X}\} = 1, \quad \mathbf{X} \geq \mathbf{0}.
 \end{aligned} \tag{3.49}$$

As compared to the problem (3.48) with a non-convex DC-type objective function, the non-convexity in the equivalent problem (3.49) is localized in the inequality constraints $\log(\beta_m) \leq t_m$, $m = 2, 3, \dots, 2L$. To deal with these non-convex constraints, we propose to use a linear approximation of the log function, e.g., the first order Taylor series of the log function, which uses the same philosophy as the original POTDC algorithm in [KRVH12]. The first order Taylor polynomial approximation of $\log(\beta)$ at β_0 is defined as

$$\log(\beta) \approx \log(\beta_0) + \frac{\beta - \beta_0}{\beta_0}. \tag{3.50}$$

Using (3.50), the optimization problem (3.49) can be reformulated as

$$\begin{aligned}
 & \max_{\mathbf{X}, \{\alpha_m, \beta_m, t_m\}} \quad \log(\text{Tr}\{\mathbf{A}_1 \mathbf{X}\}) + \sum_{m=2}^{2L} \log(\alpha_m) - \sum_{m=2}^{2L} t_m \\
 & \text{s. t.} \quad \text{Tr}\{\mathbf{A}_m \mathbf{X}\} = \alpha_m, \quad m = 2, 3, \dots, 2L \\
 & \quad \quad \text{Tr}\{\mathbf{B}_m \mathbf{X}\} = \beta_m, \quad m = 2, 3, \dots, 2L \\
 & \quad \quad \log(\beta_{0,m}) + \frac{\beta_m - \beta_{0,m}}{\beta_{0,m}} \leq t_m, \quad m = 2, 3, \dots, 2L \\
 & \quad \quad \text{Tr}\{\mathbf{B}_1 \mathbf{X}\} = 1, \quad \mathbf{X} \geq \mathbf{0}.
 \end{aligned} \tag{3.51}$$

It can be seen that for a given set of initial values $\{\beta_{0,2}, \beta_{0,3}, \dots, \beta_{0,m}\}$, the problem (3.51) is an SDP problem that can be solved efficiently using the interior-point algorithms if it is feasible [BV04]. Since the best set of initial values is unknown, it is natural to use an iterative method and update the initial values in each iteration. Here, the initial values $\{\beta_{0,2}^{(p)}, \beta_{0,3}^{(p)}, \dots, \beta_{0,m}^{(p)}\}$ at the p th step are the optimal values of β_m which are obtained by solving the problem (3.51) at the $(p-1)$ th step. It is worth stressing that, if the problem (3.51) is feasible at the p th step, then the optimal value of the cost function in (3.51) denoted as $f^{*(p)}$ should be larger or equal

to the optimal value for the same problem at the previous $(p-1)$ th step, i.e., $f^{*(p-1)}$. Otherwise, if $f^{*(p)} < f^{*(p-1)}$, it is contradictory to the objective function. Moreover, the following lemma holds for the POTDC inspired algorithm.

Lemma 3.5.1. *The solution generated by the POTDC inspired algorithm converges to the Karush-Kuhn-Tucker (KKT) point of problem (3.49).*

Proof. This conclusion comes straightforwardly from Proposition 3.2 of [BBTT10]. \square

Summarizing, the proposed iterative algorithm for solving the optimization problem (3.49) can be described as in Algorithm 4.

Algorithm 4 Iterative algorithm for solving the optimization problem (3.49)

- 1: **Initialize:** input: $\mathbf{A}_1, \mathbf{B}_1, \mathbf{A}_m, \mathbf{B}_m, \mathbf{C}$, set $\{\beta_{0,2}^{(0)}, \beta_{0,3}^{(0)}, \dots, \beta_{0,m}^{(0)}\}$, $f^{*(0)}$, maximum iteration number N_{\max} and the threshold value ϵ .
 - 2: **Main step:**
 - 3: **for** $p = 1$ to N_{\max} **do**
 - 4: Solve the problem (3.51) in order to find the optimal value $f^{*(p)}$ and $\beta_m^{(p)}$.
 - 5: $\beta_{0,m}^{(0)} = \beta_m^{(p)}$, $m = 2, 3, \dots, 2L$
 - 6: **if** $|f^{*(p)} - f^{*(p-1)}| \leq \epsilon$ **then**
 - 7: **break**
 - 8: **end if**
 - 9: **end for**
-

It should also be stressed that the initial set of $\{\beta_{0,2}^{(0)}, \beta_{0,3}^{(0)}, \dots, \beta_{0,m}^{(0)}\}$ has to be feasible. Taking into account the generalized Rayleigh quotient structure and recalling that $\mathbf{g}^H \mathbf{B}_1 \mathbf{g} = 1$, β_m can be any value between the maximum and minimum generalized eigenvalues of the matrix pair \mathbf{B}_m and \mathbf{B}_1 , i.e., $\beta_m \in \{\lambda_{\min}\{\mathbf{B}_1^{-1} \mathbf{B}_m\}, \lambda_{\max}\{\mathbf{B}_1^{-1} \mathbf{B}_m\}\}$. For example, $\beta_{0,m}^{(0)}$ can be chosen in a random way such that

$$\beta_{0,m}^{(0)} = \frac{\mathbf{a}^H \mathbf{B}_m \mathbf{a}}{\mathbf{a}^H \mathbf{B}_1 \mathbf{a}}, \quad m = 2, 3, \dots, 2L, \quad (3.52)$$

where $\mathbf{a} \in \mathbb{C}^{M_{\mathbb{R}}^2} \sim \mathcal{CN}(\mathbf{0}, \mathbf{I}_{M_{\mathbb{R}}^2})$.

Algorithm 4 provides only an approximate solution to the relaxed problem (3.44) in terms of the matrix variable \mathbf{X} . This solution is the same as the solution of the original problem (3.44) only if \mathbf{X} is a rank-1 matrix. In other words, $\hat{\mathbf{g}}$ is optimal for (3.44) only if there exists $\mathbf{X}^* = \hat{\mathbf{g}} \hat{\mathbf{g}}^H$, where \mathbf{X}^* is the solution obtained based on Algorithm 4. However, according to [HP10] (*Theorem 3.2 and Corollary 3.4*), there is no guarantee that the matrix \mathbf{X} found using Algorithm 4 has rank-1. Indeed, the latter would be guaranteed only if the number

of constraints in the SDP relaxed optimization problem would be less or equal to 3. In our problem, the number of constraints is clearly larger than 3 when ($L \geq 2$), i.e., when the number of operators is larger than one. For such a situation, a good rank-1 approximation can be obtained by using the randomization techniques [LMS⁺10], which is also described in Appendix B.3.5. Thus, using also randomization for obtaining a rank-1 approximate solution to the problem (3.44), the overall algorithm for finding an approximate solution to the sum-rate maximization problem in multi-operator TWR networks with an AF relay equipped with multiple antennas can be summarized as in Algorithm 5.

Algorithm 5 Iterative algorithm for approximately solving the problem (3.44)

- 1: **Initialize:** input: $\mathbf{A}_1, \mathbf{B}_1, \mathbf{A}_m, \mathbf{B}_m, \mathbf{C}$, set $\{\beta_{0,2}^{(0)}, \beta_{0,3}^{(0)}, \dots, \beta_{0,m}^{(0)}\}, f^{\star(0)}, R_{\text{sum},0}$, maximum iteration number $N_{\text{max}}, N_{\text{iter}}$ and the threshold value ϵ .
 - 2: **Main step:**
 - 3: Solve problem (3.49) finding \mathbf{X} with arbitrary rank
 - 4: Calculate the eigen-decomposition of \mathbf{X} as $\mathbf{X} = \mathbf{U}\mathbf{\Sigma}\mathbf{U}^{\text{H}}$;
 - 5: **for** $j = 1$ to N_{iter} **do**
 - 6: Generate $\hat{\mathbf{g}}_j = \mathbf{U}\mathbf{\Sigma}^{1/2}\mathbf{z}_j$ where $\mathbf{z}_j \in \mathbb{C}^{M_{\text{R}}^2} \sim \mathcal{CN}(\mathbf{0}, \mathbf{I}_{M_{\text{R}}^2})$.
 - 7: $\tilde{\mathbf{g}}_j = \frac{\hat{\mathbf{g}}_j \sqrt{P_{\text{R}}}}{\sqrt{\hat{\mathbf{g}}_j^{\text{H}} \mathbf{C} \hat{\mathbf{g}}_j}}$.
 - 8: Insert $\tilde{\mathbf{g}}_j$ into (3.44) to calculate $R_{\text{sum},j}$.
 - 9: **if** $R_{\text{sum},j} > R_{\text{sum},(j-1)}$ **then**
 - 10: $\mathbf{g}_{\text{opt}} = \tilde{\mathbf{g}}_j$.
 - 11: **end if**
 - 12: **end for**
-

Remark 5. Note that due to the randomization step in Algorithm 5 the optimality of the obtained solutions to problem (3.44) is not guaranteed theoretically. However, numerical results show a strong evidence that the achieved performance is optimal.

It is interesting to compare the proposed POTDC approach with the ProBaSeMO algorithm. While the performance comparison is summarized in Section 3.9, we discuss their computational complexity here. The complexity of the ProBaSeMO schemes can be roughly estimated as follows. For L pairs ProBaSeMO requires L SVDs of complex matrices of size $M_{\text{R}} \times 2(L-1)$ and L SVDs of complex matrices of size $M_{\text{R}}^2 \times 2$. Assuming that the SVD of a $M \times N$ real matrix has the complexity of $O(MN^2)$ and taking into account that a $M \times N$ complex matrix can be written equivalently as a $2M \times 2N$ real matrix, then the complexity of ProBaSeMO can be estimated as $O(L(32M_{\text{R}}^2 + 32M_{\text{R}}(L-1)^2))$. The complexity of the proposed POTDC-type algorithm is a product of the number of required iterations to the complexity of solving the SDP problem (3.51), which is higher than the complexity of the SVD.

3.6 Relay transmit power minimization

In this subsection, we determine the optimal \mathbf{g} which minimizes the transmit power at the relay subject to an SINR constraint at each UT. The optimization problem is expressed as

$$\begin{aligned} \min_{\mathbf{g}} \quad & \mathbf{g}^H \mathbf{C} \mathbf{g} \\ \text{s.t.} \quad & \frac{\mathbf{g}^H \mathbf{D}_k^{(\ell)} \mathbf{g}}{\mathbf{g}^H \mathbf{E}_k^{(\ell)} \mathbf{g} + \sigma_k^{(\ell)^2}} \geq \gamma_k^{(\ell)}, \forall k, \ell. \end{aligned} \quad (3.53)$$

Problem (3.53) is mathematically similar to the beamforming problems in [LMS⁺10] and [BPG12] which are in general non-convex. It can be further expanded into the following equivalent problem

$$\begin{aligned} \min_{\mathbf{g}} \quad & \mathbf{g}^H \mathbf{C} \mathbf{g} \\ \text{s.t.} \quad & \mathbf{g}^H \mathbf{C}_k^{(\ell)} \mathbf{g} \geq \gamma_k^{(\ell)} \sigma_k^{(\ell)^2}, \forall k, \ell. \end{aligned} \quad (3.54)$$

where $\mathbf{C}_k^{(\ell)} = \mathbf{D}_k^{(\ell)} - \gamma_k^{(\ell)} \mathbf{E}_k^{(\ell)}$. Each constraint in (3.54) is a superlevel set of a quadratic function [BV04]. Such a set is convex if and only if the quadratic function is concave, i.e., $\mathbf{C}_k^{(\ell)}$ is negative semi-definite, $\forall k, \ell$. It is clear that in this case the feasible set is empty since $\mathbf{g}^H \mathbf{C}_k^{(\ell)} \mathbf{g} \leq 0$, $\forall k, \ell$. Hence, problem (3.54) may not be solvable in polynomial time, but its approximate solution can be obtained by using either the SDP approach [LMS⁺10] or the iterative second-order cone programming (SOCP) approach [BPG12]. In the sequel we will discuss the two approaches.

In general, the SDP approach which uses the semidefinite relaxation technique (SDR) works as follows [LMS⁺10]. We introduce a new variable $\mathbf{X} = \mathbf{g} \mathbf{g}^H$ and rewrite problem (3.54) as

$$\begin{aligned} \min_{\mathbf{X}} \quad & \text{Tr}\{\mathbf{C} \mathbf{X}\} \\ \text{s.t.} \quad & \text{Tr}\{\mathbf{C}_k^{(\ell)} \mathbf{X}\} \geq \gamma_k^{(\ell)} \sigma_k^{(\ell)^2}, \forall k, \ell \\ & \mathbf{X} \geq 0, \text{rank}\{\mathbf{X}\} = 1. \end{aligned} \quad (3.55)$$

Dropping the rank-1 constraint, problem (3.55) can be approximated by the following convex SDP problem which can be solved efficiently by the interior-point method [BV04],

$$\begin{aligned} \min_{\mathbf{X}} \quad & \text{Tr}\{\mathbf{C} \mathbf{X}\} \\ \text{s.t.} \quad & \text{Tr}\{\mathbf{C}_k^{(\ell)} \mathbf{X}\} \geq \gamma_k^{(\ell)} \sigma_k^{(\ell)^2}, \forall k, \ell \end{aligned}$$

$$\mathbf{X} \geq 0. \quad (3.56)$$

Obviously, problem (3.56) is a relaxed version of the original problem (3.53), i.e., the optimal value of (3.56) is a lower bound of problem (3.53). If the optimal solution \mathbf{X}_{opt} of (3.56) is rank-1, it is also optimal for the original problem and the optimal \mathbf{g}_{opt} is the principle component of \mathbf{X}_{opt} . Due to the relaxation, \mathbf{X}_{opt} is generally not rank-1. Although a rank-1 solution of (3.56) always exists if the number of constraints in (3.56) is less or equal to three [HP10], our problem has always more than three constraints, i.e., at least two operators and two UTs per operator. Thus, we apply the randomization method in Appendix B.3.5 to extract the rank-1 approximation from \mathbf{X}_{opt} [LMS⁺10].

Since the SDP solution is in general not optimal for our problem, it is worth applying an alternative approach which is the iterative SOCP method [BPG12]. In the traditional SOCP method, the rank-1 property of the matrix $\mathbf{D}_k^{(\ell)}$ is exploited and the constraints in (3.53) are rewritten as

$$\frac{\sqrt{P_k^{(\ell)}} |\mathbf{g}^H (\mathbf{h}_{3-k}^{(\ell)\text{T}} \otimes \mathbf{h}_k^{(\ell)\text{T}})^H|}{\sqrt{\mathbf{g}^H \mathbf{E}_k^{(\ell)} \mathbf{g} + \sigma_k^{(\ell)^2}}} \geq \sqrt{\gamma_k^{(\ell)}}, \quad \forall k, \ell \quad (3.57)$$

If we introduce

$$\tilde{\mathbf{U}}_k^{(\ell)} = \begin{bmatrix} \sigma_k^{(\ell)^2} & \mathbf{0}^T \\ \mathbf{0} & \mathbf{E}_k^{(\ell)} \end{bmatrix}^{\frac{1}{2}},$$

$$\tilde{\mathbf{g}} = [1, \mathbf{g}^T]^T, \quad \tilde{\mathbf{h}}_k^{(\ell)} = [0, (\mathbf{h}_{3-k}^{(\ell)\text{T}} \otimes \mathbf{h}_k^{(\ell)\text{T}})^*]^T,$$

(3.57) can be rewritten as

$$|\tilde{\mathbf{g}}^H \tilde{\mathbf{h}}_k^{(\ell)}| \geq \sqrt{\gamma_k^{(\ell)} / P_k^{(\ell)}} \|\tilde{\mathbf{U}}_k^{(\ell)\text{H}} \tilde{\mathbf{g}}\|, \quad \forall k, \ell \quad (3.58)$$

With the conservative approximation [BPG12]

$$|\tilde{\mathbf{g}}^H \tilde{\mathbf{h}}_k^{(\ell)}| \geq \text{Re} \left\{ \tilde{\mathbf{g}}^H \tilde{\mathbf{h}}_k^{(\ell)} \right\}, \quad (3.59)$$

the non-convex part of the constraint (3.58) can be strengthened as

$$\text{Re} \left\{ \tilde{\mathbf{g}}^H \tilde{\mathbf{h}}_k^{(\ell)} \right\} \geq \sqrt{\gamma_k^{(\ell)} / P_k^{(\ell)}} \|\tilde{\mathbf{U}}_k^{(\ell)\text{H}} \tilde{\mathbf{g}}\|, \quad \forall k, \ell. \quad (3.60)$$

Constraint (3.60) is harder to fulfill than (3.58). This is also due to the fact that $\text{Re}\{\tilde{\mathbf{g}}^H \tilde{\mathbf{h}}_k^{(\ell)}\}$ can have a negative value. Introducing the auxiliary variable t and the matrix

$$\tilde{\mathbf{V}} = \begin{bmatrix} 0 & \mathbf{0}^T \\ \mathbf{0} & \mathbf{C} \end{bmatrix}^{\frac{1}{2}}, \quad (3.61)$$

problem (3.53) can be approximated by the following convex SOCP problem

$$\begin{aligned} \min_{t, \tilde{\mathbf{g}}} \quad & t \\ \text{s.t.} \quad & \|\tilde{\mathbf{V}}^H \tilde{\mathbf{g}}\| \leq t, \tilde{g}_1 = 1 \\ & \text{Re}\{\tilde{\mathbf{g}}^H \tilde{\mathbf{h}}_k^{(\ell)}\} \geq \sqrt{\gamma_k^{(\ell)} / P_k^{(\ell)}} \|\tilde{\mathbf{U}}_k^{(\ell)H} \tilde{\mathbf{g}}\|, \forall k, \ell, \end{aligned} \quad (3.62)$$

where \tilde{g}_1 is the first element of $\tilde{\mathbf{g}}$.

Since replacing (3.58) by (3.60) yields a restricted convex feasible set which is a subset of the original feasible set of problem (3.53), it guarantees that the optimal solution of (3.62) is always feasible for (3.53). However, the drawback of this approach is that the solution of (3.53) might not be in the feasible set of (3.62) and thus it may turn the original feasible problem into an infeasible one. Thus, the performance and feasibility strongly depend on how accurately the non-convex feasible set of problem (3.53) is approximated. To improve the convex approximation, we apply the iterative SOCP approach which is proposed in [BPG12]. The iterative SOCP approach guarantees that in each iteration the obtained approximate solution of the original problem is improved as compared to that of the previous iteration. It is worth mentioning that numerical results in Section 3.9 show that the SOCP approach converges to the SDP approach, which is a strong evidence that the obtained solution is globally optimal.

3.7 SINR balancing

In this section, we study the SINR balancing problem. That is, we derive optimal \mathbf{g} to maximize the minimum SINR at each UT. Recalling the SINR definition in (3.32), the SINR balancing problem can be formulated as

$$\begin{aligned} \max_{\mathbf{g}} \min_{\forall k, \ell} \quad & \eta_k^{(\ell)} \\ \text{s.t.} \quad & \mathbf{g}^H \mathbf{C} \mathbf{g} \leq P_R \end{aligned} \quad (3.63)$$

or equivalently as

$$\begin{aligned}
 & \max_{\mathbf{g}, t} && t \\
 & \text{s.t.} && \mathbf{g}^H \mathbf{C} \mathbf{g} \leq P_R, \\
 & && \frac{\mathbf{g}^H \mathbf{D}_k^{(\ell)} \mathbf{g}}{\mathbf{g}^H \mathbf{E}_k^{(\ell)} \mathbf{g} + \sigma_k^{(\ell)2}} \geq t, \forall k, \ell.
 \end{aligned} \tag{3.64}$$

Problem (3.63) is non-convex. Following the idea of SDR in the previous section, we introduce $\mathbf{X} = \mathbf{g}\mathbf{g}^H$ and drop the non-convex rank-1 constraint. The problem is then reformulated into

$$\begin{aligned}
 & \max_{\mathbf{X}, t} && t \\
 & \text{s.t.} && \text{Tr}\{\mathbf{C}\mathbf{X}\} \leq P_R, \mathbf{X} \geq 0 \\
 & && \text{Tr}\{(\mathbf{D}_k^{(\ell)} - t\mathbf{E}_k^{(\ell)})\mathbf{X}\} \geq t\sigma_k^{(\ell)2}, \forall k, \ell
 \end{aligned} \tag{3.65}$$

Problem (3.65) is a quasi-convex problem similar as in [GSS⁺10]. Hence, it can be solved using the same procedure as in [GSS⁺10], i.e., using a simple bisection search algorithm in which a feasibility problem is solved at each step. Due to the relaxation, the solution \mathbf{X}_{opt} might not be feasible for the original problem. The randomization techniques in Appendix B.3.5 is applied to obtain the final \mathbf{g} [LMS⁺10].

3.8 Widely linear relay amplification matrix design

Widely linear (WL) signal processing generalizes linear signal processing by linearly processing the real and imaginary parts of the input signals separately [ASS11]. When applied to wireless communication systems which deploy improper or non-circular modulation schemes, such as real modulation formats (e.g., binary phase-shift keying (BPSK), amplitude-shift keying (ASK)) and offset schemes (e.g., OQAM), additional degrees of freedom can be exploited. Thereby, a significant performance gain is obtained over linear signal processing methods [Ste07]. Although WL signal processing techniques have been studied for point-to-point MIMO [Ste07], [DGPV12] and the one-way relaying scenario with multiple AF relays [SH13], they have not been extended to two-way relaying scenarios with MIMO relays.

In this section, we develop WL signal processing techniques for TWR scenarios with single or multiple pairs of UTs and a MIMO AF relay. First, we propose generalized WL system models which are a prerequisite for developing WL signal processing techniques. Since WL processing can be applied at the relay and/or the UTs, a complete design requires jointly optimizing the WL precoder and decoder at the UT and the WL relay amplification matrix at

the relay. This problem is non-convex and might be intractable. Thus, we resort to a simplified model where the WL signal processing is only applied at the relay. Since this model can be transformed into an equivalent linear model, most of the linear transmit strategies can simply be extended. We design WL relay amplification matrices by adopting the optimal transmit strategies (which include the maximization of the minimum SINR subject to a relay power constraint and the minimization of the required transmit power at the relay subject to SINR constraints [ZBR⁺12]) as well as a suboptimal transmit strategy, which is the dual channel matching (DCM) scheme in [VRWH11].

3.8.1 Transformation from widely linear system model to linear system model

Let us first introduce the definition of non-circular data. According to [SS10], we have the following definition.

Definition 3.8.1. [SS10] A complex-valued random vector $\mathbf{x} \in \mathbb{C}^n$ is called *circular* if \mathbf{x} has the same probability distribution as $e^{j\alpha}\mathbf{x}$ for any given real number α ; otherwise it is called *non-circular*.

As we have mentioned before, real modulation schemes, e.g., BPSK and ASK, and complex offset modulation schemes (after some processing [GSL03]), e.g., OQAM, are non-circular modulation schemes.

To perform the WL processing, or in other words, to explore the noncircularity for the scenario in Figure 3.2, we need WL transformations of the transmitted and received complex-valued data [ASS11]. For notational simplicity, we select the complex augmented representation of the complex-valued data as defined in [ASS11]. That is, if a WL precoder $\tilde{\mathbf{w}}_k^{(\ell)} \in \mathbb{C}^2$ is applied, the transmitted data at the UT is written as:

$$\mathbf{x}_k^{(\ell)} = \tilde{\mathbf{w}}_k^{(\ell)\text{H}} \underline{\mathbf{s}}_k^{(\ell)} = \begin{bmatrix} w_{k,1}^{(\ell)*} & w_{k,2}^{(\ell)*} \end{bmatrix} \begin{bmatrix} s_k^{(\ell)} & s_k^{(\ell)*} \end{bmatrix}^{\text{T}} \quad (3.66)$$

where $\underline{\mathbf{s}}_k^{(\ell)}$ is called the complex augmented vector of $s_k^{(\ell)} \in \mathbb{C}$ and $s_k^{(\ell)}$ has zero mean and unit variance. It is further assumed that $s_k^{(\ell)}$ is strongly non-circular [SS10], i.e., $s_k^{(\ell)*} = e^{j\beta} s_k^{(\ell)}$ and $\beta \in \mathbb{R}$. For example, real modulation schemes satisfy $\beta = 0$. Thereby, $s_k^{(\ell)}$ has non-zero pseudo-variance, i.e., $\tilde{C}_k^\ell = \mathbb{E}\{s_k^{(\ell)2}\} = e^{-j\beta} \neq 0$. The selection of β will not affect our analysis in the following. Therefore, without loss of generality we assume $\beta = 0$. Moreover, the transmit power constraint at each UT has to be fulfilled such that $\mathbb{E}\{|x_k^\ell|^2\} = P_k^{(\ell)}$. Then the received

signal at the relay is

$$\mathbf{r} = \sum_{\ell=1}^L \sum_{k=1}^2 \mathbf{h}_k^{(\ell)} x_k^{(\ell)} + \mathbf{n}_R \in \mathbb{C}^{M_R} \quad (3.67)$$

where \mathbf{n}_R denote the ZMCSCG noise and $\mathbb{E}\{\mathbf{n}_R \mathbf{n}_R^H\} = \sigma_R^2 \mathbf{I}_{M_R}$. The AF relay amplifies the received data and forwards it to all the UTs simultaneously. If WL processing is applied at the relay, the signal transmitted by the relay is expressed as

$$\bar{\mathbf{r}} = \tilde{\mathbf{G}} \mathbf{r} = [\mathbf{G}_1 \quad \mathbf{G}_2] [\mathbf{r}^T \quad \mathbf{r}^H]^T \quad (3.68)$$

where $\{\mathbf{G}_1, \mathbf{G}_2\} \in \mathbb{C}^{M_R \times M_R}$ and the transmit power constraint at the relay has to be satisfied such that $\mathbb{E}\{\|\bar{\mathbf{r}}\|^2\} \leq P_R$. Assume that there is reciprocity between the uplink and downlink channels due to TDD transmission and define $\mathbf{h}_k^{(\ell)}$, $\mathbf{x}_k^{(\ell)}$, \mathbf{n}_R , $\mathbf{n}_k^{(\ell)}$, and $\mathbf{y}_k^{(\ell)}$ as the augmented complex vectors of $\mathbf{h}_k^{(\ell)}$, $x_k^{(\ell)}$, \mathbf{n}_R , $n_k^{(\ell)}$, and $y_k^{(\ell)}$, respectively. If the receiver performs WL processing, the received augmented data vector at the k th UT of the ℓ th operator is given by

$$\begin{aligned} \mathbf{y}_k^{(\ell)} = & \underbrace{\tilde{\mathbf{H}}_k^{(\ell)T} \underline{\mathbf{G}} \tilde{\mathbf{H}}_{3-k}^{(\ell)} \mathbf{x}_{3-k}^{(\ell)}}_{\text{desired signal}} + \underbrace{\tilde{\mathbf{H}}_k^{(\ell)T} \underline{\mathbf{G}} \tilde{\mathbf{H}}_k^{(\ell)} \mathbf{x}_k^{(\ell)}}_{\text{self-interference}} \\ & + \underbrace{\sum_{\substack{\bar{k}=1,2 \\ \bar{\ell} \neq \ell}} \tilde{\mathbf{H}}_k^{(\ell)T} \underline{\mathbf{G}} \tilde{\mathbf{H}}_{\bar{k}}^{(\bar{\ell})} \mathbf{x}_{\bar{k}}^{(\bar{\ell})}}_{\text{inter-operator interference}} + \underbrace{\mathbf{H}_k^{(\ell)T} \underline{\mathbf{G}} \mathbf{n}_R + \mathbf{n}_k^{(\ell)}}_{\text{effective noise}} \in \mathbb{C}^2, \end{aligned} \quad (3.69)$$

where $\tilde{\mathbf{H}}_k^{(\ell)} = \text{blkdiag}\{\mathbf{h}_k^{(\ell)}, \mathbf{h}_k^{(\ell)*}\} \in \mathbb{C}^{2M_R \times 2}$, $\underline{\mathbf{G}} = \begin{bmatrix} \mathbf{G}_1 & \mathbf{G}_2 \\ \mathbf{G}_2^* & \mathbf{G}_1^* \end{bmatrix} \in \mathbb{C}^{2M_R \times 2M_R}$, and $\mathbf{n}_k^{(\ell)}$ is the ZMCSCG noise with variance $\sigma_k^{(\ell)^2}$. If channel knowledge is available at the UTs, the self-interference term can be subtracted and we get

$$\hat{\mathbf{y}}_k^{(\ell)} = \mathbf{y}_k^{(\ell)} - \tilde{\mathbf{H}}_k^{(\ell)T} \underline{\mathbf{G}} \tilde{\mathbf{H}}_k^{(\ell)} \mathbf{x}_k^{(\ell)}. \quad (3.70)$$

An estimate of the transmitted symbol is then obtained via

$$\hat{x}_{3-k}^{(\ell)} = \tilde{\mathbf{f}}_k^{(\ell)H} \hat{\mathbf{y}}_k^{(\ell)} = \begin{bmatrix} f_{k,1}^{(\ell)*} & f_{k,2}^{(\ell)*} \end{bmatrix} \begin{bmatrix} \hat{y}_k^{(\ell)} & \hat{y}_k^{(\ell)*} \end{bmatrix}^T \quad (3.71)$$

where $\tilde{\mathbf{f}}_k^{(\ell)} \in \mathbb{C}^2$ is the WL decoder. From (3.69) it appears that to jointly design $\tilde{\mathbf{w}}_k^{(\ell)}$, $\underline{\mathbf{G}}$, and $\tilde{\mathbf{f}}_k^{(\ell)}$ is difficult since $\underline{\mathbf{G}}$ has a specific structure. Actually it has been already discussed in

Section 2.3 that for a practical system it is better to divide the transmission into two phases. In the first phase (training phase), the UTs send out only training symbols so that the relay amplification matrix is designed at the relay as described in Section 3.3.6. Afterwards, each UT estimates its equivalent channel which is $\mathbf{h}_k^{(\ell)\text{T}} \tilde{\mathbf{G}} \mathbf{h}_{3-k}^{(\ell)}$ and then designs its WL precoder and decoder based on the channel knowledge. In the second phase, the data will be transmitted using precoders, decoders and the relay amplification matrix which is designed in the training phase. Nevertheless, in this chapter we focus on the WL relay amplification matrix design in the first phase but leave the WL precoder and decoder design for future work. More specifically, the precoder and the decoder are set to $\tilde{\mathbf{w}}_k^{(\ell)\text{H}} = \begin{bmatrix} \sqrt{P_k^{(\ell)}} & 0 \end{bmatrix}$ and $\tilde{\mathbf{f}}_k^{(\ell)\text{H}} = [1 \ 0]$, $\forall k, \ell$, respectively. Then the system model in (3.69) simplifies to:

$$\begin{aligned} \hat{y}_k^{(\ell)} &= \sqrt{P_{3-k}^{(\ell)}} \mathbf{h}_k^{(\ell)\text{T}} \tilde{\mathbf{G}} \tilde{\mathbf{H}}_{3-k}^{(\ell)} \mathbf{s}_{3-k}^{(\ell)} + \sum_{\substack{\bar{k}=1,2 \\ \bar{\ell} \neq \ell}} \sqrt{P_{\bar{k}}^{(\bar{\ell})}} \mathbf{h}_k^{(\ell)\text{T}} \tilde{\mathbf{G}} \tilde{\mathbf{H}}_{\bar{k}}^{(\bar{\ell})} \mathbf{s}_{\bar{k}}^{(\bar{\ell})} + \mathbf{h}_k^{(\ell)\text{T}} \tilde{\mathbf{G}} \mathbf{n}_R + n_k^{(\ell)} \\ &= \underbrace{\sqrt{P_{3-k}^{(\ell)}} \mathbf{h}_k^{(\ell)\text{T}} \tilde{\mathbf{G}} \mathbf{h}_{3-k}^{(\ell)} \mathbf{s}_{3-k}^{(\ell)}}_{\text{desired signal}} + \underbrace{\sum_{\substack{\bar{k}=1,2 \\ \bar{\ell} \neq \ell}} \sqrt{P_{\bar{k}}^{(\bar{\ell})}} \mathbf{h}_k^{(\ell)\text{T}} \tilde{\mathbf{G}} \mathbf{h}_{\bar{k}}^{(\bar{\ell})} \mathbf{s}_{\bar{k}}^{(\bar{\ell})}}_{\text{inter-operator interference}} + \underbrace{\mathbf{h}_k^{(\ell)\text{T}} \tilde{\mathbf{G}} \mathbf{n}_R + n_k^{(\ell)}}_{\text{effective noise}} \end{aligned} \quad (3.72)$$

It is worth mentioning that equation (3.72) is a linear function with respect to $\tilde{\mathbf{G}}$ and thus arbitrary linear transmit strategies can be extended to this equivalent linear model.

3.8.2 Optimal widely linear design

In this section we address the optimal WL design of $\tilde{\mathbf{G}}$ such that the minimum SINR of the UTs is maximized subject to a total transmit power constraint at the relay or the relay transmit power is minimized subject to SINR constraints at the UTs. For this purpose we need to derive explicit expressions for the actual SINR and the actual power consumption at the relay. The SINR at the k th UT of the ℓ th operator is computed as

$$\text{SINR}_k^{(\ell)} = \frac{P_{3-k}^{(\ell)} |\mathbf{h}_k^{(\ell)\text{T}} \tilde{\mathbf{G}} \mathbf{h}_{3-k}^{(\ell)}|^2}{\sum_{\substack{\bar{k}=1,2 \\ \bar{\ell} \neq \ell}} P_{\bar{k}}^{(\bar{\ell})} |\mathbf{h}_k^{(\ell)\text{T}} \tilde{\mathbf{G}} \mathbf{h}_{\bar{k}}^{(\bar{\ell})}|^2 + \sigma_R^2 \|\mathbf{h}_k^{(\ell)\text{T}} \tilde{\mathbf{G}}\|^2 + \sigma_k^{(\ell)^2}} \quad (3.73)$$

and the actual relay transmit power is calculated by

$$\mathbb{E}\{\|\tilde{\mathbf{r}}\|^2\} = \sum_{\ell=1}^L \sum_{k=1}^2 P_k^{(\ell)} \|\tilde{\mathbf{G}} \mathbf{h}_k^{(\ell)}\|^2 + \sigma_R^2 \|\tilde{\mathbf{G}}\|_F^2. \quad (3.74)$$

Let us define $\tilde{\mathbf{g}} = \text{vec}\{\tilde{\mathbf{G}}\}$. Using the properties that $\text{Tr}\{\mathbf{\Gamma}_1\mathbf{\Gamma}_2\} = \text{Tr}\{\mathbf{\Gamma}_2\mathbf{\Gamma}_1\}$ and $\text{vec}\{\mathbf{\Gamma}_1\mathbf{X}\mathbf{\Gamma}_2\} = (\mathbf{\Gamma}_2^T \otimes \mathbf{\Gamma}_1)\text{vec}\{\mathbf{X}\}$, it is possible to further expand (3.73) and (3.74) by following a similar procedure as in [ZBR⁺12] and the same steps in Appendix C.3. Finally we get

$$\text{SINR}_k^{(\ell)} = \frac{\tilde{\mathbf{g}}^H \mathbf{D}_k^{(\ell)} \tilde{\mathbf{g}}}{\tilde{\mathbf{g}}^H (\mathbf{E}_k^{(\ell)} + \mathbf{F}_k^{(\ell)}) \tilde{\mathbf{g}} + \sigma_k^{(\ell)2}} \quad (3.75)$$

and

$$\mathbb{E}\{\|\tilde{\mathbf{r}}\|^2\} = \tilde{\mathbf{g}}^H \mathbf{A} \tilde{\mathbf{g}}, \quad (3.76)$$

where $\mathbf{D}_k^{(\ell)}$, $\mathbf{E}_k^{(\ell)}$, and $\mathbf{F}_k^{(\ell)}$ are defined as

$$\begin{aligned} \mathbf{D}_k^{(\ell)} &= P_{3-k}^{(\ell)} (\underline{\mathbf{h}}_{3-k}^{(\ell)*} \underline{\mathbf{h}}_{3-k}^{(\ell)T}) \otimes (\mathbf{h}_k^{(\ell)*} \mathbf{h}_k^{(\ell)T}) \\ \mathbf{E}_k^{(\ell)} &= \sum_{\substack{\bar{k}=1,2 \\ \bar{\ell}=1,\dots,L,\bar{\ell}\neq\ell}} P_{\bar{k}}^{(\bar{\ell})} (\underline{\mathbf{h}}_{\bar{k}}^{(\bar{\ell})*} \underline{\mathbf{h}}_{\bar{k}}^{(\bar{\ell})T}) \otimes (\mathbf{h}_k^{(\ell)*} \mathbf{h}_k^{(\ell)T}) \\ \mathbf{F}_k^{(\ell)} &= \sigma_R^2 (\mathbf{I}_{2M_R} \otimes (\mathbf{h}_k^{(\ell)} \mathbf{h}_k^{(\ell)H})^T) \\ \mathbf{A} &= \sum_{k,\ell} P_k^{(\ell)} (\underline{\mathbf{h}}_k^{(\ell)*} \underline{\mathbf{h}}_k^{(\ell)T}) \otimes \mathbf{I}_{M_R} + \sigma_R^2 \mathbf{I}_{2M_R^2}. \end{aligned} \quad (3.77)$$

Now it is possible to calculate the optimal WL relay amplification matrix $\tilde{\mathbf{G}}$ using the derived expressions (3.75) and (3.76). Our SINR balancing problem is formulated as

$$\begin{aligned} \max_{\tilde{\mathbf{g}}} \min_{\forall k,\ell} \quad & \text{SINR}_k^{(\ell)} \\ \text{s.t.} \quad & \tilde{\mathbf{g}}^H \mathbf{A} \tilde{\mathbf{g}} \leq P_R \end{aligned} \quad (3.78)$$

or equivalently

$$\begin{aligned} \max_{\tilde{\mathbf{g}}, t} \quad & t \\ \text{s.t.} \quad & \text{SINR}_k^{(\ell)} \geq t, \forall k, \ell \\ & \tilde{\mathbf{g}}^H \mathbf{A} \tilde{\mathbf{g}} \leq P_R \end{aligned} \quad (3.79)$$

Problem (3.78) is the same non-convex problem as in Section 3.7. Therefore, it can be solved efficiently using the two-step method proposed in Section 3.7. The first step is to solve the relaxed problem based on SDR together with a bisection search. Afterwards, a randomization procedure is used to get a rank-1 approximation.

The power minimization problem is formulated as

$$\begin{aligned} \min_{\tilde{\mathbf{g}}} \quad & \tilde{\mathbf{g}}^H \mathbf{A} \tilde{\mathbf{g}} \\ \text{s.t.} \quad & \frac{\tilde{\mathbf{g}}^H \mathbf{D}_k^{(\ell)} \tilde{\mathbf{g}}}{\tilde{\mathbf{g}}^H (\mathbf{E}_k^{(\ell)} + \mathbf{F}_k^{(\ell)}) \tilde{\mathbf{g}} + \sigma_k^{(\ell)^2}} \geq \gamma_k^{(\ell)}, \forall k, \ell. \end{aligned} \quad (3.80)$$

Problem (3.80) has exactly the same structure as the problem in Section 3.6. Thus, it can be solved using SDR together with the randomization procedure or the iterative SOCP approach. Here the SDR approach is used.

3.8.3 Suboptimal widely linear design and large system analysis for a single operator TWR system

The main idea of WL signal processing is to exploit the noncircularity of the transmitted symbols. However, as also pointed out in [ASS11] and [Ste07], the magnitude of the gain from a WL design depends on certain conditions. Although in general such conditions are still open for TWR scenarios, in the following we show that a simple extension of the suboptimal relay amplification matrix design may provide only limited gain over linear signal processing. This is true for our proposed WL extension of the DCM method [VRWH11] which is a simple and efficient algorithm used in single operator TWR with a MIMO AF relay. Here we only consider the single operator case, i.e., $L = 1$. In the remaining part of this section, the index (ℓ) will be dropped for simplicity. The WL model in (3.72) is then reduced to

$$\hat{y}_k = \underbrace{\sqrt{P_{3-k}} \mathbf{h}_k^T \tilde{\mathbf{G}} \mathbf{h}_{3-k} s_{3-k}}_{\text{desired signal}} + \underbrace{\mathbf{h}_k^{(\ell)T} \tilde{\mathbf{G}} \mathbf{n}_R + n_k}_{\text{effective noise}} \quad (3.81)$$

Let us first recall the linear DCM design by setting $\tilde{\mathbf{G}} = [\mathbf{G} \ \mathbf{0}]$. Then we get the linear model of our system as

$$\hat{y}_k = \underbrace{\sqrt{P_{3-k}} \mathbf{h}_k^T \mathbf{G} \mathbf{h}_{3-k} s_{3-k}}_{\text{desired signal}} + \underbrace{\mathbf{h}_k^{(\ell)T} \mathbf{G} \mathbf{n}_R + n_k}_{\text{effective noise}} \quad (3.82)$$

According to [VRWH11], the linear DCM design which is inspired by the maximum ratio combining is given by

$$\mathbf{G}_{\text{L,DCM}} = \mathbf{h}_1^* \mathbf{h}_2^H + \mathbf{h}_2^* \mathbf{h}_1^H \in \mathbb{C}^{M_R \times M_R} \quad (3.83)$$

We extend this strategy to our equivalent linear system model in (3.81) and propose our WL DCM design as

$$\tilde{\mathbf{G}}_{\text{WL,DCM}} = \mathbf{h}_1^* \mathbf{h}_2^{\text{H}} + \mathbf{h}_2^* \mathbf{h}_1^{\text{H}} = [\mathbf{h}_1^* \mathbf{h}_2^{\text{H}} + \mathbf{h}_2^* \mathbf{h}_1^{\text{H}}, \quad \mathbf{h}_1^* \mathbf{h}_2^{\text{T}} + \mathbf{h}_2^* \mathbf{h}_1^{\text{T}}] \in \mathbb{C}^{M_{\text{R}} \times 2M_{\text{R}}}. \quad (3.84)$$

Our proposed WL DCM design in (3.84) shares the same characteristics as the linear DCM design in the sense that the received signal powers at both UTs are the same.

Now we analyze the WL gain in terms of SNR using the proposed design. Taking UT 1 ($k = 1$) as an example, the SNR of UT 1 in the linear model (3.82) can be computed by

$$\text{SNR}_{\text{L},1} = \frac{\mathbb{E}\{|\sqrt{P_2} \mathbf{h}_1^{\text{T}} \mathbf{G}_{\text{L,DCM}} \mathbf{h}_2 s_2|^2\}}{\mathbb{E}\{|\mathbf{h}_1^{\text{T}} \mathbf{G}_{\text{L,DCM}} \mathbf{n}_{\text{R}}|^2\} + \sigma_1^2 \cdot \gamma_{\text{L}}^{-2}} \quad (3.85)$$

where $\gamma_{\text{L}} \in \mathbb{R}^+$ is an amplification factor which guarantees that the transmit power constraint at the relay is fulfilled, i.e.,

$$\mathbb{E}\{\|\gamma_{\text{L}} \cdot \mathbf{G}_{\text{L,DCM}} \cdot \mathbf{r}\|^2\} = P_{\text{R}}. \quad (3.86)$$

Then by using the linear DCM design the desired signal power at the UT 1 is derived as

$$\begin{aligned} \mathbb{E}\{|\sqrt{P_2} \mathbf{h}_1^{\text{T}} \mathbf{G}_{\text{L,DCM}} \mathbf{h}_2 s_2|^2\} &= P_2 |\mathbf{h}_1^{\text{T}} \mathbf{G}_{\text{L,DCM}} \mathbf{h}_2|^2 = P_2 |\mathbf{h}_1^{\text{T}} \mathbf{h}_1^* \mathbf{h}_2^{\text{H}} \mathbf{h}_2 + \mathbf{h}_1^{\text{T}} \mathbf{h}_2^* \mathbf{h}_1^{\text{H}} \mathbf{h}_2|^2 \\ &= P_2 (\|\mathbf{h}_1\|^2 \|\mathbf{h}_2\|^2 + |\mathbf{h}_1^{\text{H}} \mathbf{h}_2|^2). \end{aligned} \quad (3.87)$$

Using the fact that $\mathbf{h}_1^{\text{T}} \mathbf{h}_2^* = \mathbf{h}_2^{\text{H}} \mathbf{h}_1$ and $|\mathbf{h}_1^{\text{H}} \mathbf{h}_2| = |\mathbf{h}_2^{\text{H}} \mathbf{h}_1|$, the noise power which includes both the propagated noise power from the relay and the noise power at UT 1 is calculated by

$$\begin{aligned} &\mathbb{E}\{|\mathbf{h}_1^{\text{T}} \mathbf{G}_{\text{L,DCM}} \mathbf{n}_{\text{R}}|^2\} + \sigma_1^2 \cdot \gamma_{\text{L}}^{-2} \\ &= \sigma_{\text{R}}^2 \mathbf{h}_1^{\text{T}} \mathbf{G}_{\text{L,DCM}} \mathbf{G}_{\text{L,DCM}}^{\text{H}} \mathbf{h}_1 + \frac{\sigma_1^2}{P_{\text{R}}} (P_1 \mathbf{h}_1^{\text{H}} \mathbf{G}_{\text{L,DCM}}^{\text{H}} \mathbf{G}_{\text{L,DCM}} \mathbf{h}_1 + P_2 \mathbf{h}_2^{\text{H}} \mathbf{G}_{\text{L,DCM}}^{\text{H}} \mathbf{G}_{\text{L,DCM}} \mathbf{h}_2 \\ &\quad + \mathbb{E}\{\mathbf{n}_{\text{R}}^{\text{H}} \mathbf{G}_{\text{L,DCM}}^{\text{H}} \mathbf{G}_{\text{L,DCM}} \mathbf{n}_{\text{R}}\}) \\ &= \sigma_{\text{R}}^2 (\|\mathbf{h}_1\|^4 \|\mathbf{h}_2\|^2 + 3 \|\mathbf{h}_1\|^2 |\mathbf{h}_1^{\text{H}} \mathbf{h}_2|^2) + \sigma_1^2 \left(\frac{P_1}{P_{\text{R}}} \|\mathbf{h}_1\|^2 + \frac{P_2}{P_{\text{R}}} \|\mathbf{h}_2\|^2 \right) (\|\mathbf{h}_1\|^2 \|\mathbf{h}_2\|^2 + 3 |\mathbf{h}_1^{\text{H}} \mathbf{h}_2|^2) \\ &\quad + 2 \sigma_1^2 \sigma_{\text{R}}^2 \frac{1}{P_{\text{R}}} (\|\mathbf{h}_1\|^2 \|\mathbf{h}_2\|^2 + |\mathbf{h}_1^{\text{H}} \mathbf{h}_2|^2) \end{aligned} \quad (3.88)$$

Similarly, the SNR of UT 1 using the WL DCM design is calculated as

$$\text{SNR}_{\text{WL},1} = \frac{\mathbb{E}\{|\sqrt{P_2} \mathbf{h}_1^{\text{T}} \tilde{\mathbf{G}}_{\text{WL,DCM}} \mathbf{h}_2 s_2|^2\}}{\mathbb{E}\{|\mathbf{h}_1^{\text{T}} \tilde{\mathbf{G}}_{\text{WL,DCM}} \mathbf{n}_{\text{R}}|^2\} + \sigma_1^2 \cdot \gamma_{\text{L}}^{-2}} \quad (3.89)$$

where $\gamma_{\text{WL}} \in \mathbb{R}^+$ is determined by

$$\mathbb{E}\{\gamma_{\text{WL}} \cdot \tilde{\mathbf{G}}_{\text{WL,DCM}} \cdot \underline{\mathbf{r}}\} = P_{\text{R}}. \quad (3.90)$$

Then the desired signal power and the noise power are computed by

$$\mathbb{E}\{|\sqrt{P_2} \mathbf{h}_1^{\text{T}} \tilde{\mathbf{G}}_{\text{WL,DCM}} \mathbf{h}_2 s_2|^2\} = P_2 |2\|\mathbf{h}_1\|^2 \|\mathbf{h}_2\|^2 + |\mathbf{h}_1^{\text{H}} \mathbf{h}_2|^2 + (\mathbf{h}_2^{\text{H}} \mathbf{h}_1)^2|^2. \quad (3.91)$$

and

$$\begin{aligned} & \mathbb{E}\{|\mathbf{h}_1^{\text{T}} \tilde{\mathbf{G}}_{\text{WL,DCM}} \underline{\mathbf{n}}_{\text{R}}|^2\} + \sigma_1^2 \cdot \gamma_{\text{WL}}^{-2} \\ &= \sigma_{\text{R}}^2 \mathbf{h}_1^{\text{T}} \tilde{\mathbf{G}}_{\text{WL,DCM}} \tilde{\mathbf{G}}_{\text{WL,DCM}}^{\text{H}} \mathbf{h}_1^* + \frac{\sigma_1^2}{P_{\text{R}}} \left(P_1 \mathbf{h}_1^{\text{H}} \tilde{\mathbf{G}}_{\text{WL,DCM}}^{\text{H}} \cdot \tilde{\mathbf{G}}_{\text{WL,DCM}} \mathbf{h}_1 + P_2 \mathbf{h}_2^{\text{H}} \tilde{\mathbf{G}}_{\text{WL,DCM}}^{\text{H}} \tilde{\mathbf{G}}_{\text{WL,DCM}} \mathbf{h}_2 \right. \\ & \quad \left. + \mathbb{E}\{\underline{\mathbf{n}}_{\text{R}}^{\text{H}} \tilde{\mathbf{G}}_{\text{WL,DCM}}^{\text{H}} \tilde{\mathbf{G}}_{\text{WL,DCM}} \underline{\mathbf{n}}_{\text{R}}\} \right) \\ &= 2\sigma_{\text{R}}^2 \left(\|\mathbf{h}_1\|^4 \|\mathbf{h}_2\|^2 + 2\|\mathbf{h}_1\|^2 |\mathbf{h}_1^{\text{H}} \mathbf{h}_2|^2 + \frac{1}{2} \|\mathbf{h}_1\|^2 ((\mathbf{h}_1^{\text{H}} \mathbf{h}_2)^2 + (\mathbf{h}_2^{\text{H}} \mathbf{h}_1)^2) \right) \\ & \quad + 4\sigma_1^2 \left(\frac{P_1}{P_{\text{R}}} \|\mathbf{h}_1\|^2 + \frac{P_2}{P_{\text{R}}} \|\mathbf{h}_2\|^2 \right) \cdot \left(\|\mathbf{h}_1\|^2 \|\mathbf{h}_2\|^2 + 1.5 |\mathbf{h}_1^{\text{H}} \mathbf{h}_2|^2 + \frac{3}{4} ((\mathbf{h}_1^{\text{H}} \mathbf{h}_2)^2 + (\mathbf{h}_2^{\text{H}} \mathbf{h}_1)^2) \right) \\ & \quad + 4\sigma_1^2 \sigma_{\text{R}}^2 \frac{1}{P_{\text{R}}} \left(\|\mathbf{h}_1\|^2 \|\mathbf{h}_2\|^2 + \frac{1}{2} |\mathbf{h}_1^{\text{H}} \mathbf{h}_2|^2 + \frac{1}{4} \|\mathbf{h}_1\|^2 ((\mathbf{h}_1^{\text{H}} \mathbf{h}_2)^2 + (\mathbf{h}_2^{\text{H}} \mathbf{h}_1)^2) \right), \end{aligned} \quad (3.92)$$

correspondingly. Based on the equations (3.87), (3.88), (3.91), and (3.92) it is clear that in general we do not get a two-fold WL gain. But it is difficult to determine the exact magnitude of the WL gain since the derived expressions are complicated. Hence, to gain more insights into the achievable WL gain we perform a large system analysis, i.e., $M_{\text{R}} \rightarrow +\infty$. Let the elements of the channels \mathbf{h}_k be i.i.d Gaussian distributed with zero mean and variance one, i.e., ZMCSG. According to the law of large numbers in [Ser80] we have

$$\frac{1}{M_{\text{R}}} \mathbf{h}_i^{\text{H}} \mathbf{h}_j \xrightarrow{a.s.} \begin{cases} 1 & i = j \\ 0 & i \neq j \end{cases} \quad (3.93)$$

where $\{i, j\} \in \{1, 2\}$. Thereby, for equation (3.87) we have

$$\frac{1}{M_{\text{R}}^4} \mathbb{E}\{|\sqrt{P_2} \mathbf{h}_1^{\text{T}} \mathbf{G}_{\text{L,DCM}} \mathbf{h}_2 s_2|^2\} \xrightarrow{a.s.} P_2. \quad (3.94)$$

For equation (3.88) we can get

$$\frac{1}{M_R^3} (\mathbb{E}\{|\mathbf{h}_1^T \mathbf{G}_{L,DCM} \mathbf{n}_R|^2\} + \sigma_1^2 \cdot \gamma_{L}^{-2}) \xrightarrow{a.s.} \sigma_R^2 + \sigma_1^2 \frac{P_1 + P_2}{P_R}. \quad (3.95)$$

Similarly, for the derived signal power expression (3.91) and the derived noise power expression (3.92) we have

$$\frac{1}{M_R^4} \mathbb{E}\{|\sqrt{P_2} \mathbf{h}_1^T \tilde{\mathbf{G}}_{WL,DCM} \mathbf{h}_2 s_2|^2\} \xrightarrow{a.s.} 4P_2 \quad (3.96)$$

and

$$\frac{1}{M_R^3} (\mathbb{E}\{|\mathbf{h}_1^T \tilde{\mathbf{G}}_{WL,DCM} \mathbf{n}_R|^2\} + \sigma_1^2 \cdot \gamma_{WL}^{-2}) \xrightarrow{a.s.} 2\sigma_R^2 + 4\sigma_1^2 \frac{P_1 + P_2}{P_R}, \quad (3.97)$$

correspondingly. Therefore, when $M_R \rightarrow +\infty$, the WL gain in terms of the SNR for UT 1 is computed as

$$\eta = \frac{\text{SNR}_{WL,1}}{\text{SNR}_{L,1}} \xrightarrow{a.s.} \frac{2\sigma_R^2 + 2\sigma_1^2 \frac{P_1 + P_2}{P_R}}{\sigma_R^2 + 2\sigma_1^2 \frac{P_1 + P_2}{P_R}}. \quad (3.98)$$

If we consider the special case where $P_1 = P_2 = P_R = P$ and $\sigma_1^2 = \sigma_2^2 = \sigma_R^2 = \sigma_n^2$, then we get $\eta = 1.2$ immediately, which implies the achievable WL gain is only 20 %. However, if we have $P_1 = P_2 = \frac{P_R}{100}$ and $\sigma_1^2 = \sigma_2^2 = \sigma_R^2 = \sigma_n^2$, then $\eta = 1.96$. If P_R increases and $P_1 = P_2 \ll P_R$, then $\eta = 2$ and a two-fold WL gain can be obtained.

3.9 Simulation results

In this section, the performance of the proposed algorithms are evaluated via Monte Carlo simulations. In the first set of simulations (Figures 3.7-3.19), a single antenna is used at each UT and the proposed optimal and suboptimal algorithms are evaluated and compared to the time-shared case as well as the algorithms in [JS10] and [YZGK10]. In the second set of simulations (Figures 3.20, 3.21, 3.22), a similar evaluation is performed for multiple antennas at the UT. Here, “uXX” stands for the transmit strategy at each UT and “rXX” stands for the transmit strategy at the relay. In Figure 3.23, the effects of CSI imperfections are evaluated and discussed. Based on the simulation results of the four ProBaSeMO approaches, i.e., {BD, RBD} & {ANOMAX, RR-ANOMAX}, the BD and the RBD strategy only differ in the low SNR regime and in general “BD ANOMAX” \leq “RBD ANOMAX” < “BD RR-ANOMAX” \leq “RBD

RR-ANOMAX”.⁶ For brevity, we mainly demonstrate the performance of ”BD ANOMAX” (or ”ProBaSeMO (BA)”) and ”RBD RR-ANOMAX” (or ”ProBaSeMO (RR)”) in the sequel. Moreover, the time-shared case performance is labeled by “excl” which stands for exclusively. It means that the relay as well as the spectrum are used by different operators in a TDMA fashion. In particular, in the first two time slots, only the UTs of the first operator are served. In the next two time slots, the UTs of the second operator are served and so on.

The simulated MIMO flat fading channels $\mathbf{H}_k^{(\ell)}$ are uncorrelated Rayleigh channels except for Figure 3.22. When the channel is correlated, the spatial correlation is modeled using the Kronecker model such that the channel matrix $\mathbf{H}_k^{(\ell)}$ is obtained from

$$\mathbf{H}_k^{(\ell)} = \mathbf{R}_R^{1/2} \mathbf{H}_{w_k}^{(\ell)} \mathbf{R}_k^{(\ell)1/2}, \quad (3.99)$$

where $\mathbf{H}_{w_k}^{(\ell)} \in \mathbb{C}^{M_R \times M_U}$ represents a spatially white unit variance flat fading MIMO channel, whereas \mathbf{R}_R and $\mathbf{R}_k^{(\ell)}$ are the spatial correlation matrices with $\text{Tr}\{\mathbf{R}_R\} = M_R$ and $\text{Tr}\{\mathbf{R}_k^{(\ell)}\} = M_U$. The spatial correlation matrix \mathbf{R}_R at the relay contains ones on the main diagonal and elements with magnitude ρ_R and random phases on all the other positions.

The channel $\mathbf{H}_k^{(\ell)}$ is fixed during the training phase and the data transmission phase. The transmit power at each UT and at the relay are identical and $P_k^{(\ell)} = P_R = 1 \text{ W}$, $\forall k, \ell$. The SNR at each UT and at the relay are also identical. It is defined as

$$\text{SNR} = 1/\sigma_R^2 = 1/\sigma_k^{(\ell)2}, \quad \forall k, \ell. \quad (3.100)$$

The ANOMAX weighting factor β is set to 0.5 in all simulations (see Section 3.3.3). All the simulation results are obtained by averaging over 1000 channel realizations.

3.9.1 Single antenna at each UT

Figure 3.7 shows the system sum rate comparison when $M_U = 1$ and $L = 2$. The “Optimum” and “excl Optimum” methods are based on the power method described in Section 3.4.1. The performance of the ProBaSeMO algorithm outperforms the time-shared approach for large values of M_R as well as moderate to high SNR values. At an SNR of 35 dB, the sharing gain is nearly two-fold due to an increased multiplexing gain. The result also implies that the ProBaSeMO algorithm coincides with the optimum when M_R increases.

Figure 3.8 shows the relay transmit power vs. a common SINR constraint with $\text{SNR} = 15 \text{ dB}$, i.e., the transmit power of the UTs is 15 dB above the noise power level. “SDP” is

⁶”RBD ANOMAX”>”BD RR-ANOMAX” in the low SNR regime. When M_R increases the differences become small.

the convex approximation using SDP and the randomization technique [LMS⁺10] while “lower bound” is obtained from (3.56). “iSOCP” is the iterative SOCP technique. It can be observed that the difference of the ProBaSeMO solution to the lower bound reduces for increasing M_R . Moreover, the two convex approximation techniques SDP and iterative SOCP merge with the lower bound. This implies that both approximation techniques are accurate enough for our problem.

Figure 3.9 depicts the results corresponding to the SINR balancing approach where this time, the maximized minimum SINR vs. SNR is shown. “BiSDR” stands for SDP with rank-one extraction plus bisection search. Again the method based on convex approximation yields the best results. However, the ProBaSeMO method, which yields competitive results, requires a significantly lower computational complexity.

Additionally, the optimal linear design and the optimal widely linear design are compared in Fig. 3.10 and Fig. 3.11. “Optimal WL” stands for the optimal WL design solution while “Optimal L” stands for the optimal linear solution. Fig. 3.10 demonstrates the achievable average minimum SINR by using the optimal WL design and the linear design under different system settings. It can be concluded that in general the WL processing is more effective than the linear processing techniques. Nevertheless, when $L = 1$ the WL gain is approximately 1 dB and the gain reduces slightly when the number of antennas at the relay increases. This result fits to our analysis of the suboptimal algorithm. As L increases, the WL gain also increases. But the gain again reduces as the array size of the relay enlarges. This implies that the linear design benefits more from increased spatial dimension and the WL design is superior compared to the linear design only if there are not sufficient degrees of freedom in the spatial domain. Fig. 3.11 shows the average minimum transmit power at the relay given identical SINR constraints at all UTs. The same conclusion can be drawn. That is, the WL gain is limited when there is only a single pair of UTs. The WL gain increases as the number of pairs increases. However, it decreases as the array size at the relay increases.

Figure 3.12 demonstrates the sum rate comparison of the ProBaSeMO schemes and the proposed POTDC approach in a symmetric scenario. That is, each user has equal distance to the relay. The proposed POTDC only slightly outperforms the ProBaSeMO schemes. When the noise variance is small and the number of antennas at the relay is large, the performance difference almost vanishes.

In Figure 3.13, the ProBaSeMO algorithms are compared to other techniques from the literature. The “ZF” and “MMSE” methods are the single antenna version of algorithms proposed in [JS10]. “YZGK10” stands for the algorithm proposed in [YZGK10]. As the result suggests, the ProBaSeMO algorithms give the best performance especially from moderate to high SNRs.

When M_R increases, there will be sufficient degrees of freedom in the spatial dimension. Thus, non-pairing aware algorithms (ZF and MMSE) almost approach the performance of pairing aware algorithms with less than 1 dB difference. The ProBaSeMO methods can provide a gain of approximately 10 dB over the YZGK10 method at the high SNRs when $M_R = 8$. This implies that ANOMAX offers this performance enhancement because one major difference between the YZGK10 method and the ProBaSeMO (BA) method is that an identity matrix instead of the ANOMAX strategy in Section 3.3.3 is used as the relay amplification matrix for each sub-system. However, all the curves have the same slope in the high SNR regime which means that they yield the same multiplexing gain.

Figure 3.14 shows the sum rate as a function of the number of antennas at the relay when the SNR is 25 dB. The sharing gain of pairing aware schemes (ProBaSeMO, YZGK10) as well as non-pairing aware schemes (ZF and MMSE) increases as the array size at the relay increases. ProBaSeMO outperforms ZF and MMSE especially when only a few antennas are deployed at the relay, e.g., $M_R = 3$. This is due to the fact that the ZF and the MMSE algorithms require more antennas at the relay to null the interference. It can be also seen that the time-shared approach has a better or equal performance compared to the non-pairing aware algorithms when the relay has only a few antennas (e.g., 3 antennas). Again, the performance of the YZGK10 approach implies that the ANOMAX algorithm determines the gain obtained in the ProBaSeMO schemes.

Figure 3.15 demonstrates the system loading capability for both high SNR (25 dB) and low SNR (5 dB) when the relay has 20 antennas. It shows that increasing the number of operators which share the spectrum and the relay will increase the sharing gain. However, due to the dimensionality constraint of the SDMA based approaches, there is a turning point after which increasing number of operators will decrease the system sum rate.

Figure 3.16 demonstrates the effects of path loss on the sum rate performance for $M_R = 8$. The path loss model $P_L = 20 \log_{10}(d_k^{(\ell)})$ is applied where $d_k^{(\ell)}$ is the normalized distance between the relay and the UT. We further assume a symmetric system model, i.e., $d_1^{(\ell)} = d_1$ and $d_2^{(\ell)} = d_2 \forall \ell$. The near-far (N/F) ratio is defined as d_2/d_1 . It can be seen that the suboptimal algorithms suffer more loss when the ratio is smaller than 0.5. When an asymmetric path loss model is applied, i.e., $N/F_{ratio} = d_2^{(1)}/d_1^{(1)} = d_1^{(2)}/d_2^{(2)}$, the superiority of the optimal approach is further revealed. As shown in Figures 3.17 and 3.18, compared to the POTDC approach, the ProBaSeMO scheme and the MMSE method in [JS10] suffer more from the asymmetry of the system especially when the near-far ratio is far away from 1. When the number of antennas at the relay increases, the performance difference between the ProBaSeMO approach and the POTDC approach is even enlarged.

Figure 3.19 illustrates the uncoded system BER performance of different algorithms. Uncoded system BER is defined as the average over all UTs' uncoded BERs. Among all algorithms, RBD RR-ANOMAX provides the best performance. Not surprisingly, the RBD ANOMAX solution has a slightly worse performance than BD ANOMAX. There are two reasons. First, the low rank nature of ANOMAX will cause more bit errors in some data streams and the worst data stream dominates the BER performance. Second, compared to the BD solution, the singular value profile of the RBD solution is more imbalanced [SH08]. This will result in a worse decoding situation. Thus, substituting ANOMAX with RR-ANOMAX provides a better BER performance. Another method for improving the RBD ANOMAX performance is to use the power loading method in [SH08]. However, it requires a significantly higher computational complexity.

3.9.2 Two antennas at each UT

Figure 3.20 shows the comparison of different transmission strategies when each UT has 2 antennas. Three precoding approaches, namely, “uWF (water-filling algorithm in Section 3.3.4)”, “uDET” (dominant eigenmode transmission in Section 3.3.4) and “uJou2010” (dominant eigen beamforming in [JS10] which uses a different effective channel than “uDET”), are compared in this simulation. “rStDe” is the steepest descent method in Section 3.4.2. Compared to the time-shared approach, the ProBaSeMO approaches obtain an almost two-fold sharing gain in terms of the sum rate at an SNR of 35 dB due to the increased slope of the curves (increased spatial multiplexing gain). Moreover, the ProBaSeMO approaches have achieved the same multiplexing gain as the steepest descent method but with much less computational complexity.

In Figure 3.21, the sum rate performance is shown as a function of the number of antennas at the relay at high SNR (25 dB). As M_R increases, the slope of ProBaSeMO is higher compared to the time-shared approaches. This means that larger sharing gains are obtained when the relay has more antennas. However, when the relay has only 5 antennas, the time-shared approach slightly outperforms ProBaSeMO because the SDMA approach sacrifices the available degrees of freedom. Nevertheless, the ProBaSeMO scheme achieves the same multiplexing gain as the steepest descent method.

Figure 3.22 demonstrates the sum rate comparison of different transmission strategies when spatial correlation exists at the relay, i.e., $\rho_R = 0.9$. The ProBaSeMO algorithms with single stream transmission are robust against this kind of correlation while multiple stream transmission suffers from spatial correlation. However, the ZF and MMSE methods have a significant degradation of the performance even in the case of single stream transmission.

3.9.3 CSI imperfections

In Figure 3.23, we show the effects of the CSI imperfection on the system spectral efficiency when each UT has 2 antennas and the relay has 8 antennas. Each UT transmits 8 pilot symbols. The spectral efficiency is defined as (Number of correctly received packets \times Number of bits per packet/Total transmission time). “LS r+u” denotes that the LS channel estimation method in Section 3.3.6 is applied at all nodes while “pCSI” stands for perfect CSI. As can be seen, the ProBaSeMO approaches are not sensitive (in this simulation less than 1 dB) to channel estimation errors. Note that we have not compared to the techniques in [JS10] since each UT needs to acquire $\mathbf{H}_k^{(\ell)}$ and the CSI acquisition method is not specified in [JS10].

3.10 Discussion of the sharing gain

In this section we discuss some important findings with respect to the sharing gain, i.e.,

- What is the order of magnitude of the gain?
- What are the parameter settings such that a significant gain is achieved?

To demonstrate our findings, we use numerical simulations and the simulation parameters are the same as in Section 3.9. Moreover, we consider the single antenna UT case and select the ProBaSeMO approach as the transmit strategy for accomplishing the resource sharing among multiple operators. If we define the fractional sharing gain as

$$\text{Fractional sharing gain} = \frac{\text{Throughput of non-orthogonal sharing}}{\text{Throughput of TDMA with half the number of antennas at the relay}},$$

then the fractional sharing gain as a function of the SNR and a function of number of antennas at the relay for the two operator ($L = 2$) sharing case are demonstrated in Figure 3.4 and Figure 3.5. TDMA with half the number of antennas at the relay implies that the two operators will not only share the spectrum but will also share a relay with twice the number of antennas. As shown in Figure 3.4, the sharing gain tends to be two-fold as long as the SNR increases. Figure 3.5 shows that the sharing gain converges to two-fold as the number of antennas at the relay increases regardless of the SNR, i.e., the sharing gain saturates when there are only two operators share the spectrum and the relay.

If we increase the number of the operators L and allow the array size of the relay increases linearly as the number of operators, i.e., $M_R = 4L$, then Figure 3.6 shows that the sharing gain increases linearly as the number of operators increases. In such a case, the fractional sharing

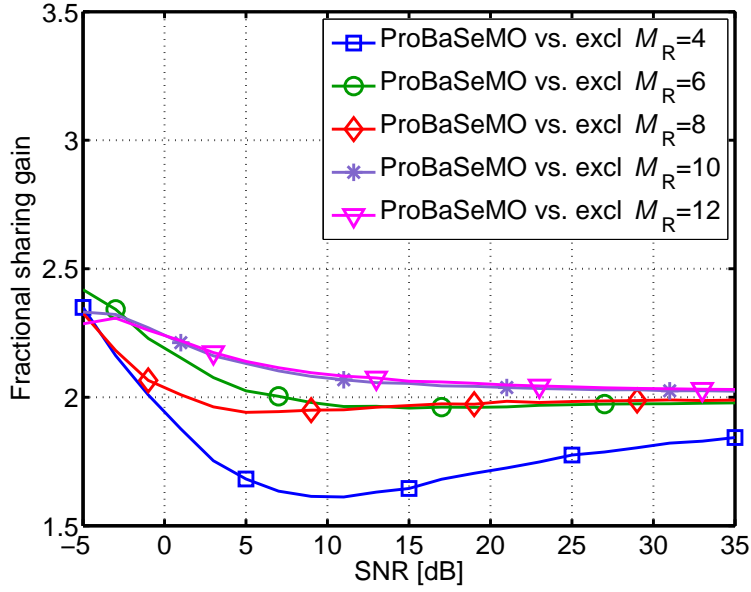


Figure 3.4: Fractional sharing gain as a function of SNR for $M_U = 1$ and $L = 2$.

gain is defined as

$$\text{Fractional sharing gain} = \frac{\text{Throughput of non-orthogonal sharing}}{\text{Throughput of TDMA with 4 antennas at the relay}}.$$

3.11 Summary

In this chapter we discuss relay transmit strategies for multi-operator two-way relaying networks with a MIMO AF relay first proposed by us in [RZHJ10, ZRH⁺12c, ZRH12b, ZH13, ZVKH13]. First, we propose the ProBaSeMO strategy inspired by the BD and RBD MU-MIMO precoding schemes. We demonstrate that all operators can serve their users by using multiple antennas at the relay via the the ProBaSeMO strategy. This ProBaSeMO strategy can be applied for both single and multiple antennas at the UTs. Transmit and receive strategies for both single-stream and multiple streams transmission are also proposed. Then, we develop optimal linear relaying strategies which can be used as benchmarks for the ProBaSeMO approach when each UT has a single antenna. The sum rate maximization problem is non-convex and in general NP-hard. The steepest descent algorithm simplifies to a dominant eigenvector problem for the single antenna UT case. It thus can be solved using a modified power method.

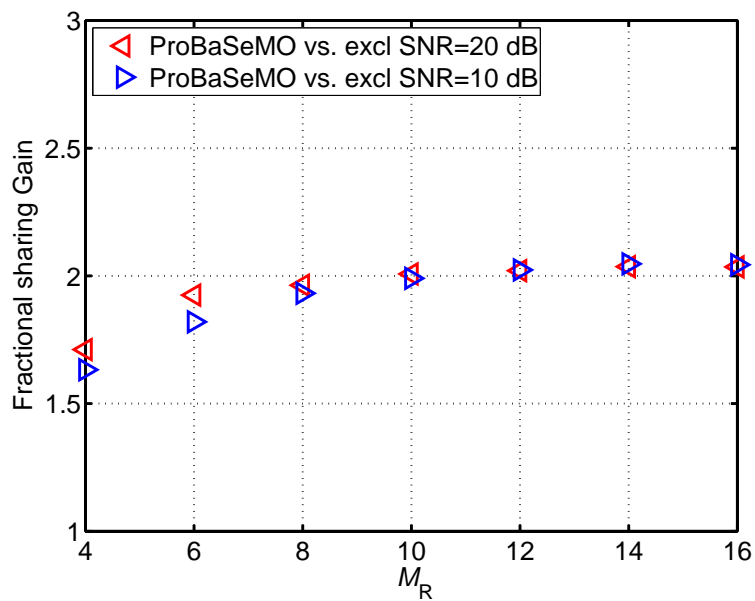


Figure 3.5: Fractional sharing gain as a function of M_R for $M_U = 1$ and $L = 2$.

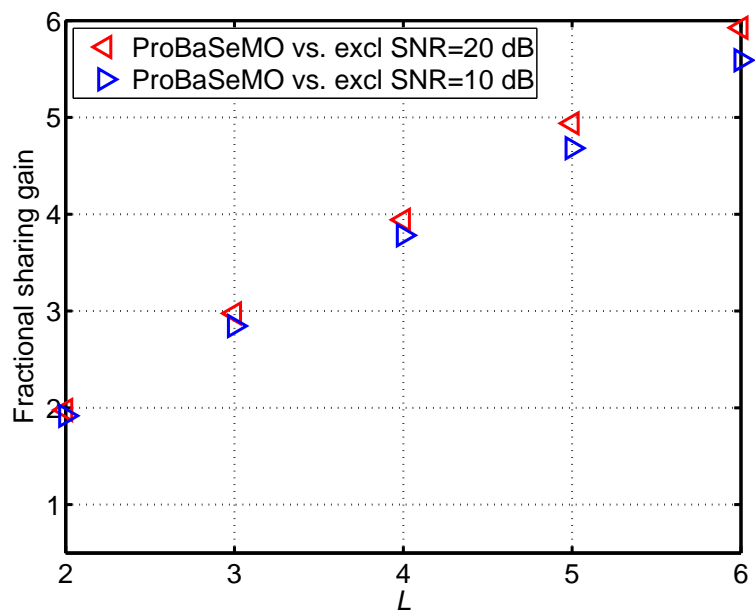


Figure 3.6: Fractional sharing gain as a function of L for $M_U = 1$ and $M_R = 4L$.

Although the steepest descent algorithm can be extended for multiple antennas UT, it requires many iterations. Thus, its computational complexity is much higher compared to the ProBaSeMO approach. In a single antenna UT case, the corresponding optimization task can be also represented as a DC programming problem. Therefore, the efficient polynomial time algorithm POTDC is extended to this multi-operator case and solves the problem approximately. Furthermore, two other QoS based system design criteria have been chosen for the design of optimal relay amplification matrices. First, we minimize the average transmit power at the relay subject to an SINR constraint per user. Second, we discuss the SINR balancing problem with average relay transmit power constraint. Both problems are generally non-convex. Thus, to solve the optimization problems, we apply convex approximation techniques based on SDP and SOCP. Finally, we address the WL design for the specific case of transmitting strictly non-circular signals. Our goal is to exploit the WL gain by applying WL signal processing to the nodes in the system. It turns out that a globally optimal WL design for our system requires a joint WL design at the UTs and at the relay. This problem is in general non-convex and NP-hard. Therefore, we resort to a suboptimal problem where the WL design is only applied at the relay. Since the considered WL model can be transformed into an equivalent linear model, arbitrary linear transmit strategies can be applied. We study the design of the optimal WL transmit strategies to maximize the minimum SINR per user or to minimize the average required transmit power at the relay. We have also proposed a suboptimal WL design, namely, the WL DCM method, for the scenario with only one operator.

Simulation results have demonstrated that

- Compared to the time-shared approach, the ProBaSeMO approach can achieve a two-fold sharing gain with many antennas at the relay or in the high SNR regime regardless of single stream transmission or multiple stream transmission at the UTs when two operators are considered. For a fixed number of antennas at the relay, a higher sharing gain can be obtained if the number of operators which share the relay increases. The sharing gain is defined as the performance comparison of the non-orthogonal sharing approaches and the time-shared approach in terms of system sum rate.
- Compared to the non-pairing aware approach in [JS10] and the pairing aware approach in [YZGK10], the ProBaSeMO approach has a better sum rate performance especially in the high SNR regime and is more robust to the spatial correlation at the relay. Moreover, less number of antennas at the relay are required to apply the ProBaSeMO approach compared to the methods in [JS10].
- The ProBaSeMO scheme has almost the same performance as the power method for the

single antenna case and suffers only a little loss compared to the steepest descent method for the multiple antennas case.

- When each UT has a single antenna and the relay power minimization and SINR balancing are system design criteria, the ProBaSeMO scheme yields competitive results compared to the convex optimization techniques especially when a large number of antennas is deployed at the relay. However, it requires much less computational complexity.
- When each UT has a single antenna and strongly non-circular modulation schemes are deployed, a WL signal processing gain is obtained by using optimal WL techniques over optimal linear techniques. The WL gain increases as the number of operators increases but it decreases as the number of antennas at the relay increases. Moreover, by taking a large number of antennas at the relay and using the law of large numbers we derive the asymptotic gain of the WL DCM scheme when compared to linear DCM, which can be only 20 % in the worst case.

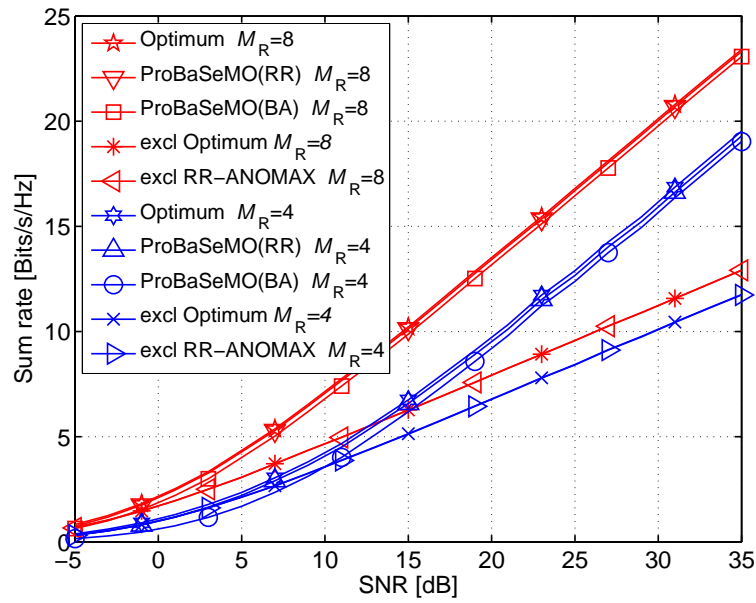


Figure 3.7: Sum rate comparison of time-shared approach and ProBaSeMO approach for $M_U = 1$ and $L = 2$.

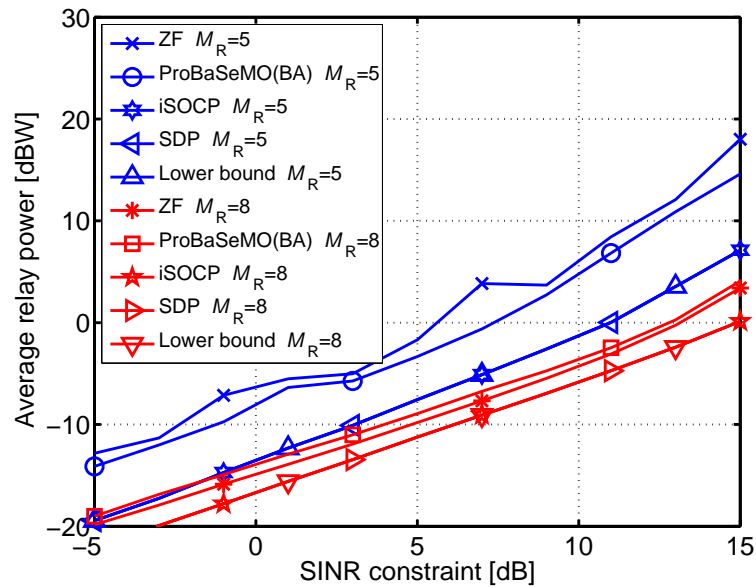


Figure 3.8: Relay transmit power vs. SINR constraint, SNR = 15 dB, 1000 channel realizations

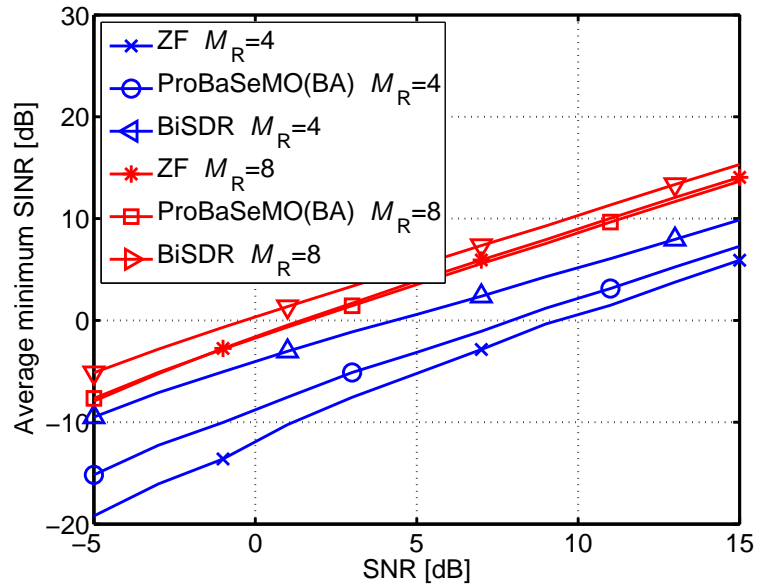


Figure 3.9: SINR balancing, $P_R = 1$ W

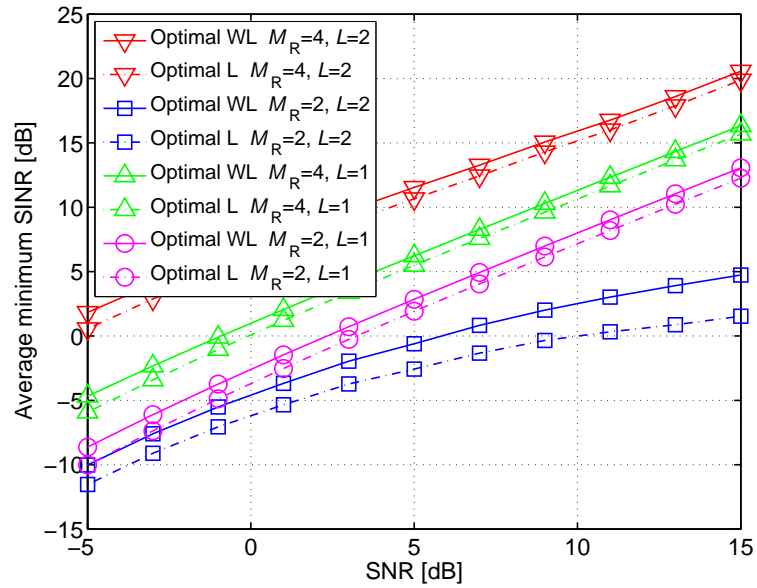


Figure 3.10: Achievable average minimum SINR by using WL design and linear design for different pairs and various number of antennas at the relay.

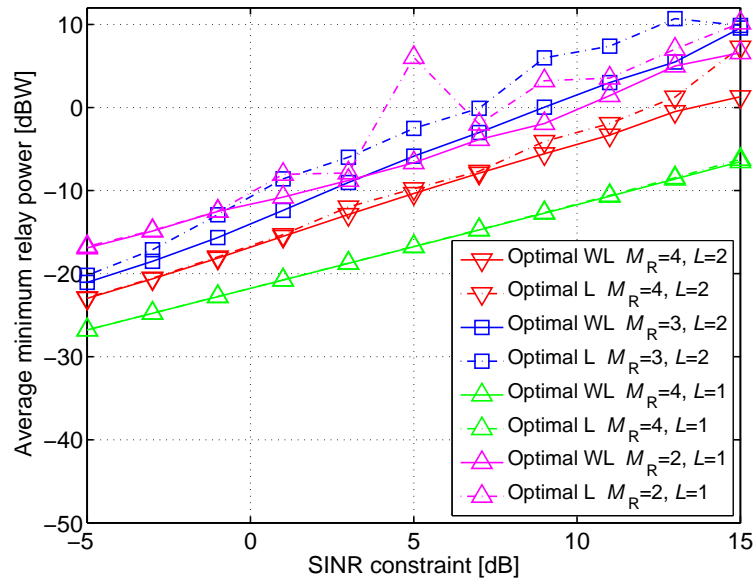


Figure 3.11: Average minimum transmit power at the relay by using WL design and linear design for different pairs and various number of antennas at the relay. SNR = 20 dB. 1000 channel realizations

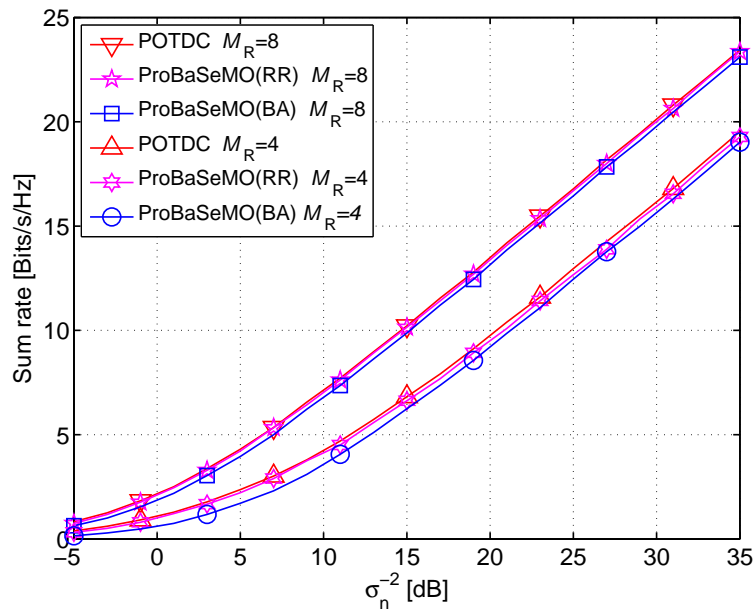


Figure 3.12: Sum rate comparison of ProBaSeMO ($\{BA, RR\}$) and POTDC approaches for $L = 2$.

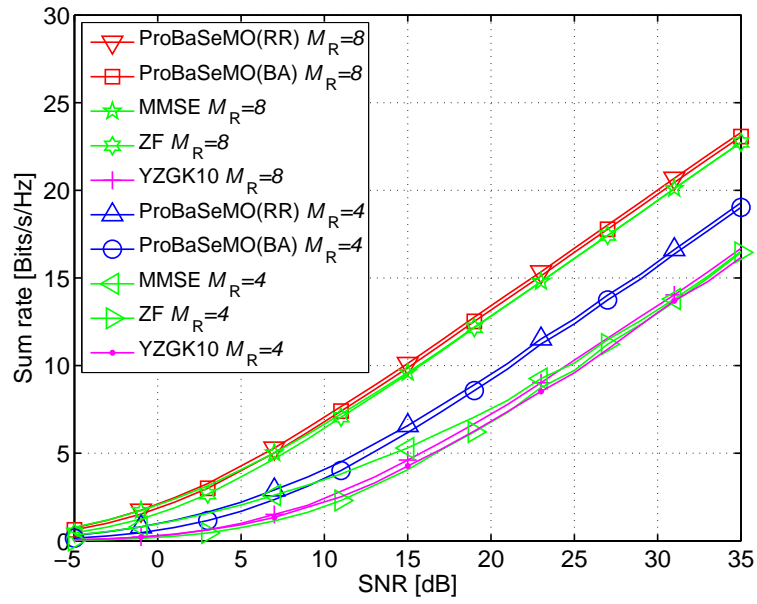


Figure 3.13: Sum rate comparison of different multi-operator TWR approaches for $M_U = 1$ and $L = 2$.

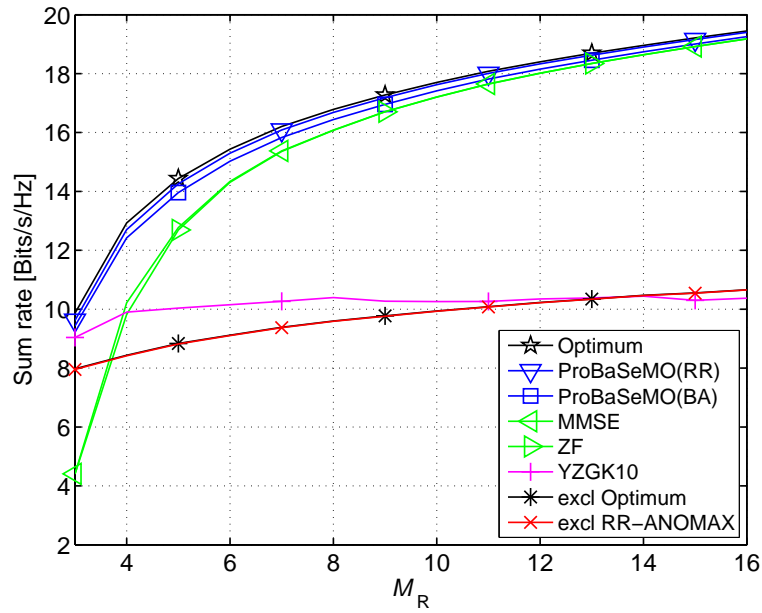


Figure 3.14: Sum rate comparison of different multi-operator TWR approaches for $M_U = 1$, SNR = 25 dB and $L = 2$.

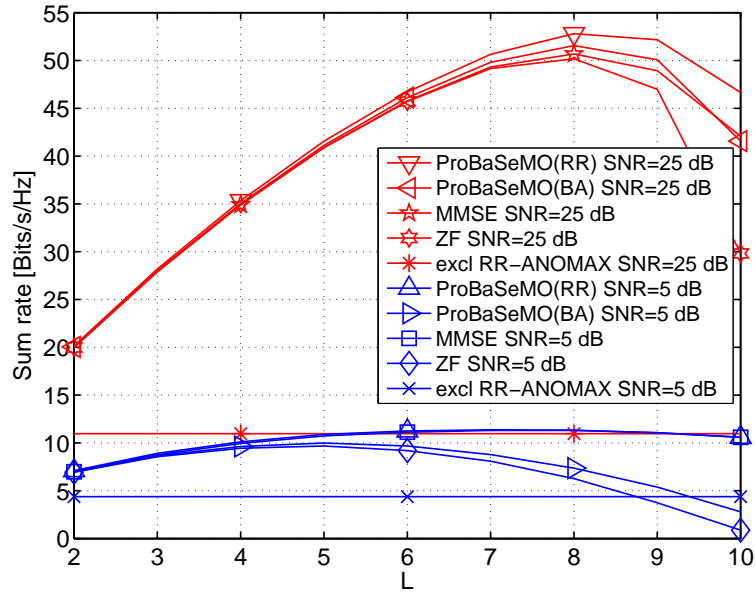


Figure 3.15: Sum rate comparison of different multi-operator TWR approaches for $M_U = 1$, SNR= 25 dB, and $M_R = 20$.

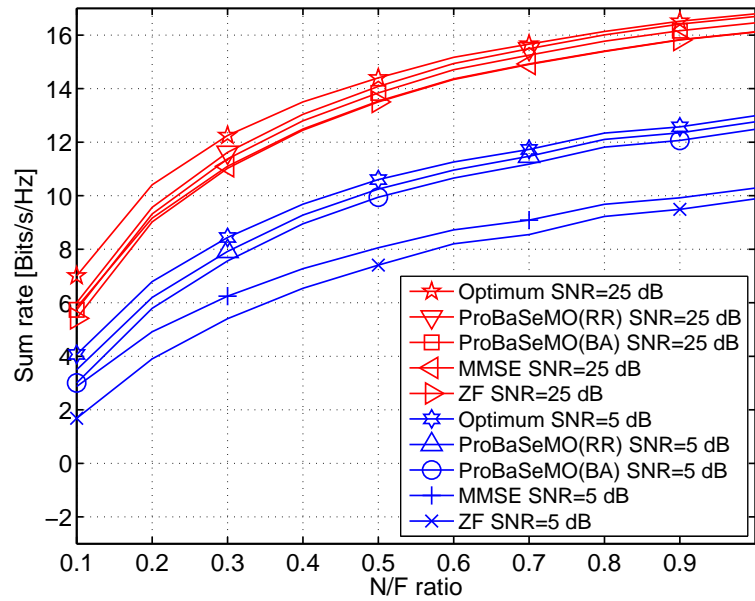


Figure 3.16: Effects of path loss of different multi-operator TWR approaches for $M_R = 8$, $M_U = 1$ and $L = 2$ in a symmetric scenario, i.e., N/F ratio = $d_2^{(\ell)} / d_1^{(\ell)} = d_2 / d_1, \forall \ell$.

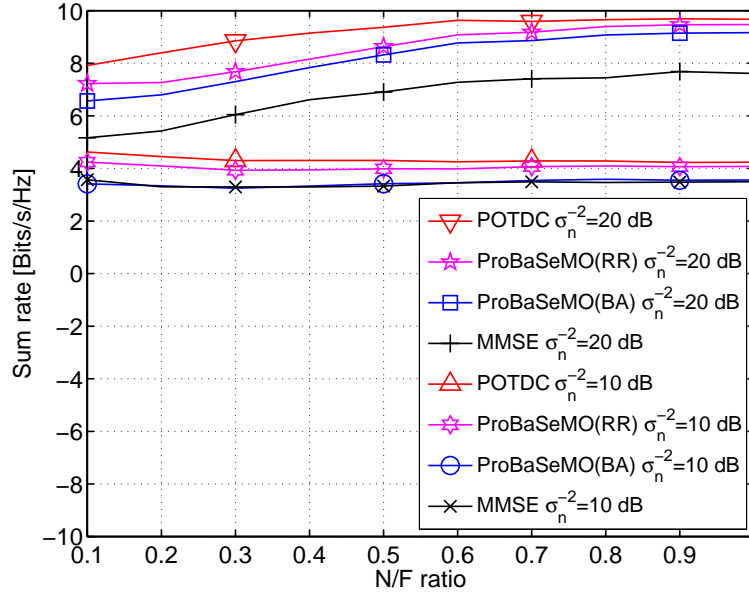


Figure 3.17: Effects of path loss of ProBaSeMO ($\{BA, RR\}$), MMSE, and POTDC approaches for $M_R = 4$ and $L = 2$ in an asymmetric scenario, i.e., N/F ratio = $d_2^{(1)}/d_1^{(1)} = d_1^{(2)}/d_2^{(2)}$.

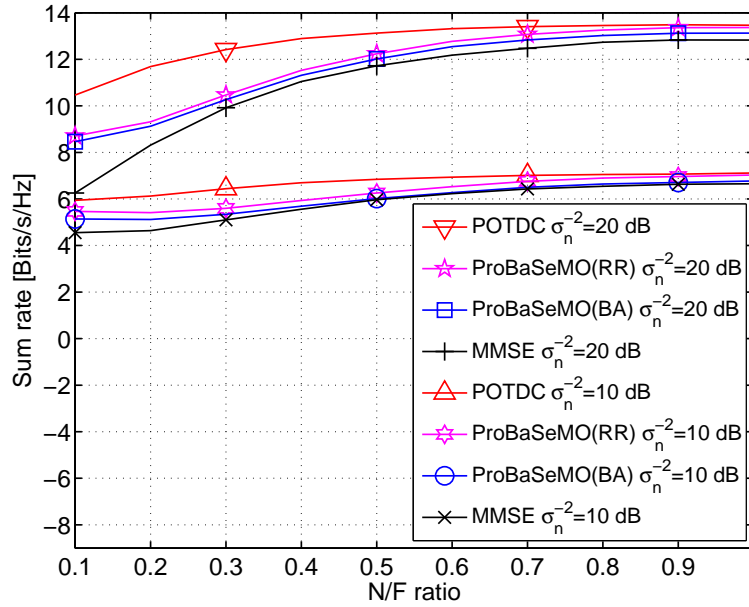


Figure 3.18: Effects of path loss of ProBaSeMO ($\{BA, RR\}$), MMSE, and POTDC approaches for $M_R = 8$ and $L = 2$ in an asymmetric scenario, i.e., N/F ratio = $d_2^{(1)}/d_1^{(1)} = d_1^{(2)}/d_2^{(2)}$.

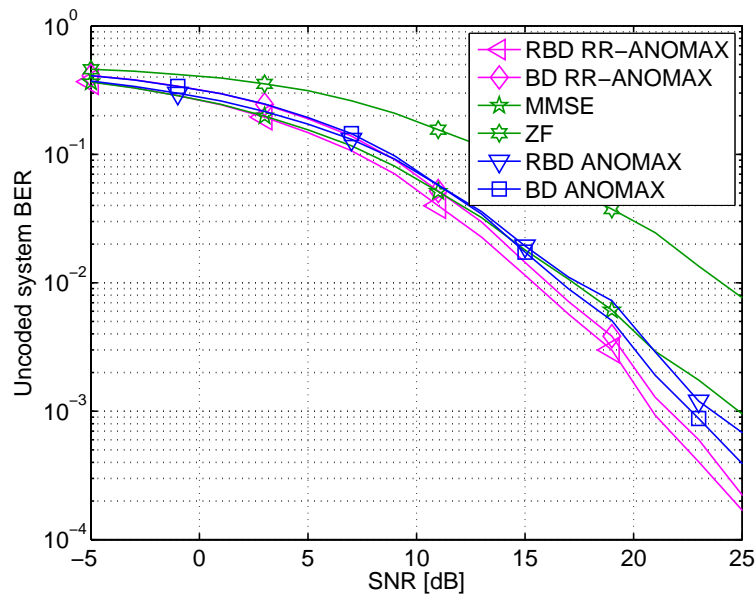


Figure 3.19: Uncoded system BER comparison of different multi-operator TWR approaches for QPSK modulation, $M_U = 1$, $M_R = 4$ and $L = 2$.

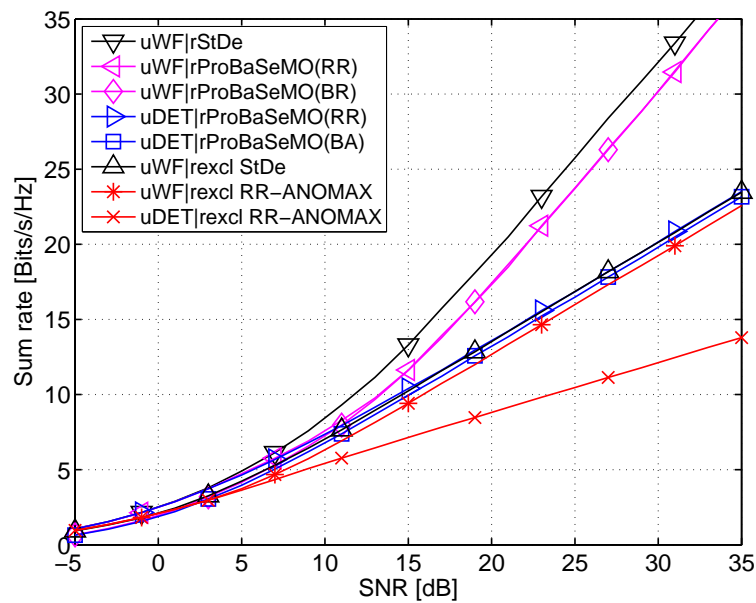


Figure 3.20: Sum rate comparison of different multi-operator TWR transmit strategies for $M_U = 2$, $M_R = 8$ and $L = 2$.

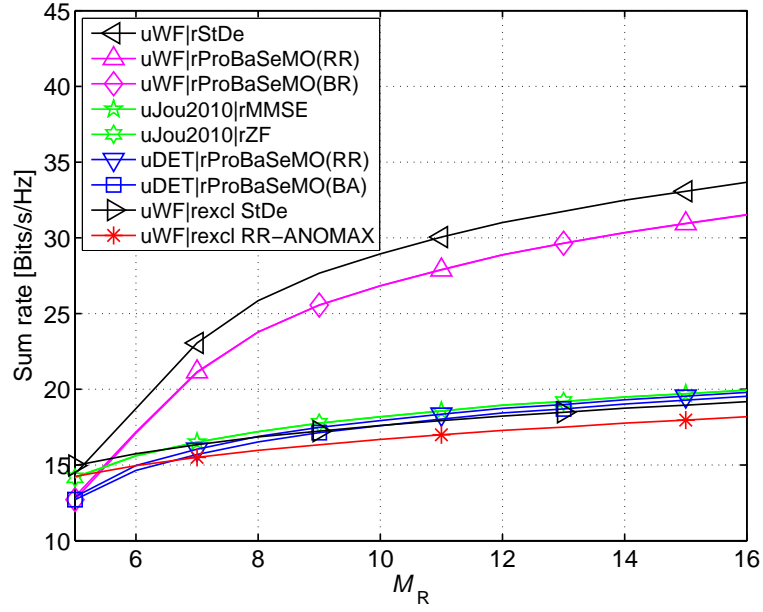


Figure 3.21: Sum rate comparison of different multi-operator TWR approaches for $M_U = 2$, SNR= 25 dB and $L = 2$.

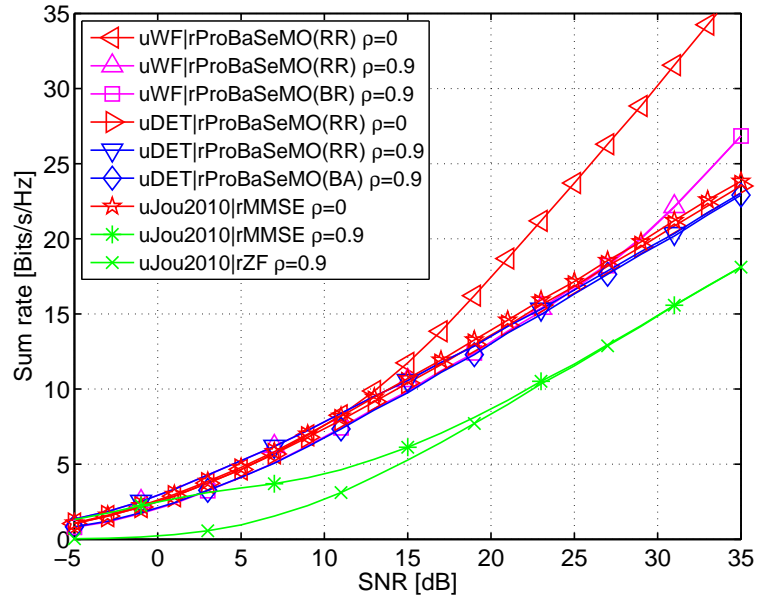


Figure 3.22: Sum rate comparison of different approaches for $M_U = 2$, $M_R = 8$, and $L = 2$ when $\rho_R = 0.9$.

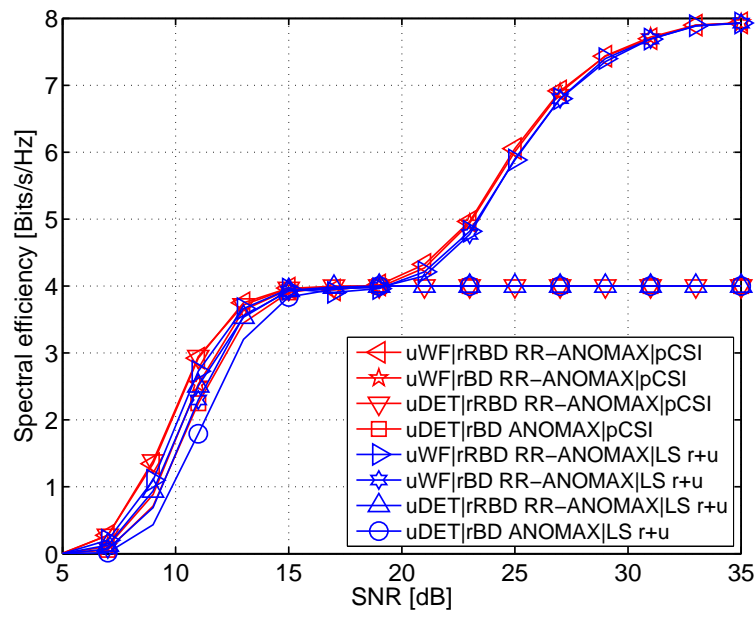


Figure 3.23: System spectral efficiency comparison of different approaches for QPSK modulation, $M_U = 2$, $M_R = 8$ and $L = 2$.

4 Multi-pair relaying networks with multiple single antenna relays

Now we consider another TWR scenario, i.e., a multi-pair TWR network with multiple single antenna AF relays. The sum rate maximization problem subject to a total transmit power constraint of the relays in the network or individual relay transmit power constraints is studied. Due to the structure of the network, we shift from the design of relay amplification matrices to the design of relay amplification coefficients for each relay. The major challenge comes when each relay has its own transmit power constraint. Considering different types of power constraints, we divide this chapter into two parts. In the first part, we investigate the optimization problem under a total relay transmit power constraint [ZRH⁺12c]. First, we show that the problem is a monotonic optimization problem and propose a polyblock approximation algorithm for obtaining the global optimum. However, this algorithm is only suitable for benchmarking because of its high computational complexity. After observing that the necessary optimality condition for our problem is similar to that of the generalized eigenvalue problem, we propose to use the power method as in Section 3.4 which can approach the optimum recursively. Finally, we propose the total signal to interference plus noise ratio (SINR) eigen-beamformer which is a closed-form suboptimal solution that reduces the computational complexity significantly. In the second part we study the sum rate maximization problem where each relay has its own transmit power constraint [ZRH12a]. Again, we show that the polyblock algorithm can be applied with a few modifications. Afterwards, inspired by the polynomial time difference of convex functions (POTDC) method [KRVH12], we develop a suboptimal solution which has lower complexity but comparable performance. To further reduce the computational complexity, we propose two other algorithms, i.e., the modified total SINR eigen-beamformer and an interference neutralization based design which are the low SNR and high SNR approximations of the original optimization problem, respectively.

4.1 Problem description and state of the art

The optimal beamforming design for the sum rate maximization in AF TWR networks with one pair of users and multiple single antenna AF relays has been studied in [HNSG10] and [DS10]. Only a few references deal with multi-pair AF TWR networks, which include adaptive power allocation [LXDL10] and distributed beamforming [WCY⁺11]. Reference [LXDL10]

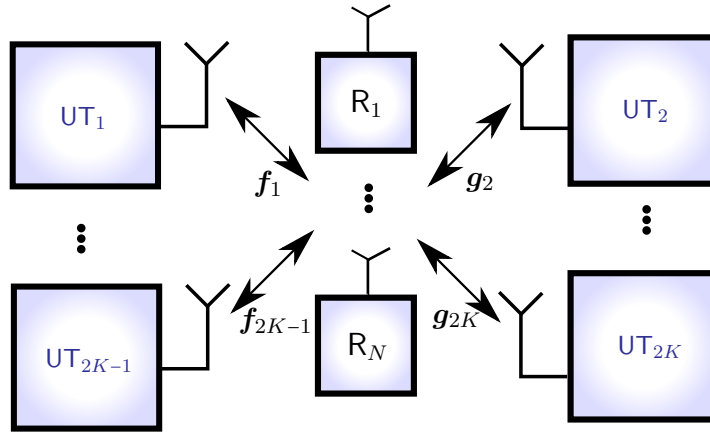


Figure 4.1: Multi-pair two-way relaying with multiple single antenna amplify and forward relays.

deals with the adaptive power allocation problem while assuming different pairs of UTs access the network using different frequency bins, i.e., no inter-pair interference is created during the data transmission. Reference [WCY⁺11] proposes suboptimal beamforming techniques for networks with inter-pair interference, where the strategy is to first null the inter-pair interference using a ZF method and then optimize the interference-free system. When the inter-pair interference is involved in the sum rate maximization problem, it is non-convex and in general NP-hard.

The sum rate maximization problem with non-orthogonal network access has not been studied prior to our work [ZRH⁺12c] and [ZRH12a]. The optimum beamforming design for maximizing the sum rate of this system is developed in [ZRH⁺12c]. However, a sum power constraint is assumed in [ZRH⁺12c]. Thereby, this motivates us to extend it to the case where each relay has its own transmit power constraint in [ZRH12a] because this case has not been dealt with before. Moreover, it is mathematically more difficult as will be shown in Section 4.4.

4.2 System model

The scenario under investigation is shown in Fig. 4.1. K pairs of single antenna users would like to communicate with each other via the help of N single antenna relays. We assume perfect synchronization and the channel is frequency flat and quasi-static block fading. The vector channel from the $(2k-1)$ -th user (on the left-hand side of Fig. 4.1) to the relays is denoted as $\mathbf{f}_{2k-1} = [f_{2k-1,1}, f_{2k-1,2}, \dots, f_{2k-1,N}]^T \in \mathbb{C}^N$, while the channel from the $(2k)$ -th user (on the right-hand side of Fig. 4.1) to the relay is denoted as $\mathbf{g}_{2k} = [g_{2k,1}, g_{2k,2}, \dots, g_{2k,N}]^T \in \mathbb{C}^N$, for

$k \in \{1, 2, \dots, K\}$. For notational simplicity, we assume an ideal TDD system, i.e., the channels are *reciprocal*. The transmission takes two time slots. In the first time slot, the signal received at all relays can be combined in a vector as

$$\mathbf{r} = \sum_{k=1}^K (\mathbf{f}_{2k-1} s_{2k-1} + \mathbf{g}_{2k} s_{2k}) + \mathbf{n}_R \in \mathbb{C}^N \quad (4.1)$$

where s_{2k-1} and s_{2k} are i.i.d. symbols with zero mean and unit power. The vector \mathbf{n}_R denotes the ZMCSCG noise and $\mathbb{E}\{\mathbf{n}_R \mathbf{n}_R^H\} = \sigma_R^2 \mathbf{I}_N$.

Afterwards, the AF relays broadcast the weighted signal as

$$\bar{\mathbf{r}} = \mathbf{W} \cdot \mathbf{r} \quad (4.2)$$

where $\mathbf{W} = \text{diag}\{\mathbf{w}^*\}$ and $\mathbf{w} = [w_1, w_2, \dots, w_N]^T$ is the vector which consists of the N complex weights of all the relays.

In the second time slot, the received signal at the $(2k-1)$ -th user (on the left-hand side of Fig. 4.1) is expressed as [WCY⁺11]

$$\begin{aligned} y_{2k-1} = & \underbrace{\mathbf{w}^H \mathbf{F}_{2k-1} \mathbf{g}_{2k} s_{2k}}_{\text{desired signal}} + \underbrace{\mathbf{w}^H \mathbf{F}_{2k-1} \mathbf{f}_{2k-1} s_{2k-1}}_{\text{self-interference}} \\ & + \underbrace{\mathbf{w}^H \mathbf{F}_{2k-1} \sum_{\substack{\ell \neq k \\ \ell=1}}^K (\mathbf{f}_{2\ell-1} s_{2\ell-1} + \mathbf{g}_{2\ell} s_{2\ell})}_{\text{inter-pair interference}} + \underbrace{\mathbf{w}^H \mathbf{F}_{2k-1} \mathbf{n}_R + n_{2k-1}}_{\text{effective noise}} \end{aligned} \quad (4.3)$$

where $\mathbf{F}_{2k-1} = \text{diag}\{\mathbf{f}_{2k-1}\}$ and n_{2k-1} is the ZMCSCG noise with variance σ_{2k-1}^2 . The SINR of the m -th user can be calculated as

$$\text{SINR}_{2k-1} = \frac{\mathbf{w}^H \mathbf{B}_{2k-1} \mathbf{w}}{\mathbf{w}^H (\mathbf{D}_{2k-1} + \mathbf{E}_{2k-1}) \mathbf{w} + \sigma_{2k-1}^2} \quad (4.4)$$

where $\mathbf{D}_{2k-1} = \sum_{\ell \neq k}^K (\tilde{\mathbf{h}}_{2k-1, \ell}^{(o)} \tilde{\mathbf{h}}_{2k-1, \ell}^{(o)H} + \tilde{\mathbf{h}}_{2k-1, \ell}^{(e)} \tilde{\mathbf{h}}_{2k-1, \ell}^{(e)H})$ and $\mathbf{B}_{2k-1} = \mathbf{h}_{2k-1} \mathbf{h}_{2k-1}^H$ are $N \times N$ positive semidefinite Hermitian matrices. The matrices \mathbf{D}_{2k-1} and \mathbf{B}_{2k-1} are related to the interference power and the desired signal power, respectively, ($\mathbf{h}_{2k-1} = \mathbf{f}_{2k-1} \odot \mathbf{g}_{2k}$, $\tilde{\mathbf{h}}_{2k-1, \ell}^{(o)} = \mathbf{f}_{2k-1} \odot \mathbf{f}_{2\ell-1}$ and $\tilde{\mathbf{h}}_{2k-1, \ell}^{(e)} = \mathbf{f}_{2k-1} \odot \mathbf{g}_{2\ell}$). The term which is related to the forwarded noise from the relay is denoted by an $N \times N$ full rank diagonal matrix $\mathbf{E}_{2k-1} = \sigma_R^2 \mathbf{F}_{2k-1} \mathbf{F}_{2k-1}^H$. Similar SINR expression can be obtained when $m = 2k$. Furthermore, the total transmit power is given by

$\mathbb{E}\{\|\bar{\mathbf{r}}\|^2\} = \mathbf{w}^H \mathbf{\Gamma} \mathbf{w}$ with

$$\mathbf{\Gamma} = \sum_{k=1}^K (\mathbf{F}_{2k-1} \mathbf{F}_{2k-1}^H + \mathbf{G}_{2k} \mathbf{G}_{2k}^H) + \sigma_{\text{R}}^2 \mathbf{I}_N, \quad (4.5)$$

where $\mathbf{G}_{2k} = \text{diag}\{\mathbf{g}_{2k}\}$. The i -th relay's transmit power is given by $\mathbb{E}\{\|\bar{r}_i\|^2\} = \mathbf{w}^H \mathbf{\Upsilon}_i \mathbf{w}$ with $\mathbf{\Upsilon}_i = \Gamma_{i,i} \mathbf{e}_i \mathbf{e}_i^H$. The vector \mathbf{e}_i is the i -th column of an identity matrix. The scalar $\Gamma_{i,i}$ is the (i, i) -th element of the diagonal matrix $\mathbf{\Gamma}$.

Assume that perfect channel knowledge can be obtained such that the self-interference terms can be canceled. Our goal is to find the weight vector \mathbf{w} such that the sum rate of the system is maximized subject to a sum power constraint or individual relay transmit power constraints.

4.3 Sum rate maximization under a total relay transmit power constraint

Hereafter, for notational simplicity, we define an index m to substitute the indices k such that $m \in \{1, 2, \dots, 2K\}$. Let P_{R} be the total transmit power consumed by the relays in the network. The optimization problem can be formulated as

$$\begin{aligned} \max_{\mathbf{w}} \quad & \frac{1}{2} \sum_{m=1}^{2K} \log_2(1 + \text{SINR}_m) \\ \text{subject to} \quad & \mathbb{E}\{\|\bar{\mathbf{r}}\|^2\} \leq P_{\text{R}}, \end{aligned} \quad (4.6)$$

where the factor $1/2$ is due to the two channel uses (half duplex).

To simplify the optimization problem we note that the inequality constraint in (4.6) has to be satisfied with equality at optimality. Otherwise, the optimal \mathbf{w} can be scaled up to satisfy the constraint with equality while increasing the objective function, which contradicts the optimality. Inserting the constraint into the objective function in (4.6), the original problem can be reformulated as an *unconstrained* optimization problem

$$\max_{\mathbf{w}} \prod_{m=1}^{2K} \frac{\mathbf{w}^H \mathbf{A}_m \mathbf{w}}{\mathbf{w}^H \mathbf{C}_m \mathbf{w}} \quad (4.7)$$

where $\mathbf{C}_m = \mathbf{D}_m + \mathbf{E}_m + \frac{\sigma_m^2}{P_{\text{R}}} \mathbf{\Gamma}$ and $\mathbf{A}_m = \mathbf{B}_m + \mathbf{C}_m$ are positive definite. Problem (4.7) is equivalent to (4.6) since the objective function is homogeneous and any scaling in \mathbf{w} does not change the optimality. Nevertheless, if $\bar{\mathbf{w}}$ is the solution to (4.7), it should be scaled to fulfill

the transmit power constraint, i.e., the optimal solution to (4.6) is given by

$$\mathbf{w} = \sqrt{\frac{P_R}{\bar{\mathbf{w}}^H \mathbf{\Gamma} \bar{\mathbf{w}}}} \bar{\mathbf{w}}. \quad (4.8)$$

Problem (4.7) is non-convex and in general NP-hard.

4.3.1 Generalized polyblock algorithm

Monotonic optimization (see [Tuy00], [PT03]) deals with the maximization or minimization of an increasing function over an intersection of normal and reverse normal sets. The polyblock approximation approach is a unified algorithm to find the global optimum of the monotonic optimization problem. Prior work that used this approach in the area of wireless communications can be found in [QZH09], [JL10]. We show that the problem (4.7) is a monotonic optimization problem and then propose a version of the polyblock algorithm to solve it. A polyblock approach is also summarized in Appendix C.7.2.

Proposition 4.3.1. *Problem (4.7) is a monotonic optimization problem.*

Proof. Problem (4.7) is equivalent to the following problem

$$\max_{\mathbf{y}} \{\Phi(\mathbf{y}) | \mathbf{y} \in \mathbb{D}\} \quad (4.9)$$

where $\Phi(\mathbf{y}) = \prod_{m=1}^{2K} y_m$ and $\mathbb{D} = \mathbb{G} \cap \mathbb{L}$. The sets $\mathbb{G} = \{\mathbf{y} \in \mathbb{R}_+^{2K} | y_m \leq \max_{\mathbf{w}} \frac{\mathbf{w}^H \mathbf{A}_m \mathbf{w}}{\mathbf{w}^H \mathbf{C}_m \mathbf{w}}, \mathbf{w} \in \mathbb{C}^N\}$ and $\mathbb{L} = \{\mathbf{y} \in \mathbb{R}_+^{2K} | y_m \geq \min_{\mathbf{w}} \frac{\mathbf{w}^H \mathbf{A}_m \mathbf{w}}{\mathbf{w}^H \mathbf{C}_m \mathbf{w}}\}$ are normal set and reverse normal set, respectively. The function $\Phi(\mathbf{y})$ is an increasing function since $\Phi(\bar{\mathbf{y}}) \geq \Phi(\tilde{\mathbf{y}})$ for $\bar{\mathbf{y}} \geq \tilde{\mathbf{y}}$. Then the proof of the equivalence follows similar steps as in [PT03]. Thus, problem (4.7) is a monotonic optimization problem. The definitions of increasing function, normal set, and reverse normal set are the same as in [PT03]. \square

A polyblock \mathbb{P} with vertex set $\mathbb{T} \subset \mathbb{R}_+^{2K}$ is defined as the finite union of all the boxes $[\mathbf{0}, \mathbf{z}]$, $\mathbf{z} \in \mathbb{T}$. It is dominated by its proper vertices. A vertex \mathbf{z} is proper if there is no $\bar{\mathbf{z}} \neq \mathbf{z}$ and $\bar{\mathbf{z}} \geq \mathbf{z}$ for $\bar{\mathbf{z}} \in \mathbb{T}$.

According to Proposition 2 in [PT03], the global maximum of the problem (4.9), if exists, is attained on $\partial^+ \mathbb{D}$, i.e., the upper boundary of \mathbb{D} . The main idea of the polyblock approximation algorithm for solving (4.9) is to approximate $\partial^+ \mathbb{D}$ by polyblocks, i.e., construct a nested sequence of polyblocks which approximate \mathbb{D} from above, that is,

$$\mathbb{P}_1 \supset \mathbb{P}_2 \supset \dots \supset \mathbb{D} \text{ s.t. } \max_{\mathbf{y} \in \mathbb{P}_k} \Phi(\mathbf{y}) \rightarrow \max_{\mathbf{y} \in \mathbb{D}} \Phi(\mathbf{y}) \quad (4.10)$$

when $k \rightarrow \infty$ and $\mathbf{y}_k \geq \mathbf{y}_\ell$ for all $\ell \geq k$.

Now we outline how to construct the subset \mathbb{P}_k in our case, which is clearly the critical step of a polyblock approximation. Let \mathbb{T}_k be the proper vertex set of \mathbb{P}_k and define the maximizer at iteration k as

$$\bar{\mathbf{y}}_k \in \arg \max_{\bar{\mathbf{y}}} \{\Phi(\bar{\mathbf{y}}) | \bar{\mathbf{y}} \in \mathbb{T}_k\}. \quad (4.11)$$

Compute the unique intersection point of $\partial^+ \mathbb{D}$ and $\bar{\mathbf{y}}_k$ as $\hat{\mathbf{y}}_k = \gamma_k \bar{\mathbf{y}}_k$ with $\gamma_k \in [0, 1]$. Then the proper vertex set \mathbb{T}_{k+1} of \mathbb{P}_{k+1} in step $k+1$ is the set obtained by substituting $\bar{\mathbf{y}}_k$ in \mathbb{T}_k with the new vertices $\{\bar{\mathbf{y}}_k^1, \dots, \bar{\mathbf{y}}_k^{2K}\}$ defined by

$$\bar{\mathbf{y}}_k^m = \bar{\mathbf{y}}_k - (\bar{y}_{k,m} - \hat{y}_{k,m}) \mathbf{e}_m, \quad m = 1, \dots, 2K \quad (4.12)$$

and removing all the improper vertices¹ as well as the vertices not belonging to \mathbb{L} . The scalar $\bar{y}_{k,m}$ is the m -th element of $\bar{\mathbf{y}}_k$ and $\mathbf{e}_m \in \mathbb{R}_+^{2K}$ is the m -th unit vector. The factor γ_k is calculated as [PT03]

$$\gamma_k = \max_{\mathbf{w}} \min_m \frac{\mathbf{w}^H \mathbf{A}_m \mathbf{w}}{\bar{y}_{k,m} \mathbf{w}^H \mathbf{C}_m \mathbf{w}}. \quad (4.13)$$

Although (4.13) is non-convex, it is an easier sub-problem which can be solved approximately (η -optimality)² using the algorithm in [GSS⁺10]. Finally, the proposed (ϵ, η) -optimal solution using the polyblock algorithm is described in Algorithm 6. The proof of the global convergence follows similar steps as in [PT03].

Algorithm 6 (ϵ, η) -optimal polyblock algorithm for solving (4.7)

- 1: **Initialize:** set initial vertex set $\mathbb{T}_0 = \{\mathbf{b}\}$ ³, maximum iteration number N_{\max} , and the threshold values ϵ, η .
 - 2: **Main step:**
 - 3: **for** $k = 1$ to N_{\max} **do**
 - 4: Solve (4.11) and (4.13) finding $\bar{\mathbf{y}}_k$ and η -optimal γ_k .
 - 5: Construct a smaller polyblock \mathbb{P}_k using $\bar{\mathbf{y}}_k$ and γ_k .
 - 6: **if** $\max_m \{(\bar{y}_{k,m} - \hat{y}_{k,m}) / \bar{y}_{k,m}\} \leq \epsilon$ **then**
 - 7: **break**
 - 8: **end if**
 - 9: **end for**
-

¹A vertex is improper if it is dominated by other vertices in the same set. For example, if $\{\mathbf{y}_1, \mathbf{y}_2\} \in \mathbb{T}$ and $\mathbf{y}_2 \geq \mathbf{y}_1$, then \mathbf{y}_1 is dominated by \mathbf{y}_2 and thus \mathbf{y}_1 is improper [PT03].

²The η -optimality means that the stopping criterion or the tolerance factor of the iterative algorithm is η .

³Here $\mathbf{b} \in \mathbb{R}_+^{2K}$ satisfies $b_m = \max_{\mathbf{w}} \frac{\mathbf{w}^H \mathbf{A}_m \mathbf{w}}{\mathbf{w}^H \mathbf{C}_m \mathbf{w}}, m = 1, \dots, 2K$.

4.3.2 Extended GPM algorithm

Clearly, problem (4.7) can also be solved using the GPM algorithm in Section 3.4.1, which is also applied in [LYC08]. Although the GPM algorithm converges fast in practice and the numerical results provide a strong evidence that it provides globally optimal solution (compared to the polyblock approach), we can neither prove its optimality nor characterize its convergence behavior theoretically. The analytic study of it is not trivial.

Let us briefly review the GPM method of Section 3.4.1. According to the optimality condition, all the local maximizers for the problem (4.7) should satisfy

$$\left. \frac{\partial \lambda(\mathbf{w})}{\partial \mathbf{w}} \right|_{\mathbf{w}=\bar{\mathbf{w}}} = 0 \quad (4.14)$$

where $\lambda(\mathbf{w}) = \prod_{m=1}^{2K} \frac{\mathbf{w}^H \mathbf{A}_m \mathbf{w}}{\mathbf{w}^H \mathbf{C}_m \mathbf{w}}$. After differentiation and some algebraic manipulation, the condition in (4.14) can be converted into

$$\mathbf{V}(\bar{\mathbf{w}})\bar{\mathbf{w}} = \lambda(\bar{\mathbf{w}})\mathbf{Q}(\bar{\mathbf{w}})\bar{\mathbf{w}} \quad (4.15)$$

where $\mathbf{V}(\bar{\mathbf{w}}) = \sum_{m=1}^{2K} (\prod_{i \neq m} \bar{\mathbf{w}}^H \mathbf{A}_i \bar{\mathbf{w}}) \mathbf{A}_m$ and $\mathbf{Q}(\bar{\mathbf{w}}) = \sum_{m=1}^{2K} (\prod_{i \neq m} \bar{\mathbf{w}}^H \mathbf{C}_i \bar{\mathbf{w}}) \mathbf{C}_m$. Equation (4.15) is a generalized eigenvalue problem and $\lambda(\bar{\mathbf{w}})$ can be thought as the generalized eigenvalue of matrices $\mathbf{V}(\bar{\mathbf{w}})$ and $\mathbf{Q}(\bar{\mathbf{w}})$. Thus, the maximum generalized eigenvalue $\lambda_{\max}(\bar{\mathbf{w}})$ is the maximum of the problem (4.7). Since both matrices are functions of $\bar{\mathbf{w}}$, a closed-form solution is not possible. Therefore, in Section 3.4.1 we propose to apply the recursive power method of [GL96] to obtain the solution. In [GL96], it is shown that the original power method converges only if the largest eigenvalue is dominant and the convergence speed depends on the ratio between the largest and the second largest eigenvalues. Although we can only demonstrate this via numerical simulations, we claim that GPM should have similar features as the original power method. Thus, the following conjecture is given.

Conjecture 1. The GPM algorithm converges if there is a dominant eigenvalue. The convergence behavior depends on the dispersion of the eigenvalue profiles of the matrices of \mathbf{A}_m and \mathbf{C}_m .

Moreover, it is observed that the GPM algorithm converges faster in the high SNR regime with a given error tolerance factor. For a detailed implementation one can be referred to Section 3.4.1.

4.3.3 Total SINR Eigen-Beamformer

Although the polyblock algorithm and the GPM algorithm solve the problem (4.7) in an optimal way, they require many iterations. In this section, we propose a closed-form sub-optimal design. This closed-form solution is based on the observation that for our scenario nulling the inter-pair interferences by forcing every interference term to zero is equivalent to nulling the sum of the inter-pair interferences. That is, if the sum of the interference powers $\mathbf{w}^H(\sum_{m=1}^{2K} \mathbf{D}_m)\mathbf{w} = \sum_{m=1}^{2K}(\mathbf{w}^H \mathbf{D}_m \mathbf{w}) = 0$, it is clear that $\mathbf{w}^H \mathbf{D}_m \mathbf{w} = 0$, for all m since $\mathbf{D}_m \geq 0$.

Let us define $\mathbf{S}_{\text{tot}} = \sum_{m=1}^{2K} \mathbf{B}_m$ and $\mathbf{U}_{\text{tot}} = \sum_{m=1}^{2K} \mathbf{C}_m$. Thus, $\mathbf{w}^H \mathbf{S}_{\text{tot}} \mathbf{w}$ and $\mathbf{w}^H \mathbf{U}_{\text{tot}} \mathbf{w}$ are the sum of the signal power and the sum of the interference plus noise power of all the users, respectively. Then the proposed total SINR eigen-beamformer solves the following problem

$$\max_{\mathbf{w}} \frac{\mathbf{w}^H \mathbf{S}_{\text{tot}} \mathbf{w}}{\mathbf{w}^H \mathbf{U}_{\text{tot}} \mathbf{w}}. \quad (4.16)$$

It is obvious that the optimal value of (4.16) is the dominant eigenvalue $\lambda_{\max}\{\mathbf{U}_{\text{tot}}^{-1} \mathbf{S}_{\text{tot}}\}$ and the optimal \mathbf{w} is the corresponding dominant eigenvector of the matrix $\mathbf{U}_{\text{tot}}^{-1} \mathbf{S}_{\text{tot}}$ (\mathbf{U}_{tot} is always invertible due to the noise term). In the end, a scaling has to be performed as in (4.8).

Remark 6. Although all the proposed algorithms do not have any requirements on N , to cancel the interference completely $N > 2K(K-1)$ is required since the rank of the sum of the interference terms is equal to $\text{rank}\{\sum_{m=1}^{2K} \mathbf{D}_m\} = 2K(K-1)$ [WCY⁺11]. If $N \leq 2K(K-1)$, the results will be unfair for some users since they will suffer from extremely lower throughput compared to the other users.

4.4 Sum rate maximization under individual relay transmit power constraints

Let $P_{R,i}$ be the transmit power constraint of the i -th relay in the network. The optimization problem can be formulated as

$$\begin{aligned} \max_{\mathbf{w}} \quad & \frac{1}{2} \sum_{m=1}^{2K} \log_2(1 + \text{SINR}_m) \\ \text{subject to} \quad & \mathbb{E}\{\|\bar{r}_i\|^2\} \leq P_{R,i}, \forall i \in \{1, 2, \dots, N\}. \end{aligned} \quad (4.17)$$

Using the quadratic reformulation in Section 4.2, problem (4.17) can be rewritten as

$$\begin{aligned} \max_{\mathbf{w}} \quad & \prod_{m=1}^{2K} \frac{\mathbf{w}^H \bar{\mathbf{A}}_m \mathbf{w} + \sigma_u^2}{\mathbf{w}^H \bar{\mathbf{C}}_m \mathbf{w} + \sigma_u^2} \\ \text{subject to} \quad & \mathbf{w}^H \mathbf{\Upsilon}_i \mathbf{w} \leq P_{R,i}, \forall i \end{aligned} \quad (4.18)$$

or equivalently

$$\begin{aligned} \max_{\mathbf{w}} \quad & \sum_{m=1}^{2K} (\log(\mathbf{w}^H \bar{\mathbf{A}}_m \mathbf{w} + \sigma_u^2) - \log(\mathbf{w}^H \bar{\mathbf{C}}_m \mathbf{w} + \sigma_u^2)) \\ \text{subject to} \quad & \mathbf{w}^H \mathbf{\Upsilon}_i \mathbf{w} \leq P_{R,i}, \forall i \end{aligned} \quad (4.19)$$

where $\bar{\mathbf{C}}_m = \mathbf{D}_m + \mathbf{E}_m$ and $\bar{\mathbf{A}}_m = \mathbf{B}_m + \bar{\mathbf{C}}_m$ are positive definite, and $\mathbf{\Upsilon}_i$ is defined below equation (4.5). Note that for simplicity the scalar $\frac{1}{2}$ is dropped and the natural logarithm is used instead. The formulations (4.18) or (4.19) are still non-convex.

4.4.1 Generalized polyblock Algorithm

In Section 4.3.1 we have proven that the sum rate maximization problem in such a relay network with a total power constraint satisfies the monotonic optimization framework. Similarly, problem (4.18) is also a monotonic optimization problem which can be solved using a unified algorithm, which is called the polyblock approximation approach [PT03]. In the following we prove that the problem (4.18) is a monotonic optimization problem and then adapt the polyblock algorithm to solve it.

Problem (4.18) is equivalent to the following problem

$$\max_{\mathbf{y}} \{\Phi(\mathbf{y}) | \mathbf{y} \in \mathbb{D}\} \quad (4.20)$$

where $\Phi(\mathbf{y}) = \prod_{m=1}^{2K} y_m$ and $\mathbb{D} = \mathbb{G} \cap \mathbb{L}$. The sets $\mathbb{G} = \{\mathbf{y} \in \mathbb{R}_+^{2K} | y_m \leq \max_{\mathbf{w}} \frac{\mathbf{w}^H \bar{\mathbf{A}}_m \mathbf{w} + \sigma_u^2}{\mathbf{w}^H \bar{\mathbf{C}}_m \mathbf{w} + \sigma_u^2}\}$ and $\mathbb{L} = \{\mathbf{y} \in \mathbb{R}_+^{2K} | y_m \geq \min_{\mathbf{w}} \frac{\mathbf{w}^H \bar{\mathbf{A}}_m \mathbf{w} + \sigma_u^2}{\mathbf{w}^H \bar{\mathbf{C}}_m \mathbf{w} + \sigma_u^2}\}$ are a normal set and a reverse normal set, respectively [PT03]. The domain of \mathbf{w} is defined as $\{\mathbf{w} \in \mathbb{C}^N | \mathbf{w}^H \mathbf{\Upsilon}_i \mathbf{w} \leq P_{R,i}, \forall i\}$. Moreover, the function $\Phi(\mathbf{y})$ is an increasing function since $\Phi(\bar{\mathbf{y}}) \geq \Phi(\tilde{\mathbf{y}})$, $\forall \bar{\mathbf{y}} \geq \tilde{\mathbf{y}}$. Thereby, problem (4.18) is the maximization of an increasing function over an intersection of normal and reverse normal sets. As shown in [PT03], such a formulation is a monotonic optimization problem. The definitions of the increasing function, the normal set, and the reverse normal set are the same as in [PT03].

Following the same procedure as in Section 4.3.1, the (ϵ, η) -optimal solution of problem

(4.18) is obtained. Note that the major difference between the problem in Section 4.3.1 and our problem is the calculation of $\gamma_k \in (0, 1]$ at the k -th step. The scalar γ_k determines the unique intersection between the ray through $\mathbf{0}$ and $\bar{\mathbf{y}}_k$ and the upper boundary $\partial^+ \mathbb{D}$ where $\bar{\mathbf{y}}_k$ is the vertex in \mathbb{T}_k which maximizes the function $\Phi(\mathbf{y})$. Instead of solving an unconstrained max-min problem as in Section 4.3.1, we need to solve the following constrained problem

$$\begin{aligned} \gamma_k = \max_{\mathbf{w}} \min_m & \frac{\mathbf{w}^H \bar{\mathbf{A}}_m \mathbf{w} + \sigma_u^2}{\bar{y}_{k,m} \mathbf{w}^H \bar{\mathbf{C}}_m \mathbf{w} + \sigma_u^2} \\ \text{subject to} & \mathbf{w}^H \boldsymbol{\Upsilon}_i \mathbf{w} \leq P_{R,i}, \forall i \end{aligned} \quad (4.21)$$

Similar as in [ZRH⁺12c], problem (4.21) is solved using semidefinite relaxation together with the bisection search (the concept of this method is elaborated in Section 4.4.3).

4.4.2 POTDC inspired approach

The computational complexity of the polyblock algorithm can be non-polynomial time in the worst case. Thus, it is worth to look for a polynomial time solution. In this section, we introduce a polynomial time solution which is similar as in Section 3.5.

Let us first define $\mathbf{X} = \mathbf{w}\mathbf{w}^H$. Using the SDR technique and dropping the rank-1 constraint, problem (4.19) can be reformulated as

$$\begin{aligned} \min_{\mathbf{X}, \alpha_m, \beta_m, \forall m} & - \sum_{m=1}^{2K} \log(\alpha_m) - \left(- \sum_{m=1}^{2K} \log(\beta_m) \right) \\ \text{subject to} & \text{Tr}\{\boldsymbol{\Upsilon}_i \mathbf{X}\} \leq P_{R,i}, \forall i, \\ & \text{Tr}\{\bar{\mathbf{A}}_m \mathbf{X}\} + \sigma_u^2 = \alpha_m, \\ & \text{Tr}\{\bar{\mathbf{C}}_m \mathbf{X}\} + \sigma_u^2 = \beta_m, \forall m, \\ & \mathbf{X} \geq 0. \end{aligned} \quad (4.22)$$

The objective function of problem (4.22) is a DC problem and therefore is non-convex and in general NP-hard. Inspired by the POTDC algorithm in [KRVH12], we replace the concave part of the objective function in (4.22) by its linear approximation, i.e., $\log(\beta_m)$ is replaced by its first order Taylor polynomial $\log(\beta_{0,m}) + \frac{\beta_m - \beta_{0,m}}{\beta_{0,m}}, \forall m$. After the substitutions, the cost function in (4.22) becomes convex. Finally, we obtain the following problem:

$$\min_{\mathbf{X}, \alpha_m, \beta_m, t_m, \forall m} - \sum_{m=1}^{2K} \log(\alpha_m) + \sum_{m=1}^{2K} t_m$$

$$\begin{aligned}
 \text{subject to } & \text{Tr}\{\mathbf{\Upsilon}_i \mathbf{X}\} \leq P_{R,i}, \forall i, \mathbf{X} \geq 0 \\
 & \text{Tr}\{\bar{\mathbf{A}}_m \mathbf{X}\} + \sigma_u^2 = \alpha_m, \\
 & \text{Tr}\{\bar{\mathbf{C}}_m \mathbf{X}\} + \sigma_u^2 = \beta_m \\
 & \log(\beta_{0,m}) + \frac{1}{\beta_{0,m}}(\beta_m - \beta_{0,m}) \leq t_m.
 \end{aligned} \tag{4.23}$$

Problem (4.23) is a convex SDP problem and can be solved using the standard interior-point algorithm [BV04].

Clearly, the first order Taylor polynomial approximation in problem (4.23) is the exact Taylor expansion of $\log(\beta_m)$ in (4.22) only if $\beta_{0,m}$ is equal to the optimal $\beta_{\text{opt},m}$. Thus, similarly as in Section 3.5, we apply the same iterative algorithm as in Algorithm 4 for obtaining the optimal \mathbf{X}_{opt} of problem (4.23). The proposed algorithm, which is described in Algorithm 7, has preserved the convergence properties from the original POTDC. That is, the optimal values obtained over the iterations are non-decreasing. Furthermore, the proposed algorithm provides a polynomial-time solution since it solves a sequence of convex problems. In the end, to obtain \mathbf{w}_{opt} we need to extract a rank-1 solution from \mathbf{X}_{opt} . In our work, the randomization technique described in [LMS⁺10] and Appendix B.3.5 is applied.

Algorithm 7 POTDC approach for solving problem (4.23)

- 1: **Initialize:** set initial values $\beta_{0,m}, \forall m$, maximum iteration number N_{max} and the tolerance factor ϵ .
 - 2: **Main step:**
 - 3: **for** $p = 1$ to N_{max} **do**
 - 4: Solve (4.23) finding optimal value $f^{*(p)}$ and $\beta_m^{(p)}$.
 - 5: $\beta_{0,m}^{(p+1)} = \beta_m^{(p)}, m = 1, \dots, 2K$
 - 6: **if** $\left| f^{*(p)} - f^{*(p-1)} \right| \leq \epsilon$ **then**
 - 7: **break**
 - 8: **end if**
 - 9: **end for**
-

4.4.3 Modified total SINR Eigen-Beamformer

Although the POTDC inspired algorithm has a comparable performance and guaranteed polynomial time solution compared to the polyblock algorithm, it requires iterations (approximately 10-20 iterations are required in general) and therefore is still computationally inefficient. To further reduce the computational complexity, we propose a low SNR approximation of problem (4.17), i.e., the total SINR eigen-beamformer (denoted as ToT in the simulation

results). As stated in Section 4.3.3, the total SINR eigen-beamformer aims at maximizing the ratio between the sum of the received signal powers of all the UTs and the sum of interference plus noise power of all the UTs. This beamformer design can be applied to our problem but a closed-form solution as in Section 4.3.3 cannot be obtained due to the individual relay power constraints. In the following we apply the concept of the total SINR eigen-beamformer and develop the solution to it.

Let us define $\mathbf{S}_{\text{tot}} = \sum_{m=1}^{2K} \mathbf{B}_m$ and $\mathbf{U}_{\text{tot}} = \sum_{m=1}^{2K} \bar{\mathbf{C}}_m$. Thus, $\mathbf{w}^H \mathbf{S}_{\text{tot}} \mathbf{w}$ and $\mathbf{w}^H \mathbf{U}_{\text{tot}} \mathbf{w}$ are the sum of the signal power and the sum of the interference power plus the forwarded noise power from all the relays, respectively. Then our proposed total SINR eigen-beamformer solves the following problem

$$\begin{aligned} \max_{\mathbf{w}} \quad & \frac{\mathbf{w}^H \mathbf{S}_{\text{tot}} \mathbf{w}}{\mathbf{w}^H \mathbf{U}_{\text{tot}} \mathbf{w} + 2K\sigma_u^2} \\ \text{subject to} \quad & \mathbf{w}^H \mathbf{\Upsilon}_i \mathbf{w} \leq P_{R,i}, \forall i \end{aligned} \quad (4.24)$$

Although problem (4.24) is in general non-convex and NP-hard, it is well studied in the literature, e.g., [GSS⁺10], [LPP11]. In our work, we use the SDR together with a bisection search which is similar to [GSS⁺10]. In the following we briefly introduce this algorithm. Applying the SDR method, problem (4.24) is reformulated as

$$\begin{aligned} \min_{\mathbf{X}, t} \quad & -t \\ \text{subject to} \quad & \text{Tr}\{\mathbf{\Upsilon}_i \mathbf{X}\} \leq P_{R,i}, \forall i, \mathbf{X} \geq 0 \\ & \text{Tr}\{(t\mathbf{U}_{\text{tot}} - \mathbf{S}_{\text{tot}})\mathbf{X}\} \leq -2Kt\sigma_u^2, \forall i \end{aligned} \quad (4.25)$$

For a fixed t , problem (4.25) is a feasibility check problem. Thereby, the optimal \mathbf{X}_{opt} can be obtained via a bisection search over an interval $[t_{\min}, t_{\max}]$. In our case, we select $t_{\min} = 0$ and $t_{\max} = \mathcal{P}((\mathbf{U}_{\text{tot}} + 2K\sigma_u^2 \mathbf{\Gamma} / (\sum_i P_{R,i}))^{-1} \mathbf{S}_{\text{tot}})$, where $\mathbf{\Gamma}$ is defined in equation (4.5). After obtaining \mathbf{X}_{opt} , the optimal beamforming vector \mathbf{w}_{opt} is found using the randomization techniques described in [LMS⁺10].

Next we prove that problem (4.24) is the low SNR approximation of the original problem (4.17). Applying the Taylor expansion of the logarithmic function $\log(1+x)$, we have $\forall m$

$$\log\left(1 + \frac{\mathbf{w}^H \mathbf{B}_m \mathbf{w}}{\mathbf{w}^H (\mathbf{D}_m + \mathbf{E}_m) \mathbf{w} + \sigma_u^2}\right) \approx \frac{\mathbf{w}^H \mathbf{B}_m \mathbf{w}}{\mathbf{w}^H (\mathbf{D}_m + \mathbf{E}_m) \mathbf{w} + \sigma_u^2}.$$

Using the fact that in the low SNR regime ($\sigma_R^2 \rightarrow +\infty$) $\mathbf{w}^H \mathbf{D}_m \mathbf{w} \ll \mathbf{w}^H \mathbf{E}_m \mathbf{w} \approx \sigma_R^2, \forall m$ and

thus $\mathbf{w}^H(\mathbf{D}_{\bar{m}} + \mathbf{E}_{\bar{m}})\mathbf{w} \approx \mathbf{w}^H(\mathbf{D}_{\bar{n}} + \mathbf{E}_{\bar{n}})\mathbf{w}$ for $\bar{m} \neq \bar{n}$ and $\{\bar{m}, \bar{n}\} \in \{1, \dots, 2K\}$, we can rewrite the objective function in (4.17) as

$$\begin{aligned} & \sum_{m=1}^{2K} \log \left(1 + \frac{\mathbf{w}^H \mathbf{B}_m \mathbf{w}}{\mathbf{w}^H (\mathbf{D}_m + \mathbf{E}_m) \mathbf{w} + \sigma_u^2} \right) \approx \sum_{m=1}^{2K} \frac{\mathbf{w}^H \mathbf{B}_m \mathbf{w}}{\mathbf{w}^H (\mathbf{D}_m + \mathbf{E}_m) \mathbf{w} + \sigma_u^2} \\ & \approx \frac{\sum_{m=1}^{2K} \mathbf{w}^H \mathbf{B}_m \mathbf{w}}{\sum_{m=1}^{2K} (\mathbf{w}^H (\mathbf{D}_m + \mathbf{E}_m) \mathbf{w} + \sigma_u^2)} = \frac{\mathbf{w}^H \mathbf{S}_{\text{tot}} \mathbf{w}}{\mathbf{w}^H \mathbf{U}_{\text{tot}} \mathbf{w} + 2K \sigma_u^2}. \end{aligned}$$

4.4.4 Interference neutralization based design

In this section, we propose a high SNR approximation of the original problem (4.17). The proposed algorithm is based on the interference neutralization which is a technique that tunes the interfering signals such that they neutralize each other at the receiver [MDF08a]. Mathematically, interference neutralization for our scenario requires that

$$\begin{cases} (\mathbf{f}_{2k-1} \odot \mathbf{f}_{2\ell-1})^H \mathbf{w} = 0 & \forall \ell, k, \ell \neq k \\ (\mathbf{f}_{2k-1} \odot \mathbf{g}_{2\ell})^H \mathbf{w} = 0 & \forall \ell, k, \ell \neq k \\ (\mathbf{g}_{2k} \odot \mathbf{f}_{2\ell-1})^H \mathbf{w} = 0 & \forall \ell, k, \ell \neq k \\ (\mathbf{g}_{2k} \odot \mathbf{g}_{2\ell})^H \mathbf{w} = 0 & \forall \ell, k, \ell \neq k. \end{cases} \quad (4.26)$$

where the first two equations, which are from equation (4.3), represent the interference from odd-indexed (i.e., $(2\ell - 1)$ -th) users and even-indexed (i.e., (2ℓ) -th) users to another odd-indexed (i.e., $(2k - 1)$ -th) user. Similar as equation (4.3), the received signal model for the even-indexed (i.e., $(2k)$ -th) users can be obtained and thus we get the last two equations of (4.26).

Utilizing the commutative property of the Hadamard product, $2K(K - 1)$ duplicated equations in (4.26) are removed and we have

$$\mathbf{H}^{(e)} \cdot \mathbf{w} = \mathbf{0}. \quad (4.27)$$

where $\mathbf{H}^{(e)}$ has a dimension of $2K(K - 1) \times N$. Define $\bar{i} \in \{1, \dots, K\}$ and $\bar{j} \in \{\bar{i} + 1, \dots, K\}$. The matrix $\mathbf{H}^{(e)}$ is generated by

$$\mathbf{H}^{(e)} = \left[\mathbf{f}_{2\bar{i}-1}^* \odot \mathbf{f}_{2\bar{j}-1}^* \quad \mathbf{f}_{2\bar{i}-1}^* \odot \mathbf{g}_{2\bar{j}}^* \quad \mathbf{g}_{2\bar{i}}^* \odot \mathbf{f}_{2\bar{j}-1}^* \quad \mathbf{g}_{2\bar{i}}^* \odot \mathbf{g}_{2\bar{j}}^* \right]^T.$$

Equation (4.27) is solvable only if the null space of $\mathbf{H}^{(e)}$ is not empty, i.e., $N > 2K(K-1)$. Define the SVD of $\mathbf{H}^{(e)} = \mathbf{U}\mathbf{\Sigma}[\mathbf{V}_s \ \mathbf{V}_n]^H$, where \mathbf{V}_n contains the last $(N - 2K(K-1))$ right singular vectors and thus forms an orthonormal basis for the null subspace of $\mathbf{H}^{(e)}$. Without loss of generality, we define the interference neutralization based beamformer (denoted as IntNeu in the simulation results) as $\mathbf{w} = \mathbf{V}_n \bar{\mathbf{w}}$, where $\bar{\mathbf{w}} \in \mathbb{C}^{N-2K^2+2K}$ has a smaller dimension than $\mathbf{w} \in \mathbb{C}^N$. In other words, searching over $\bar{\mathbf{w}}$ yields a lower computational complexity. Furthermore, observing that we have $\mathbf{w}^H \mathbf{E}_m \mathbf{w} \rightarrow \sigma_R^2, \forall m$ also in the high SNR regime ($\sigma_R^2 \rightarrow 0$), the cost function in (4.19) is then reformulated as

$$\sum_{m=1}^{2K} \log(\bar{\mathbf{w}}^H \mathbf{V}_n^H \bar{\mathbf{A}}_m \mathbf{V}_n \bar{\mathbf{w}} + \sigma_u^2) - \sum_{m=1}^{2K} \log(\sigma_R^2 + \sigma_u^2) \quad (4.28)$$

Replacing the cost function in (4.19) by (4.28) and dropping the constant terms, we obtain the following problem

$$\begin{aligned} \max_{\bar{\mathbf{w}}} \quad & \sum_{m=1}^{2K} \log(\bar{\mathbf{w}}^H \bar{\mathbf{A}}_m \bar{\mathbf{w}} + \sigma_u^2) \\ \text{subject to} \quad & \bar{\mathbf{w}}^H \bar{\mathbf{\Upsilon}}_i \bar{\mathbf{w}} \leq P_{R,i}, \forall i \end{aligned} \quad (4.29)$$

where $\bar{\mathbf{A}}_m = \mathbf{V}_n^H \mathbf{A}_m \mathbf{V}_n, \forall m$ and $\bar{\mathbf{\Upsilon}}_i = \mathbf{V}_n^H \mathbf{\Gamma}_{ii} \mathbf{e}_i \mathbf{e}_i^H \mathbf{V}_n$. Again applying the SDR, we have the following convex SDP problem

$$\begin{aligned} \min_{\bar{\mathbf{X}}, \bar{\alpha}_m, \forall m} \quad & - \sum_{m=1}^{2K} \log(\bar{\alpha}_m) \\ \text{subject to} \quad & \text{Tr}\{\bar{\mathbf{\Upsilon}}_i \bar{\mathbf{X}}\} \leq P_{R,i}, \forall i, \mathbf{X} \geq 0 \\ & \text{Tr}\{\bar{\mathbf{A}}_m \bar{\mathbf{X}}\} + \sigma_u^2 = \bar{\alpha}_m. \end{aligned} \quad (4.30)$$

where $\bar{\mathbf{X}} = \bar{\mathbf{w}} \bar{\mathbf{w}}^H$. After obtaining the optimal $\bar{\mathbf{X}}_{\text{opt}}$, the rank-1 extraction of $\mathbf{V}_n \bar{\mathbf{X}}_{\text{opt}} \mathbf{V}_n^H$, which is computed using the randomization technique, yields the final \mathbf{w}_{opt} .

4.5 Simulation results

In this section, the performance of the proposed algorithms is evaluated via Monte-Carlo simulations. The simulated flat fading channels are spatially uncorrelated Rayleigh fading channels. The total relay power P_R is fixed to unity. The noise variances at all nodes are the same, i.e., $\sigma_R^2 = \sigma_u^2$ and thus $\text{SNR} = 1/\sigma_u^2$. There are $K = 2$ pairs of users in the network. All the simulation results are obtained by averaging over 1000 channel realizations.

4.5.1 A sum transmit power constraint for the relays in the network

“Polyblock”, “GPM”, “Total SINR”, and “Method 1” denote the algorithms in Sections 4.3.1, 4.3.2, 4.3.3, and [WCY⁺11], respectively. For the polyblock algorithm, $\epsilon = 10^{-1}$ and $\eta = 10^{-6}$.

Figure 4.2 shows the comparison of different algorithms with $N = 5$ relays and $N = 12$ relays in the network. “Method 1” is available only for the case $N = 12$ since it requires that $N \geq 2K^2 + K$. It is obvious that “Polyblock”, “GPM” and “Total SINR” outperform “Method 1”. One possible reason is that in “Method 1” a part of the transmit power is used to force the self-interference power to a certain level. The polyblock algorithm performs slightly worse than the GPM algorithm. This is due to the (ϵ, η) -optimality. Moreover, the total SINR eigen-beamformer performs almost the same as the optimal solution with a small number of relays ($N = 5$) and suffers only a small loss when many relays ($N = 12$) exist.

Figures 4.3, 4.4, and 4.5 demonstrate the convergence behavior of the POTDC inspired algorithm, the GPM algorithm, and the polyblock approach, when a total transmit power constraint is considered, respectively. As can be seen, the POTDC approach provides the fastest convergence speed in all cases. The polyblock approach provides the worst convergence behavior. As we discussed in Section 4.3.2, the convergence speed of the GPM scheme increases when the number of relays increases in the network or the SNR is high.

4.5.2 Individual relay transmit power constraints

“Polyblock”, “POTDC”, “ToT”, and “IntNeu” denote the algorithms in Sections 4.4.1, 4.4.2, 4.4.3, and 4.4.4, respectively. For the polyblock algorithm, the POTDC algorithm, and the ToT algorithm, the stopping criterion is set to be a tolerance factor of 10^{-4} .

Figure 4.6 shows the comparison of different algorithms with $N = 6$ relays and $N = 12$ relays in the network. Clearly, the POTDC algorithm has close to optimal performance especially in the low SNR regime and when there is a sufficient number of relays in the network (e.g., $N = 12$). Thus, the POTDC algorithm can also be used as a benchmark for the other suboptimal algorithms since it has a lower computational complexity but a comparable performance when compared to the global optimal solution.

Figure 4.7 demonstrates the comparison of different suboptimal algorithms. As depicted in the figure, the modified total SINR eigen-beamformer (denoted by “ToT”) and the interference neutralization based design (denoted by “IntNeu”) show a low SNR performance and a high SNR performance of the global optimum solution, respectively. Moreover, when there are enough relays in the network, both the distributed total SINR eigen-beamformer and the interference neutralization based design are very close to the optimum solution but have a

much lower computational complexity.

4.6 Summary

In this chapter, we investigate the sum rate maximization problem in multi-pair AF TWR networks with multiple single antenna relays, which has been firstly studied by us in [ZRH⁺12c, ZRH12a]. Unlike the multi-operator TWR networks in Chapter 3, a relay transmit beamformer instead of a relay amplification matrix has to be designed. Given a total network power constraint, the optimization problem is quite similar to the one in Sections 3.4.1 and 3.5 and thus the power method and the POTDC based approach can be directly applied. But it is not possible to apply the ProBaSeMO approach here. When a sum power constraint is considered, the optimization problem fits into the monotonic optimization framework and thus can be solved using the generalized polyblock approximation algorithm. Since the optimality condition yields a generalized eigenvalue problem, we apply the GPM algorithm, which is based on the power method in Sections 3.4.1. To reduce the computational complexity, we propose the total SINR eigen-beamformer which maximizes the total SINR of the network. When each relay in the network has its own transmit power constraint, the optimization problem becomes more challenging. Most of the aforementioned methods cannot be applied directly. Nevertheless, by modifying the polyblock algorithm and the POTDC approach, it is possible to solve the optimization problem accordingly. Again, considering the computational complexity, we propose a modified version of the total SINR eigen-beamformer method. The modified total SINR eigen-beamformer is a low SNR approximation of the original problem. We also propose an interference neutralization based design which provides a high SNR approximation of the optimum solution.

Simulation results have illustrated that

- When a sum relay transmit power is considered, all the proposed algorithms outperform the state of the art algorithm in [WCY⁺11]. Moreover, the proposed total SINR eigen-beamformer only suffers a little loss compared to the polyblock algorithm and the GPM algorithm.
- When each relay has its own transmit power constraint, the achievable system sum rate is slightly worse compared to the case with a total transmit power constraint. Moreover, the proposed modified total SINR eigen-beamformer is close to the polyblock algorithm and the generalized POTDC algorithm when there is a sufficient number of relays in the network. The same performance can be observed for the proposed interference neu-

tralization based design, which has the lowest computational complexity among all the proposed algorithms.

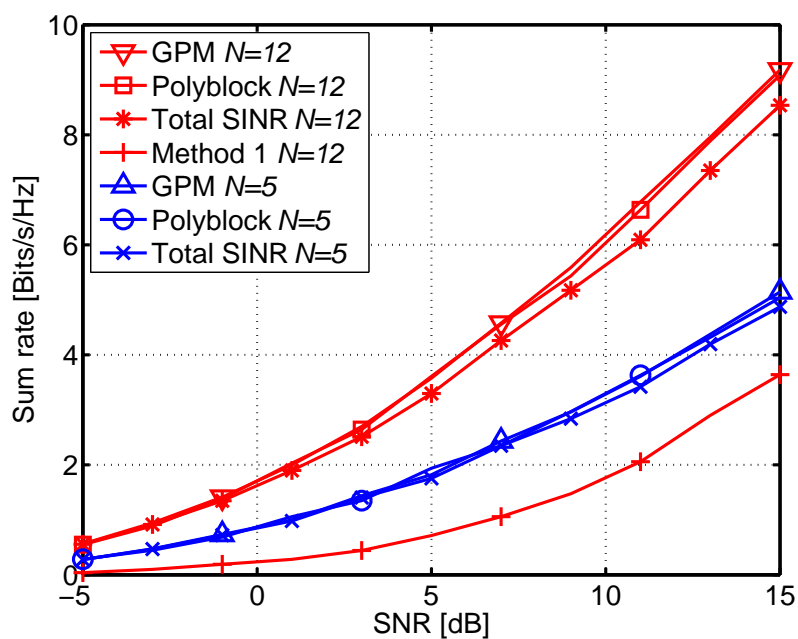


Figure 4.2: Sum rate comparison of the proposed algorithms under a total transmit power constraint.

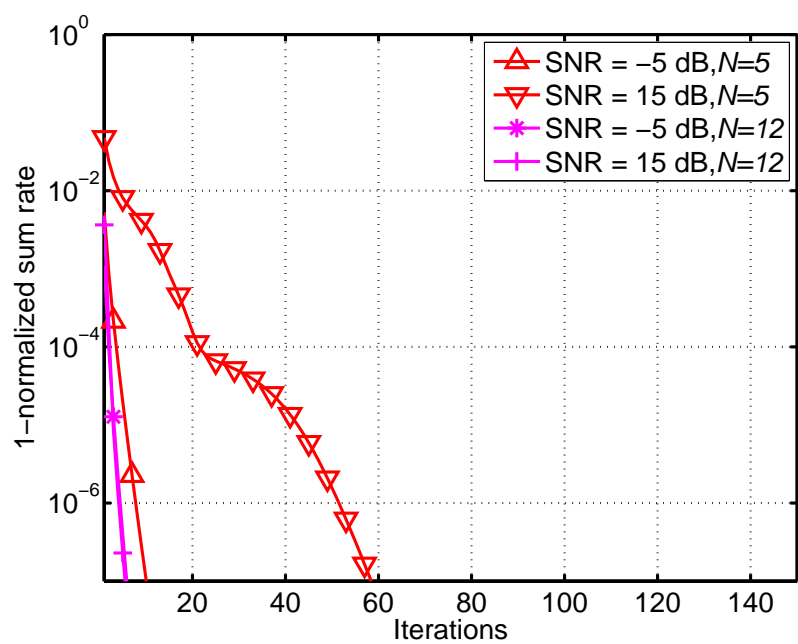


Figure 4.3: Convergence property of the POTDC inspired method with different N and SNRs. Averaged over 100 channel realizations.

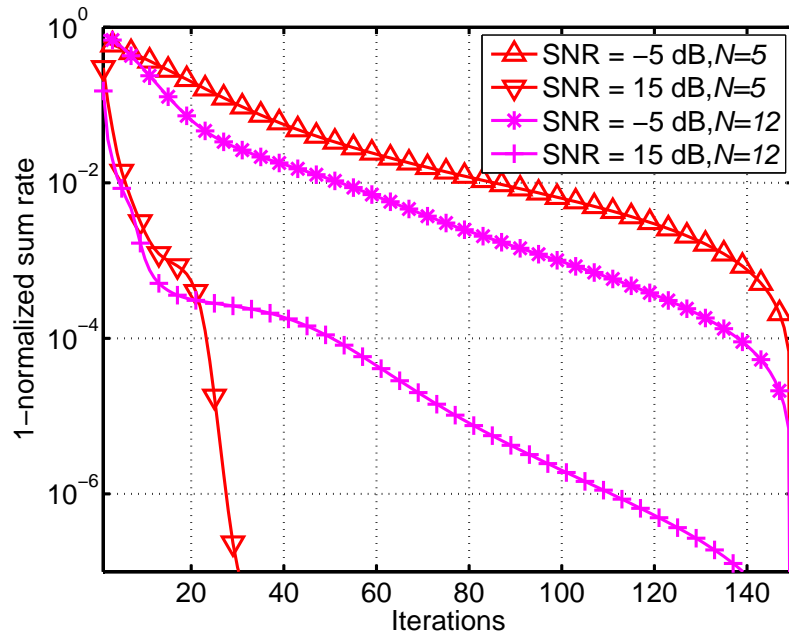


Figure 4.4: Convergence property of GPM with different N and SNRs. Averaged over 100 channel realizations.

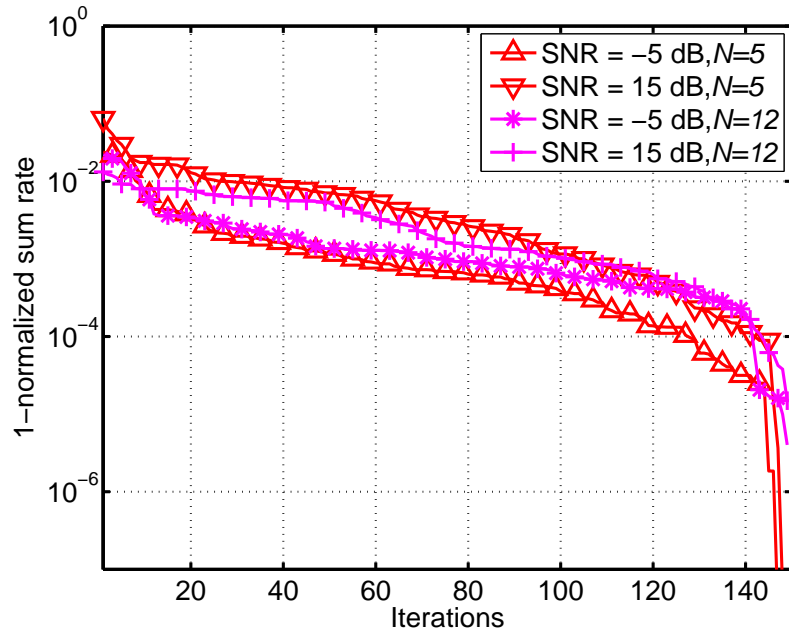


Figure 4.5: Convergence property of the polyblock approach with different N and SNRs. Averaged over 100 channel realizations.

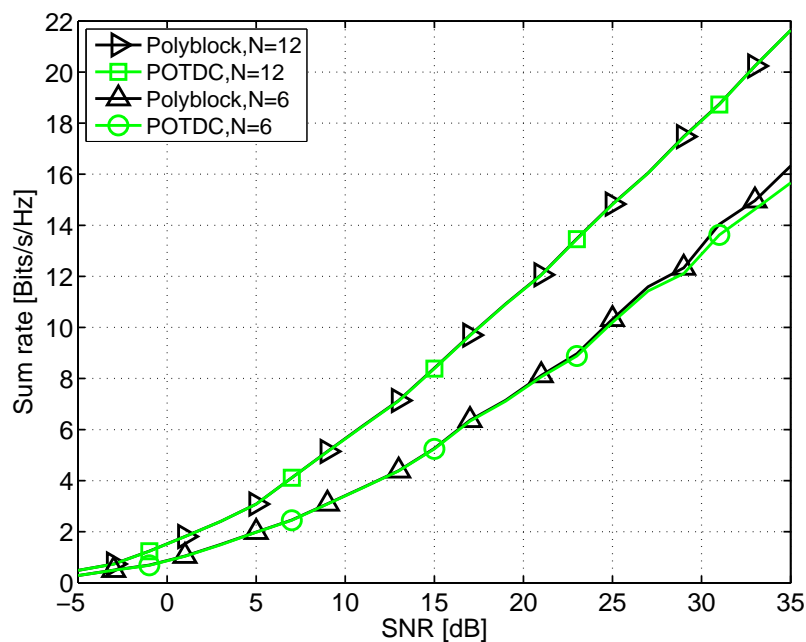


Figure 4.6: Sum rate comparison of the polyblock algorithm and the POTDC algorithm under individual relay transmit power constraints.

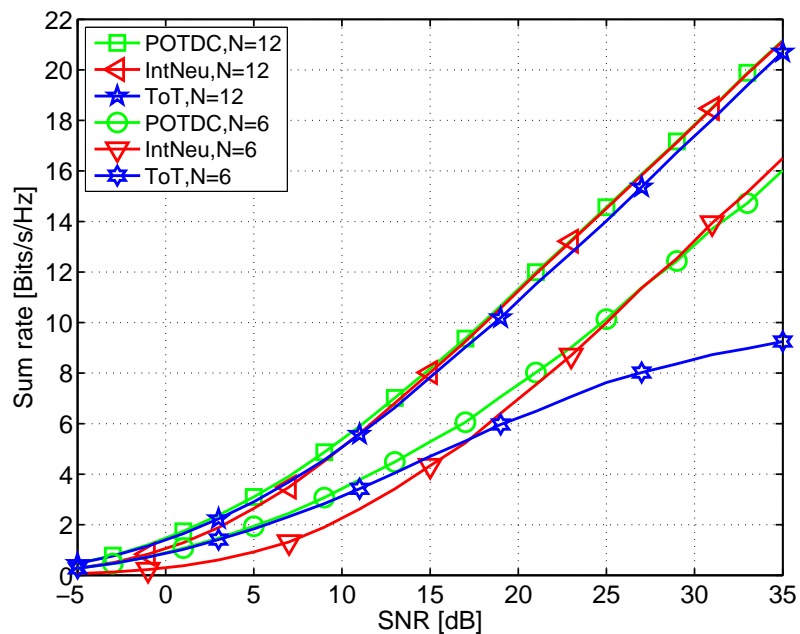


Figure 4.7: Sum rate comparison of the POTDC algorithm, the total SINR eigen-beamformer (low SNR approximation), and the interference neutralization based design (high SNR approximation) under individual relay transmit power constraints.

5 Multi-pair relaying networks with non-cooperative repeaters

In this chapter we look at a more general multi-pair TWR scenario, i.e., a TWR network with multiple repeaters and smart relays, where the smart relays use the AF relaying strategy. The relaying network here is more general because the scenarios, which are studied in previous chapters, can be seen as special cases of the considered scenario. Our contribution is summarized as a general framework to optimize different system utility functions in a TWR with repeaters and smart relay nodes with and without interference neutralization [ZHJH14c, ZHJH14a, ZHJH14b]. In this part, we first introduce the system model and perform necessary algebraic manipulations on it in Section 5.3. Then in Section 5.4 we derive necessary and sufficient conditions for realizing interference-free transmission using interference neutralization. Afterwards, we design optimal relay amplification matrices, which minimize the required transmit power at the relays subject to minimum SINR constraints, maximize the minimum SINR of the users subject to relay transmit power constraint(s), or maximize the weighted system sum rate subject to relay transmit power constraint(s), regardless whether the smart relays in the network have a total transmit power limit or individual transmit power limits in Sections 5.5, 5.6, and 5.7, respectively. Finally, the proposed methods are evaluated in Section 5.8 and a conclusion is drawn in Section 5.9.

5.1 State of the art

Interference is one major bottleneck on the capacity of wireless networks. Recently a number of new ideas and techniques have been developed in network information theory [EK11]. These approaches led to the optimal resource allocation and transceiver design of single-hop multi-cell systems [BJ13]. However, in modern networks such as LTE and WiMAX [IEE09], wireless links can be connected using layer-1 repeaters (simple amplifiers) [Sei09, BSR⁺13]. The advantage of non-regenerative relaying strategies is that the relay is transparent to the modulation and coding schemes and thus offers a flexible implementation. Furthermore, it induces negligible signal processing delays [BUK⁺09]. The notion of *relay-without-delays*, also known as instantaneous relays if the relays are memoryless [EH05, EHM07, CJ09, LJ11], refers to relays that forward signals consisting of both current symbol and symbols in the past, instead of only the past symbols as in conventional relays. Therefore, we assume that the relays

employ an AF, i.e., a non-regenerative, strategy.

In multi-hop interference networks, one way to manage interference is to choose the transmit and receive strategies such that the interference components cancel over different paths when arriving at a destination node. This is usually termed as interference neutralization (IN). IN has been applied to eliminate interference in various single-carrier systems, such as deterministic channels [MDF08b, MDT09], together with other interference management techniques, e.g., interference separation, interference alignment, and interference suppression. For two-hop relay channels IN is studied in [BUK⁺09, BW05] where it is termed multi-user ZF relaying. In [LLL13], the generalized degrees of freedom of a two-way MIMO relay interference channel are studied. In [RW07] partial and complete interference cancellation in two-way and two-path relaying is proposed and compared. Finally, in [ZRH12a] and in Chapter 4, the maximization of the sum rate of a multi-pair two-way AF relaying network where each relay has its individual power constraint is studied. In [LJ13] the degrees of freedom of the two-cell two-hop MIMO interference channel are described and an interference-free relay transmission scheme is proposed. Instantaneous relay channels are considered in [HJ12] and interference neutralization is compared to the optimal relaying strategy obtained by non-convex complex optimization.

In relay-enhanced cellular systems, instantaneous relays originate from the coexistence of layer-1 repeaters and smart non-regenerative relays. Both operate on the same time scale: Signals traveling over layer-1 repeaters and smart AF relays arrive symbol-synchronous at the receivers (see example LTE scenario in [HJG13b]). This results in an effective instantaneous relay model. In an adversarial environment in which receivers act as well-behaved but curious nodes, the IN technique can be successfully applied to avoid information leakage [HJG13b].

When multiple pairs of users access the network via the help of MIMO relays, the design of the relay amplification matrices becomes more complicated. This is due to the fact that each pair of users in this network suffers from the interference caused by the other users especially in the high SNR regime. Thus, the inter-pair interference has to be dealt with properly. Previous work on multi-pair TWR systems with a single MIMO relay includes optimal designs [FWY13], [TW12], [ZBR⁺12] and suboptimal designs [YZGK10], [ZRH12b], [JS10]. All the suboptimal schemes use the concept of interference cancellation or suppression. In [JS10], closed-form relay transmit strategies are obtained based on ZF and MMSE criteria. In [YZGK10], the relay amplification matrix is designed using a singular value decomposition (SVD) to null the interference. A more general SVD-based algorithm is proposed in [ZRH12b], where the design principle is to null the inter-pair interference first and then to optimize each sub-system (pair) independently. Conversely, an optimal design does not necessarily rely on interference cancellation. Moreover, the known optimal designs use the fact that the

relay amplification matrix can be stacked into a vector. Thereby, system utilities such as max-min fairness in [TW12] and power minimization in [ZBR⁺12] (in Section 3.6) turn into quadratic programming problems, which can be solved using convex optimization techniques. In [FWY13], this approach was generalized such that all the utility functions are reformulated as a max-min fairness problem.

Nevertheless, IN has not been studied for a general multi-pair TWR network with multiple AF relays prior to our work. The general scenario can include the TWR scenario with direct user terminal links (via dummy repeaters) or not. Thereby, it is more general than the multi-pair two-way MIMO relay interference channel. Furthermore, our system operates with finite relay and terminal transmit power. Therefore the feasibility of IN depends on the system parameters (number of antennas and links) but also on the terminal and relay transmit powers. Moreover, neither optimal relay transmit strategies nor IN based suboptimal strategies have been studied prior to our work. Therefore, our problem is more general. But it is also more challenging due to the involvement of multiple relays, which can have their own transmit power limitation.

5.2 Our contributions

In this chapter, we develop a general framework to optimize different system utility functions in a two-way relay network with repeater and smart relay nodes with and without interference neutralization. Sufficient and necessary conditions for interference neutralization under different system settings have been characterized and proven. Optimal relay amplification matrices, which minimize the required transmit power at the relay subject to minimum SINR constraints, maximize the minimum SINR of the users subject to relay transmit power constraint(s), and maximize the weighted system sum rate subject to relay transmit power constraint(s) have been derived regardless whether the smart relays in the network have a total transmit power limit or individual transmit power limits. The major contributions are summarized in the following.

5.2.1 Distributed relay nodes vs. relay clusters

To have a better network resource management, given a total number of antennas, we study the problem of antenna assignment in a relay-assisted wireless network. This is a relevant question in network planning and resource management. In one extreme, it is possible to group all antennas in one mega relay which is powerful and manages all network resources and traffic. In another extreme, we can use a single antenna per relay, such as in sensor networks.

Or, as a compromise between both schemes, bundles of antennas are distributed in various locations in the network. We discuss the feasibility of interference neutralization with two-way relaying in these settings in Section 5.4.

We provide a very interesting result which shows *how the required total number of antennas in the network decreases when clusters of relays can be formed*. For example, when single antenna relays cannot cooperate with each other, one needs $NM_R \geq 2K(K-1)$ antennas in total, where N , M_R , and K denote the number of relays, the number of antennas at each relay and the number of user pairs, respectively. However, if we allow 3 single antenna relays to form a cluster - a multi-antenna relay, the number of antennas required in the network decreases by half: $NM_R \geq K(K-1)$.

5.2.2 The minimum required transmit power to perform IN

To neutralize the interference, a certain amount of power has to be available at the relay. Then the question arises regarding the minimum required transmit power to perform IN in the network. This problem is solved and analytic solutions are provided in Section 5.4. Similar to the discussion about the distribution of the antennas, the general trend is that the required power decreases as the number of antennas at each relay increases. It increases as the number of pairs increases. However, the decrease is not monotonic. Moreover, for fixed K , we show that the required transmit power depends on the value of $\frac{1}{2}NM_R(M_R+1) - 2K(K-1)$, which represents the available spatial dimensions that can be used to scale down the required transmit power. The higher this value is, the less power is required to perform IN.

5.2.3 Optimal relay amplification matrices

For the considered scenario it is interesting to know the optimal relay amplification matrices under different system utility functions, e.g., minimizing the required transmit power at the relay, balancing the achievable SINR of the users, and maximizing the weighted sum rate. Although IN nulls the interference in the system, in general the structure of the considered optimization problems remains unchanged after the interference is canceled. This is due to the forwarded noise of the AF relaying strategy. Thus, the system with and without IN share the same optimal solution. The difference is that less parameters need to be optimized after applying IN. Moreover, the optimal solution for the case where the relays in the network have a total transmit power limit can be extended to the case where each relay has its own transmit power limit. Furthermore, all the formulated problems are in general non-convex QCQP problems. But they can be relaxed into SDP problems using SDR techniques. Numerical

results show that the obtained solutions are almost always rank-1. Specifically, when the SINR balancing problem is considered, we propose a generalized Dinkelbach-type (DT) algorithm, which includes two versions, namely, DT-1 and DT-2. The convergence speed of the proposed algorithm is proven to be at least linearly in general. If a DT-2 algorithm is applied, a better convergence can be obtained. When the weighted sum rate problem is considered, we propose a polyblock approach which can be applied to obtain a globally optimal solution.

5.2.4 Orthogonal vs non-orthogonal resource access

In such an interference limited network, one way to avoid the interference is to let the users access the resources in the network, e.g., the smart relays, in an orthogonal way. This leads to the question when it is better to perform an orthogonal resource access than a non-orthogonal resource access, and vice versa. We answer this question by comparing our proposed non-orthogonal relay access schemes to an orthogonal relay access scheme, where the smart relays are used by different pairs of users in a time-shared approach as described in Section 5.8. Simulation results show that the non-orthogonal approach is preferred when the noise power is low and when there are many antennas at the relay (given a fixed $N \cdot M_R$).

5.3 Preliminaries

5.3.1 System model

The scenario under investigation is shown in Figure 5.1, where K pairs of single antenna UTs communicate with each other via the help of N smart relays and K dumb repeaters. Each smart relay has M_R antennas. All the nodes are half-duplex. We assume that the channel is frequency flat and quasi-static block fading. The channel vector from the $(2k-1)$ -th UT to the n -th relay is denoted as $\mathbf{f}_{2k-1,n} \in \mathbb{C}^{M_R}$ ($n \in \{1, \dots, N\}$) and the cascaded channel vector of the $(2k-1)$ -th UT to all the relays is $\mathbf{f}_{2k-1} = [\mathbf{f}_{2k-1,1}^T, \dots, \mathbf{f}_{2k-1,N}^T]^T \in \mathbb{C}^{NM_R}$. Meanwhile, the channel from the $(2k)$ -th user to the n -th relay is denoted as $\mathbf{g}_{2k,n} \in \mathbb{C}^{M_R}$ and the cascaded channel vector of the $(2k)$ -th UT to all the relays is $\mathbf{g}_{2k} = [\mathbf{g}_{2k,1}^T, \dots, \mathbf{g}_{2k,N}^T]^T \in \mathbb{C}^{NM_R}$, for $k \in \{1, 2, \dots, K\}$. The repeaters in the network do not cooperate with each other and amplify only their received signals [HJ12]. Therefore, the equivalent channel from the i -th UT to the j -th UT via the network of repeaters is modeled as an effective channel, which is denoted as $h_{i,j}$ ($\{i, j\} \in \{1, \dots, 2K\}$). We assume that the reciprocity holds for the smart relay channel as well as for the repeaters' channels such that $h_{i,j} = h_{j,i}$. This is valid in an ideal TDD system. The signals passing through the repeaters and the smart relays are assumed to arrive at the

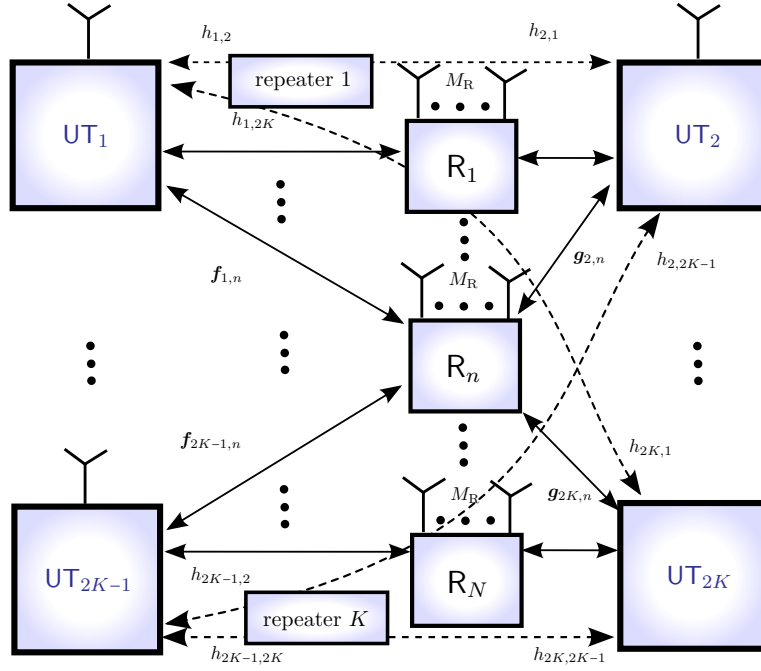


Figure 5.1: Multi-pair two-way relaying with multiple repeaters and amplify-and-forward relays where each relay has M_R antennas.

destination at the same time (symbol-synchronous). The transmission takes two time slots. In the first time slot, all the UTs transmit to the relays and the repeaters. The signals received at the n -th relay can be combined in a vector as

$$\mathbf{r}_n = \sum_{k=1}^K (\mathbf{f}_{2k-1,n} s_{2k-1} + \mathbf{g}_{2k,n} s_{2k}) + \mathbf{n}_{R,n} \in \mathbb{C}^{M_R} \quad (5.1)$$

where s_m ($m \in \{1, 2, 3, \dots, 2K\}$) is i.i.d. with zero mean and variance P_m and $\mathbf{n}_{R,n}$ represents ZMCSCG noise with covariance matrix $\mathbb{E}\{\mathbf{n}_{R,n} \mathbf{n}_{R,n}^H\} = \sigma_R^2 \mathbf{I}_{M_R}$, for all $1 \leq n \leq N$. In the second time slot, the repeaters simply amplify and forward the received signal while the n -th relay amplifies its received signal and transmits

$$\bar{\mathbf{r}}_n = \mathbf{W}_n \mathbf{r}_n \quad (5.2)$$

where $\mathbf{W}_n \in \mathbb{C}^{M_R \times M_R}$ is the relay amplification matrix. The relay transmit power constraint has to be fulfilled such that

$$\mathbb{E}\{\|\bar{\mathbf{r}}_n\|^2\} \leq P_{R,\max}^{(\text{Ind})}, \quad \text{for all } 1 \leq n \leq N, \quad (5.3)$$

if identical individual relay power constraints are considered, e.g., as in [ZRH12a]. Alternatively,

$$\sum_{n=1}^N \mathbb{E}\{\|\bar{\mathbf{r}}_n\|^2\} \leq P_{R,\max}, \quad (5.4)$$

if a total sum relay power constraint is considered, e.g. as in [ZRH⁺12c]. Finally, the received signal at the $(2k-1)$ -th user can be written as

$$\begin{aligned} y_{2k-1} = & \underbrace{(h_{2k-1,2k} + \mathbf{f}_{2k-1}^T \tilde{\mathbf{W}} \mathbf{g}_{2k})}_{\text{desired signal}} s_{2k} + \underbrace{(h_{2k-1,2k-1} + \mathbf{f}_{2k-1}^T \tilde{\mathbf{W}} \mathbf{f}_{2k-1})}_{\text{self-interference}} s_{2k-1} \\ & + \underbrace{\sum_{\substack{\ell \neq k \\ \ell=1}}^K (h_{2k-1,2\ell-1} + \mathbf{f}_{2k-1}^T \tilde{\mathbf{W}} \mathbf{f}_{2\ell-1}) s_{2\ell-1}}_{\text{from left inter-pair interference}} + \underbrace{\sum_{\substack{\ell \neq k \\ \ell=1}}^K (h_{2k-1,2\ell} + \mathbf{f}_{2k-1}^T \tilde{\mathbf{W}} \mathbf{g}_{2\ell}) s_{2\ell}}_{\text{from right inter-pair interference}} + \underbrace{\mathbf{f}_{2k-1}^T \tilde{\mathbf{W}} \bar{\mathbf{n}}_R + n_{2k-1}}_{\text{effective colored noise}} \end{aligned}$$

where $\bar{\mathbf{n}}_R = [\mathbf{n}_{R,1}^T \ \dots \ \mathbf{n}_{R,N}^T]^T$ and $\tilde{\mathbf{W}} \in \mathbb{C}^{NM_R \times NM_R}$ is a block diagonal matrix which is defined as $\tilde{\mathbf{W}} = \text{blkdiag}\{\mathbf{W}_n\}_{n=1}^N$ and n_{2k-1} denotes the ZMCSCG noise with variance σ_U^2 , for all $1 \leq k \leq K$. Assume that the CSI is known at the receiver. The self-interference term can be subtracted and thus we get

$$\hat{y}_{2k-1} = y_{2k-1} - (h_{2k-1,2k-1} + \mathbf{f}_{2k-1}^T \tilde{\mathbf{W}} \mathbf{f}_{2k-1}) s_{2k-1}. \quad (5.5)$$

5.3.2 Derivation of the SINR and the actual transmit power of the relays without interference neutralization

The goal of this section is to arrive at quadratic formulas for the SINR expressions and the transmit power constraints at the relay with or without IN. The derived quadratic forms are highlighted by boxes.

Let $\tilde{\mathbf{w}} = [\text{vec}\{\mathbf{W}_1\}^T \ \dots \ \text{vec}\{\mathbf{W}_N\}^T]^T \in \mathbb{C}^{NM_R^2}$. Define $\tilde{\mathbf{F}}_{2k-1} = \text{unvec}_{M_R \times N}\{\mathbf{f}_{2k-1}\}$, $\tilde{\mathbf{G}}_{2k} = \text{unvec}_{M_R \times N}\{\mathbf{g}_{2k}\}$, $\tilde{\mathbf{F}}_{2\ell-1} = \text{unvec}_{M_R \times N}\{\mathbf{f}_{2\ell-1}\}$ and $\tilde{\mathbf{G}}_{2\ell} = \text{unvec}_{M_R \times N}\{\mathbf{g}_{2\ell}\}$. Define $\mathbf{h}_{2k-1,2k} = \text{vec}\{\tilde{\mathbf{G}}_{2k} \diamond \tilde{\mathbf{F}}_{2k-1}\}$, $\mathbf{h}_{2k-1,2\ell-1} = \text{vec}\{\tilde{\mathbf{F}}_{2\ell-1} \diamond \tilde{\mathbf{F}}_{2k-1}\}$ and $\mathbf{h}_{2k-1,2\ell} = \text{vec}\{\tilde{\mathbf{G}}_{2\ell} \diamond \tilde{\mathbf{F}}_{2k-1}\}$. Define $\tilde{\mathbf{H}}_{2k-1} = \text{blkdiag}\{\mathbf{I}_{M_R} \otimes \mathbf{f}_{2k-1,n}\}_{n=1}^N$. The received effective data in (5.5) can be rewritten as

$$\begin{aligned} \hat{y}_{2k-1} = & (h_{2k-1,2k} + \mathbf{h}_{2k-1,2k}^T \tilde{\mathbf{w}}) s_{2k} \\ & + \sum_{\substack{\ell \neq k \\ \ell=1}}^K (h_{2k-1,2\ell-1} + \mathbf{h}_{2k-1,2\ell-1}^T \tilde{\mathbf{w}}) s_{2\ell-1} + \sum_{\substack{\ell \neq k \\ \ell=1}}^K (h_{2k-1,2\ell} + \mathbf{h}_{2k-1,2\ell}^T \tilde{\mathbf{w}}) s_{2\ell} + \tilde{\mathbf{w}}^T \tilde{\mathbf{H}}_{2k-1} \bar{\mathbf{n}}_R + n_{2k-1}. \end{aligned}$$

The SINR of the $(2k-1)$ -th UT is calculated as

$$\gamma_{2k-1} = \frac{P_{2k-1}^{(S)}}{P_{2k-1}^{(I)} + P_{2k-1}^{(N)}}$$

where the signal power $P_{2k-1}^{(S)}$, the interference power $P_{2k-1}^{(I)}$, and the effective noise power $P_{2k-1}^{(N)}$ are defined as $P_{2k-1}^{(S)} = P_{2k} |h_{2k-1,2k} + \mathbf{h}_{2k-1,2k} \tilde{\mathbf{w}}|^2$, $P_{2k-1}^{(I)} = \sum_{\substack{\ell \neq k \\ \ell=1}}^K (P_{2\ell-1} |h_{2k-1,2\ell-1} + \mathbf{h}_{2k-1,2\ell-1} \tilde{\mathbf{w}}|^2 + P_{2\ell} |h_{2k-1,2\ell} + \mathbf{h}_{2k-1,2\ell} \tilde{\mathbf{w}}|^2)$, and $P_{2k-1}^{(N)} = \sigma_{\text{R}}^2 \|\tilde{\mathbf{w}}^T \bar{\mathbf{H}}_{2k-1}\|^2 + \sigma_{\text{U}}^2$.

Utilizing the Charnes-Cooper transform [CC62], we let $\boldsymbol{\eta}_1/\beta_1 = \tilde{\mathbf{w}}$ and $\mathbf{w}_1 = [\boldsymbol{\eta}_1^T \quad \beta_1]^T \in \mathbb{C}^{NM_{\text{R}}^2+1}$, where $\beta_1 \in \mathbb{C}$ is arbitrary with $|\beta_1| = 1$. Then we can express the signal power $P_{2k-1}^{(S)}$ as

$$P_{2k-1}^{(S)} = P_{2k} |h_{2k-1,2k} + \mathbf{h}_{2k,2k-1}^T \tilde{\mathbf{w}}|^2 = \frac{P_{2k}}{|\beta_1|^2} |\beta_1 \cdot h_{2k-1,2k} + \mathbf{h}_{2k,2k-1}^T \boldsymbol{\eta}_1|^2 = \mathbf{w}_1^H \mathbf{E}_{2k-1}^{(g)} \mathbf{w}_1,$$

where $\mathbf{E}_{2k-1}^{(g)} = P_{2k} \bar{\mathbf{h}}_{2k-1,2k}^* \bar{\mathbf{h}}_{2k-1,2k}^T$ and $\bar{\mathbf{h}}_{i,j} = [\mathbf{h}_{i,j}^T \quad h_{i,j}]^T$, $\forall i, j$. It is straightforward to apply similar derivations to the interference power $P_{2k-1}^{(I)}$ and the effective noise power $P_{2k-1}^{(N)}$. The generalized SINR expression of the $(2k-1)$ -th UT is then given by

$$\boxed{\gamma_{2k-1} = \frac{\mathbf{w}_1^H \mathbf{E}_{2k-1}^{(g)} \mathbf{w}_1}{\mathbf{w}_1^H \mathbf{F}_{2k-1}^{(g)} \mathbf{w}_1}} \quad (5.6)$$

where

$$\mathbf{F}_{2k-1}^{(g)} = \sum_{\substack{\ell \neq k \\ \ell=1}}^K (P_{2\ell-1} \bar{\mathbf{h}}_{2k-1,2\ell-1}^* \bar{\mathbf{h}}_{2k-1,2\ell-1}^T + P_{2\ell} \bar{\mathbf{h}}_{2k-1,2\ell}^* \bar{\mathbf{h}}_{2k-1,2\ell}^T) + \text{blkdiag}\{\sigma_{\text{R}}^2 \bar{\mathbf{H}}_{2k-1}^* \bar{\mathbf{H}}_{2k-1}^T, \sigma_{\text{U}}^2\}.$$

Define $\bar{\mathbf{F}}_n = [\mathbf{f}_{1,n} \quad \dots \quad \mathbf{f}_{2K-1,n}] \in \mathbb{C}^{M_{\text{R}} \times K}$, $\bar{\mathbf{G}}_n = [\mathbf{g}_{2,n} \quad \dots \quad \mathbf{g}_{2K,n}] \in \mathbb{C}^{M_{\text{R}} \times K}$, $\forall n$, $\mathbf{P}_o = \text{blkdiag}\{P_{2k-1}\}_{k=1}^K \in \mathbb{C}^{K \times K}$, and $\mathbf{P}_e = \text{blkdiag}\{P_{2k}\}_{k=1}^K \in \mathbb{C}^{K \times K}$. The total transmit power of the relays in the network is computed by

$$\begin{aligned} \sum_{n=1}^N \mathbb{E}\{\|\bar{\mathbf{r}}_n\|^2\} &= \sum_{n=1}^N \|\mathbf{W}_n (\bar{\mathbf{F}}_n \mathbf{P}_o^{\frac{1}{2}} + \bar{\mathbf{G}}_n \mathbf{P}_e^{\frac{1}{2}} + \sigma_{\text{R}}^2 \mathbf{I}_{M_{\text{R}}})\|_{\text{F}}^2 \\ &= \sum_{n=1}^N \|\text{vec}\{\mathbf{W}_n (\bar{\mathbf{F}}_n \mathbf{P}_o^{\frac{1}{2}} + \bar{\mathbf{G}}_n \mathbf{P}_e^{\frac{1}{2}} + \sigma_{\text{R}}^2 \mathbf{I}_{M_{\text{R}}})\}\|^2 = \tilde{\mathbf{w}}^H \tilde{\mathbf{C}}_0^{(g)} \tilde{\mathbf{w}} = \boxed{\frac{1}{|\beta_1|^2} \mathbf{w}_1^H \bar{\mathbf{C}}_0^{(g)} \mathbf{w}_1} \end{aligned} \quad (5.7)$$

where $\tilde{\mathbf{C}}_0^{(g)} = \text{blkdiag}\{(\bar{\mathbf{F}}_n^* \mathbf{P}_o \bar{\mathbf{F}}_n^T + \bar{\mathbf{G}}_n^* \mathbf{P}_e \bar{\mathbf{G}}_n^T + \sigma_R^2 \mathbf{I}_{M_R}) \otimes \mathbf{I}_{M_R}\}_{n=1}^N \in \mathbb{C}^{NM_R^2 \times NM_R^2}$ and $\bar{\mathbf{C}}_0^{(g)} = \text{blkdiag}\{\tilde{\mathbf{C}}_0^{(g)}, 0\}$. The actual transmit power of the n -th relay can be expressed as

$$\mathbb{E}\{\|\bar{\mathbf{r}}_n\|^2\} = \tilde{\mathbf{w}}^H \tilde{\mathbf{C}}_n^{(g)} \tilde{\mathbf{w}} = \boxed{\frac{1}{|\beta_1|^2} \mathbf{w}_1^H \bar{\mathbf{C}}_n^{(g)} \mathbf{w}_1} \quad (5.8)$$

where $\tilde{\mathbf{C}}_n^{(g)}$ is obtained by setting all the elements in $\tilde{\mathbf{C}}_0^{(g)}$ to zero except for the n -th M_R^2 -by- M_R^2 matrix on the main diagonal and $\bar{\mathbf{C}}_n^{(g)} = \text{blkdiag}\{\tilde{\mathbf{C}}_n^{(g)}, 0\}$.

The total transmit power constraint of the relays in the network can be expanded as

$$\sum_{n=1}^N \mathbb{E}\{\|\bar{\mathbf{r}}_n\|^2\} \leq P_{R,\max} \Leftrightarrow \boxed{\mathbf{w}_1^H \mathbf{C}_0^{(g)} \mathbf{w}_1 \leq 0} \quad (5.9)$$

where $\mathbf{C}_0^{(g)} = \text{blkdiag}\{\tilde{\mathbf{C}}_0^{(g)}, -P_{R,\max}\}$. The individual power constraint for each relay can be obtained as

$$\mathbb{E}\{\|\bar{\mathbf{r}}_n\|^2\} \leq P_{R,\max}^{(\text{Ind})}, \forall n \Leftrightarrow \boxed{\mathbf{w}_1^H \mathbf{C}_n^{(g)} \mathbf{w}_1 \leq 0, \forall n} \quad (5.10)$$

where $\mathbf{C}_n^{(g)} = \text{blkdiag}\{\tilde{\mathbf{C}}_n^{(g)}, -P_{R,\max}^{(\text{Ind})}\}$.

5.4 Interference neutralization

5.4.1 Feasibility of interference neutralization

In this section we show how the relay forwarding strategy can be chosen to neutralize all interference and which conditions are necessary and sufficient to achieve this. To this end, the following equalities must be satisfied at the same time. For all $\ell, k \in \{1, \dots, K\}, \ell \neq k$,

$$h_{2k-1,2\ell-1} + \mathbf{f}_{2k-1}^T \tilde{\mathbf{W}} \mathbf{f}_{2\ell-1} = 0 \quad (5.11a)$$

$$h_{2k-1,2\ell} + \mathbf{f}_{2k-1}^T \tilde{\mathbf{W}} \mathbf{g}_{2\ell} = 0 \quad (5.11b)$$

$$h_{2k,2\ell-1} + \mathbf{g}_{2k}^T \tilde{\mathbf{W}} \mathbf{f}_{2\ell-1} = 0 \quad (5.11c)$$

$$h_{2k,2\ell} + \mathbf{g}_{2k}^T \tilde{\mathbf{W}} \mathbf{g}_{2\ell} = 0. \quad (5.11d)$$

Equation (5.11a) describes the interference from any odd-indexed (i.e., $(2\ell - 1)$ -th) UT to another odd-indexed (i.e., $(2k - 1)$ -th) UT. Similarly (5.11b), (5.11c), (5.11d) describe the interference from any even-indexed UT to another odd-indexed UT, from any odd-indexed UT to another even-indexed UT and from any even-indexed UT to another even-indexed UT, respectively. The feasibility conditions in (5.11) can be quantified by four parameters: the

number of relay nodes N , the number of antennas at each relay node M_R , the number of UT pairs K , and the maximum available power at the relay. The conditions are summarized in the following main result:

Theorem 5.4.1. *Assume that we have a two-way relay channel with $2K$ UTs and N relay nodes each with M_R antennas. The interference neutralization requirements, given in (5.11), can be satisfied if and only if both of the following criteria are satisfied:*

1. *The total available number of antennas in the network should satisfy*

$$2K(K-1) \leq \frac{1}{2}NM_R(M_R+1). \quad (5.12)$$

2. *Given the interference neutralization solution as $\tilde{\mathbf{w}}^{(1)}$, the available relay power should satisfy*

$$P_{R,\max} \geq \tilde{\mathbf{w}}^{(1)\text{H}} \tilde{\mathbf{C}}_0^{(g)} \tilde{\mathbf{w}}^{(1)} \quad (5.13)$$

if a total transmit power constraint is considered. Or

$$P_{R,\max}^{(\text{Ind})} \geq \tilde{\mathbf{w}}^{(1)\text{H}} \tilde{\mathbf{C}}_n^{(g)} \tilde{\mathbf{w}}^{(1)}, \forall 1 \leq n \leq N \quad (5.14)$$

if individual transmit power constraints are considered.

Proof. Please refer to Appendix C.4.1. □

If all the antennas in the network are grouped together to form a single relay or are distributed such that each relay has a single antenna, we have the following results.

Corollary 5.4.2. *In the special case of a single relay node $N = 1$ with M_R antennas, condition (5.12) implies that $M_R \geq 2(K-1)$. At the other extreme, $N > 1$ relays and each with a single antenna $M_R = 1$, condition (5.12) simplifies to $N \geq 2K(K-1)$.*

Proof. When $N = 1$ and $M_R > 1$, by applying the roots of quadratic equations, condition (5.12) means that

$$M_R \geq \left\lceil \frac{-1 + \sqrt{16K^2 - 16K + 1}}{2} \right\rceil = 2(K-1).$$

The equality can be verified using proof by contradiction. That is, we prove that $1 + \frac{-1 + \sqrt{16K^2 - 16K + 1}}{2} \leq 2(K-1)$ is false. After some algebraic manipulation, the previous condition simplifies to $K \leq 1$, which is contradictory with our assumption that $K > 1$. Therefore, $M_R \geq 2(K-1)$. When $N > 1$ and $M_R = 1$, the proof is straightforward. □

From Corollary 5.4.2 follows that the gain of cooperation is going from $2(K-1)$ to $2K(K-1)$. Furthermore, the IN solution $\tilde{\mathbf{w}}^{(1)}$ can be expressed in a generic form as follows.

Lemma 5.4.3. *Assume that interference neutralization is feasible, i.e., the two conditions in Theorem 5.4.1 are fulfilled. The interference neutralization solution $\tilde{\mathbf{w}}^{(1)}$, using the vectorized representation of $\tilde{\mathbf{W}}$, must satisfy the following form:*

$$\tilde{\mathbf{w}}^{(1)} = \mathbf{c} + \mathbf{B}\mathbf{v} \quad (5.15)$$

where \mathbf{c} is a known vector, \mathbf{B} is a known projection matrix, and \mathbf{v} is an arbitrary vector. More specifically, let $\mathbf{K}_{M_R^2}$ be a commutation matrix as defined in [Lue96]. Define the SVD of $\bar{\mathbf{K}} = \mathbf{I}_N \otimes (\mathbf{I}_{M_R^2} - \mathbf{K}_{M_R^2})$ as $\bar{\mathbf{K}} = \mathbf{U}\Sigma[\mathbf{V}_s \quad \mathbf{V}_n]^H$ where $\mathbf{V}_n \in \mathbb{C}^{NM_R^2 \times (NM_R^2 - r_1)}$ spans the null space of $\bar{\mathbf{K}}$ and r_2 is the rank of $\bar{\mathbf{K}}$, where we have $r_1 = \frac{1}{2}NM_R(M_R - 1)$. The interference neutralization solution is computed as

$$\tilde{\mathbf{w}}^{(1)} = \mathbf{V}_n \left((\mathbf{A}\mathbf{V}_n)^+ \mathbf{b} + \left(\mathbf{I}_{NM_R^2 - r_1} - (\mathbf{A}\mathbf{V}_n)^+ \mathbf{A}\mathbf{V}_n \right) \mathbf{v} \right) \quad (5.16)$$

where $\mathbf{v} \in \mathbb{C}^{\frac{1}{2}NM_R(M_R+1)}$ contains $\left(\frac{1}{2}NM_R(M_R+1) - 2K(K-1)\right)$ signal dimensions that can be used for further system improvements. Define $\bar{i} \in \{1, \dots, K\}$ and $\bar{j} \in \{\bar{i} + 1, \dots, K\}$. The column-vector $\mathbf{b} \in \mathbb{C}^{2K(K-1)}$ is generated by

$$\mathbf{b} = - \left[h_{2\bar{i}-1, 2\bar{j}-1} \quad h_{2\bar{i}-1, 2\bar{j}} \quad h_{2\bar{i}, 2\bar{j}-1} \quad h_{2\bar{i}, 2\bar{j}} \right]^T, \forall \bar{i}, \bar{j}$$

and the corresponding $\mathbf{A} \in \mathbb{C}^{2K(K-1) \times NM_R^2}$ is generated via

$$\mathbf{A} = \left[\mathbf{h}_{2\bar{i}-1, 2\bar{j}-1} \quad \mathbf{h}_{2\bar{i}-1, 2\bar{j}} \quad \mathbf{h}_{2\bar{i}, 2\bar{j}-1} \quad \mathbf{h}_{2\bar{i}, 2\bar{j}} \right]^T, \forall \bar{i}, \bar{j}.$$

Proof. Please refer to Appendix C.4.2. □

Corollary 5.4.4. *Assume that interference neutralization is feasible. When $M_R = 1$ and $N > 1$, the interference neutralization solution simplifies to*

$$\tilde{\mathbf{w}}^{(1)} = \mathbf{A}^+ \mathbf{b} + (\mathbf{I}_N - \mathbf{A}^+ \mathbf{A}) \mathbf{v}.$$

Define the SVD $(\mathbf{I}_{M_R^2} - \mathbf{K}_{M_R^2}) = \mathbf{U}_3 \Sigma_3 [\mathbf{V}_{s,3} \quad \mathbf{V}_{n,3}]^H$ where $\mathbf{V}_{n,3} \in \mathbb{C}^{M_R^2 \times (\frac{1}{2}M_R(M_R+1))}$ contains the last $(\frac{1}{2}M_R(M_R+1))$ columns. When $N = 1$ and $M_R > 1$, the interference neutralization

solution simplifies to

$$\tilde{\mathbf{w}}^{(I)} = \mathbf{V}_{n,3} \left((\mathbf{A}\mathbf{V}_{n,3})^+ \mathbf{b} + \left(\mathbf{I}_{\frac{1}{2}M_R(M_R+1)} - (\mathbf{A}\mathbf{V}_{n,3})^+ \mathbf{A}\mathbf{V}_{n,3} \right) \mathbf{v} \right).$$

Proof. Please refer to Appendix C.4.2. □

Finally, the following statements are direct consequences of Lemma 5.4.3.

Corollary 5.4.5. 1. If $2K(K-1) < \frac{1}{2}NM_R(M_R+1)$, the required minimum total transmit power of the relays in the network (if considered) is computed as

$$P_{R,\max} = \mathbf{c}^H \tilde{\mathbf{C}}_0^{(g)} \mathbf{c} - \mathbf{b}_p^H \mathbf{A}_p^+ \mathbf{b}_p$$

where $\mathbf{A}_p = \mathbf{B}^H \tilde{\mathbf{C}}_0^{(g)} \mathbf{B}$ and $\mathbf{b}_p = \mathbf{B}^H \tilde{\mathbf{C}}_0^{(g)} \mathbf{c}$, while the required minimum individual transmit power (if considered) is calculated by

$$P_{R,\max}^{(\text{Ind})} = \max_n \left(\mathbf{c}^H \tilde{\mathbf{C}}_n^{(g)} \mathbf{c} - \mathbf{b}_{p,n}^H \mathbf{A}_{p,n}^+ \mathbf{b}_{p,n} \right)$$

where $\mathbf{A}_{p,n} = \mathbf{B}^H \tilde{\mathbf{C}}_n^{(g)} \mathbf{B}$ and $\mathbf{b}_{p,n} = \mathbf{B}^H \tilde{\mathbf{C}}_n^{(g)} \mathbf{c}$. Otherwise, if $2K(K-1) = \frac{1}{2}NM_R(M_R+1)$, the required minimum total transmit power is $P_{R,\max} = \mathbf{c}^H \tilde{\mathbf{C}}_0^{(g)} \mathbf{c}$ while the required minimum individual transmit power is given by $P_{R,\max}^{(\text{Ind})} = \max_n \mathbf{c}^H \tilde{\mathbf{C}}_n^{(g)} \mathbf{c}$.

2. If both conditions in Theorem 5.4.1 are satisfied, then $\tilde{\mathbf{w}}^{(I)} = \mathbf{c}$ is a closed-form IN solution. Moreover, it is a minimum norm solution such that $\|\tilde{\mathbf{w}}^{(I)}\|$ is minimized.
3. If condition (5.12) or condition (5.13) (or (5.14)) is violated, then

$$\tilde{\mathbf{w}}^{(I)} = \mathbf{c},$$

when condition (5.12) is violated, or

$$\tilde{\mathbf{w}}^{(I)} = \mathbf{c} \sqrt{\frac{P_{R,\max}}{\mathbf{c}^H \tilde{\mathbf{C}}_0^{(g)} \mathbf{c}}} \left(\text{or } \tilde{\mathbf{w}}^{(I)} = \mathbf{c} \sqrt{\frac{P_{R,\max}^{(\text{Ind})}}{\max_n \mathbf{c}^H \tilde{\mathbf{C}}_n^{(g)} \mathbf{c}}} \right),$$

when condition (5.13) (or (5.14)) is violated, is a least square solution which minimizes the weighted sum of the interference power in the network, i.e.,

$$\tilde{\mathbf{w}}^{(I)} = \arg \min_{\tilde{\mathbf{w}}} \sum_{k=1}^K \left(\frac{1}{P_{2k-1}} P_{2k-1}^{(I)} + \frac{1}{P_{2k}} P_{2k}^{(I)} \right).$$

Proof. Please refer to Appendix C.4.3. □

Remark

Remark 7. When there are no dumb repeaters in the network, i.e., $h_{i,j} = 0, \forall i, j$, to neutralize/cancel the interference in the network no additional constraints are imposed on the available powers of the relays, i.e., (5.13) or (5.14) is not required. However, condition (5.12) has to be satisfied with inequality, i.e., $2K(K-1) < \frac{1}{2}NM_R(M_R+1)$. This holds true also for the extreme cases. That is, from Corollary 5.4.2, when there is a single multi-antenna relay in the network, we should have $M_R > 2(K-1)$. When each relay has a single antenna, we should have $N > 2K(K-1)$. These results coincide with our findings in Chapters 3 and 4.

5.4.2 SINR and the actual transmit power of the relays after interference neutralization

Taking the $(2k-1)$ -th UT as an example, the interference term $P_{2k-1}^{(I)}$ is zero after applying IN. We consider the generalized IN solution in Lemma 1. By using the Charness-Cooper transform, we let $\boldsymbol{\eta}_2/\beta_2 = \mathbf{v}$ and $\mathbf{w}_2 = \begin{bmatrix} \boldsymbol{\eta}_2^T & \beta_2 \end{bmatrix}^T \in \mathbb{C}^{r_B+1}$ where $\beta_2 \in \mathbb{C}$ and $|\beta_2| = 1$. Define \mathbf{e}_{r_B+1} as the (r_B+1) -th column of the identity matrix \mathbf{I}_{r_B+1} . Then the SINR expression of the $(2k-1)$ -th UT becomes

$$\gamma_{2k-1} = \frac{\mathbf{w}_2^H \mathbf{E}_{2k-1}^{(n)} \mathbf{w}_2}{\mathbf{w}_2^H \mathbf{F}_{2k-1}^{(n)} \mathbf{w}_2} \quad (5.17)$$

where $\mathbf{E}_{2k-1}^{(n)} = P_{2k} \tilde{\mathbf{h}}_{2k-1,2k}^* \tilde{\mathbf{h}}_{2k-1,2k}^T$, $\tilde{\mathbf{h}}_{i,j} = \begin{bmatrix} \mathbf{h}_{i,j}^T \mathbf{B} & h_{i,j} + \mathbf{h}_{i,j}^T \mathbf{c} \end{bmatrix}^T, \forall i, j$, $\mathbf{F}_{2k-1}^{(n)} = \sigma_R^2 \tilde{\mathbf{H}}_{2k-1}^H \tilde{\mathbf{H}}_{2k-1} + \sigma_U^2 \mathbf{e}_{r_B+1} \mathbf{e}_{r_B+1}^H$, and $\tilde{\mathbf{H}}_{2k-1} = \begin{bmatrix} \tilde{\mathbf{H}}_{2k-1}^T \mathbf{B} & \tilde{\mathbf{H}}_{2k-1}^T \mathbf{c} \end{bmatrix}$.

Clearly, compared to \mathbf{w}_1 in (5.6), \mathbf{w}_2 has fewer elements to be optimized, i.e., a lower computational complexity. Conversely, \mathbf{w}_2 possesses fewer signal dimensions to utilize, i.e., a worse performance in general. In other words, IN provides a balance between the performance and the computational complexity.

Define $\tilde{\mathbf{C}}_0^{(n)} = \begin{bmatrix} \mathbf{B} & \mathbf{c} \end{bmatrix}^H \tilde{\mathbf{C}}_0^{(g)} \begin{bmatrix} \mathbf{B} & \mathbf{c} \end{bmatrix}$ and $\tilde{\mathbf{C}}_n^{(n)} = \begin{bmatrix} \mathbf{B} & \mathbf{c} \end{bmatrix}^H \tilde{\mathbf{C}}_n^{(g)} \begin{bmatrix} \mathbf{B} & \mathbf{c} \end{bmatrix}, \forall n$. The actual total transmit power of the relays in the network and actual individual transmit powers at the relays after applying IN are calculated by

$$\sum_{n=1}^N \mathbb{E}\{\|\tilde{\mathbf{r}}_n\|^2\} = \tilde{\mathbf{w}}^H \tilde{\mathbf{C}}_0^{(g)} \tilde{\mathbf{w}} = \frac{1}{|\beta_2|^2} \mathbf{w}_2^H \tilde{\mathbf{C}}_0^{(n)} \mathbf{w}_2 \quad (5.18)$$

and

$$\mathbb{E}\{\|\bar{\mathbf{r}}_n\|^2\} = \tilde{\mathbf{w}}^H \tilde{\mathbf{C}}_n^{(g)} \tilde{\mathbf{w}} = \boxed{\frac{1}{|\beta_2|^2} \mathbf{w}_2^H \bar{\mathbf{C}}_n^{(n)} \mathbf{w}_2, \forall n}. \quad (5.19)$$

Moreover, the total power constraint and the individual power constraints are rewritten as

$$\boxed{\mathbf{w}_2^H \mathbf{C}_0^{(n)} \mathbf{w}_2 \leq 0} \quad (5.20)$$

and

$$\boxed{\mathbf{w}_2^H \mathbf{C}_n^{(n)} \mathbf{w}_2 \leq 0, \forall n}, \quad (5.21)$$

respectively, where we have $\mathbf{C}_0^{(n)} = \bar{\mathbf{C}}_0^{(n)} - P_{R,\max} \mathbf{e}_{r_{B+1}} \mathbf{e}_{r_{B+1}}^H$ and $\mathbf{C}_n^{(n)} = \bar{\mathbf{C}}_n^{(n)} - P_{R,\max}^{(\text{Ind})} \mathbf{e}_{r_{B+1}} \mathbf{e}_{r_{B+1}}^H$.

In summary, IN does not change the structure of the SINR expressions and the structure of the power constraints compared to Section 5.3.2. Therefore, the same kind of optimization problems are formulated, as shown in Sections 5.5, 5.6, and 5.7. For notational simplicity, we unify the derived expressions with or without IN. By using the superindex m instead of $2k-1$ (or $2k$), we define the SINR of the m -th UT with or without IN as

$$\gamma_m = \frac{\mathbf{w}^H \mathbf{E}_m \mathbf{w}}{\mathbf{w}^H \mathbf{F}_m \mathbf{w}} \quad (5.22)$$

where $\mathbf{w} \in \{\mathbf{w}_1, \mathbf{w}_2\}$, $\mathbf{E}_m \in \{\mathbf{E}_m^{(g)}, \mathbf{E}_m^{(n)}\}$, and $\mathbf{F}_m \in \{\mathbf{F}_m^{(g)}, \mathbf{F}_m^{(n)}\}$. We have $\mathbf{E}_m \geq 0$ and $\mathbf{F}_m > 0$, $\forall m$. The sum transmit power constraint (5.9), (5.20) or individual transmit power constraints (5.10), (5.21) are generalized as

$$\mathbf{w}^H \mathbf{C}_0 \mathbf{w} \leq 0 \quad (5.23)$$

and

$$\mathbf{w}^H \mathbf{C}_n \mathbf{w} \leq 0, \quad (5.24)$$

correspondingly, where $\mathbf{C}_0 \in \{\mathbf{C}_0^{(g)}, \mathbf{C}_0^{(n)}\}$ and $\mathbf{C}_n \in \{\mathbf{C}_n^{(g)}, \mathbf{C}_n^{(n)}\}$.

In the following we design the beamforming vector \mathbf{w} subject to various system design criteria.

Remark 8. If the optimal \mathbf{w}_{opt} is obtained, the optimal $\tilde{\mathbf{w}}_{\text{opt}}$ is computed via $\tilde{\mathbf{w}}_{\text{opt}} = \boldsymbol{\eta}_{1,\text{opt}}/\beta_{1,\text{opt}}$ or $\tilde{\mathbf{w}}_{\text{opt}} = \mathbf{c} + \mathbf{B}\boldsymbol{\eta}_{2,\text{opt}}/\beta_{2,\text{opt}}$. Afterwards, the cascaded relay amplification matrix $\check{\mathbf{W}}_{\text{opt}}$ can be computed as

$$\check{\mathbf{W}}_{\text{opt}} = \text{unvec}_{M_R \times N M_R} \{\tilde{\mathbf{w}}_{\text{opt}}\} \quad (5.25)$$

Finally, the n -th relay's amplification matrix $\mathbf{W}_{n,\text{opt}}$ is given by M_R columns of $\check{\mathbf{W}}_{\text{opt}}$ starting

from the $((n-1)M_R + 1)$ -th column.

5.5 Relay power minimization

In this section, we introduce the relay power minimization problems subject to QoS constraints. To this end, we first define the following two types of power metrics

1. the individual relay power metric $P_{R,n}(\mathbf{w}) = \mathbf{w}^H \bar{\mathbf{C}}_n \mathbf{w}$, $\forall 1 \leq n \leq N$
2. the sum relay power metric $P_{R,\text{sum}}(\mathbf{w}) = \sum_{n=1}^N P_{R,n}(\mathbf{w}) = \mathbf{w}^H \bar{\mathbf{C}}_0 \mathbf{w}$

where $\bar{\mathbf{C}}_n \in \{\bar{\mathbf{C}}_n^{(g)}, \bar{\mathbf{C}}_n^{(n)}\}$ and $\bar{\mathbf{C}}_0 \in \{\bar{\mathbf{C}}_0^{(g)}, \bar{\mathbf{C}}_0^{(n)}\}$. Moreover, we consider two utility functions. The min-max relay power utility is to minimize the maximum relay power over all relays:

$$P_{R,\text{max}}(\mathbf{w}) = \max_n P_{R,n}(\mathbf{w}). \quad (5.26)$$

The sum relay power utility is to minimize the total required relay power $P_{R,\text{sum}}(\mathbf{w})$ in the network. Denote the general relay power optimization metric as $P_R(\mathbf{w})$, which represents $P_{R,\text{max}}(\mathbf{w})$ or $P_{R,\text{sum}}(\mathbf{w})$. Note that $P_R(\mathbf{w})$ in the expressions above are convex functions of \mathbf{w} . In the following, the optimization problem can be formulated using the the general relay power optimization metric. The proposed algorithm applies to all power constraints with minor modifications. Recall the achievable SINR for user m with or without interference neutralization from (5.22) as γ_m . Let $\beta \in \{\beta_1, \beta_2\}$. The relay power minimization problem subject to SINR constraints is given by

$$\begin{aligned} \min_{\mathbf{w}} \quad & P_R(\mathbf{w}) \\ \text{s.t.} \quad & \gamma_m \geq \eta_m, \quad m = 1, \dots, 2K, \end{aligned} \quad (5.27a)$$

$$\mathbf{w}^H \mathbf{C}_c \mathbf{w} = 1 \quad (5.27b)$$

where η_m is the target SINR value for user m . Constraint (5.27b) comes from the fact that $|\beta| = 1$ and $\mathbf{C}_c = \text{blkdiag}\{\mathbf{0}, 1\}$. Although the cost function of problem (5.27) is convex, constraint (5.27a) is non-convex in general. Therefore, problem (5.27) is a non-convex QCQP problem. It may not be solvable in polynomial time. But its approximate solution can be obtained by using either the SDP approach [LMS⁺10] or the SOCP approach [BV04]. In our work we adopt the SDP approach.

The SDP approach uses the SDR technique [LMS⁺10]. By introducing a new variable $\mathbf{X} = \mathbf{w}\mathbf{w}^H$ we can rewrite problem (5.27) as

$$\begin{aligned} \min_{\mathbf{X}} \quad & P_R(\mathbf{X}) \\ \text{s.t.} \quad & \text{Tr}\{(\mathbf{E}_m - \eta_m \mathbf{F}_m)\mathbf{X}\} \geq 0, \quad m = 1, \dots, 2K, \\ & \text{Tr}\{\mathbf{C}_c \mathbf{X}\} = 1, \mathbf{X} \geq 0, \text{rank}\{\mathbf{X}\} = 1 \end{aligned} \quad (5.28)$$

where $P_R(\mathbf{X}) = \max_n \text{Tr}\{\bar{\mathbf{C}}_n \mathbf{X}\}$ if individual power constraints are considered and $P_R(\mathbf{X}) = \text{Tr}\{\bar{\mathbf{C}}_0 \mathbf{X}\}$ if the sum power constraint is considered. Dropping the rank-1 constraint, problem (5.28) can be approximated by the following convex SDP problem

$$\begin{aligned} \min_{\mathbf{X}} \quad & P_R(\mathbf{X}) \\ \text{s.t.} \quad & \text{Tr}\{(\mathbf{E}_m - q_m \mathbf{F}_m)\mathbf{X}\} \geq 0, \quad m = 1, \dots, 2K, \\ & \text{Tr}\{\mathbf{C}_c \mathbf{X}\} = 1, \mathbf{X} \geq 0, \end{aligned} \quad (5.29)$$

which can be solved efficiently using the standard interior-point algorithm [BV04]. If the optimal solution of problem (5.29) is a rank-1 matrix, it is also the optimal solution to the original problem (5.28). Otherwise, rank-1 extraction techniques in [LMS⁺10] should be applied. Since we have more than three constraints, a rank-1 solution is not guaranteed for our problem (5.29) according to [HP10, Theorem 3.2 & Corollary 3.4]. Hence, the randomization technique, which is a rank-1 approximation technique [LMS⁺10], is used to get an approximate solution, finally.

5.6 SINR balancing

The SINR balancing problem is another QoS based system design criterion. It aims at maximizing the minimum SINR of the UTs in the network subject to transmit power constraints at the relay. In the following we discuss the SINR balancing solution with or without IN.

Define $f_\kappa(\mathbf{X}) = \text{Tr}\{\mathbf{C}_\kappa \mathbf{X}\}$ where \mathbf{X} can have arbitrary rank. Let $f_\kappa(\mathbf{w}\mathbf{w}^H) = \mathbf{w}^H \mathbf{C}_\kappa \mathbf{w}$ represent the rank-1 case. The optimization problem with a sum power constraint or individual power constraints can be generalized as

$$\begin{aligned} \max_{\mathbf{w}} \min_m \quad & \gamma_m \\ \text{s.t.} \quad & \mathbf{w}^H \mathbf{C}_c \mathbf{w} = 1 \\ & f_\kappa(\mathbf{w}\mathbf{w}^H) \leq 0, \quad \forall \kappa \in \mathcal{N}, \end{aligned} \quad (5.30)$$

where $\mathcal{N} = \{0\}$ if a total power constraint is considered and $\mathcal{N} = \{1, \dots, N\}$ if individual power constraints are considered.

Problem (5.30) is non-convex. But its approximate solution can be obtained using the same SDP approach as in Section 5.5. After replacing $\mathbf{w}\mathbf{w}^H$ by \mathbf{X} , (5.30) can be rewritten as

$$\begin{aligned} \lambda_{\text{opt}} = \max_{\mathbf{X}} \min_m & \frac{\text{Tr}\{\mathbf{E}_m \mathbf{X}\}}{\text{Tr}\{\mathbf{F}_m \mathbf{X}\}} \\ \text{s.t.} & \text{Tr}\{\mathbf{C}_c \mathbf{X}\} = 1 \\ & f_\kappa(\mathbf{X}) \leq 0, \forall \kappa \in \mathcal{N}. \end{aligned} \quad (5.31)$$

If the optimal solution \mathbf{X}_{opt} to problem (5.31) is rank-1, it is also the optimal solution to the original problem (5.30). Similarly as in Section 5.5, a rank-1 solution is not guaranteed since there are more than three constraints in (5.31). Hence, the randomization technique in [LMS⁺10] and Appendix B.3.5 is applied at the end to get an approximate solution. From now on, concerning the convergence speed of our proposed iterative solutions, we introduce two methods, namely, the bisection search method and the Dinkelbach-type algorithm. To distinguish the convergence speed, we give the following definition.

Definition 5.6.1. [NW99] Consider the sequence $\lambda^{(p)}$, which converges to λ_{opt} as a limit. The sequence $\lambda^{(p)}$ is said to converge with an order q to λ_{opt} if

$$\lim_{p \rightarrow +\infty} \frac{|\lambda^{(p+1)} - \lambda_{\text{opt}}|}{|\lambda^{(p)} - \lambda_{\text{opt}}|^q} = \delta. \quad (5.32)$$

The number q is called the Q-order of convergence where ‘‘Q’’ stands for quotient.

- $\delta \in (0, 1)$ and $q = 1$, it is Q-linearly convergent.
- $\delta = 0$ and $q = 1$, it is Q-superlinearly convergent.
- $\delta > 0$ and $q > 1$, it is said that the Q-order of convergence is q , e.g., Q-quadratic convergent for $q = 2$.

In general, sequences with higher q converge faster [NW99].

5.6.1 The bisection search method

Problem (5.31) is equivalent to the following optimization problem

$$\max_{\mathbf{X}, t} t$$

$$\begin{aligned}
& \text{s.t.} \quad \text{Tr}\{\mathbf{C}_c \mathbf{X}\} = 1 \\
& \quad \quad f_\kappa(\mathbf{X}) \leq 0, \forall \kappa \in \mathcal{N} \\
& \quad \quad \text{Tr}\{(t\mathbf{F}_m - \mathbf{E}_m)\mathbf{X}\} \leq 0, \forall m.
\end{aligned} \tag{5.33}$$

For fixed t , (5.33) is a convex SDP problem. Moreover, t represents the minimum SINR of the UTs in the network and thus it has a finite interval, e.g., $[0, t_{\max}]$. Hence, problem (5.33) can be solved using bisection search method as discussed in [LMS⁺10]. That is, we solve the following feasibility problem in each iteration.

$$\begin{aligned}
& \text{find} \quad \mathbf{X} \\
& \text{s.t.} \quad \text{Tr}\{\mathbf{C}_c \mathbf{X}\} = 1 \\
& \quad \quad f_\kappa(\mathbf{X}) \leq 0, \forall \kappa \in \mathcal{N} \\
& \quad \quad \text{Tr}\{(t\mathbf{F}_m - \mathbf{E}_m)\mathbf{X}\} \leq 0, \forall m
\end{aligned} \tag{5.34}$$

where t is updated using the bisection search method. A possible choice of t_{\max} for our problem will be

$$t_{\max} = \max_m \lambda_{\max}\{\mathbf{F}_m^{-1} \mathbf{E}_m\}. \tag{5.35}$$

The intuition of (5.35) comes from the fact that our SINR expressions γ_m in (5.22) are generalized Rayleigh quotients. It is well known that the Rayleigh quotient is bounded between the maximum and minimum eigenvalues of the matrix $\mathbf{F}_m^{-1} \mathbf{E}_m$. The details of the bisection search method are found in [LMS⁺10]. The bisection search method is linearly convergent since in each iteration the search space is reduced by half such that we have $q = 1$ and $\delta = 1/2$.

5.6.2 Parametric programming via Dinkelbach-type algorithms

Parametric optimization can be also used to solve fractional programming problems like (5.31). When the formulated parametric optimization problem is solved using the Dinkelbach approach, a better convergence speed might be obtained [CF91]. In the following, we develop Dinkelbach-type algorithms for our problems and analyze their convergence behavior.

A parametric programming of (5.31) is formulated as

$$\begin{aligned}
f(\lambda) = \max_{\mathbf{X}} \min_m \quad & \text{Tr}\{\mathbf{E}_m \mathbf{X}\} - \lambda \text{Tr}\{\mathbf{F}_m \mathbf{X}\} \\
& \text{s.t.} \quad \text{Tr}\{\mathbf{C}_c \mathbf{X}\} = 1 \\
& \quad \quad f_\kappa(\mathbf{X}) \leq 0, \forall \kappa \in \mathcal{N}
\end{aligned} \tag{5.36}$$

where parametric here implies that we consider the solution of this optimization problem for various values of λ . This formulation is especially useful if $f(\lambda)$ is a convex function with respect to \mathbf{X} , because it is easier to solve a convex problem (5.36) than a non-convex problem (5.31)¹. Problem (5.36) is equivalent to (5.31) if $f(\lambda) = 0$ [CF91]. Thus, this gives rise to finding the root of the equation $f(\lambda) = 0$. A Newton's method for finding the roots of the function uses the following iterative process

$$\lambda^{(p+1)} = \lambda^{(p)} - \frac{f(\lambda^{(p)})}{\partial_{\lambda} f(\lambda^{(p)})}. \quad (5.37)$$

In general, finding the gradient $\partial_{\lambda} f(\lambda^{(p)}) = \left. \frac{\partial f(\lambda)}{\partial \lambda} \right|_{\lambda=\lambda^{(p)}}$ is non-trivial. When problem (5.36) contains only a single ratio, i.e., the minimization is not involved such that the index m can be dropped, a subgradient of $f(\lambda)$ at $\lambda^{(p)}$ can be found to be $-\text{Tr}\{\mathbf{F}\mathbf{X}^{(p)}\}$ [Din67]. Thus, using this subgradient instead, we get the following update rule

$$\lambda^{(p+1)} = \lambda^{(p)} + \frac{f(\lambda^{(p)})}{\text{Tr}\{\mathbf{F}\mathbf{X}^{(p)}\}} = \frac{\text{Tr}\{\mathbf{E}\mathbf{X}^{(p)}\}}{\text{Tr}\{\mathbf{F}\mathbf{X}^{(p)}\}}, \quad (5.38)$$

and this method is called Dinkelbach's algorithm [Din67]. Compared to the bisection method, Dinkelbach's algorithm converges superlinearly given that the feasible region is compact and λ is finite².

Dinkelbach's algorithm has been extended to the case with multiple ratios in [CF91]. If the update of $\lambda^{(p+1)}$ is calculated as

$$\lambda^{(p+1)} = \min_m \frac{\text{Tr}\{\mathbf{E}_m \mathbf{X}^{(p)}\}}{\text{Tr}\{\mathbf{F}_m \mathbf{X}^{(p)}\}}, \quad (5.39)$$

and in each iteration we solve the following problem

$$\begin{aligned} \max_{\mathbf{X}} \min_m \quad & \text{Tr}\{\mathbf{E}_m \mathbf{X}\} - \lambda^{(p)} \text{Tr}\{\mathbf{F}_m \mathbf{X}\} \\ \text{s.t.} \quad & \text{Tr}\{\mathbf{C}_c \mathbf{X}\} = 1 \\ & f_{\kappa}(\mathbf{X}) \leq 0, \quad \forall \kappa \in \mathcal{N}, \end{aligned} \quad (5.40)$$

which is equivalent to

$$\max_{\mathbf{X}, t_1} \quad t_1$$

¹The cost function in (5.31) is quasi-convex.

² λ of our problem is bounded between $\min_m \lambda_{\min}\{\mathbf{F}_m^{-1} \mathbf{E}_m\}$ and $\max_m \lambda_{\max}\{\mathbf{F}_m^{-1} \mathbf{E}_m\}$

$$\begin{aligned}
\text{s.t. } & \text{Tr}\{\mathbf{C}_c \mathbf{X}\} = 1 \\
& f_\kappa(\mathbf{X}) \leq 0, \forall \kappa \in \mathcal{N}, \\
& \text{Tr}\{\mathbf{E}_m \mathbf{X}\} - \lambda^{(p)} \text{Tr}\{\mathbf{F}_m \mathbf{X}\} \geq t_1, \forall m,
\end{aligned}$$

it is called Dinkelbach Type-I (DT-1) algorithm in [CF91] and was used for solving the max-min SINR problem in multi-pair TWR networks in [FWY13]. Unfortunately, it is revealed in [CFS85] that in general the DT-1 algorithm converges only linearly since the subgradient is not unique anymore. Thus, a modified version of the DT-1 algorithm with a better convergence is proposed in [CFS86]. The proposed method is named as the DT-2 algorithm [CF91] and the following problem is solved in each iteration instead

$$\begin{aligned}
& \max_{\mathbf{X}} \min_m \frac{\text{Tr}\{\mathbf{E}_m \mathbf{X}\} - \lambda^{(p)} \text{Tr}\{\mathbf{F}_m \mathbf{X}\}}{\text{Tr}\{\mathbf{F}_m \mathbf{X}^{(p-1)}\}} \\
\text{s.t. } & \text{Tr}\{\mathbf{C}_c \mathbf{X}\} = 1 \\
& f_\kappa(\mathbf{X}) \leq 0, \forall \kappa \in \mathcal{N}.
\end{aligned} \tag{5.41}$$

Hence, we propose a generalized Dinkelbach algorithm which is summarized in Algorithm 8 and we have the following lemma.

Lemma 5.6.1. *The generalized Dinkelbach-type algorithm in Algorithm 8 has the following properties:*

1. *it solves (5.31).*
2. *it has at least a linear convergence when (5.40) is used while a better convergence is achieved when (5.41) is applied.*

Proof. Please refer to Appendix C.6. □

A trivial initial point $\lambda^{(1)}$ for the proposed algorithm is

$$\lambda^{(1)} = \min_m \frac{\mathbf{w}_{\text{ini}}^H \mathbf{E}_m \mathbf{w}_{\text{ini}}}{\mathbf{w}_{\text{ini}}^H \mathbf{F}_m \mathbf{w}_{\text{ini}}} \tag{5.42}$$

where $\mathbf{w}_{\text{ini}} = [\mathbf{0}^T \ 1]^T$ is a feasible solution to problem (5.31).

Clearly, both (5.40) and (5.41) can be formulated into standard SDP problems, which are solved using the interior-point algorithm in [BV04]. Taking into account the guaranteed convergence speed of the Dinkelbach-type algorithms, we conclude that Algorithm 8 provides a

polynomial-time solution. Moreover, from numerical examples we observe that Algorithm 8 converges much faster than the bisection search method.

Algorithm 8 The generalized Dinkelbach algorithm

- 1: **Initialize:** set a feasible $\lambda^{(1)}$, e.g., using (5.42), maximum iteration number N_{\max} and the threshold value v .
 - 2: **Main step:**
 - 3: **for** $p = 1$ to N_{\max} **do**
 - 4: Obtain $(\mathbf{X}^{(p)}, t_1^{(p)})$ by solving
 (5.40) if DT-1 is applied;
 (5.41) if DT-2 is applied.
 - 5: Calculate $\lambda^{(p+1)}$ using (5.39)
 - 6: **if** $|t_1^{(p)}| \leq v$ **then**
 - 7: return $\mathbf{X}^{(p)}$
 - 8: **end if**
 - 9: **end for**
-

5.7 Weighted sum rate maximization

In this section, we discuss the weighted sum rate maximization problem. The weighted sum rate maximization problem for our scenario with or without IN can be formulated as

$$\begin{aligned}
 \max_{\mathbf{w}} \quad & \frac{1}{2} \sum_{m=1}^{2K} \alpha_m \log_2(1 + \gamma_m) \\
 \text{s. t.} \quad & \mathbf{w}^H \mathbf{C}_c \mathbf{w} = 1 \\
 & f_\kappa(\mathbf{w} \mathbf{w}^H) \leq 0, \forall \kappa \in \mathcal{N}
 \end{aligned} \tag{5.43}$$

where $\alpha_m \in [0, 1]$ is a given weighting factor for the m th UT's rate and $\sum_m \alpha_m = 1$. When $\alpha_m = \frac{1}{2K}, \forall m$, problem (5.43) is a sum rate maximization problem. As discussed in our previous work ([ZRH12a], [ZRH⁺12c]) and also in Chapter 4, similar sum rate maximization problems can be solved using monotonic optimization. Monotonic optimization ([Tuy00], [PT03]) deals with the maximization or minimization of an *increasing function* over an intersection of normal and reverse normal sets. A generic algorithm for solving monotonic optimization problems is the polyblock approximation approach [PT03]. In the following we solve problem (5.43) using the polyblock approach, which is also applied in Chapter 4.

Let us start by introducing new variables $y_m \in \mathbb{R}_+$ and reformulate (5.43) as

$$\begin{aligned}
 & \max_{\mathbf{w}, y_m, \forall m} \sum_{m=1}^{2K} \alpha_m \log(y_m) \\
 & \text{s. t. } \mathbf{w}^H \mathbf{C}_c \mathbf{w} = 1 \\
 & \quad f_\kappa(\mathbf{w} \mathbf{w}^H) \leq 0, \forall \kappa \in \mathcal{N} \\
 & \quad y_m \leq \max_{\mathbf{w}} \frac{\mathbf{w}^H \bar{\mathbf{E}}_m \mathbf{w}}{\mathbf{w}^H \mathbf{F}_m \mathbf{w}}, \forall m \\
 & \quad y_m \geq \min_{\mathbf{w}} \frac{\mathbf{w}^H \bar{\mathbf{E}}_m \mathbf{w}}{\mathbf{w}^H \mathbf{F}_m \mathbf{w}}, \forall m
 \end{aligned} \tag{5.44}$$

where $\bar{\mathbf{E}}_m = \mathbf{E}_m + \mathbf{F}_m$ and the factor 1/2 is dropped for simplicity. Define the sets

$$\mathbb{G} = \left\{ \mathbf{y} \in \mathbb{R}_+^{2K} : y_m \leq \max_{\mathbf{w}} \frac{\mathbf{w}^H \bar{\mathbf{E}}_m \mathbf{w}}{\mathbf{w}^H \mathbf{F}_m \mathbf{w}}, \mathbf{w} \in \mathbb{F}, \forall m \right\},$$

and

$$\mathbb{L} = \left\{ \mathbf{y} \in \mathbb{R}_+^{2K} : y_m \geq \min_{\mathbf{w}} \frac{\mathbf{w}^H \bar{\mathbf{E}}_m \mathbf{w}}{\mathbf{w}^H \mathbf{F}_m \mathbf{w}} \geq 1, \mathbf{w} \in \mathbb{F}, \forall m \right\}.$$

where $\mathbb{F} = \{\mathbf{w} | \mathbf{w}^H \mathbf{C}_c \mathbf{w} = 1, f_\kappa(\mathbf{w} \mathbf{w}^H) \leq 0, \forall \kappa \in \mathcal{N}\}$. Let $\mathbb{D} = \mathbb{G} \cap \mathbb{L}$ and formulate the following optimization problem

$$\begin{aligned}
 & \max_{\mathbf{y}} \Phi(\mathbf{y}) \\
 & \text{s. t. } \mathbf{y} \in \mathbb{D}
 \end{aligned} \tag{5.45}$$

where we have $\Phi(\mathbf{y}) = \sum_{m=1}^{2K} \alpha_m \log(y_m)$. Clearly, given a global optimal solution \mathbf{y}_{opt} of (5.45), then an optimal \mathbf{w}_{opt} should exist and it is a global optimizer of (5.44). In the following we solve problem (5.45) using the polyblock algorithm. For this purpose, we introduce the following lemma.

Lemma 5.7.1. *Problem (5.45) is a monotonic optimization problem.*

Proof. Please refer to Appendix C.7.1. □

According to [Tuy00], a monotonic optimization problem can be solved using the polyblock outer approximation algorithm which is described in Appendix C.7.2. The main idea of the polyblock approach is to iteratively create an outer approximation of \mathbb{G} using a sequence of polyblocks, where a polyblock $\mathbb{P}^{(p)}$ is a union of a finite number of hypercubes and it can be

represented with its vertex set $\mathbb{T}^{(p)} = \{z_1, \dots, z_L\}$, assume that there are L vertices in the set. To build up the next polyblock $\mathbb{P}^{(p+1)}$, one fundamental step is to find the unique intersection between the boundary of \mathbb{G} , which is denoted as $\partial^+ \mathbb{G}$, and the line segment connecting the origin and $z_{\text{opt}}^{(p)}$, where $z_{\text{opt}}^{(p)} \in \mathbb{T}^{(p)}$ and $\Phi(z_{\text{opt}}^{(p)}) \geq \Phi(z)$, $\forall z \in \mathbb{T}^{(p)}$. Mathematically, the following problem has to be solved

$$\mu^{(p)} = \max_{\mu \in (0,1]} \mu, \quad \text{s. t.} \quad \mu z_{\text{opt}}^{(p)} \in \mathbb{D}, \quad (5.46)$$

which is equivalent to the following optimization problem

$$\begin{aligned} \mu^{(p)} = \max_{\mathbf{w}} \min_m \frac{\mathbf{w}^H \bar{\mathbf{E}}_m \mathbf{w}}{z_{\text{opt},m}^{(p)} \mathbf{w}^H \mathbf{F}_m \mathbf{w}} \\ \text{s.t.} \quad \mathbf{w}^H \mathbf{C}_c \mathbf{w} = 1 \\ f_\kappa(\mathbf{w} \mathbf{w}^H) \leq 0, \quad \forall \kappa \in \mathcal{N}. \end{aligned} \quad (5.47)$$

Problem (5.47) is similar to the SINR balancing problem in Section 5.6. Thus, we solve it using the SDR technique, i.e., by replacing $\mathbf{w} \mathbf{w}^H$ by \mathbf{X} we get

$$\begin{aligned} \mu^{(p)} = \max_{\mathbf{X}} \min_m \frac{\text{Tr}\{\bar{\mathbf{E}}_m \mathbf{X}\}}{\text{Tr}\{z_{\text{opt},m}^{(p)} \mathbf{F}_m \mathbf{X}\}} \\ \text{s.t.} \quad \text{Tr}\{\mathbf{C}_c \mathbf{X}\} = 1 \\ f_\kappa(\mathbf{X}) \leq 0, \quad \forall \kappa \in \mathcal{N}. \end{aligned} \quad (5.48)$$

Problem (5.48) can be solved approximately (ν -optimality) using the bisection search method or the Dinkelbach-type algorithms. Similarly as in Section 5.6, a rank-1 solution is not guaranteed for (5.48). Thus, problem (5.46) cannot be solved exactly. For a polyblock algorithm, if its sub-problem like (5.46) is not solved exactly, to guarantee the convergence of the polyblock algorithm, further restrictions have to be given [PT03]. To find these restrictions explicitly for our problem is usually non-trivial, e.g., [UB12], and might be intractable. Moreover, concerning the computational complexity, we resort to a simplified implementation as given in Algorithm 9. The (ϵ, ν) -optimal polyblock algorithm implies that the following problem instead of (5.44) is solved.

$$\begin{aligned} \max_{\mathbf{X}, y_m, \forall m} \quad & \sum_{m=1}^{2K} \alpha_m \log(y_m) \\ \text{s. t.} \quad & \text{Tr}\{\mathbf{C}_c \mathbf{X}\} = 1 \\ & f_\kappa(\mathbf{X}) \leq 0, \quad \forall \kappa \in \mathcal{N} \end{aligned}$$

Algorithm 9 (ϵ, ν) -optimal polyblock algorithm for weighted sum rate maximization given fixed weighting factor α_m

- 1: **Initialize:** set initial vertex set $\mathbb{T}_0 = \{\mathbf{z}_0\}$, maximum iteration number N_{\max} , and the threshold values ϵ, ν .
 - 2: **Main step:**
 - 3: **for** $p = 1$ to N_{\max} **do**
 - 4: Find $\mathbf{z}_{\text{opt}}^{(p)}$ as described in Appendix C.7.2.
 - 5: Solve (5.48) to find $\mathbf{X}^{(p)}$ and ν -optimal $\mu^{(p)}$.
 - 6: Construct a smaller polyblock $\mathbb{P}^{(p+1)}$ as described in Appendix C.7.2.
 - 7: **if** $|\Phi(\mathbf{y}^{(p+1)}) - \Phi(\mathbf{y}^{(p)})| \leq \epsilon$ **then**
 - 8: **return** $\mathbf{X}^{(p)}$
 - 9: **end if**
 - 10: **end for**
 - 11: Obtain the optimal \mathbf{w} from $\mathbf{X}^{(p)}$ using the randomization technique in [LMS⁺10].
-

$$\begin{aligned}
y_m &\leq \max_{\mathbf{X}} \frac{\text{Tr}\{\bar{\mathbf{E}}_m \mathbf{X}\}}{\text{Tr}\{\mathbf{F}_m \mathbf{X}\}}, \quad \forall m \\
y_m &\geq \min_{\mathbf{X}} \frac{\text{Tr}\{\bar{\mathbf{E}}_m \mathbf{X}\}}{\text{Tr}\{\mathbf{F}_m \mathbf{X}\}}, \quad \forall m
\end{aligned} \tag{5.49}$$

Note that the two stopping criteria, i.e., the maximum iteration number N_{\max} and the tolerance factors (ϵ, ν) , reduce the computational complexity of the polyblock algorithm in Algorithm 9. But in general the obtained solutions are not globally optimal and thus only (ϵ, ν) -optimal solutions are achieved for problem (5.49). Moreover, the randomization based rank-1 approximation in the end of Algorithm 9 drives the final solution further away from the globally optimal solution.

Remark 9. Although the polyblock algorithm has guaranteed convergence, it is in general not a polynomial time algorithm. Its convergence speed depends on the initial vertex set \mathbb{T}_0 , the threshold value $(\epsilon, \nu)^3$ as well as the problem size $2K$ [PT03]. In practice it is only suitable as a benchmark algorithm.

5.8 Simulation results

The proposed algorithms in Sections 5.5, 5.6, and 5.7 are evaluated using Monte-Carlo simulations. The simulated channels $\mathbf{f}_{m,n}$, $\mathbf{g}_{m,n}$, and $h_{i,j}$ are uncorrelated flat Rayleigh fading and all their elements have zero mean and unit variance. The transmit powers at each UT are identical

³Practically, it suffices to set $\nu = \epsilon/4K$ [PT03].

and $P_m = 1$ W, $\forall m$. When SINR balancing and sum rate maximization are considered, the total power constraint of the relays is set to $P_{R,\max} = 1$ W while individual power constraints are set to $P_{R,\max}^{(\text{Ind})} = P_{R,\max}/N$. Moreover, the noise power at each UT and at each relay are also identical and $\sigma_U^2 = \sigma_R^2 = \sigma_n^2$. “Opt-FP” and “Opt-IP” denote the proposed algorithms with a total transmit power constraint and individual transmit power constraints. “Opt-xx-INL” and “Opt-xx” denote the cases with and without IN, where “xx” represents “FP” or “IP”. All the simulation results are obtained by averaging over 1000 channel realizations and $K = 2$ pairs of users are considered.

The feasibility region of interference neutralization is visualized in Figure 5.2. When M_R is fixed, the minimum number of relays which is required for interference neutralization increases exponentially as the number of pairs increases, although less relays are needed when M_R is large. Meanwhile, if N is fixed, the minimum number of antennas at the relay increases almost linearly as K increases. Again, less antennas are required when N is large. Moreover, if the total number of antennas in the network is fixed, Figure 5.2 suggests that a better choice to neutralize the interference in the network is to have more antennas at each relay.

Figure 5.3 illustrates an asymptotic analysis of the IN condition (5.12). When $K, M_R \rightarrow \infty$ and the ratio $\alpha = \frac{K}{M_R}$ remains as a constant, we have $N \geq 4 \frac{K(K-1)}{M_R(M_R+1)} \rightarrow 4\alpha^2$. That is, N grows quadratically with respect to the ratio α . As shown in Figure 5.3, as long as the ratio is small, even with a small M_R the exact results will coincide with the asymptotic results.

Figures 5.4, 5.5, and 5.6 demonstrate the minimum required total transmit power for interference neutralization, which is averaged over 1000 channel realizations. In general, the required transmit power increases as the number of pairs increases. It decreases as the number of antennas at the relay increases. However, the decrease is not monotonic. This phenomenon depends on the value of the function $f(K, M_R, N) = \frac{1}{2}NM_R(M_R + 1) - 2K(K - 1)$. According to Lemma C.4.3 in Appendix C.4.3, $f(K, M_R, N)$ represents the additional spatial dimensions which can be used to scale down the required power. For example, we have $f(K = 2, M_R = 1, N = 4) = 0$. Thus, the required power only depends on the channel realizations. The required power is high and a strong fluctuation can happen if the noise power changes, as shown in Figure 5.6. Moreover, the CDF curve converges slowly as shown in Figure 5.5. The same interpretation can be given to the cases $(K = 3, M_R = 3, N = 2)$ and $(K = 4, M_R = 3, N = 4)$. Furthermore, if K is fixed, e.g., $K = 3$, we have $f(K = 3, M_R = 4, N = 2) = 8$ and $f(K = 2, M_R = 5, N = 1) = 3$. This explains why the required transmit power increases from $(K = 3, M_R = 4, N = 2)$ to $(K = 2, M_R = 5, N = 1)$. Finally, Figure 5.6 implies that the required transmit power varies slightly as the noised power changes.

Figure 5.7 shows the minimum required transmit power as a function of the required mini-

mum SINR. Given a fixed value of $M_R \cdot N$, in general, more relays require more transmit power at the relay. One explanation is that fewer antennas at the relay yield a smaller feasibility range and thus fewer degrees of freedom in the spatial domain, which can be used to reach the SINR requirements. Due to a similar reason, when IN is applied, more power has to be consumed to achieve the desired SINR. However, as the required SINR increases, the required power with IN increases slower than for the case without IN. Moreover, it is worth mentioning that numerical results show that the relaxed problem, i.e., problem (5.29), provides almost always a rank-1 solution⁴. We observe the same behavior for all the other simulations of SDR based solutions.

Figure 5.8 demonstrates the required number of iterations for the bisection method and the DT algorithms. Although in general all the proposed algorithms converge linearly, as discussed in Section 5.6, simulation results show that the DT algorithms converge in fewer iterations compared to the bisection search method. Compared to the DT-1 algorithm, the DT-2 algorithm converges faster when the noise power is high. When the noise power is low, it can happen that the DT-2 algorithm will take more iterations. However, we observe that if IN is applied, all the proposed algorithms take fewer iterations. The difference between convergence speeds of different algorithms reduces. In the following, all the simulation results are obtained using the DT-2 algorithm. Figures 5.9 illustrates the SINR balancing performance under two different system settings, i.e., $N = 2, M_R = 4$ and $N = 4, M_R = 2$. Other than the proposed algorithms, the following two algorithms have also been compared. The first one is denoted as “Non-smart”, which refers to the scheme where smart relays are not deployed. The second one is denoted as “TDMA”. This scheme refers to an orthogonal resource access where each pair of the UTs utilize the relays and repeaters in the network in a time-division multiple access (TDMA) fashion. Thus, for a fair comparison, peak power constraints are used in the simulation and the simulation results obtained using the “TDMA” scheme are additionally divided by K . Clearly, when there are no smart relays in the network, the presence of interferences will significantly affect the system performance. On the other hand, the orthogonal resource access scheme “TDMA” has its benefits especially when the system is noise limited. Among the two non-orthogonal resource access schemes, the IN scheme provides a balance between the computational complexity and the performance. Moreover, when the total number of antennas is limited in a network, to have a better system performance, it is more reasonable to have a few relays but many antennas at each relay.

When the system sum rate is considered as depicted in Figure 5.10, the difference between the algorithm with or without IN is quite small. Moreover, the proposed non-orthogonal

⁴For the case with IN, this refers to the matrix $[\mathbf{B} \quad \mathbf{c}]^H \mathbf{X}_{\text{opt}} [\mathbf{B} \quad \mathbf{c}]$.

schemes outperform the orthogonal schemes significantly.

5.9 Summary

In this chapter we study the feasibility problem of neutralizing the interference for a AF TWR network with multiple repeaters and smart relays. The necessary and sufficient conditions for IN have been derived. Moreover, a general framework to design optimal relay amplification matrices subject to different system design criteria, i.e., minimize the required transmit power at the relays subject to minimum SINR constraints, maximize the minimum SINR of the UTs subject to relay transmit power constraint(s), and maximize the weighted system sum rate subject to relay transmit power constraint(s), has been developed for such a scenario with or without IN, regardless whether the smart relays in the network have a total transmit power limit or individual transmit power limits.

Simulation results have demonstrated that

- When the number of antennas at each relay is fixed, the minimum number of relays which is required for IN increases exponentially as the number of pairs increases. When the number of relays is fixed, the minimum required number of antennas at each relay increases almost linearly as the number of pairs increases. These results suggest that a better choice to perform IN in the network is to have more antennas at each relay.
- In general, the required relay transmit power to perform IN increases as the number of UT pairs increases. It decreases as the number of antennas at each relay increases although the decrease is not monotonic due to the available spatial dimensions, which can be used to reduce the required relay transmit power for neutralizing the interference.
- To guarantee the required minimum SINR at each UT, the minimum required relay transmit power increases if the number of relays in the network increases, given a fixed value of $M_R \cdot N$. This is because less spatial dimensions can be used to satisfy the minimum SINR requirements. When IN is applied, more power are required since additional power might be required to neutralize the interference.
- In general, the proposed DT algorithms yield a better convergence behavior than the traditional bisection search algorithm. Compared to the TDMA scheme, the proposed non-orthogonal schemes are especially better when the noise is weak or when there are many number of antennas at each relay. When IN is applied, the performance is worse

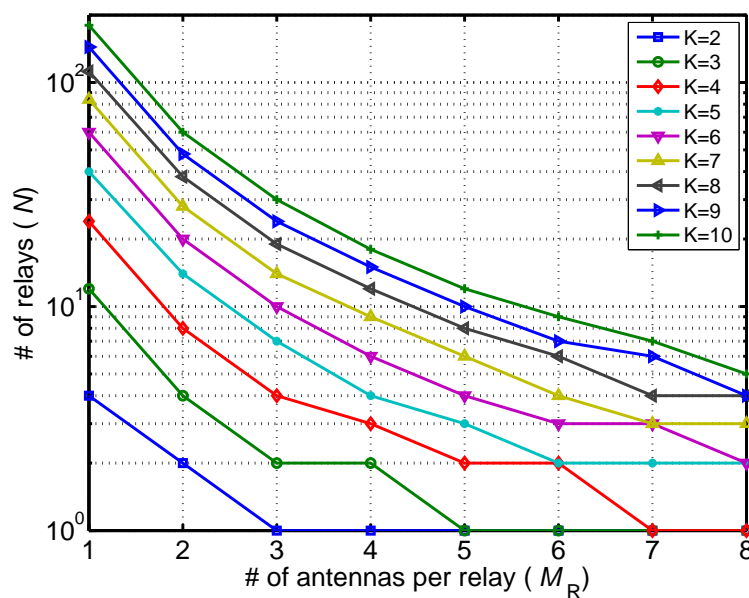


Figure 5.2: An illustration of condition (5.12) in Theorem 5.4.1. Given the number of user pairs K , the feasible region of interference neutralization consists of all pairs (M_R, N) which are on or above the plotted curve.

than the optimal performance. However, the performance difference reduces as the number of antennas at each relay increases. A similar performance is observed when sum rate maximization is the system design criterion.

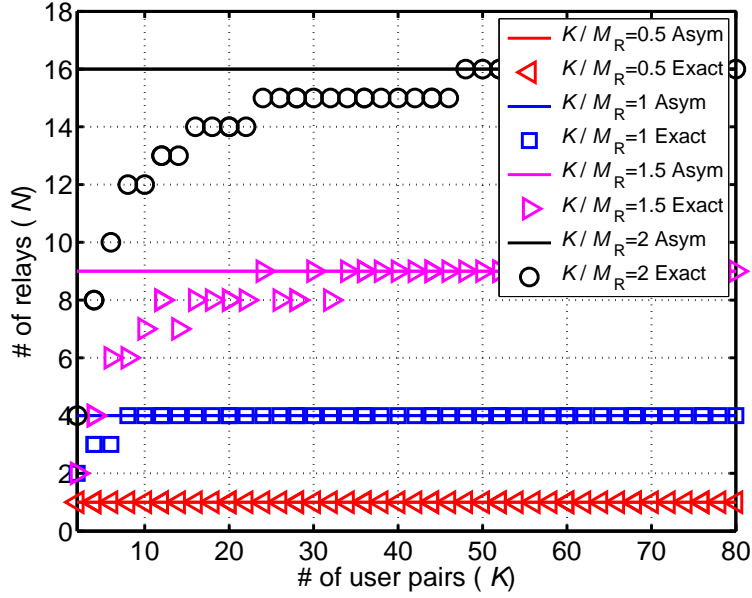


Figure 5.3: An illustration of the asymptotic analysis of (5.12) in Theorem 5.4.1. Let $K, M_R \rightarrow \infty$ and the ratio $\frac{K}{M_R}$ be a constant.

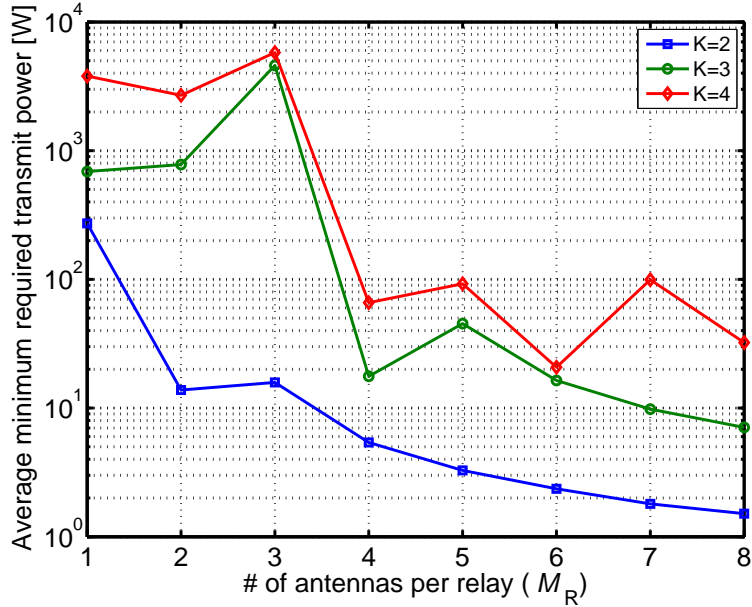


Figure 5.4: An illustration of the average minimum required total transmit power as a function of M_R . Given K and M_R , N is the minimum integer value which satisfies (5.12). In other words, N is the corresponding value on the curves of Figure 5.2. $\sigma_n^{-2} = 15$ dB.

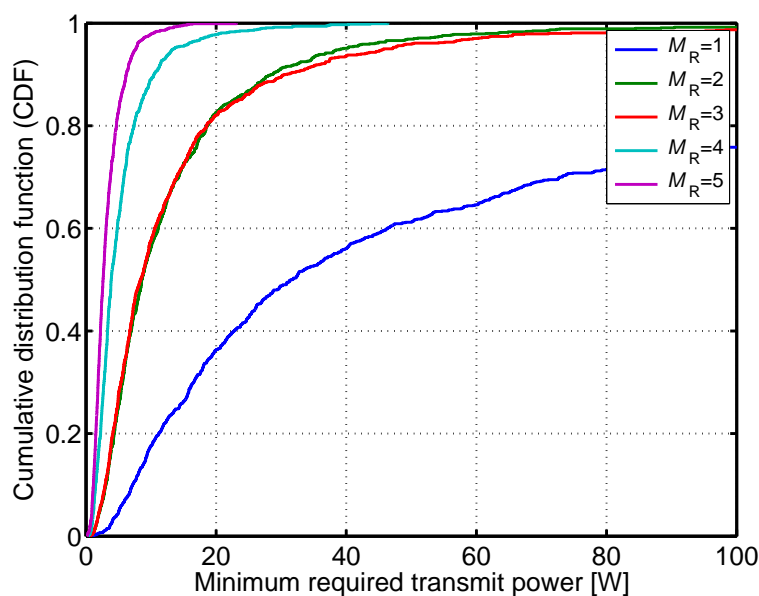


Figure 5.5: The cumulative distribution function (CDF) of the minimum required total transmit power under different pairs of (M_R, N) for $K = 2$ and $\sigma_n^{-2} = 15$ dB. M_R and N are calculated in the same way as in Figure 5.4.

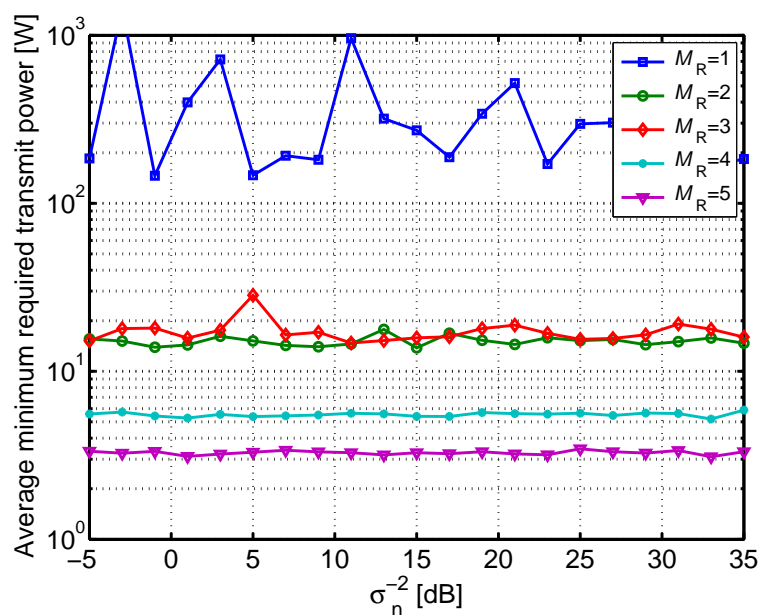


Figure 5.6: An illustration of the average minimum required total transmit power as a function of σ_n^{-2} . We have $K = 2$. M_R and N are calculated in the same way as in Figure 5.4.

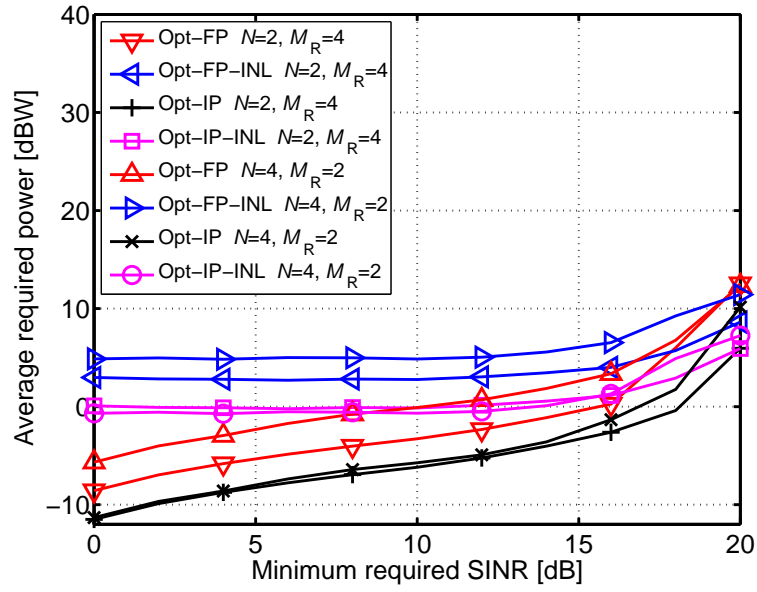


Figure 5.7: A comparison of the minimum required transmit power with and without interference neutralization.

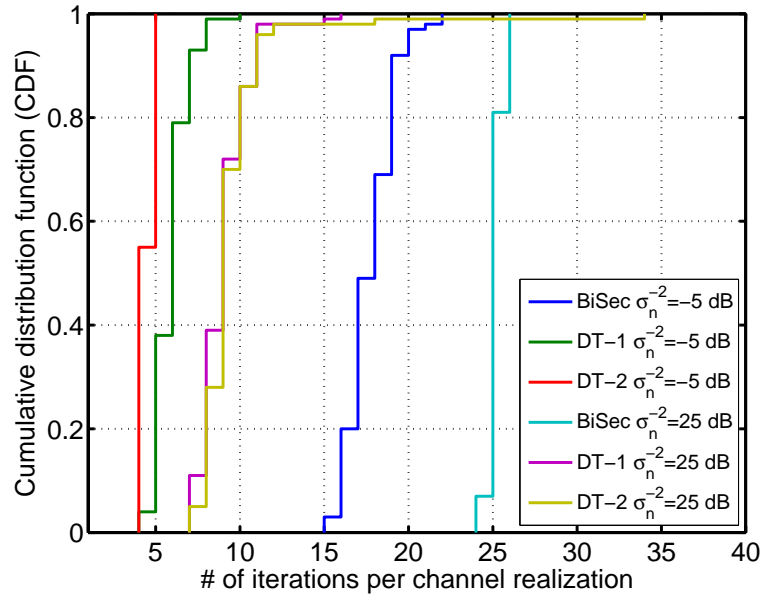


Figure 5.8: A demonstration of the convergence speed of the bisection search method (“BiSec”), the DT-1 algorithm (“DT-1”), and the DT-2 algorithm (“DT-2”) without IN. $N = 2$ and $M_R = 4$.

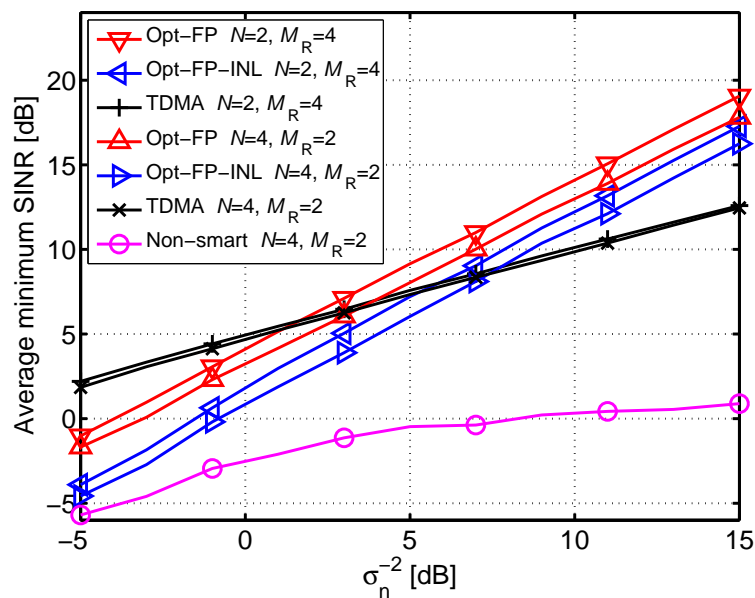


Figure 5.9: A comparison of the achievable minimum SINR using the state of art algorithm and the proposed algorithm.

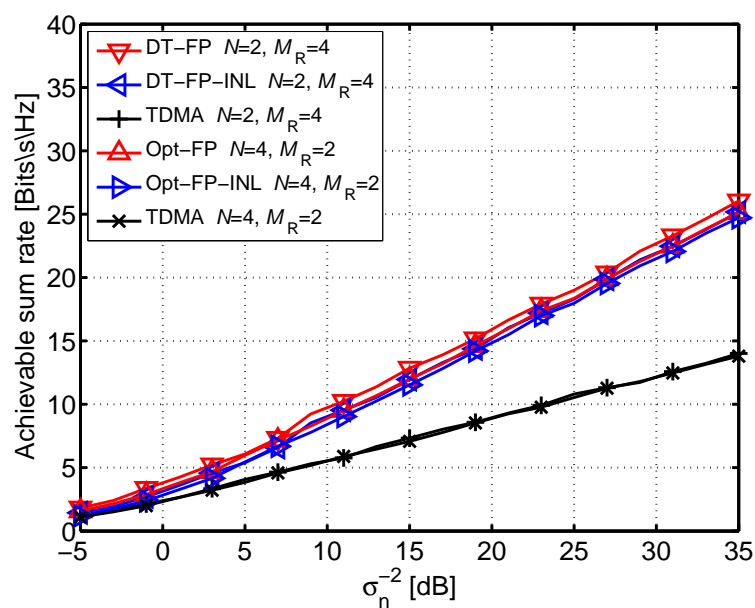


Figure 5.10: Maximum achievable sum rate with and without interference neutralization.

6 Relay broadcasting channel

Now we shift our focus from a multi-pair scenario to a multi-user downlink scenario, which is a typical scene for modern cellular networks. More specifically, we consider relay broadcasting channel with a MIMO AF relay where a MIMO BS and multiple single antenna UTs exchange messages via the relay. The precoding matrix at the BS and the relay amplification matrix should be designed. Moreover, multi-user scheduling should be also taken into account. This results in a complicated cross-layer design problem which is in general difficult to solve. To avoid the prohibitive complexity, we focus on the design of the precoder and decoder matrices at the BS as well as the relay amplification matrix while assuming that the UT scheduling is fixed. We develop suboptimal MIMO transmission techniques for both the BS and the relay [ZRH11]. The proposed suboptimal schemes are based on conventional channel inversion (CI), ProBaSeMO and zero-forcing dirty paper coding (ZFDPC), respectively. All the proposed algorithms are also compared to the state of the art algorithm in [TS09].

6.1 Problem description and state of the art

When relays are placed at the cell edge to boost the coverage, it is likely that each relay has to support multiple users. This motivates the development of multi-user MIMO relaying techniques, where the relay forwards data to and from multiple users. Compared to the multi-pair multi-user scenarios discussed in Chapters 3, 4, and 5, the major difference is that the BS sends multiple data streams to different UTs, i.e., broadcasting instead of unicasting. In such a situation, a proper user scheduling is inevitable. It is clear that a joint design of user scheduling techniques and MIMO transmission techniques cannot be avoided if one would like to optimize the system performance. This may result in a non-tractable optimization problem. Thus, most of the known work (including our work [ZRH11]) focuses on the design of novel MIMO transmission techniques while assuming that the user scheduling algorithm is fixed.

Prior work on the OWR broadcasting channel includes [TCHC06], [CTJC08], [YH10], and [AHV10]. In [TCHC06] a relay precoder design based on the SVD and a low-complexity user selection algorithm are proposed. In [CTJC08] the authors propose upper and lower bounds on the achievable sum rate assuming ZFDPC precoding at the BS. In [YH10] a ZFDPC strategy is also applied such that the relay precoder design problem reduces to a power allocation problem. Afterwards, the authors develop a so called generalized water-filling (GWF) algo-

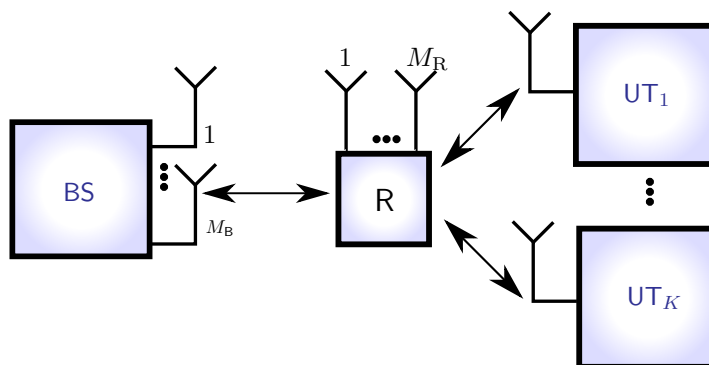


Figure 6.1: Multi-user two-way relaying with a MIMO amplify and forward relay.

rithm to solve the remaining problem. In [AHV10] the authors consider a relay broadcasting channel with BS cooperation. Again, non-linear precoding techniques, i.e., iterative Tomlinson Harashima precoding (THP) based schemes, are used such that the problem turns into a power allocation problem. Moreover, in this reference the authors use the multiuser fairness instead of the system sum rate in [YH10] as the design criterion. However, all the proposed techniques for one-way relaying scenario cannot be applied to the two-way relaying scenario directly. References dealing with multi-user two-way relaying include beamforming with an AF relay [TS09], beamforming with a DF relay [EW08a], relaying protocols with repeaters [WM07] as well as the performance analysis of a channel inversion (CI) based transmit precoder design in [DKTL11]. In general, only [TS09] and [DKTL11] discuss the precoder design problem for a MIMO AF relay broadcasting channel and they consider only the CI based techniques. Therefore, this motivates us to develop other advanced linear or non-linear precoding techniques.

6.2 Data model

The scenario under investigation is shown in Figure 6.1. Due to the poor quality of the direct channel between the BS and the UTs, they can only communicate with each other with the help of the relay. Assume that we have K single antenna UTs. The BS is equipped with M_B antennas and the relay has M_R antennas. For notational simplicity, in the rest of our work we assume that $M_B = K$. The channel is flat fading. The channel between the k th user and the relay is denoted by $\mathbf{h}_k \in \mathbb{C}^{M_R}$. The channel between the BS and the relay is full rank and denoted by $\mathbf{H}_B \in \mathbb{C}^{M_R \times M_B}$.

The two-way AF relaying protocol consists of two transmission phases: in the first phase

all the users and the BS transmit their data simultaneously to the relay. Let the BS transmit the data symbol vector $\mathbf{d}_B = [d_{B,1}, \dots, d_{B,K}]^T \in \mathbb{C}^K$ using the transmit beamforming matrix $\mathbf{F}_B \in \mathbb{C}^{M_B \times K}$. The data symbols in \mathbf{d}_B are independently distributed with zero mean and unit variance. Let us further assume that $d_{B,k}$ is the symbol transmitted from the BS to the k th UT and the relay knows the order of the data streams from the BS. The total power at the BS is denoted by P_B . The transmit power constraint can be written as

$$\mathbb{E}\{\|\mathbf{F}_B \mathbf{d}_B\|^2\} = \text{Tr}\{\mathbf{F}_B \mathbf{F}_B^H\} = P_B. \quad (6.1)$$

Then, the received signal vector at the relay is given by

$$\mathbf{r} = \sum_{k=1}^K \mathbf{h}_k \cdot d_k + \mathbf{H}_B \mathbf{F}_B \mathbf{d}_B + \mathbf{n}_R \in \mathbb{C}^{M_R}, \quad (6.2)$$

where d_k is the transmitted scalar from the k th user to the BS and $\mathbf{n}_R \in \mathbb{C}^{M_R}$ is the ZMCSCG noise with $\mathbb{E}\{\mathbf{n}_R \mathbf{n}_R^H\} = \sigma_R^2 \mathbf{I}_{M_R}$. Moreover, we assume that each user has identical transmit power P_U and the transmit power constraint is equivalent to $\mathbb{E}\{|d_k|^2\} \leq P_U$.

In the second phase, the relay amplifies the received signal and then forwards it to all the UTs as well as the BS. The signal transmitted by the relay can be expressed as

$$\bar{\mathbf{r}} = \gamma_0 \cdot \mathbf{G} \cdot \mathbf{r}. \quad (6.3)$$

where $\mathbf{G} \in \mathbb{C}^{M_R \times M_R}$ is the relay amplification matrix and $\gamma_0 \in \mathbb{R}^+$ is chosen such that the transmit power constraint at the relay is fulfilled, i.e.,

$$\mathbb{E}\{\|\bar{\mathbf{r}}\|^2\} = \text{Tr}\{\gamma_0^2 \cdot \mathbf{G}\{P_U \mathbf{H}_U \mathbf{H}_U^H + P_B \mathbf{H}_B \mathbf{F}_B \mathbf{F}_B^H \mathbf{H}_B^H + \sigma_R^2 \mathbf{I}_{M_R}\} \mathbf{G}^H\} = P_R, \quad (6.4)$$

where $\mathbf{H}_U = [\mathbf{h}_1, \dots, \mathbf{h}_K] \in \mathbb{C}^{M_R \times K}$ is the concatenated channel matrix of all UTs.

For notational simplicity, we assume that the reciprocity assumption between the first and second phase channels is valid. This assumption is fulfilled in a TDD system if identical calibrated RF chains are applied. Then the received signal vector at the BS can be expressed as

$$\begin{aligned} \mathbf{y}_B &= \mathbf{W}_B (\mathbf{H}_B^T \bar{\mathbf{r}} + \mathbf{n}_B) \\ &= \underbrace{\gamma_0 \mathbf{W}_B \mathbf{H}_B^T \mathbf{G} \mathbf{H}_U \mathbf{d}_U}_{\text{useful signal}} + \underbrace{\gamma_0 \mathbf{W}_B \mathbf{H}_B^T \mathbf{G} \mathbf{H}_B \mathbf{F}_B \mathbf{d}_B}_{\text{self-interference}} + \underbrace{\gamma_0 \mathbf{W}_B \mathbf{H}_B^T \mathbf{G} \mathbf{n}_R + \mathbf{W}_B \mathbf{n}_B}_{\text{effective noise}} \in \mathbb{C}^{M_R} \end{aligned} \quad (6.5)$$

where $\mathbf{d}_U = [d_1, \dots, d_K]^T \in \mathbb{C}^K$ is the concatenated data vector of all the UTs and $\mathbf{n}_B \in \mathbb{C}^{M_B}$ is the ZMCSCG noise with $E\{\mathbf{n}_B \mathbf{n}_B^H\} = \sigma_B^2 \mathbf{I}_{M_B}$. The receive beamforming matrix is denoted by $\mathbf{W}_B \in \mathbb{C}^{K \times M_B}$. It can be seen from (6.5) that the BS only experiences the self-interference caused by its own transmitted signal. If the BS has perfect channel knowledge, the self-interference can be subtracted.

On the other hand, the received scalar y_k at the k th UT can be written as

$$\begin{aligned}
 y_k = \mathbf{h}_k^T \bar{\mathbf{r}} + n_k = & \underbrace{\gamma_0 \mathbf{h}_k^T \mathbf{G} \mathbf{H}_B \mathbf{f}_{B,k} d_{B,k}}_{\text{useful signal}} + \underbrace{\gamma_0 \mathbf{h}_k^T \mathbf{G} \mathbf{h}_k d_k}_{\text{self-interference}} \\
 + & \underbrace{\sum_{\substack{m=1 \\ m \neq k}}^K \gamma_0 \mathbf{h}_k^T \mathbf{G} \mathbf{H}_B \mathbf{f}_{B,m} d_{B,m}}_{\text{interference from other streams to other UTs}} + \underbrace{\sum_{\substack{j=1 \\ j \neq k}}^K \gamma_0 \mathbf{h}_k^T \mathbf{G} \mathbf{h}_j d_j}_{\text{interference from other UTs}} + \underbrace{\gamma_0 \mathbf{h}_k^T \mathbf{G} \mathbf{n}_R + n_k}_{\text{effective noise}} \quad (6.6)
 \end{aligned}$$

where $\mathbf{f}_{B,k}$ is the k th column of \mathbf{F}_B and n_k is ZMCSCG noise at each UT with identical variance σ_U^2 . As can be seen from (6.6), unlike the BS, each UT experiences self-interference, interference caused by other UTs, and the interference caused by the signal which is transmitted from the BS but intended for another UT.

The overall sum rate of the system could be written as

$$R_{\text{sum}} = R_U + R_B \quad (6.7)$$

where R_B and R_U are the achievable data rate at the BS and the cumulated achievable data rate at all UTs, respectively. The optimization problem to find the relay amplification matrix structure which maximizes (6.7) subject to the transmit power constraints in (6.1) and (6.4) is non-convex. To avoid a non-tractable optimization problem, we resort to suboptimal algorithms instead.

In [TS09], a linear beamforming is proposed such that

$$\begin{aligned}
 \mathbf{G} &= \gamma_1 (\mathbf{H}_U^T)^{-1} \mathbf{H}_U^{-1} \\
 \mathbf{F}_B &= \gamma_2 \mathbf{H}_B^{-1} \mathbf{H}_U \\
 \mathbf{W}_B &= \mathbf{H}_U^T (\mathbf{H}_B^T)^{-1} \quad (6.8)
 \end{aligned}$$

where γ_1 and γ_2 are the normalizing coefficients satisfying the transmit power constraint at the relay and the BS, respectively.

However, it can be seen that the inverses of \mathbf{H}_U and \mathbf{H}_B do not always exist. Hence, this

method can not be always utilized since (6.8) requires that $M_R = M_B = K$. Our algorithms in Sections 6.3.1, 6.3.2, and 6.3.3 are applicable for a broader range of antenna configurations. We specify the corresponding dimensionality constraints below.

Moreover, inspired by the ProBaSeMO approach in Section 3.3, we decompose \mathbf{G} into

$$\mathbf{G} = \mathbf{G}_T \cdot \mathbf{G}_S \cdot \mathbf{G}_R \in \mathbb{C}^{M_R \times M_R} \quad (6.9)$$

6.3 Transmit strategies design for the BS and the relay

6.3.1 Channel inversion based design

In this section, we introduce a straightforward beamforming design based on CI. Using this method, orthogonal channels are created between the BS and the UTs for interference free communication. This algorithm can efficiently eliminate the self-interference as well as the co-channel interference. However, the well-known disadvantage of it is the enhancement of the noise power.

Let us define $\mathbf{H} = \begin{bmatrix} \mathbf{H}_B & \mathbf{H}_U \end{bmatrix} \in \mathbb{C}^{M_R \times (K+M_B)}$. The CI receive beamforming is then given by

$$\mathbf{G}_R = \mathbf{H}^+ = (\mathbf{H}^H \mathbf{H})^{-1} \mathbf{H}^H \quad (6.10)$$

and the transmit beamforming is given by $\mathbf{G}_T = \mathbf{G}_R^T$.

In this case, the matrix \mathbf{G}_S is chosen to be a block matrix of the form $\mathbf{G}_S = \mathbf{\Pi}_2 \otimes \mathbf{I}_K \in \mathbb{C}^{2 \cdot K \times 2 \cdot K}$, where $\mathbf{\Pi}_2 = \begin{bmatrix} 0 & 1 \\ 1 & 0 \end{bmatrix}$ is the exchange matrix which ensures that the BS and the UTs will not receive their own transmitted signals. Furthermore, for simplicity, we choose $\mathbf{F}_B = \mathbf{W}_B = \sqrt{\frac{P_B}{M_B}} \mathbf{I}_{M_B}$. As can be seen from (6.10), this CI method requires that $M_R \geq 2K$. Moreover, compared to the other algorithms proposed in the following sections, the complexity for calculating the Moore-Penrose pseudoinverse is much lower.

6.3.2 ProBaSeMO inspired approach

For simplicity, we again choose $\mathbf{F}_B = \mathbf{W}_B = \sqrt{\frac{P_B}{M_B}} \mathbf{I}_{M_B}$ in this section. Let us further fix the order of the users such that the k th user communicates with the BS only via the k th antenna at the BS. Then this system can be treated as multiple pairs of single antenna users which communicate with each other with the help of the relay. Clearly, this kind of architecture possesses the same mathematical model as in Chapter 3. Thus, all proposed schemes in Chapter 3 can be applied. But the optimal algorithms in Chapter 3 are suboptimal for the relay broadcasting channel.

Therefore, for simplicity, we recommend the ProBaSeMO scheme and more specifically, BD combined with ANOMAX, since according to our work in Chapter 3 it provides the best trade-off between performance and computational complexity. Here we extend the BD ANOMAX method to the relay broadcasting channel.

First, define $\mathbf{G}_T = [\mathbf{G}_T^{(1)}, \dots, \mathbf{G}_T^{(K)}] \in \mathbb{C}^{M_R \times KM_R}$, $\mathbf{G}_S = \text{blkdiag} \left\{ \mathbf{G}_S^{(k)} \right\}_{k=1}^K \in \mathbb{C}^{KM_R \times KM_R}$, and $\mathbf{G}_R = [\mathbf{G}_R^{(1)\text{T}}, \dots, \mathbf{G}_R^{(K)\text{T}}]^\text{T} \in \mathbb{C}^{KM_R \times M_R}$, where $\mathbf{G}_T^{(k)}$, $\mathbf{G}_S^{(k)}$, and $\mathbf{G}_R^{(k)} \in \mathbb{C}^{M_R \times M_R}$. BD ANOMAX consists of two steps. In the first step, the system is converted into K parallel independent sub-systems via the BD design of \mathbf{G}_R and \mathbf{G}_T . Then, in the second step, for each single-pair two-way relaying sub-system, we use the ANOMAX algorithm [RH09] to calculate $\mathbf{G}_S^{(k)}$.

Let us define the combined channel matrix $\tilde{\mathbf{H}}^{(k)}$ for all UTs except for the k th UT as

$$\tilde{\mathbf{H}}^{(k)} = \begin{bmatrix} \mathbf{H}^{(1)} & \dots & \mathbf{H}^{(k-1)} & \mathbf{H}^{(k+1)} & \dots & \mathbf{H}^{(K)} \end{bmatrix}, \quad (6.11)$$

where $\mathbf{H}^{(k)} = \begin{bmatrix} \mathbf{h}_{B,k} & \mathbf{h}_k \end{bmatrix}$ and $\mathbf{h}_{B,k}$ is the k th column of \mathbf{H}_B .

Let $\tilde{L}^{(k)} = \text{rank}\{\tilde{\mathbf{H}}^{(k)}\}$ and calculate the singular value decomposition (SVD)

$$\tilde{\mathbf{H}}^{(k)} = \begin{bmatrix} \tilde{\mathbf{U}}_s^{(k)} & \tilde{\mathbf{U}}_n^{(k)} \end{bmatrix} \tilde{\Sigma}^{(k)} \tilde{\mathbf{V}}^{(k)\text{H}}. \quad (6.12)$$

where $\tilde{\mathbf{U}}_n^{(k)}$ contains the last $(M_R - \tilde{L}^{(k)})$ left singular vectors. Thus, $\tilde{\mathbf{U}}_n^{(k)}$ forms an orthogonal basis for the null space of $\tilde{\mathbf{H}}^{(k)}$. Therefore, we choose $\mathbf{G}_R^{(k)} = \tilde{\mathbf{U}}_n^{(k)} \tilde{\mathbf{U}}_n^{(k)\text{H}} \in \mathbb{C}^{M_R \times M_R}$ which is a projection matrix that projects any matrix into the null space of $\tilde{\mathbf{H}}^{(k)}$. Due to the channel reciprocity, we can simply set $\mathbf{G}_T^{(k)} = \mathbf{G}_R^{(k)\text{T}}$.

Next, we define the matrix

$$\mathbf{K}_\beta^{(k)} = \left[\beta \left((\mathbf{G}_R^{(k)} \mathbf{h}_k) \otimes (\mathbf{G}_T^{(k)\text{T}} \mathbf{h}_{B,k}) \right) \quad (1 - \beta) \left((\mathbf{G}_R^{(k)} \mathbf{h}_{B,k}) \otimes (\mathbf{G}_T^{(k)\text{T}} \mathbf{h}_k) \right) \right],$$

which is needed to calculate the ANOMAX solution of $\mathbf{G}_S^{(k)}$ [RH09]. The parameter $\beta \in [0, 1]$ is a weighting factor.

Then we compute the SVD of $\mathbf{K}_\beta^{(k)}$ as $\mathbf{K}_\beta^{(k)} = \mathbf{U}_\beta^{(k)} \Sigma_\beta^{(k)} \mathbf{V}_\beta^{(k)\text{H}}$. Let the first column of $\mathbf{U}_\beta^{(k)}$, i.e., the dominant left singular vector of $\mathbf{K}_\beta^{(k)}$ be denoted by $\mathbf{u}_{\beta,1}^{(k)}$. According to the ANOMAX concept, the matrix $\mathbf{G}_S^{(k)}$ is then obtained via

$$\mathbf{G}_S^{(k)} = \text{unvec}_{M_R \times M_R} \left\{ \mathbf{u}_{\beta,1}^{(k)*} \right\}. \quad (6.13)$$

In this chapter we use equal weighting and therefore β is set to 0.5. This algorithm has the

dimensionality constraint that $M_R > (2K - 2)$.

6.3.3 ZFDPC based design

The multi-antenna BS has the ability of jointly encoding its transmitted data streams or of jointly decoding of its received data streams. To further make use of this capability, we introduce the ZFDPC based beamforming design.

Let us partition $\mathbf{G}_R = \begin{bmatrix} \mathbf{G}_B^T & \mathbf{G}_U^T \end{bmatrix}^T$ and assume that $\mathbf{G}_T = \mathbf{G}_R^T$. Moreover, let $L_U = \text{rank}(\mathbf{H}_U)$ and define the SVD of \mathbf{H}_U as

$$\mathbf{H}_U = \begin{bmatrix} \mathbf{U}_{U,s} & \mathbf{U}_{U,n} \end{bmatrix} \boldsymbol{\Sigma}_U \mathbf{V}_U^H \in \mathbb{C}^{M_R \times K}. \quad (6.14)$$

where $\mathbf{U}_{U,n}$ contains the last $\bar{L}_U = M_R - L_U$ left singular vectors. Thus, with the same reasoning as in Section 6.3.2, we choose

$$\mathbf{G}_B = \mathbf{U}_{U,n} \mathbf{U}_{U,n}^H \in \mathbb{C}^{M_R \times M_R}.$$

Furthermore, let us define $\mathbf{G}_S = \mathbf{\Pi}_2 \otimes \mathbf{I}_{M_R} \in \mathbb{C}^{2 \cdot M_R \times 2 \cdot M_R}$ and $\mathbf{0}_{K \times K}$ to be the K -by- K matrix with all zero elements. Then the concatenated received signal at the BS and all UTs can be written as

$$\begin{bmatrix} \mathbf{y}_B \\ \mathbf{y}_U \end{bmatrix} = \underbrace{\begin{bmatrix} \gamma_0 \mathbf{W}_B \mathbf{H}_B^T \mathbf{G} \mathbf{H}_B \mathbf{F}_B & \mathbf{W}_B \mathbf{H}_B^T \mathbf{G}_B^T \mathbf{G}_U \mathbf{H}_U \\ \mathbf{H}_U^T \mathbf{G}_U^T \mathbf{G}_B \mathbf{H}_B \mathbf{F}_B & \mathbf{0}_{K \times K} \end{bmatrix}}_{\mathbf{H}_{\text{eff}}} \cdot \begin{bmatrix} \mathbf{d}_B \\ \mathbf{d}_U \end{bmatrix} + \tilde{\mathbf{n}} \in \mathbb{C}^{(M_B + K)}. \quad (6.15)$$

In equation (6.15), the first M_B rows represent the received signal at the BS (\mathbf{y}_B). We further assume that the BS has perfect channel knowledge, and thus, the self-interference term which corresponds to the upper left block of \mathbf{H}_{eff} can be subtracted from \mathbf{y}_B . Then, the system is further decomposed into two-sub systems where the upper right part is equivalent to the uplink of a one-way relay broadcast channel and the lower left part is equivalent to the downlink of a one-way relay multiple access channel. In the next step, we show how to design \mathbf{G}_U , \mathbf{F}_B , and \mathbf{W}_B using ZFDPC.

ZFDPC is a suboptimal beamforming solution which has been used in several multi-user MIMO relaying references ([YH10], [TCHC06], [EW08a]). Thus, we will also modify the ZFDPC design for our scenario.

First, we apply the QR decomposition and the SVD to the channel matrices \mathbf{H}_U and $\mathbf{G}_B \mathbf{H}_B$

respectively,

$$\mathbf{H}_U^T = \mathbf{M}_U \mathbf{Q}_U \in \mathbb{C}^{K \times M_R}, \quad (6.16)$$

where $\mathbf{M}_U \in \mathbb{C}^{K \times M_R}$ is a lower triangular matrix and $\mathbf{Q}_U \in \mathbb{C}^{M_R \times M_R}$ is a unitary matrix. The SVD of $\mathbf{G}_B \mathbf{H}_B$ is denoted by $\mathbf{G}_B \mathbf{H}_B = \mathbf{U}_B \mathbf{\Sigma}_B \mathbf{V}_B^H \in \mathbb{C}^{M_R \times M_B}$. Then the linear processing matrix \mathbf{G}_U can be expressed as:

$$\mathbf{G}_U = \mathbf{U}_B^* \mathbf{Q}_U^* \in \mathbb{C}^{M_R \times M_R}. \quad (6.17)$$

Moreover, the precoding matrix \mathbf{F}_B is chosen as $\mathbf{F}_B = \sqrt{\frac{P_B}{M_B}} \mathbf{V}_B$ and the decoding matrix \mathbf{W}_B is constructed as $\mathbf{W}_B = \mathbf{F}_B^T \in \mathbb{C}^{M_B \times M_B}$.

Inserting \mathbf{G}_U , \mathbf{F}_B and \mathbf{W}_B into (6.15), the upper right matrix in \mathbf{H}_{eff} is converted into an upper-triangular matrix while the lower left part of it is converted into a lower-triangular matrix, as shown in the following.

$$\begin{bmatrix} \mathbf{y}_B \\ \mathbf{y}_U \end{bmatrix} = \underbrace{\begin{bmatrix} \gamma_0 \mathbf{W}_B \mathbf{H}_B^T \mathbf{G} \mathbf{H}_B \mathbf{F}_B & \sqrt{\frac{P_B}{M_B}} \mathbf{\Sigma}_B^T \mathbf{M}_U^T \\ \sqrt{\frac{P_B}{M_B}} \mathbf{M}_U \mathbf{\Sigma}_B & \mathbf{0}_{K \times K} \end{bmatrix}}_{\mathbf{H}_{\text{eff}}} \begin{bmatrix} \mathbf{d}_B \\ \mathbf{d}_U \end{bmatrix} + \tilde{\mathbf{n}} \in \mathbb{C}^{(M_B+K)}.$$

Assuming that the BS has also perfect knowledge of the interference signals, it can utilize a successive interference cancellation (SIC) receiver to decode each data stream. For each UT, the interference can be canceled by applying a DPC coding at the BS with perfect knowledge of the interfering signals. Unfortunately, the ZFDPC design has also a dimensionality constraint, which means $M_R \geq 2K$. Furthermore, since this is a non-linear algorithm, it has the highest computational complexity among the three proposed algorithms.

6.3.4 Simulation results

In this section, the performance of the proposed algorithms is evaluated via Monte-Carlo simulations. The simulated MIMO flat fading channels \mathbf{h}_k and \mathbf{H}_B are spatially uncorrelated Rayleigh fading channels. The SNRs at all nodes are defined as $\text{SNR} = 1/\sigma_B^2 = 1/\sigma_R^2 = 1/\sigma_U^2$. All the simulation results are obtained by averaging over 1000 channel realizations. ‘‘CI’’, ‘‘ProBaSeMO(BA)’’, ‘‘OWR ZFDPC’’, and ‘‘Toh09’’ denote the algorithms in Sections 6.3.1, 6.3.2, 6.3.3 and [TS09], respectively. Note that the curves labeled ‘‘Toh09’’ in our results are obtained by using the pseudo-inverse of \mathbf{H}_B and \mathbf{H}_U in (6.8).

As can be seen from Figure 6.2, ‘‘ProBaSeMO(BA)’’ provides the best performance and is 8 dB better than ‘‘Toh09’’ in the high SNR regime. The ‘‘OWR ZFDPC’’ curve is as good as

“CI” and is close to “ProBaSeMO(BA)”. However, it should be noted that “OWR ZFDPC” has the highest complexity. Moreover, all the curves have the same slope at high SNRs which implies that they possess the same multiplexing gain.

Figure 6.3 show the system loading when $M_R = 20$ and the SNRs at all nodes are 25 dB. It can be seen that due to the dimensionality constraint for “ProBaSeMO(BA)” and “CI”, there is an inflexion point after which increasing the number of UTs will decrease the system sum rate. For “OWR ZFDPC”, although there seems to be also an inflexion point when the system is heavily loaded (at $K = 9$), the sum rate does not drop as quickly as in the case of the other two algorithms.

6.4 Summary

In this chapter we discuss our proposed precoding techniques (at both BS and relay) in [ZRH11] for the multi-user two-way relay broadcasting channel with a MIMO AF relay. We propose three suboptimal algorithms, namely, the CI approach, the ProBaSeMO (BA) approach and the ZFDPC based design, for computing the transmit and receive beamforming matrices at the BS as well as the linear amplification matrix at the relay. The CI approach relies on the existence of the inverse of the compound channel. Although it can be easily implemented, it amplifies the noise and thus the performance is limited. The ProBaSeMO approach is applied while assuming that the precoder and decoder of the BS are fixed. Thus, its performance might be far from the optimal performance. Although the ZFDPC approach also requires a sufficient number of antennas at the relay, it suffers only a little when the number of user pairs K increases compared to the two approaches before. But it has a high computational complexity.

Simulation results have illustrated that

- When there are sufficient antennas at the relay, the proposed algorithms have almost the same performance. Among the proposed algorithms “ProBaSeMO(BA)” provides the best balance between complexity and performance. All the algorithms outperform the algorithm in [TS09].
- When the system is heavily loaded, i.e., the required number of antennas at the BS and at the relay for performing the proposed algorithms are satisfied with a small margin, “OWR ZFDPC” can still perform well due to its non-linear nature.

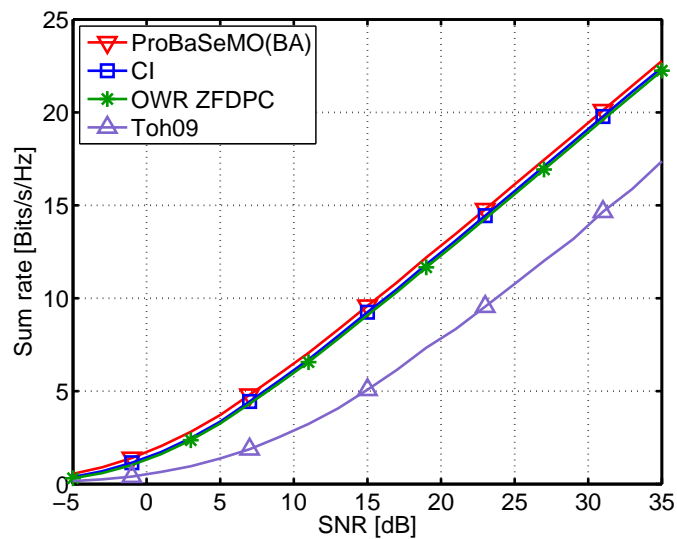


Figure 6.2: Sum rate comparison for $M_R = 8$ and $K = 2$.

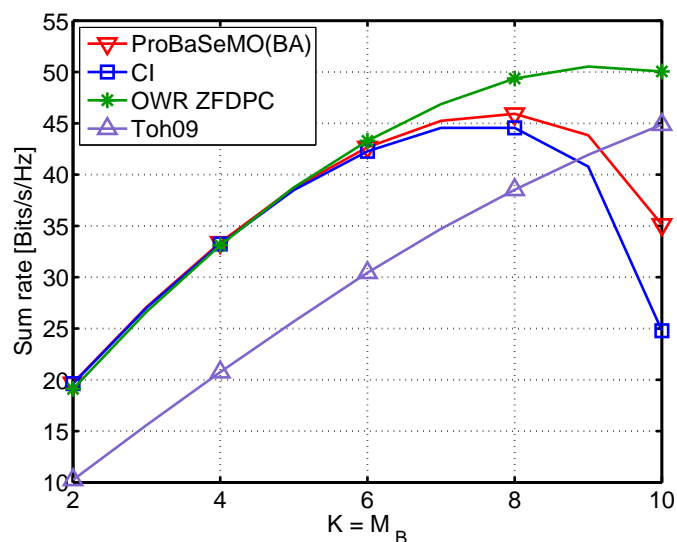


Figure 6.3: Sum rate comparison for $M_R = 20$ and $\text{SNR} = 25$ dB.

7 Summary of the two-way relaying networks

7.1 Summary of contributions

This part of the thesis devotes to the signal processing algorithms design for TWR networks with AF relays. Our major contributions are summarized as:

- The projection based separation of multiple operators (ProBaSeMO) algorithm has been proposed to accomplish the relay-assisted physical resource sharing in a TWR network with a MIMO AF relay [RZHJ10], [ZRH12b]. The ProBaSeMO algorithm is flexible and can be extended to the multi-antenna user case and can be adjusted for different utility functions. We have also demonstrated that in a two operator case the non-orthogonal sharing approach can provide a two-fold gain in terms of sum rate compared to the time shared approach when the SNR is large enough and when there are many antennas at the relay. For the aforementioned time shared approach the relay is assumed to have half number of antennas. If in a time shared approach only 4 antennas are at the relay and the number of antennas at the relay increases linearly as the number of operators in the non-orthogonal sharing approach, i.e., four times the number of operators, then the sharing gain increases linearly with the number of operators.
- The sum rate maximization problem of a multi-operator TWR network with a MIMO AF relay has been solved using the gradient based solutions or the POTDC inspired algorithm [ZVKH13]. Compared to the gradient based solution in [ZRH12b], the POTDC algorithm provides a polynomial-time solution. Compared to the ProBaSeMO scheme, the POTDC algorithm or the gradient based solution is especially suitable for a near-far scenario.
- Optimal relay amplification matrices, which minimize the transmit power at the relay subject to SINR constraints at the UTs or maximize the minimum SINR constraints subject to the transmit power constraint at the relay, have been derived for a TWR network with a MIMO AF relay [ZBR⁺12]. The former problem is solved using the iterative SOCP approach, which has a lower computational complexity compared to the conventional SDP approach. The latter problem is solved using a bisection search together with a SDP approach.

- To exploit the non-circularity of the source signals by using WL processing at the relay, widely linear relay amplification matrices have been developed for a TWR network with a MIMO AF relay [ZH13]. Optimal widely linear relay amplification matrices have been derived, which can minimize the transmit power at the relay or maximize the minimum SINR at the UTs. A suboptimal solution has been derived based on the DCM method. Moreover, a large scale analysis has been performed and analytic results on the achievable widely linear gain have been obtained. If the available transmit power at the relay is much larger than the available transmit power at the UTs, a two-fold widely linear gain is achieved.
- Sum rate maximization problems have been addressed for cooperative multi-pair TWR networks with multiple single antenna AF relays [ZRH⁺12c], [ZRH12a]. Global optimal solutions have been obtained regardless whether a total transmit power in the network is considered or individual transmit power constraints per relay are considered. The solutions are obtained using the monotonic optimization framework. Suboptimal solutions, which have close to optimal solution, have also been developed based on other design criteria, e.g., maximizing the total SINR.
- We have studied interference neutralization problems for non-regenerative TWR networks [ZHJH14c], [ZHJH14a], [ZHJH14b]. The considered relaying network contains multiple multi-antenna AF relays and dummy repeaters. Necessary and sufficient conditions for interference neutralization have been derived. Moreover, a general framework to optimize different system utility functions in such a network with and without interference neutralization has been developed.
- We have considered the beamforming design problem for a two-way relay broadcasting channel with a MIMO AF relay [ZRH11]. To optimize the performance of this channel, a joint design of the precoder and the decoder at the BS and the relay amplification matrix at the relay has to be performed. Nevertheless, we resort to suboptimal solutions. Linear transmit strategies have been designed using the channel inversion criterion or the ProBaSeMO concept. A non-linear transmit strategy has also been proposed based on the ZFDPC method.

We would like to emphasize that for all the considered mutli-operator/multi-pair TWR scenarios the proposed non-orthogonal resource access schemes, i.e., SDMA based solutions, are better than the orthogonal resource access schemes, i.e., TDMA based schemes, especially when there are many antennas at each relay, there are many relays in the network, or the noise

is weak. More related contributions that are not explicitly discussed in this thesis but worth mentioning are:

- Different types of relay sharing scenarios have been presented in [LZR⁺11], [ABZ⁺12]. We have developed novel physical layer solutions to accomplish different types of relaying sharing. The developed algorithms provide a significant sharing gain compared to an exclusive resource sharing approach.
- In [GZV⁺12], [GVJ⁺13a], and [GVJ⁺13b] we study a three-node TWR channel, where each node has multiple antennas and the relay uses the DF relaying strategy. Moreover, the superposition coding scheme is applied. Our task is to maximize the achievable rate region by optimizing the transmit strategies at the relay as well as at the UTs. By analyzing active constraints at the optimality, we have proven that the optimal transmit strategy problem can be decoupled into several power allocation problems, all of which can be solved using the water-filling algorithm. Thus, analytical solutions have been obtained at the end.
- We have proposed a novel channel estimation scheme for estimating the channel between the UTs and the relays in a TWR channel with multiple MIMO AF relays [ZNH14]. The proposed scheme is based on the block component decomposition. It is more flexible compared to the state of the art channel estimation schemes since it allows the relay to apply a full relay amplification matrix instead of a diagonal relay amplification matrix. This will become a major enabler for further optimizing the relay amplification matrix in the training phase.

7.2 Future work

Two-way relaying is a promising technique for satisfying the high data rate needs in the future dense networks since it is cost efficient, flexible and uses the spectrum in a more efficient way (compared to the traditional one-way relaying). Nevertheless, to deploy the TWR protocol in future wireless systems, there are still many practical and theoretical issues needed to be solved especially on the PHY and MAC layer. In my opinion, future researches shall address the following areas:

- The fundamental information theory limit of the TWR system is still unknown. Although AF and DF relaying strategies have been intensively studied in the literature, the best relaying strategy in a certain scenario is still unclear. Thus, it makes sense to study the fundamental limits of the TWR systems.

- There are still remaining problems regarding the relay transmit strategy design of a multi-pair TWR scenario or a TWR based relay broadcast channel. For example, energy efficient relay transmit strategies have not been studied for multi-pair TWR scenarios. Similarly, distributed beamforming design for a system with multiple single or multiple-antenna relays should be investigated. Optimal transmit strategies subject to peak power constraint(s) should be studied because in a practical RF chain a peak power constraint per antenna is more realistic compared to an average power constraint. When each user has multiple antennas, optimal joint design of the relay amplification matrix and the precoder and the decoder at the users need to be investigated. If strongly non-circular signals are transmitted and each user has multiple antennas, a joint WL design of the relay amplification matrix and the precoder and the decoder at the users should be investigated. It is also important to study the analytic performance of the proposed transmit strategies, e.g., the analytic sharing gain of the ProBaSeMO scheme.
- To achieve the best performance, perfect CSI is desired. However, in practice it is difficult to obtain perfect CSI. Therefore, robust transmit strategies to combat the imperfect CSI, which are already existing for MU-MIMO downlink systems, e.g., [ZRH13], should be studied.
- The beamforming design requires certain CSI knowledge, e.g., instantaneous CSI, second order statistics of the CSI. For TWR systems, it is natural to estimate the channels and design the beamforming matrices at the relay. However, it has been shown in [RH10b] that the traditional training based channel estimation method is inefficient for obtaining the CSI at the relay. A more efficient pilot design together with channel estimation algorithms or even blind channel estimation schemes shall be studied.
- Unlike conventional cellular networks, there is no widely used topology for relay planning in existing networks. One of the reasons is that relay networks are interference limited networks. Although relays help to improve the network quality, they might also create interference to the macro-cell users. Such effects have not really been well studied. Novel resource allocation (or cross layer design) algorithms, e.g., scheduling of the macro-cell users and relay users, relay selection, are needed especially when the system is fully loaded.
- In a system with two-way relays the uplink and downlink communications links are coupled. This may leads to difficulties when introducing the TWR protocol into modern cellular networks such as LTE or LTE-A that are based on multicarrier techniques.

In LTE the air interfaces for the downlink, i.e., OFDMA, and the uplink, i.e., single carrier frequency division multiple access (SC-FDMA), are different. To use the TWR techniques more efficiently, a joint consideration of the air interface of the downlink and the uplink might be required. Moreover, if the channels of different subcarriers are correlated, a chunk based design of the relay transmit strategies for the considered scenarios can be considered. That is, instead of a per subcarrier design, the transmit strategy for a group of subcarriers can be designed based on their equivalent channel. This is computationally more efficient compared to a per subcarrier design.

- Link adaptation is well adopted in modern wireless communication systems as an efficient closed-loop method for improving the system performance. How the relay should behave in the link adaptation procedure in relay-assisted networks is an interesting issue to address. For example, when the DF relay is applied, the relay decodes the received signal and thus can provide a metric for the quality of the CSI of the instantaneous channel. It can then inform the communication partners so that they can change their modulation and coding schemes (MCSs) accordingly.
- Compared to the OWR protocol, the TWR protocol might be more sensitive to synchronization errors since in the first phase it requires the signals from the two users to arrive at the relay at the same time. Thus, the impact of imperfect synchronization (either timing errors or carrier frequency offsets (CFOs)) shall be investigated.

Part II

Full-duplex wireless communication systems

This part of the thesis is devoted to the development of transmit strategies to enable a simultaneous transmission and reception of a full-duplex (FD) transceiver with limited dynamic range. The major challenge of enabling a FD operation is that the loop-back self-interference (SI) is much stronger (60 - 100 dB) than the received desired signal [CJLK10]. The SI has to be suppressed. Otherwise, it will prevent correctly detecting and decoding of the desired signal. Due to the limited dynamic range and imperfect RF chains at the transceiver, current SI cancellation techniques cannot provide efficient SI suppression in realistic scenarios (although in experiments the reported suppression is up to 80 dB [JCK⁺11]).

Therefore, in Chapter 8 we develop flexible digital SI cancellation techniques for FD point-to-point (P2P) systems. More specifically, we propose to exploit the multiple antennas at both the transmitter and the receiver, i.e., MIMO techniques. To this end, a novel SI (limited dynamic range) aware transmit beamforming based FD MIMO system model is proposed. Optimal transmit strategies, which maximize the sum rate for the MISO and the MIMO setup, are derived. Analytic solutions are obtained using convex analysis. Since the proposed transmit strategies require channel state information (CSI) at the transmitter, which is imperfect in practice, robust transmit strategies to combat worst-case CSI errors are also proposed. In Chapter 9 we deal with other drawbacks of the current SI cancellation techniques. That is, imperfect RF chains can result in residual SI, which can affect the system performance as well as the design of transmit strategies. Thus, we develop efficient transmit strategies, which maximize the signal to leakage plus noise ratio (SLNR), and power adjustment techniques to combat the residual interference. In contrast to the existing approach in [DMBS12] and [Cir14], our proposed approaches do not require the CSI to be invariant over every two consecutive time slots. It is worth emphasizing that the proposed design concepts in this part can be extended to a OWR scenario with an AF FD relay [ZTH13a], [TZH14].

A summary of our achievements and an overview of possible future work are finally provided in Chapter 10. Proofs and derivations are moved to Appendix D to enhance the readability.

8 Self-interference aware transmit strategies for full-duplex point-to-point MIMO systems

This chapter is devoted to the optimal linear transmit strategies for a full-duplex (FD) point-to-point (P2P) MIMO system with limited dynamic range. We first motivate the necessity of developing self-interference (limited dynamic range) aware transmit strategies for a FD P2P MIMO system in Section 8.1. Afterwards, we describe the self-interference (SI) limited FD system in Section 8.2. Optimal linear transmit strategies are then developed to maximize the achievable sum rate of the FD MIMO system [ZTLH12] in Section 8.3. The proposed transmit strategies require CSI at the transmitter, which is imperfect in practice. Therefore, robust transmit strategies to combat the imperfect CSI [ZTH13b] are introduced in Section 8.4. Finally, the proposed algorithms are evaluated via numerical simulations in Section 8.5.

8.1 Motivation and state of the art

Full-duplex (FD) wireless systems have the potential to double the system spectral efficiency compared to half-duplex (HD) systems [JCK⁺11]. The main difficulty in implementing a FD system is that the strong loop-back SI exceeds the limited dynamic range at the receiver, i.e., 60 - 100 dB stronger as reported in [CJLK10]. This phenomenon is critical since it saturates the receiver which will not only prevent the correct reception of the desired signal but may also damage the device. Thus, to exploit the advantages of FD operations, the SI has to be suppressed. The receiver knows its transmitted symbols. Ideally, if the CSI is available at the receiver, the SI can be estimated and thus can be subtracted. This kind of SI cancellation technique is also called time-domain cancellation [RWW11], which is supposed to be applied at the digital baseband of the receiver. However, in practice, the components of RF chains (e.g., the power amplifier (PA) and analog-to-digital converter (ADC)) have limited dynamic range. For example, as the receiver automatic gain control (AGC) keeps the total ADC input at a constant level, higher SI power requires a larger dynamic range. Otherwise, the desired signal power is reduced and thus its resolution is weak, which will result in a bad performance of the transceiver. For more details regarding the linearity and dynamic range of the transceiver chain we refer to [KSA⁺14] and the references therein. In other words, a perfect digital domain SI subtraction is far from realistic. Therefore, different SI suppression approaches have been proposed to realize FD transceivers and especially SISO FD systems. Most of the proposed

Table 8.1: A summary of the existing SI cancellation techniques.

	SI cancellation techniques	References	Institute ^a
Analog	Antenna attenuation	[Kha10], [EDDS11]	RiceU, UWaterloo, AaltoU
	RF cancellation ^b	[CJLK10], [JCK ⁺ 11], [SPS11]	StanfordU, RiceU
digital	time domain cancellation ^c	[RWW11], [HLM ⁺ 12]	AaltoU, UCRS
	frequency domain cancellation ^d	[RVW13], [ZTLH12]	TUIL, AaltoU

^aThe research institutes include Stanford University (StanfordU), Aalto University (AaltoU), Rice University (RiceU), University of California Riverside (UCRS), University of Waterloo (UWaterloo), etc..

^bThis includes Balun effect, auxiliary transmit chains, etc.

^cThis includes receiver-side subtraction and spatial-temporal transmit beamforming

^dThis includes spatial suppression techniques, e.g., null space projection and SI aware transmit beamforming

approaches involve advanced concepts in both RF transceiver architecture and digital signal processing at the receiver. The simplest approach is to use directional transmit and receive antennas to decouple the transmit and receive signals [EDDS11], which is also known as antenna attenuation. However, this approach is only suitable when the transmit antennas and the receive antennas are sufficiently separated. In [CJLK10], a RF cancellation approach was proposed, which requires two transmit antennas. By proper position adjustment, the signals of both transmit antennas overlap destructively at the receive antenna, which leads to a certain degree of SI cancellation. This approach can be regarded as a static beamforming approach and has the drawback that it is only suitable for narrow band transmissions and requires accurate manual tuning of antenna positions. In [JCK⁺11] and [SPS11], more advanced approaches are proposed, which can cope with larger bandwidths. In [JCK⁺11] a balun is used at the transmit antenna input to feed an inverted as well as amplitude and phase adjusted version of the RF transmit signal to the output of the receive antenna to cancel the SI. In [SPS11], an auxiliary transmit path is used to feed a cancellation signal to the receiver input for RF cancellation, where the cancellation signal is a preprocessed version of the own transmitted signal to match the actual signal. These SI cancellation methods can be categorized as RF cancellation techniques. If both the transmitter and the receiver have multiple antennas, then spatial domain suppression techniques can be deployed to null the SI, i.e., the precoding matrix at the transmitter and the decoding matrix at the receiver are jointly designed such that the SI is nullified [RWW11] and [RVW13]. Clearly, the spatial domain suppression techniques are also performed in the digital domain. The existing SI cancellation techniques are summarized in Table 8.1.

Nevertheless, the cancellation ability of the RF cancellation schemes has not yet been verified in real-world applications and thus their stability is unknown. The extension of these schemes for MIMO systems is unclear. Actually, it is possible that after the RF cancellation, the receiver might be still saturated. On the other hand, the spatial domain suppression techniques will in general consume the available spatial dimensions and thus the multiplexing gain of the system is significantly effected. This issue is also pointed out in [RVW13]. Moreover, in [RWW11] and [RVW13], the time-domain subtraction technique and the spatial domain suppression techniques are treated as competitors. Yet, there is another possibility which is ignored. That is, the time-domain subtraction technique can be combined with the spatial domain suppression techniques to provide an enhanced digital domain SI cancellation and/or to improve the resulted system performance. For this purpose, we propose the concept of the SI aware transmit beamforming. That is, when the spatial domain suppression techniques are deployed, we design the transmit beamformer such that the SI power is suppressed up to a certain threshold, instead of zero-forcing (ZF) as in [RVW13]. The residual SI will be canceled using the time domain cancellation technique. There are several benefits of this design concept. Compared to pure spatial domain suppression techniques, the multiplexing gain of the system can be preserved depending on the threshold. Compared to the pure time-domain subtraction technique, the SI is suppressed before going through the transceiver with a limited dynamic range. Therefore, more dynamic range will be reserved for the desired signal, and the saturation of the receiver RF chain due to a strong loop-back SI can be avoided. Our concept can be realized by setting an additional constraint on the received SI power. Based on the proposed method, optimal transmit strategies can be developed such that the system performance is improved and the SI is suppressed. However, to achieve the best performance, perfect CSI is required, which is difficult to obtain in practice. Thus, robust design approaches which take into account the imperfections of the CSI such as [WP09] are important for a realistic system implementation. Therefore, we also develop robust transmit strategies by applying a worst-case deterministic channel error model in case of imperfect CSI.

8.2 System model

Two transceivers with identical hardware configurations communicate with each other as depicted in Figure 8.1. Each transceiver has M_t transmit antennas and M_r receive antennas. The transmitter and the receiver at the same transceiver are indexed by $\{i, j\} \in \{1, 2\}$ and $i \neq j$. We assume perfect synchronization. The channel is frequency flat and quasi-static block fading. The desired channel from the i -th transmitter to the i -th receiver is denoted as $\mathbf{H}_{ii} \in \mathbb{C}^{M_r \times M_t}$

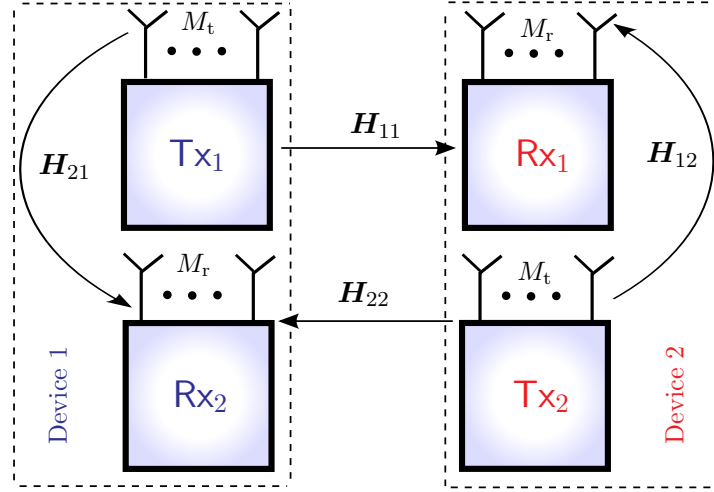


Figure 8.1: The sketch of a symmetric full-duplex point-to-point MIMO system.

while the SI channel from the i -th transmitter to the j -th receiver is $\mathbf{H}_{ji} \in \mathbb{C}^{M_r \times M_t}$. All the channels have full rank, i.e., $\text{rank}(\mathbf{H}_{ii}) = \text{rank}(\mathbf{H}_{ji}) = \min(M_r, M_t)$.

Let the i -th transmitter transmits the data vector \mathbf{s}_i with the precoding matrix $\mathbf{W}_i \in \mathbb{C}^{M_t \times r_i}$, where r_i is the number of transmitted data streams of the corresponding transmitter. Then its transmitted signal vector \mathbf{x}_i can be written as

$$\mathbf{x}_i = \mathbf{W}_i \mathbf{s}_i \quad (8.1)$$

with the transmit power constraint $\mathbb{E}\{\|\mathbf{x}_i\|^2\} \leq \epsilon_i P_i^{(\text{TH})}$ where $\epsilon_i \in \mathbb{R}^+$. The elements of \mathbf{s}_i are independently distributed with zero mean and unit variance. Moreover, we define a SI power constraint as

$$\mathbb{E}\{\eta_j \|\mathbf{H}_{ij} \mathbf{x}_j\|^2\} \leq P_i^{(\text{TH})}, \quad (8.2)$$

where $\eta_j \in \mathbb{R}^+$ denotes the ratio between the path-loss of the SI channel and the path-loss of the desired channel, i.e., the near-far ratio, and $P_i^{(\text{TH})}$ denotes the threshold of the received SI power, which should be achieved by using the spatial domain (in other words, SDMA) suppression techniques. Note that the effects of antenna attenuation (if applied) and RF cancellation techniques (if applied) can be taken into account using the factor η_j , i.e., treated as artificial path loss. A smaller η_j means that more SI suppression is provided by antenna attenuation and the RF cancellation techniques. The factor ϵ_i represents the ratio between the maximum allowable transmit power and the maximum allowable SI power of the i -th transceiver. As will be discussed in Section 8.3, when η_j is fixed, ϵ_i decides whether the spatial

dimensions are used to suppress the SI or not. The constraint (8.2) implies that if the SI power is below this required threshold, the SI suppression is sufficient and the received signal power, including the desired signal power and the residual SI power, is within the dynamic range of the receiver. The received signal at the i -th receiver is written as

$$\mathbf{y}_i = \underbrace{\mathbf{H}_{ii}\mathbf{x}_i}_{\text{desired signal}} + \underbrace{\sqrt{\eta_j}\mathbf{H}_{ij}\mathbf{x}_j}_{\text{residual SI}} + \mathbf{n}_i \in \mathbb{C}^{M_r} \quad (8.3)$$

where \mathbf{n}_i denotes the zero-mean circularly symmetric complex Gaussian (ZMCSCG) noise and $\mathbb{E}\{\mathbf{n}_i\mathbf{n}_i^H\} = \sigma_n^2\mathbf{I}_{M_r}$, $\forall i$. If channel knowledge is available at the receiver, the residual SI can be subtracted using the time-domain subtraction technique since the transceiver knows its own transmitted signal. If we further ignore the remaining SI after the subtraction, the received signal is simplified as

$$\hat{\mathbf{y}}_i = \mathbf{H}_{ii}\mathbf{x}_i + \mathbf{n}_i \in \mathbb{C}^{M_r} \quad (8.4)$$

One biggest advantage of this design, as will be seen in Section 8.3, is that it decouples the design of the precoders of the two transmitters, which cannot be achieved in general, e.g., [DMBS12]. One important assumption of this design is that the threshold has to be known in advance. We will discuss this assumption at the end of Section 8.3.

Given the above system model and assuming perfect channel knowledge at the transmitter, in the following we develop linear transmit strategies which maximize the system sum rate and derive analytic solutions for the MIMO and the MISO setup, respectively.

8.3 Optimal linear transmit strategies for sum rate maximization

In this section we solve the sum rate maximization problem for the MISO and the MIMO setup separately.

8.3.1 MISO setup

The sum rate maximization problem for the MISO setup is given by:

$$\begin{aligned} \max_{\mathbf{w}_i} \quad & \sum_{i=1}^2 \log_2 (1 + \mathbf{w}_i^H \mathbf{h}_{ii}^H \mathbf{h}_{ii} \mathbf{w}_i) \\ \text{s. t.} \quad & \mathbf{w}_i^H \mathbf{w}_i \leq \epsilon_i P_i^{(\text{TH})} \\ & \eta_i \mathbf{w}_i^H \mathbf{h}_{ji}^H \mathbf{h}_{ji} \mathbf{w}_i \leq P_i^{(\text{TH})}, \quad i \in \{1, 2\}, \end{aligned} \quad (8.5)$$

where $\mathbf{w}_i \in \mathbb{C}^N$, $\mathbf{h}_{ii}^T \in \mathbb{C}^N$, $\mathbf{h}_{ji}^T \in \mathbb{C}^N$ are vector versions of \mathbf{W}_i , \mathbf{H}_{ii} , \mathbf{H}_{ji} , respectively. Since in problem (8.5) the design of \mathbf{w}_1 and \mathbf{w}_2 can be decoupled, it is equivalent to solving the following sub-problem, $\forall i$,

$$\begin{aligned} \max_{\mathbf{w}_i} \quad & \mathbf{w}_i^H \mathbf{h}_{ii}^H \mathbf{h}_{ii} \mathbf{w}_i \\ \text{s. t.} \quad & \mathbf{w}_i^H \mathbf{w}_i \leq \epsilon_i P_i^{(\text{TH})} \\ & \eta_i \mathbf{w}_i^H \mathbf{h}_{ji}^H \mathbf{h}_{ji} \mathbf{w}_i \leq P_i^{(\text{TH})} \end{aligned} \quad (8.6)$$

Problem (8.6) is non-convex QCQP problem. As we have discussed in Section 3.6, a common approach to solve (8.6) is to apply the SDR technique to first obtain a convex problem [HP10], as also introduced in Appendix B.3.5. That is, define $\mathbf{X}_i = \mathbf{w}_i \mathbf{w}_i^H$. By dropping the rank-1 constraint on \mathbf{X}_i , $\forall i$, we get the following convex problem

$$\begin{aligned} \max_{\mathbf{X}_i} \quad & \text{Tr}\{\mathbf{h}_{ii}^H \mathbf{h}_{ii} \mathbf{X}_i\} \\ \text{s. t.} \quad & \mathbf{X}_i \geq 0, \text{Tr}\{\mathbf{X}_i\} \leq \epsilon_i P_i^{(\text{TH})} \\ & \text{Tr}\{\eta_i \mathbf{h}_{ji}^H \mathbf{h}_{ji} \mathbf{X}_i\} \leq P_i^{(\text{TH})}. \end{aligned} \quad (8.7)$$

A rank-1 optimal solution of (8.7) is the solution to the original problem. Fortunately, according to *Corollary 3.4* in [HP10], problem (8.7) has a guaranteed rank-1 solution and thus the iterative rank-1 extraction technique in [HP10] can be used.

Nevertheless, the interior-point algorithm only provides numerical solutions which do not give all the insights of the problem. If possible, an analytic solution is preferred. To this end, we analyze the active¹ and inactive constraints of problem (8.6). The following proposition is derived.

Proposition 8.3.1. *At the optimality of problem (8.6), $\forall i$,*

- i) The transmit power constraint is always active. This implies that either both the transmit power constraint and the SI power constraint are active or only the transmit power constraint is active.*
- ii) If the SI power constraint is inactive, the optimal transmit strategy is the maximum ratio transmission (MRT) scheme, i.e., $\mathbf{w}_{\text{opt},i} = \frac{\sqrt{\epsilon_i P_i^{(\text{TH})}} \mathbf{h}_{ii}^H}{\|\mathbf{h}_{ii}\|}$. A two-fold FD gain in terms of sum rate is achievable.*

¹Active constraints means that at the optimality the constraints are satisfied with equality [BV04].

Proof. Please see Appendix D.1. \square

When both of the constraints in (8.6) are active, an analytic solution can be derived and the following corollary is obtained.

Corollary 8.3.2. Define the orthogonal complement of $\mathbf{h}_{ji}^H \in \mathbb{C}^{M_t}$ as $\mathbf{\Pi}_{\mathbf{h}_{ji}^H}^\perp = \mathbf{I}_{M_t} - \frac{\mathbf{h}_{ji}^H \mathbf{h}_{ji}}{\|\mathbf{h}_{ji}\|^2} \in \mathbb{C}^{M_t \times M_t}$. When both of the constraints in (8.6) are active, the optimal beamformer is given by

$$\mathbf{w}_{\text{opt},i} = \frac{\mathbf{h}_{ji}^H}{\|\mathbf{h}_{ji}\|^2} \sqrt{\frac{P_i^{(\text{TH})}}{\eta_i}} \cdot e^{j\alpha_{\text{opt},i}} + \mathbf{\Pi}_{\mathbf{h}_{ji}^H}^\perp \cdot \mathbf{b}_{\text{opt},i} \quad (8.8)$$

where $\mathbf{b}_{\text{opt},i} = (v_{\text{opt},i} \mathbf{I}_{M_t} - \mathbf{z}_{v,i}^H \mathbf{z}_{v,i})^{-1} \mathbf{z}_{v,i}^H \mathbf{z}_{s,i} \in \mathbb{C}^{M_t}$, $\mathbf{z}_{v,i} = \mathbf{h}_{ii} \mathbf{\Pi}_{\mathbf{h}_{ji}^H}^\perp \in \mathbb{C}^{1 \times M_t}$, $\mathbf{z}_{s,i} = \frac{\mathbf{h}_{ii} \mathbf{h}_{ji}^H}{\|\mathbf{h}_{ji}\|^2} \sqrt{\frac{P_i^{(\text{TH})}}{\eta_i}} \in \mathbb{C}$, $v_{\text{opt},i} = \|\mathbf{z}_{v,i}\|^2 - \frac{|z_{s,i}| \|\mathbf{z}_{v,i}\|}{\sqrt{(\epsilon_i - \frac{1}{\eta_i \|\mathbf{h}_{ji}\|^2}) P_i^{(\text{TH})}}}$, and $\alpha_{\text{opt},i} = \arg \left\{ \frac{\mathbf{h}_{ii} \mathbf{\Pi}_{\mathbf{h}_{ji}^H}^\perp \cdot \mathbf{b}_{\text{opt},i}}{\mathbf{h}_{ii} \mathbf{h}_{ji}^H} \right\}$.

Proof. Please see Appendix D.2. \square

8.3.2 MIMO setup

The sum rate maximization problem for the MIMO setup is formulated as:

$$\begin{aligned} \max_{\mathbf{Q}_i} \quad & \sum_{i=1}^2 \log_2 \left(\left| \mathbf{I}_M + \frac{1}{\sigma_n^2} \mathbf{H}_{ii} \mathbf{Q}_i \mathbf{H}_{ii}^H \right| \right) \\ \text{s. t.} \quad & \mathbf{Q}_i \geq 0, \quad \text{Tr}\{\mathbf{Q}_i\} \leq \epsilon_i P_i^{(\text{TH})} \\ & \text{Tr}\{\eta_i \mathbf{H}_{ji} \mathbf{Q}_i \mathbf{H}_{ji}^H\} \leq P_i^{(\text{TH})}, \quad i \in \{1, 2\}, \end{aligned} \quad (8.9)$$

where $\mathbf{Q}_i = \mathbf{W}_i \mathbf{W}_i^H$. Since in problem (8.9) the design of \mathbf{Q}_1 and \mathbf{Q}_2 is not coupled so that we can design them separately, i.e., $\forall i$, we solve

$$\begin{aligned} \min_{\mathbf{Q}_i} \quad & -\log \left(\left| \mathbf{I}_M + \frac{1}{\sigma_n^2} \mathbf{H}_{ii} \mathbf{Q}_i \mathbf{H}_{ii}^H \right| \right) \\ \text{s. t.} \quad & \mathbf{Q}_i \geq 0, \quad \text{Tr}\{\mathbf{Q}_i\} \leq \epsilon_i P_i^{(\text{TH})} \\ & \text{Tr}\{\eta_i \mathbf{H}_{ji} \mathbf{Q}_i \mathbf{H}_{ji}^H\} \leq P_i^{(\text{TH})}. \end{aligned} \quad (8.10)$$

According to [BV04], problem (8.10) is a convex problem since both the cost function and the constraints are convex. Thus, it can be solved using the interior-point algorithm in [BV04]. Define the EVD of $\mathbf{Q}_i = \mathbf{U}_i \mathbf{\Sigma}_i \mathbf{U}_i^H$. The optimal precoding matrix is given by $\mathbf{W}_{i,\text{opt}} = \mathbf{U}_i \mathbf{\Sigma}_i^{\frac{1}{2}}$.

Similar as in the MISO setup, we investigate the possibility of obtaining an analytic solution to problem (8.10). We start by first pointing out that at least one of the constraints in (8.10) is active at the optimality. Otherwise, the optimal $\mathbf{Q}_{i,\text{opt}}$ can be scaled up to satisfy at least one of the constraints with equality while increasing the objective function, which contradicts the optimality. Based on this fact, we are able to prove the following proposition.

Proposition 8.3.3. *At the optimality of problem (8.10), the following statements hold:*

- i) If the transmit power constraint is active while the SI power constraint is inactive, the analytic solution is obtained by using the SVD of \mathbf{H}_{ii} together with the water-filling (WF) power allocation, i.e., the optimal solution for a HD P2P system. Two-fold gain is achievable;*
- ii) If the transmit power constraint is inactive while the SI power constraint is active, the analytic solution is given by the WF power allocation over the eigenmodes of the effective channel $\mathbf{H}_{ii}\mathbf{H}_{ji}^+$.*

Proof. Case i): after dropping the inactive SI power constraint, the remaining problem is the same as the capacity achieving precoder design problem for a HD MIMO system [PNG03]. Thereby, the solution is the well-known WF solution [PNG03].

Case ii): Let us define $\hat{\mathbf{Q}}_i = \mathbf{H}_{ji}\mathbf{Q}_i\mathbf{H}_{ji}^H$. If the pseudoinverse of $\mathbf{H}_{ji}^+ = (\mathbf{H}_{ji}^H\mathbf{H}_{ji})^{-1}\mathbf{H}_{ji}^H$ ($M \geq N$ is required) exists, then we have $\mathbf{Q}_i = \mathbf{H}_{ji}^+\hat{\mathbf{Q}}_i\mathbf{H}_{ji}^{+H}$. Problem (8.10) is reformulated as

$$\begin{aligned} \min_{\hat{\mathbf{Q}}_i} \quad & -\log \left(\left| \mathbf{I}_M + \frac{1}{\sigma_n^2} \mathbf{H}_{ii}\mathbf{H}_{ji}^+\hat{\mathbf{Q}}_i\mathbf{H}_{ji}^{+H}\mathbf{H}_{ii}^H \right| \right) \\ \text{s. t.} \quad & \hat{\mathbf{Q}}_i \geq 0, \quad \text{Tr}\{\eta_i\hat{\mathbf{Q}}_i\} = P_i^{(\text{TH})} \end{aligned} \quad (8.11)$$

Problem (8.11) has the same formulation as the MIMO capacity achieving problem for a HD system in [PNG03] and thus it can be solved using the WF algorithm. This solution is called inverse WF. \square

When both constraints are active, an analytic solution is in general difficult to obtain. A possible routine for obtaining an analytic solution for such a situation is to apply the Karush-Kuhn-Tucker (KKT) conditions in [BV04] and Appendix B.2, which are first-order necessary conditions for optimality. The intention behind this approach is that the solution obtained from the KKT conditions (if it exists) is also globally optimal since our problem is a convex problem. For the case $M_r = M_t = 2$ an analytic solution is derived in the following proposition.

Proposition 8.3.4. Define the EVD of $\mathbf{A}_{ii} = \mathbf{H}_{ii}^H \mathbf{H}_{ii} / \sigma_n^2 = \mathbf{U}_{ii} \cdot \text{diag} \{ \boldsymbol{\lambda}_{ii} \} \mathbf{U}_{ii}^H$ and $\mathbf{B}_{ji} = \mathbf{H}_{ji}^H \mathbf{H}_{ji} = \mathbf{U}_{ji} \cdot \text{diag} \{ \boldsymbol{\lambda}_{ji} \} \mathbf{U}_{ji}^H$, where $\boldsymbol{\lambda}_{ii} = [\lambda_{ii,1}, \dots, \lambda_{ii, M_t}]^T$ and $\boldsymbol{\lambda}_{ji} = [\lambda_{ji,1}, \dots, \lambda_{ji, M_t}]^T$ are the corresponding eigenvalue profiles of \mathbf{A}_{ii} and \mathbf{B}_{ji} , respectively. Define $\mathbf{U}_{ji}^H \mathbf{A}_{ii} \mathbf{U}_{ji} = \begin{bmatrix} a_{11} & a_{12} \\ a_{12}^* & a_{22} \end{bmatrix}$ where $a_{11} \in \mathbb{R}$, $a_{22} \in \mathbb{R}$, and $a_{12} \in \mathbb{C}$. When $M_r = M_t = 2$ and both constraints are active at the optimality of problem (8.10), $\forall i$, the optimal \mathbf{Q}_i is computed as

$$\mathbf{Q}_{\text{opt},i} = \begin{cases} \mathbf{Q}_{\text{PSD},i} & \text{if } \mathbf{Q}_{\text{PSD},i} \geq 0; \\ \mathbf{U}_{ji} \begin{bmatrix} |v_{i,1}| e^{j\alpha_i} \\ |v_{i,2}| \end{bmatrix} \begin{bmatrix} |v_{i,1}| e^{j\alpha_i} \\ |v_{i,2}| \end{bmatrix}^H \mathbf{U}_{ji}^H & \text{otherwise,} \end{cases} \quad (8.12)$$

where $\mathbf{Q}_{\text{PSD},i} = (\rho_i \mathbf{I}_{M_t} + v_i \eta_i \mathbf{B}_{ji})^{-1} - \mathbf{A}_{ii}^{-1}$, $\rho_i = \frac{\lambda_{ji,1}}{\lambda_{ji,1} \bar{z}_i - z_i} + \frac{\lambda_{ji,2}}{\lambda_{ji,2} \bar{z}_i - z_i}$, $v_i = \frac{1}{\bar{z}_i - \lambda_{ji,1} \bar{z}_i} + \frac{1}{\bar{z}_i - \lambda_{ji,2} \bar{z}_i}$, $\bar{z}_i = \epsilon_i P_i^{(\text{TH})} + \sum_{m=1}^2 \lambda_{ii,m}^{-1}$, $\bar{z}_i = P_i^{(\text{TH})} / \eta_i + \text{Tr} \{ \mathbf{B}_{ji} \mathbf{A}_{ii}^{-1} \}$, $|v_{i,1}| = \sqrt{\frac{P_i^{(\text{TH})} / \eta_i - \lambda_{ji,2} \epsilon_i P_i^{(\text{TH})}}{\lambda_{ji,1} - \lambda_{ji,2}}}$, $|v_{i,2}| = \sqrt{\frac{\lambda_{ji,1} \epsilon_i P_i^{(\text{TH})} - P_i^{(\text{TH})} / \eta_i}{\lambda_{ji,1} - \lambda_{ji,2}}}$, and $\alpha_i = \arg \{ a_{12} \}$.

Proof. Please see Appendix D.3. □

Remark

Remark 10. When the proposed concept is applied to a SISO setup, the optimal solution is readily available. The sum rate maximization problem for the SISO setup is given by

$$\begin{aligned} \max_{P_i} \quad & \sum_{i=1}^2 \log_2(1 + P_i |h_{ii}|^2) \\ \text{s. t.} \quad & P_i \leq \epsilon_i P_i^{(\text{TH})} \\ & P_i \eta_i |h_{ji}|^2 \leq P_i^{(\text{TH})}, \quad i \in \{1, 2\}. \end{aligned} \quad (8.13)$$

Since in this case only the transmit power $P_i \in \mathbb{R}_+$ can be tuned, an analytic solution is obtained as $P_{\text{opt},i} = \min \left(\epsilon_i P_i^{(\text{TH})}, \frac{P_i^{(\text{TH})}}{\eta_i |h_{ji}|^2} \right)$.

Remark 11. Compared to a pure HD system, our design concept results in a HD system with an additional constraint, i.e., the SI power constraint. This can be interpreted as that each transceiver maximizes its own performance while suppressing the interference, which it causes to the received signal from the other transmitter, up to a certain level. Clearly, this design requires that $P_i^{(\text{TH})}$ is known a priori. This is possible in practice. For example, a typical received signal power in a LTE system is -83.9 dBm [RVW13]. The value of $P_i^{(\text{TH})}$ can be set

to a fraction of -83.9 dBm such that the SI power is sufficiently low. That is, the threshold $P_i^{(\text{TH})}$ is fixed. When $P_i^{(\text{TH})}$ is fixed, it can happen that the received signal power is still worse than the received SI power. For example, if there are not sufficient spatial dimensions, which can be used to suppress the SI and thus the transmit power has to be reduced to satisfy the SI power constraint. Since the transmit power is reduced, the received power is reduced and might be smaller than the received SI power. If one of the desired channels is weak, this phenomenon can also happen. In such a situation, instead of fixing $P_i^{(\text{TH})}$, we propose to update $P_i^{(\text{TH})}$ iteratively. That is, the two transceivers coordinate with each other in the design of their own transmit strategy. Since only the value of $P_i^{(\text{TH})}$, i.e., a scalar, needs to be exchanged, it will not bring a large burden to the system.

8.4 Worst-case design for transmit power minimization

8.4.1 Data model under imperfect CSI

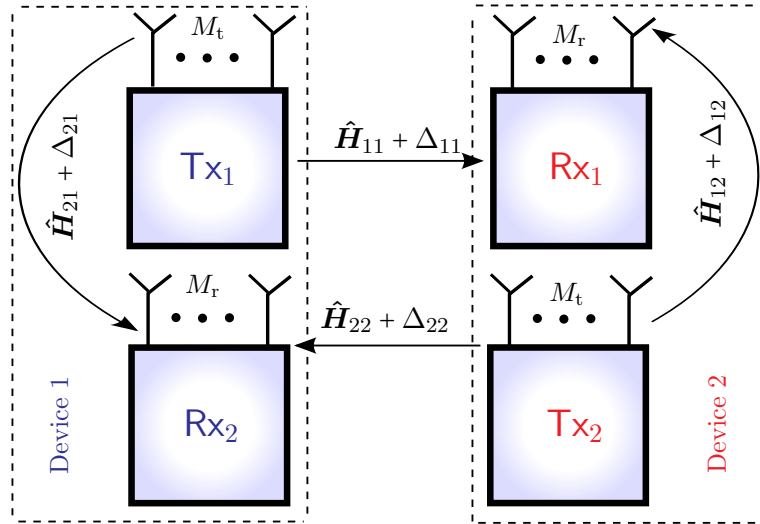


Figure 8.2: A symmetric FD point-to-point system with deterministic channel errors.

In practice, the CSI at the transmitter can be obtained by directly estimating the channel at the transmitter when TDD is applied and the RF end is calibrated, or by feeding back the estimated channel at the receiver side when FDD is applied. The imperfect channel estimation and/or the limited feedback capability cause CSI errors at the transmitter. Therefore, a robust design to combat CSI errors is essential for a practical system implementation. Although the FD operation, i.e., at the same time and on the same frequency, makes it possible to estimate

the channel directly at the transmitter, it is unclear what kind of calibration has to be used such that the reciprocity holds for a FD communication link and thus there might be calibration errors. Therefore, we apply a general CSI error model as in [WP09]. That is, the imperfect CSI is modeled as

$$\mathbf{H}_{ii} = \hat{\mathbf{H}}_{ii} + \mathbf{\Delta}_{ii}, \quad \mathbf{H}_{ij} = \hat{\mathbf{H}}_{ij} + \mathbf{\Delta}_{ij}, \quad \forall i, j \in \{1, 2\}, \quad (8.14)$$

where $\hat{\mathbf{H}}_{ii}$ and $\hat{\mathbf{H}}_{ij}$ are the estimated channels. The corresponding CSI errors are modeled deterministically using $\mathbf{\Delta}_{ii}$ and $\mathbf{\Delta}_{ij}$ and they are bounded by ellipsoids [WP09] such that

$$\text{Tr}\{\mathbf{\Delta}_{ii} \mathbf{T}_{ii} \mathbf{\Delta}_{ii}^H\} \leq \gamma_{ii}, \quad \text{Tr}\{\mathbf{\Delta}_{ij} \mathbf{T}_{ij} \mathbf{\Delta}_{ij}^H\} \leq \gamma_{ij}, \quad \forall i, j \in \{1, 2\}, \quad (8.15)$$

where $\{\mathbf{T}_{ii}, \mathbf{T}_{ij}\} \succ 0$ characterize the shape of the uncertainty region of the CSI errors and \succ stands for positive definite [WP09]. It is further assumed that $\mathbf{\Delta}_{ii}$ and $\mathbf{\Delta}_{ij}$ are independent from each other. Given the CSI error model in (8.14), we can subtract the estimated SI term $\hat{\mathbf{H}}_{ij} \mathbf{x}_j$. Then the received signal at the i th receiver can be rewritten as

$$\mathbf{y}_i = \underbrace{(\hat{\mathbf{H}}_{ii} + \mathbf{\Delta}_{ii}) \mathbf{x}_i}_{\text{desired signal}} + \underbrace{\mathbf{\Delta}_{ij} \mathbf{x}_j}_{\text{residual SI}} + \mathbf{n}_i \quad (8.16)$$

Let us define the total SINR at the i th receiver as the ratio between the sum of the received signal power and the sum of the received interference plus noise power at all antennas of the i th receiver. Then it is calculated as

$$\text{SINR}_i = \frac{\text{Tr}\{(\hat{\mathbf{H}}_{ii} + \mathbf{\Delta}_{ii}) \mathbf{Q}_i (\hat{\mathbf{H}}_{ii} + \mathbf{\Delta}_{ii})^H\}}{\text{Tr}\{\mathbf{\Delta}_{ij} \mathbf{Q}_j \mathbf{\Delta}_{ij}^H\} + M_r \sigma_n^2} \quad (8.17)$$

and the SI constraint is computed by

$$\mathbb{E}\{\|\mathbf{H}_{ij} \mathbf{x}_j\|^2\} = \text{Tr}\{(\hat{\mathbf{H}}_{ij} + \mathbf{\Delta}_{ij}) \mathbf{Q}_j (\hat{\mathbf{H}}_{ij} + \mathbf{\Delta}_{ij})^H\} \leq P_i^{(\text{TH})}. \quad (8.18)$$

Our goal is to design worst-case optimal covariance matrices \mathbf{Q}_i , $\forall i$, which minimize the total required transmit power of the system subject to total SINR constraints and SI constraints. Afterwards, the robust transmit beamforming \mathbf{F}_i is determined by $\mathbf{F}_i = \mathbf{Q}_i^{\frac{1}{2}}$.

8.4.2 Worst-case transmit strategies

Our worst-case total transmit power minimization problem can be formulated as the following min-max problem:

$$\begin{aligned}
 & \min_{\mathbf{Q}_i, \Delta_{ii}, \Delta_{ij}, \forall i} \max_{\forall i, j} \sum_i \text{Tr}\{\mathbf{Q}_i\} \\
 \text{s.t.} \quad & \frac{\text{Tr}\{(\hat{\mathbf{H}}_{ii} + \Delta_{ii})\mathbf{Q}_i(\hat{\mathbf{H}}_{ii} + \Delta_{ii})^H\}}{\text{Tr}\{\Delta_{ij}\mathbf{Q}_j\Delta_{ij}^H\} + M_r\sigma_n^2} \geq \eta_i \\
 & \text{Tr}\{(\hat{\mathbf{H}}_{ij} + \Delta_{ij})\mathbf{Q}_j(\hat{\mathbf{H}}_{ij} + \Delta_{ij})^H\} \leq P_i^{(\text{TH})} \\
 & \text{Tr}\{\Delta_{ii}\mathbf{T}_{ii}\Delta_{ii}^H\} \leq \gamma_{ii}, \quad \text{Tr}\{\Delta_{ij}\mathbf{T}_{ij}\Delta_{ij}^H\} \leq \gamma_{ij}, \quad \mathbf{Q}_i \geq 0, \forall i, j \in \{1, 2\}, \quad (8.19)
 \end{aligned}$$

where $\eta_i > 0$ are the SINR requirements. Noticing that the objective function in (8.19) is independent of Δ_{ii} and Δ_{ij} , $\forall i, j$, we can reformulate the cost function and get the following equivalent problem:

$$\begin{aligned}
 & \min_{\mathbf{Q}_i, \forall \Delta_{ii}, \Delta_{ij}} \sum_i \text{Tr}\{\mathbf{Q}_i\} \\
 \text{s.t.} \quad & \frac{\text{Tr}\{(\hat{\mathbf{H}}_{ii} + \Delta_{ii})\mathbf{Q}_i(\hat{\mathbf{H}}_{ii} + \Delta_{ii})^H\}}{\text{Tr}\{\Delta_{ij}\mathbf{Q}_j\Delta_{ij}^H\} + M_r\sigma_n^2} \geq \eta_i \quad (8.20a)
 \end{aligned}$$

$$\text{Tr}\{(\hat{\mathbf{H}}_{ij} + \Delta_{ij})\mathbf{Q}_j(\hat{\mathbf{H}}_{ij} + \Delta_{ij})^H\} \leq P_i^{(\text{TH})} \quad (8.20b)$$

$$\text{Tr}\{\Delta_{ii}\mathbf{T}_{ii}\Delta_{ii}^H\} \leq \gamma_{ii}, \quad \text{Tr}\{\Delta_{ij}\mathbf{T}_{ij}\Delta_{ij}^H\} \leq \gamma_{ij}, \quad \mathbf{Q}_i \geq 0, \forall i, j \in \{1, 2\}. \quad (8.20c)$$

Problem (8.20) is still non-convex since its constraints are infinite, i.e., we need to solve (8.20) for every feasible Δ_{ii} and Δ_{ij} which makes it intractable. Nevertheless, by applying the S-procedure and the Schur complement as in [WP09], it is possible to convert problem (8.22) into a SDP problem. For this purpose, we reformulate the constraint (8.20a) such that its dependence on Δ_{ii} and Δ_{ij} is separated. Let us introduce slack variables $t_i > 0$ [BV04]. Then (8.20a) can be split into the following two constraints.

$$\begin{aligned}
 & \text{Tr}\{(\hat{\mathbf{H}}_{ii} + \Delta_{ii})\mathbf{Q}_i(\hat{\mathbf{H}}_{ii} + \Delta_{ii})^H\} \geq t_i\eta_i \\
 & \text{Tr}\{\Delta_{ij}\mathbf{Q}_j\Delta_{ij}^H\} + M_r\sigma_n^2 \leq t_i \quad (8.21)
 \end{aligned}$$

Replacing (8.20a) with its equivalent constraints in (8.21), we get

$$\min_{\mathbf{Q}_i, t_i, \forall \Delta_{ii}, \Delta_{ij}} \sum_i \text{Tr}\{\mathbf{Q}_i\}$$

$$\text{s.t. } \text{Tr}\{(\hat{\mathbf{H}}_{ii} + \mathbf{\Delta}_{ii})\mathbf{Q}_i(\hat{\mathbf{H}}_{ii} + \mathbf{\Delta}_{ii})^H\} \geq t_i \eta_i \quad (8.22a)$$

$$\text{Tr}\{\mathbf{\Delta}_{ij}\mathbf{Q}_j\mathbf{\Delta}_{ij}^H\} + M_r \sigma_n^2 \leq t_i \quad (8.22b)$$

$$\text{Tr}\{(\hat{\mathbf{H}}_{ij} + \mathbf{\Delta}_{ij})\mathbf{Q}_j(\hat{\mathbf{H}}_{ij} + \mathbf{\Delta}_{ij})^H\} \leq P_i^{(\text{TH})} \quad (8.22c)$$

$$\text{Tr}\{\mathbf{\Delta}_{ii}\mathbf{T}_{ii}\mathbf{\Delta}_{ii}^H\} \leq \gamma_{ii} \quad (8.22d)$$

$$\text{Tr}\{\mathbf{\Delta}_{ij}\mathbf{T}_{ij}\mathbf{\Delta}_{ij}^H\} \leq \gamma_{ij} \quad (8.22e)$$

$$\mathbf{Q}_i \geq 0, t_i > 0, \forall i, j \in \{1, 2\}. \quad (8.22f)$$

Now let us review the definitions of the S-procedure and the Schur complement from [BV04].

Lemma 8.4.1. (*S-procedure [BV04]*) Let $\mathbf{A}_k = \mathbf{A}_k^H \in \mathbb{C}^{m \times m}$, $\mathbf{b}_k \in \mathbb{C}^m$, and $c_k \in \mathbb{R}$ where $k \in \{1, 2\}$. Then

$$\mathbf{x}^H \mathbf{A}_1 \mathbf{x} + 2 \cdot \text{Re}\{\mathbf{b}_1^H \mathbf{x}\} + c_1 \leq 0$$

implies

$$\mathbf{x}^H \mathbf{A}_2 \mathbf{x} + 2 \cdot \text{Re}\{\mathbf{b}_2^H \mathbf{x}\} + c_2 \leq 0$$

if and only if there exists a $\mu \geq 0$ such that

$$\mu \begin{bmatrix} \mathbf{A}_1 & \mathbf{b}_1 \\ \mathbf{b}_1^H & c_1 \end{bmatrix} - \begin{bmatrix} \mathbf{A}_2 & \mathbf{b}_2 \\ \mathbf{b}_2^H & c_2 \end{bmatrix} \geq 0 \quad (8.23)$$

provided there exists a point $\hat{\mathbf{x}}$ with

$$\hat{\mathbf{x}}^H \mathbf{A}_1 \hat{\mathbf{x}} + 2 \cdot \text{Re}\{\mathbf{b}_1^H \hat{\mathbf{x}}\} + c_1 < 0. \quad (8.24)$$

Lemma 8.4.2. (*Schur complement [BV04]*) Let

$$\mathbf{\Gamma} = \begin{bmatrix} \mathbf{A} & \mathbf{B}^H \\ \mathbf{B} & \mathbf{D} \end{bmatrix} \quad (8.25)$$

be a Hermitian matrix. Then $\mathbf{\Gamma} \geq 0$ if and only if $\mathbf{D} - \mathbf{B}^H \mathbf{A}^{-1} \mathbf{B} \geq 0$ (assuming $\mathbf{A} > 0$), or $\mathbf{A} - \mathbf{B}^H \mathbf{D}^{-1} \mathbf{B} \geq 0$ (assuming $\mathbf{D} > 0$).

Define $\boldsymbol{\delta}_{ii} = \text{vec}\{\mathbf{\Delta}_{ii}^H\}$ and $\boldsymbol{\delta}_{ij} = \text{vec}\{\mathbf{\Delta}_{ij}^H\}$ where $\text{vec}\{\cdot\}$ stacks the columns of a matrix into a vector. Using the fact that $\text{Tr}\{\mathbf{A}\mathbf{B}\mathbf{C}\mathbf{D}\} = \text{vec}\{\mathbf{A}^H\}^H (\mathbf{D}^H \otimes \mathbf{B}) \text{vec}\{\mathbf{C}\}$ where \otimes stands for the Kronecker product, the constraint (8.22a) can be further expanded as

$$\text{Tr}\{(\hat{\mathbf{H}}_{ii} + \mathbf{\Delta}_{ii})\mathbf{Q}_i(\hat{\mathbf{H}}_{ii} + \mathbf{\Delta}_{ii})^H\}$$

$$\begin{aligned}
 &= \text{Tr}\{\Delta_{ii}\mathbf{Q}_i\Delta_{ii}^H + 2 \cdot \text{Re}\{\hat{\mathbf{H}}_{ii}\mathbf{Q}_i\Delta_{ii}^H\} + \hat{\mathbf{H}}_{ii}\mathbf{Q}_i\hat{\mathbf{H}}_{ii}^H\} \\
 &= \delta_{ii}^H(\mathbf{I}_{M_r} \otimes \mathbf{Q}_i)\delta_{ii} + 2 \cdot \text{Re}\{\text{vec}\{\hat{\mathbf{H}}_{ii}^H\}^H(\mathbf{I}_{M_r} \otimes \mathbf{Q}_i)\delta_{ii}\} + \text{Tr}\{\hat{\mathbf{H}}_{ii}\mathbf{Q}_i\hat{\mathbf{H}}_{ii}^H\} - t_i\eta_i \geq 0 \quad (8.26)
 \end{aligned}$$

Similarly, constraints (8.22b)-(8.22e) can be also rewritten as the following quadratic forms, respectively.

$$\delta_{ij}^H(\mathbf{I}_{M_r} \otimes \mathbf{Q}_j)\delta_{ij} + M_r\sigma_n^2 - t_i \leq 0 \quad (8.27a)$$

$$\delta_{ij}^H(\mathbf{I}_{M_r} \otimes \mathbf{Q}_j)\delta_{ij} + 2 \cdot \text{Re}\{\text{vec}\{\hat{\mathbf{H}}_{ij}^H\}^H(\mathbf{I}_{M_r} \otimes \mathbf{Q}_j)\delta_{ij}\} + \text{Tr}\{\hat{\mathbf{H}}_{ij}\mathbf{Q}_j\hat{\mathbf{H}}_{ij}^H\} - P_i^{(\text{TH})} \leq 0 \quad (8.27b)$$

$$\delta_{ii}^H(\mathbf{I}_{M_r} \otimes \mathbf{T}_{ii})\delta_{ii} - \gamma_{ii} \leq 0 \quad (8.27c)$$

$$\delta_{ij}^H(\mathbf{I}_{M_r} \otimes \mathbf{T}_{ij})\delta_{ij} - \gamma_{ij} \leq 0 \quad (8.27d)$$

Since δ_{ii} and δ_{ij} are independent, we can deal with the constraints (8.22a), (8.22d) ((8.26) and (8.27c), respectively) and (8.22b), (8.22c), (8.22e) ((8.27a), (8.27b), and (8.27d), respectively) separately. Clearly, according to Lemma 8.4.1, (8.26) and (8.27c) hold if and only if there exists $\mu_i \geq 0$ such that

$$\begin{bmatrix} \mathbf{I}_{M_r} \otimes (\mathbf{Q}_i + \mu_i\mathbf{T}_{ii}) & (\mathbf{I}_{M_r} \otimes \mathbf{Q}_i)\text{vec}\{\hat{\mathbf{H}}_{ii}^H\} \\ \text{vec}\{\hat{\mathbf{H}}_{ii}^H\}^H(\mathbf{I}_{M_r} \otimes \mathbf{Q}_i) & \text{Tr}\{\hat{\mathbf{H}}_{ii}\mathbf{Q}_i\hat{\mathbf{H}}_{ii}^H\} - t_i\eta_i - \mu_i\gamma_{ii} \end{bmatrix} \geq 0 \quad (8.28)$$

To further simplify the constraint (8.28), we apply Lemma 8.4.2. Then it is worth mentioning that we need to distinguish the two cases $\mu_i > 0$ and $\mu_i = 0$ since \mathbf{Q}_i^{-1} might not exist when $\mu_i = 0$ [WP09]. For $\mu_i > 0$, using Lemma 8.4.2, (8.28) is equivalent to

$$\begin{aligned}
 &\text{Tr}\{\hat{\mathbf{H}}_{ii}\mathbf{Q}_i\hat{\mathbf{H}}_{ii}^H\} - t_i\eta_i - \mu_i\gamma_{ii} - \text{vec}\{\hat{\mathbf{H}}_{ii}^H\}^H(\mathbf{I}_{M_r} \otimes \mathbf{Q}_i)(\mathbf{I}_{M_r} \otimes (\mathbf{Q}_i + \mu_i\mathbf{T}_{ii}))^{-1} \\
 &\quad \cdot (\mathbf{I}_{M_r} \otimes \mathbf{Q}_i)\text{vec}\{\hat{\mathbf{H}}_{ii}^H\} \geq 0
 \end{aligned}$$

which can be further simplified to

$$\text{Tr}\{\hat{\mathbf{H}}_{ii}\mathbf{Q}_i\hat{\mathbf{H}}_{ii}^H\} - \text{Tr}\{\hat{\mathbf{H}}_{ii}\mathbf{Q}_i(\mathbf{Q}_i + \mu_i\mathbf{T}_{ii})^{-1}\mathbf{Q}_i\hat{\mathbf{H}}_{ii}^H\} - t_i\eta_i - \mu_i\gamma_{ii} \geq 0. \quad (8.29)$$

To decouple the matrix inverse term from (8.29), we introduce an auxiliary variable $\mathbf{Z}_i \in \mathbb{C}^{M_t \times M_t}$. By using the fact that $\text{Tr}\{\mathbf{A}\mathbf{B}\} = \text{Tr}\{\mathbf{B}\mathbf{A}\}$, the constraint (8.29) can be written as the following two constraints.

$$\text{Tr}\{\hat{\mathbf{H}}_{ii}^H\hat{\mathbf{H}}_{ii}(\mathbf{Q}_i - \mathbf{Z}_i)\} - t_i\eta_i - \mu_i\gamma_{ii} \geq 0 \quad (8.30a)$$

$$\mathbf{Q}_i(\mathbf{Q}_i + \mu_i\mathbf{T}_{ii})^{-1}\mathbf{Q}_i \leq \mathbf{Z}_i \quad (8.30b)$$

Using Lemma 8.4.2 again, (8.30b) can be equivalently transformed into

$$\begin{bmatrix} \mathbf{Z}_i & \mathbf{Q}_i \\ \mathbf{Q}_i & \mathbf{Q}_i + \mu_i \mathbf{T}_{ii} \end{bmatrix} \geq 0 \quad (8.31)$$

Furthermore, it can be proven that the case $\mu_i = 0$ can be integrated into the new constraints (8.30a) and (8.31) by following a similar proof as in [WP09]. Thereby, the infinite constraints (8.22a) and (8.22d) with respect to Δ_{ii} are successfully reformulated into two equivalent convex constraints (8.30a) and (8.31).

However, there are three instead of two sets of infinite constraints with respect to Δ_{ii} , i.e., (8.22b), (8.22c), and (8.22e), which does not fulfill the structure of the original S-procedure. Therefore, it is not straightforward to apply the same derivation. To tackle this problem, we notice that the feasible region for the three constraints is equivalent to the intersection of the feasible region of any two constraints. For instance, we can choose the sets $\{(8.22b), (8.22e)\}$ and $\{(8.22c), (8.22e)\}$ as the two pairs. Then the intersection of the feasible region of these two pairs of constraints will give us exactly the same feasible region for the case with three constraints. The benefits of doing this is that for each pair we can apply the original S-procedure. Thus, we can convert the infinite constraints into equivalent convex constraints as we have done for (8.22a) and (8.22d). Finally, the constraints (8.22b) and (8.22e) can be transformed into the following equivalent convex constraints

$$\text{Tr}\{\hat{\mathbf{H}}_{ij}^H \hat{\mathbf{H}}_{ij} (-\mathbf{Q}_j - \mathbf{Y}_i)\} - \kappa_i \gamma_{ij} + P_i^{(\text{TH})} \geq 0 \quad (8.32a)$$

$$\begin{bmatrix} \mathbf{Y}_i & -\mathbf{Q}_j \\ -\mathbf{Q}_j & -\mathbf{Q}_j + \kappa_i \mathbf{T}_{ij} \end{bmatrix} \geq 0 \quad (8.32b)$$

where $\kappa_i \geq 0$ and $\mathbf{Y}_i \in \mathbb{C}^{M_t \times M_t}$ are auxiliary variables. The constraints (8.22c) and (8.22e) can be converted to

$$t_i - M_r \sigma_n^2 - \lambda_i \gamma_{ij} \geq 0 \quad (8.33a)$$

$$\begin{bmatrix} \mathbf{X}_i & -\mathbf{Q}_j \\ -\mathbf{Q}_j & -\mathbf{Q}_j + \lambda_i \mathbf{T}_{ij} \end{bmatrix} \geq 0 \quad (8.33b)$$

where $\lambda_i \geq 0$ and $\mathbf{X}_i \in \mathbb{C}^{M_t \times M_t}$ are auxiliary variables. Thereby, the three constraints (8.22b), (8.22c), and (8.22e) can now be substituted by the equivalent four convex constraints (8.32a), (8.32b), (8.33a), and (8.33b).

Replacing (8.22a), (8.22b), (8.22c), (8.22d), and (8.22e) with (8.30a), (8.31), (8.32a), (8.32b),

(8.33a), and (8.33b), problem (8.22) is reformulated as

$$\begin{aligned}
 & \min_{\substack{\mathbf{Q}_i, \mathbf{X}_i, \mathbf{Y}_i, \mathbf{Z}_i, \\ t_i, \mu_i, \kappa_i, \lambda_i}} \sum_i \text{Tr}\{\mathbf{Q}_i\} \\
 \text{s.t. } & \text{Tr}\{\hat{\mathbf{H}}_{ii}^H \hat{\mathbf{H}}_{ii} (\mathbf{Q}_i - \mathbf{Z}_i)\} - t_i \eta_i - \mu_i \gamma_{ii} \geq 0 \\
 & \text{Tr}\{\hat{\mathbf{H}}_{ij}^H \hat{\mathbf{H}}_{ij} (-\mathbf{Q}_j - \mathbf{Y}_i)\} - \kappa_i \gamma_{ij} + P_i^{(\text{TH})} \geq 0 \\
 & t_i - M_r \sigma_n^2 - \lambda_i \gamma_{ij} \geq 0 \\
 & \begin{bmatrix} \mathbf{Z}_i & \mathbf{Q}_i \\ \mathbf{Q}_i & \mathbf{Q}_i + \mu_i \mathbf{T}_{ii} \end{bmatrix} \geq 0, \quad \begin{bmatrix} \mathbf{Y}_i & -\mathbf{Q}_j \\ -\mathbf{Q}_j & -\mathbf{Q}_j + \kappa_i \mathbf{T}_{ij} \end{bmatrix} \geq 0, \quad \begin{bmatrix} \mathbf{X}_i & -\mathbf{Q}_j \\ -\mathbf{Q}_j & -\mathbf{Q}_j + \lambda_i \mathbf{T}_{ij} \end{bmatrix} \geq 0 \\
 & \mathbf{Q}_i \geq 0, t_i > 0, \quad \mu_i \geq 0, \kappa_i \geq 0, \lambda_i \geq 0, \forall i, j \in \{1, 2\}.
 \end{aligned} \tag{8.34}$$

Problem (8.34) is a convex SDP problem. Thus, it can be solved efficiently using the standard interior-point algorithm in [BV04].

8.5 Simulation results

In this section the proposed algorithms are evaluated using Monte-Carlo simulations. The generated channels are uncorrelated Rayleigh flat fading. For simplicity, we have $\epsilon_i = \epsilon$, $\eta_i = \eta$, and $P_i^{(\text{TH})} = P$, $\forall i$. The threshold power P is set to unity and the SNR is defined as $\text{SNR} = \epsilon / \sigma_n^2$. All the simulation results are averaged over 1000 channel realizations. To demonstrate whether and under which conditions a FD system can achieve a two-fold gain compared to a HD system in terms of the sum rate, we define the HD baseline system. The HD baseline system has the same hardware configurations (e.g., the same number of transmit and receive antennas, the same transmit power constraints, etc.) as the transceiver in the FD system. It works in a TDD HD mode, i.e., at each time slot, the HD system only receives or transmits the data. The applied transmit strategies are capacity achieving, i.e., MRT for the MISO setup and the SVD-based WF solution for the MIMO setup. Other than these optimal solutions, the performance of suboptimal transmit strategies for the FD system is also demonstrated in the simulations. For the MIMO case, we show the performance of the classical WF solution and the inverse WF (IWF) solution derived in Section 8.3.2. This is done by first calculating the WF or IWF solution and then scaling the obtained solution such that both constraints in (8.10) are satisfied. The same procedure is also applied to the selected suboptimal algorithms for the MISO setup. For a FD MISO setup, we also demonstrate the performance of the MRT

and the ZF strategy ².

8.5.1 Achievable sum rate with perfect CSI

Let “FD-Opt” denotes the optimal FD solution using the interior-point algorithm. “HD” denotes the optimal HD solution. “FD-WF” denotes the WF solution. “FD-IWF” denotes the IWF solution. “FD-MRT” denotes the MRT solution. “FD-ZF” denotes the ZF solution.

Figures 8.3, 8.4, and 8.5 demonstrate the achievable sum rate of a FD MIMO system. The parameters ϵ and η can be seen as the indicator of the direct (e.g., creating a negative copy of the transmitted signal at the receiver, e.g., using the axillary transmit chain in [SPS11]) and the indirect (e.g., artificially introducing path-loss, e.g., techniques in [EDDS11]) RF SI cancellation ability, respectively. The smaller the ϵ or the η is, the higher is the RF cancellation ability of the FD system. Clearly, the three subfigures imply that compared to a HD MIMO system a two-fold gain in terms of the sum rate is only achievable in the high SNR regime and when ϵ or η is small enough. It is also observed that the suboptimal solution WF and IWF is not far from the optimal solution. When the SI cancellation ability is weak, i.e., in the low SNR regime and when ϵ or η is big, the optimal solution corresponds to the IWF algorithm and a two-fold gain is not obtainable. When the SI cancellation ability is strong, the optimal solution corresponds to the WF algorithm.

A similar observation can be obtained for the MISO setup in Figures 8.6, 8.7, and 8.8. That is, the suboptimal algorithms MRT and ZF have close to optimum performance. When the SI cancellation ability is strong, the MRT method corresponds to the optimal scheme. When the SI cancellation ability is weak, the ZF solution is close to the optimal solution. However, interestingly, it can be seen that as ϵ increases the gain of using a FD system is constant. Even though the gain of using a FD system decreases as η increases, the degradation is quite small compared to the MIMO setup. This implies that for a MISO setup the transmit strategies act not only as an aid of the RF cancellation techniques but also as a replacement of them. This advantage is due to the fact that in the MISO case the transmitter can allocate as much power as possible to the null space of the SI channel and this amount of power will also contribute to the sum rate maximization. However, this ability is limited in the MIMO setup due to the existence of the co-channel interference created by the multiple stream transmission.

²The transmitter transmits into the null space of the SI channel

8.5.2 Minimum required transmit power with imperfect CSI

The noise level is normalized to be unity and we have $\mathbf{T}_{ii} = \mathbf{T}_{ij} = \mathbf{I}_{M_t}, \forall i, j$. “Robust” stands for the solution of (8.34). “Non-Robust” stands for the solution where problem (8.20) is first solved by assuming $\mathbf{\Delta}_{ii} = \mathbf{\Delta}_{ij} = \mathbf{0}, \forall i, j$ and then the obtained solution is scaled such that the constraints are satisfied. We further define $\nu_1 = \gamma_{ii}, \forall i$ and $\nu_2 = \gamma_{ji}/\gamma_{ii}, \forall i, j$ to represent the channel error intensity for the desired channel and the SI channel, respectively [WP09].

Figure 8.9 demonstrates the comparison of the robust design and the non-robust design over different SINR requirements. The channel error intensity of the SI channel is much smaller than that of the desired channel, i.e., $\nu_2 = 10^{-3} \ll 1$. It can be seen that as the SINR requirements increase the robust design outperforms the non-robust design. Moreover, the gain increases as the the channel error intensity becomes higher.

Figure 8.10 compares the performance of the robust design and the non-robust design when the channel error intensity varies. Clearly, as the channel error intensity of both the SI channel and the desired channel increases, the robust design performs better compared to the non-robust design. When the array size increases, a higher gain is obtained. This is an interesting result since more antennas not only provide more degrees of freedom but also increase the SI. Hence, it is surprising to observe that the robust design significantly benefits from the enlarged array size.

8.6 Summary

In this chapter, we discuss our proposed SI aware transmit strategies for a FD P2P MIMO system, which are developed in [ZTLH12] and [ZTH13b]. The proposed transmit strategies are SDMA techniques, which are aware of the SI cancellation provided by other cancellation techniques such as RF cancellation techniques and other digital cancellation techniques. By tuning a SI threshold, the proposed transmit strategies can balance between the spatial SI cancellation and the multiplexing gain of the resulting FD system. Given a SI threshold, optimal transmit strategies, which maximize the sum rate of the system for a MIMO/MISO setup, are derived using convex optimization. Moreover, analytic solutions are obtained by using convex analysis. Since the proposed transmit strategies rely on the CSI at the transmitter side, which is imperfect in practice, we consider the worst-case beamforming design which minimizes the required transmit power subject to total SINR requirements and SI constraints. More specifically, the CSI errors are modeled deterministically and are bounded by ellipsoids. The resulting optimization problem is non-convex. We have reformulated it into a convex problem using the S-procedure.

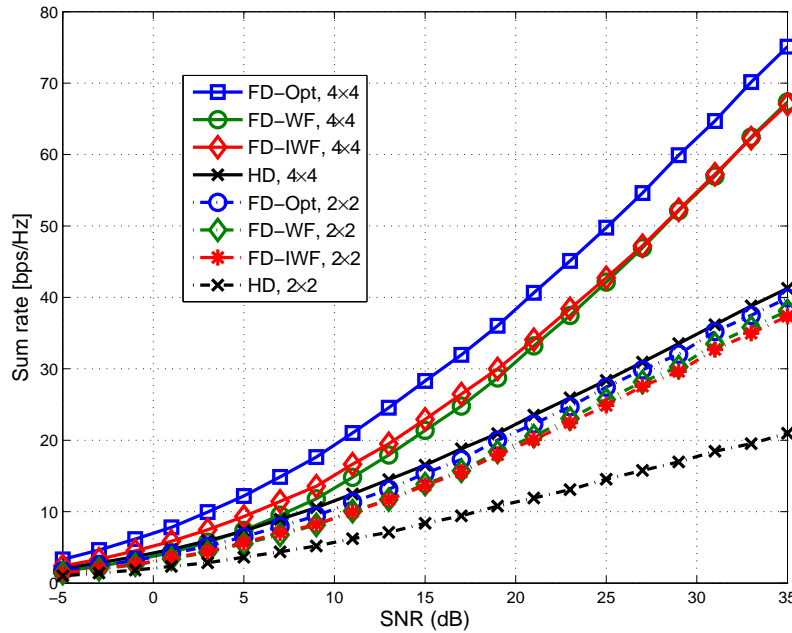


Figure 8.3: Achievable sum rate as a function of SNR for a FD system with a MIMO setup, $\epsilon = \eta = 1$.

Simulation results have demonstrated that

- Compared to the HD baseline system a two-fold gain in terms of the sum rate is achievable when the SI cancellation provided by the other cancellation techniques is sufficient. In a MISO setup, the achievable gain is less affected by the SI cancellation provided by the other cancellation techniques because there are a sufficient number of spatial dimensions, which can be used to suppress the SI.
- The proposed robust beamforming design is superior compared to the non-robust design especially when the channel error intensity is high and there are many antennas at the transmitter and at the receiver.

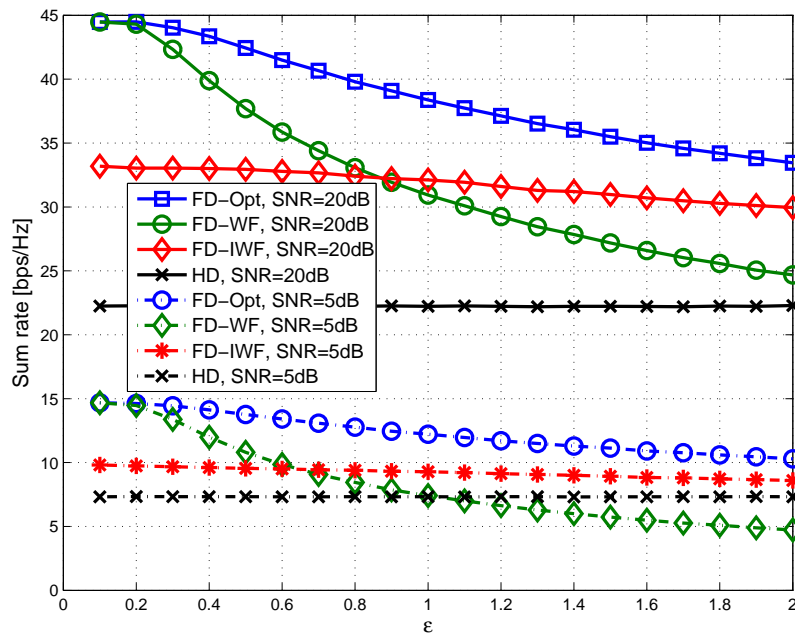


Figure 8.4: Achievable sum rate as a function of ϵ for a FD system with a MIMO setup, $M_r = M_t = 4$, $\eta = 1$.

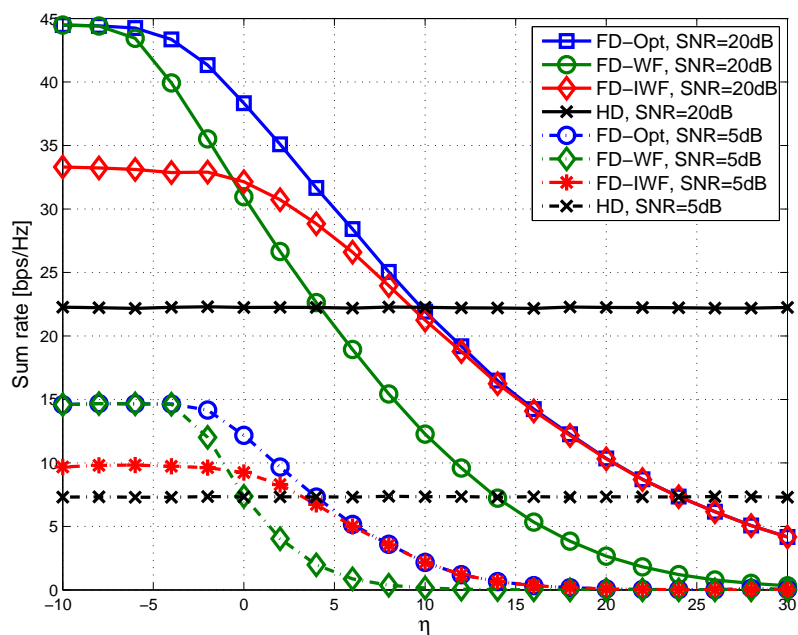


Figure 8.5: Achievable sum rate as a function of η for a FD system with a MIMO setup, $M_r = M_t = 4$, $\epsilon = 1$.

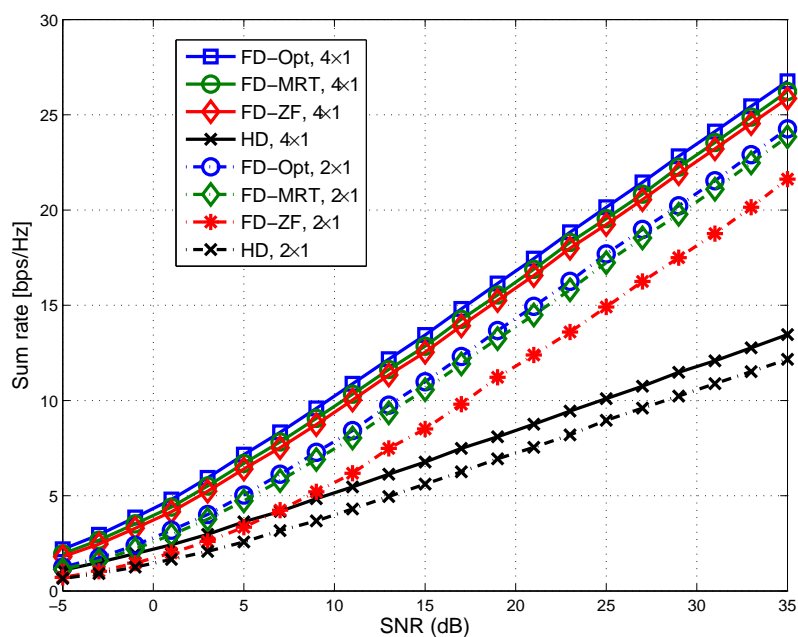


Figure 8.6: Achievable sum rate as a function of SNR for a FD system with a MISO setup, $\epsilon = \eta = 1$.

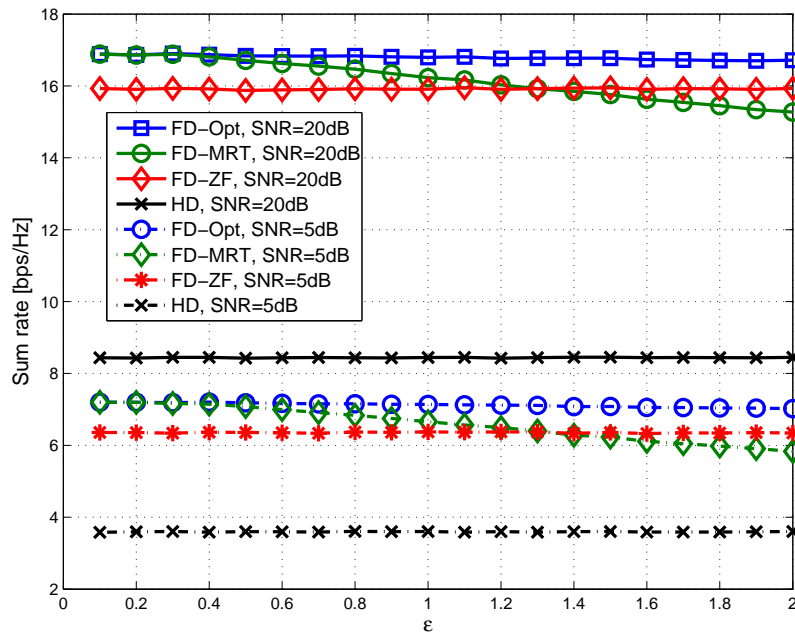


Figure 8.7: Achievable sum rate as a function of ϵ for a FD system with a MISO setup, $M_t = 4$, $\eta = 1$.

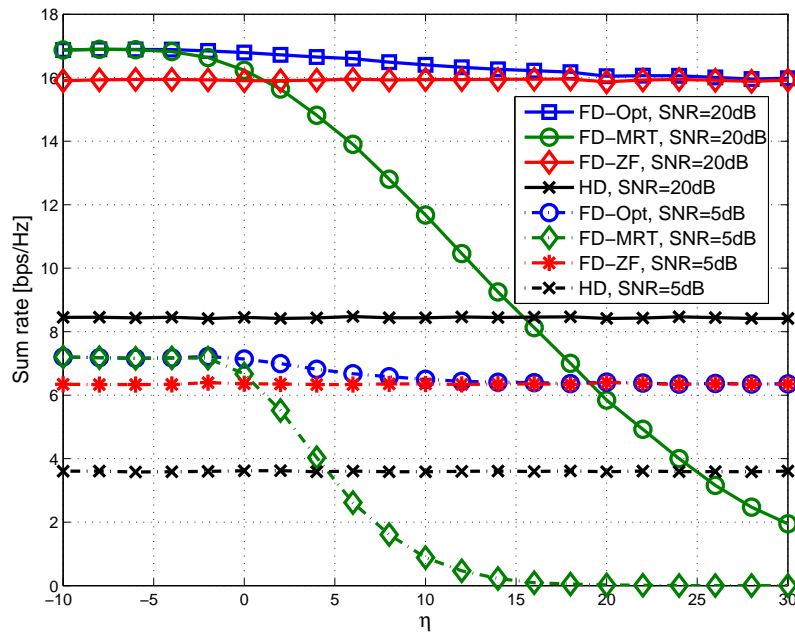


Figure 8.8: Achievable sum rate as a function of η for a FD system with a MISO setup, $M_t = 4$, $\epsilon = 1$.

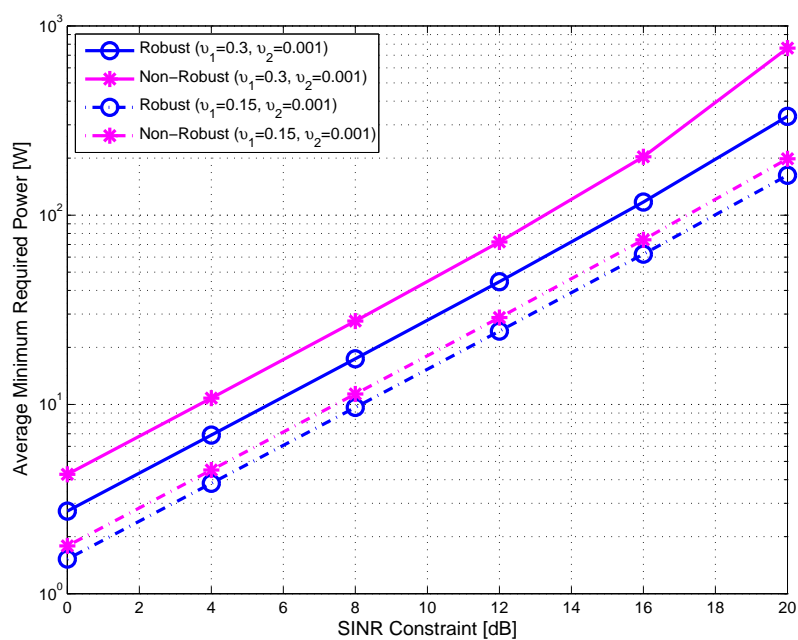


Figure 8.9: Average minimum required power vs. SINR constraint $\eta = \eta_i, \forall i$, $M_t = M_r = 2$, $P_i^{(\text{ref})} = 60$ dBW, $\forall i$.

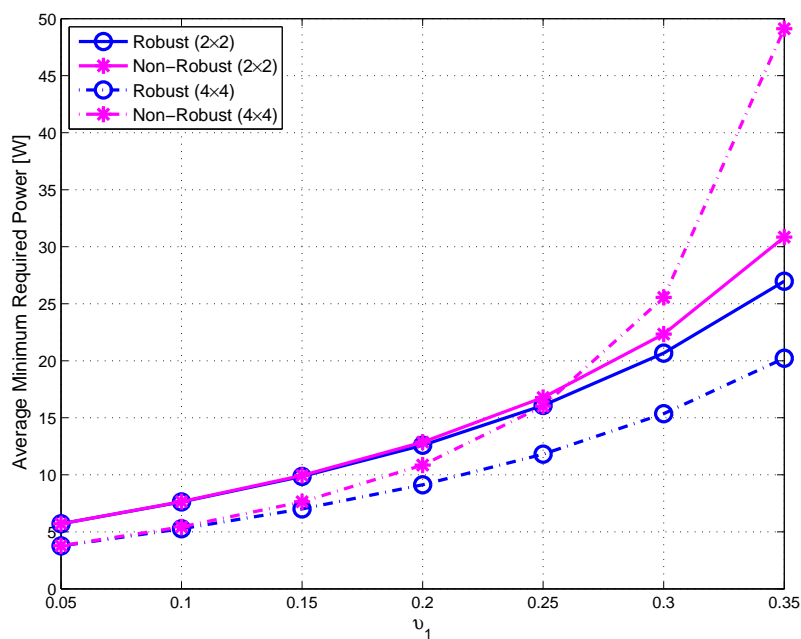


Figure 8.10: Average minimum required power vs. $v_1, v_2 = 0.01, \eta_i = 5$ dB, $\forall i, P_i^{(\text{ref})} = 40$ dBW, $\forall i$.

9 Transmit strategies for full-duplex systems with imperfect RF chain

In this chapter, we study transmit strategies for a full-duplex point-to-point system with imperfect RF chains [ZTH13c]. When the RF chain is imperfect, finding optimal transmit strategies which maximize the system sum rate corresponds to a joint design of the precoders at the two transmitters. To avoid prohibitive computational complexity, we resort to suboptimal solutions. First, we propose the signal to leakage plus noise ratio (SLNR) based precoder design for the MISO and the MIMO setup in Section 9.3. The SLNR based precoder design avoids the joint design of the precoders at the two transmitters and also provides a closed-form solution. Notice that properly adjusting the transmit power can also improve the performance of a FD system. We develop power adjustment schemes which maximize the system sum rate for SISO, MISO, and MIMO scenarios in Section 9.4. Analytic solutions for optimal power adjustment are also obtained. Furthermore, we discuss how to adjust the power to take into account the max-min fairness of the system.

9.1 Problem description and our contributions

As discussed in Chapter 8, where the SI cancellation techniques, including the antenna attenuation, RF domain cancellation techniques, and digital domain cancellation techniques proposed in [JCK⁺11], [DS10], [DMBS12], [SPS11], and [RWW11], are combined, ideally the SI can be completely removed. However, due to practical RF imperfections, e.g., ADC quantization noise and oscillator phase noise, some residual SI will exist [DMBS12]. It is critical especially when only simple SI cancellation techniques are deployed in the system, i.e., only SI subtraction in the digital baseband of the receiver is used [KSA⁺14]. The residual SI will significantly influence optimal transmit strategies of the two communicating devices. Depending on the strength of the residual SI, optimal transmit strategies for a HD P2P system, e.g., total power transmission for SISO, maximum ratio transmission (MRT) for MISO, and an SVD together with water-filling (WF) for MIMO, can be far from optimal for the resulting HD system. If the residual SI is not well handled, it can still prevent us from exploiting the benefits of FD wireless communications. This motivates the development of robust signal processing techniques to combat the imperfections in the RF chain. Transmit strategies to combat imperfect RF chains are studied in [DMBS12]. Moreover, to guarantee a HD performance in the worst case,

i.e., the achievable sum rate is never worse than that of a HD baseline scenario, the design in [DMBS12] is performed for two consecutive time slots (assuming that the CSI remains the same). The formulated optimization problem is non-convex and a gradient projection (GP) based method is proposed to solve it. The GP method is a type of gradient method and thus does neither achieve a global optimality nor has a guaranteed polynomial time solution. Moreover, switching from a FD mode to a HD mode prevents the simultaneous transmission and reception of a FD system, which itself is an important property of a FD system, e.g., if a reduced round-trip time is more desired.

Therefore, we develop efficient transmit strategies for a FD system with imperfect RF chains. The developed transmit strategies can be designed in every time slot. The resulting sum rate maximization problem is non-convex and NP-hard, similarly as in [DMBS12]. Hence, we resort to suboptimal solutions. We first propose precoding techniques which take into account the trade-offs between increasing the achievable rate and reducing the residual SI power. To this end, we exploit the statistics of the residual SI and develop SLNR based precoders which have closed-form solutions for both the MISO and the MIMO setup. On the other hand, properly controlling the transmit power can also improve the performance of a FD system. Thereby, given a fixed precoder we design optimal power scaling factors to achieve a better performance for the system. That is, power scaling factors which maximize the achievable sum rate are developed for SISO and MISO while power scaling factors which maximize the sum SINR are found for MIMO. Considering the fairness in the system, we also develop power adjustment schemes which maximize the minimum SINR in the system. The proposed power adjustment algorithms can be further combined with the proposed precoding algorithms to enhance the performance. It is worth emphasizing that the major difference between the contributions in this chapter and the contributions in Chapter 8 can be summarized as: in Chapter 8 we propose an advanced SI aware transmit precoding algorithm. We assume that after applying the existing SI cancellation techniques and the proposed scheme the SI can be significantly reduced or completely removed and thus the residual SI is ignorable. In this chapter we apply only SI subtraction in the digital baseband of the receiver. In general the residual SI is strong and might be non-linear. We model the nonlinearity and other distortions such as ADC quantization noise using a simplified model, i.e., an additive Gaussian distortion model [DMBS12]. Based on this simplified model, we develop efficient transmit precoders to combat the imperfections from the RF chain. This model has also been used in [Cir14] for the design of optimal transmit strategies under multiple linear constraints.

9.2 System model

We consider a FD P2P MIMO system with two identical transceivers. Each transceiver has M_r receive antennas and M_t transmit antennas. The channel is flat fading and has full rank. Perfect synchronization is also assumed. The desired channel between the i -th ($i \in \{1, 2\}$) transmitter and the i -th receiver is denoted as $\mathbf{H}_{ii} \in \mathbb{C}^{M_r \times M_t}$ while the SI channel from the j -th ($j \in \{1, 2\}$ and $j \neq i$) transmitter to the i -th receiver is denoted as $\mathbf{H}_{ij} \in \mathbb{C}^{M_r \times M_t}$. As derived in [DMBS12], the received signal at the i -th receiver is written as:

$$\begin{aligned} \mathbf{y}_i &= \underbrace{\sqrt{\rho_i} \mathbf{H}_{ii} (\mathbf{x}_i + \mathbf{e}_i^t) + \sqrt{\eta_i} \mathbf{H}_{ij} (\mathbf{x}_j + \mathbf{e}_j^t)}_{\mathbf{u}_i} + \mathbf{n}_i + \mathbf{e}_i^r \\ &= \underbrace{\sqrt{\rho_i} \mathbf{H}_{ii} \mathbf{x}_i}_{\text{desired signal}} + \underbrace{\sqrt{\eta_i} \mathbf{H}_{ij} \mathbf{x}_j}_{\text{suppressible SI}} + \underbrace{\sqrt{\rho_i} \mathbf{H}_{ii} \mathbf{e}_i^t + \sqrt{\eta_i} \mathbf{H}_{ij} \mathbf{e}_j^t + \mathbf{n}_i + \mathbf{e}_i^r}_{\text{insuppressible interference + Noise}} \end{aligned} \quad (9.1)$$

where $\rho_i \in \mathbb{R}_+$ and $\eta_i \in \mathbb{R}_+$ determine the strength of the desired and SI channel, respectively. The transmitted data vector \mathbf{x}_i has zero mean and covariance matrix $\mathbb{E}\{\mathbf{x}_i \mathbf{x}_i^H\} = \mathbf{Q}_i$, $\forall i$. The maximum allowable transmit power for each transmitter is P_{\max} . Let us define the received covariance matrix $\mathbb{E}\{\mathbf{u}_i \mathbf{u}_i^H\} = \mathbf{\Phi}_i$, where \mathbf{u}_i is defined in equation (9.1). Then the vectors $\mathbf{e}_i^t \sim \mathcal{CN}(\mathbf{0}, \kappa \cdot \text{Diag}\{\mathbf{Q}_i\})$ and $\mathbf{e}_i^r \sim \mathcal{CN}(\mathbf{0}, \beta \cdot \text{Diag}\{\mathbf{\Phi}_i\})$ denote the transmit error signal and the receive error signal of the RF chains, respectively. The scalars $\kappa \in \mathbb{R}_+$ ($\kappa \ll 1$) and $\beta \in \mathbb{R}_+$ ($\beta \ll 1$) denote the ratio between the transmit error power and the transmit power and the ratio of the receive error power to the received power, respectively [DMBS12]. The vector \mathbf{n}_i denotes the ZMCSCG noise and $\mathbb{E}\{\mathbf{n}_i \mathbf{n}_i^H\} = \sigma_n^2 \mathbf{I}_{M_r}$, $\forall i$. If channel knowledge is available at the receiver, then the suppressible interference in (9.1) can be subtracted. Since the error vectors \mathbf{e}_i^t and \mathbf{e}_i^r are not correlated with the signal vector \mathbf{x}_i , $\forall i$ [DMBS12], the interference plus noise power at the i th receiver is computed as

$$\begin{aligned} P_i^{(\text{IN})} &= \mathbb{E}\{\|\sqrt{\rho_i} \mathbf{H}_{ii} \mathbf{e}_i^t\|^2\} + \mathbb{E}\{\|\sqrt{\eta_i} \mathbf{H}_{ij} \mathbf{e}_j^t\|^2\} + \mathbb{E}\{\|\mathbf{e}_i^r\|^2\} + \mathbb{E}\{\|\mathbf{n}_i\|^2\} \\ &= \mathbb{E}\{\|\sqrt{\rho_i} \mathbf{H}_{ii} \mathbf{e}_i^t\|^2\} + \mathbb{E}\{\|\sqrt{\eta_i} \mathbf{H}_{ij} \mathbf{e}_j^t\|^2\} + \beta \text{Diag}\{\mathbb{E}\{\|\sqrt{\rho_i} \mathbf{H}_{ii} \mathbf{x}_i\|^2\} + \mathbb{E}\{\|\sqrt{\eta_i} \mathbf{H}_{ij} \mathbf{x}_j\|^2\}\} \\ &\quad + \mathbb{E}\{\|\sqrt{\rho_i} \mathbf{H}_{ii} \mathbf{e}_i^t\|^2\} + \mathbb{E}\{\|\sqrt{\eta_i} \mathbf{H}_{ij} \mathbf{e}_j^t\|^2\} + \mathbb{E}\{\|\mathbf{n}_i\|^2\} \} + \mathbb{E}\{\|\mathbf{n}_i\|^2\} \end{aligned} \quad (9.2)$$

Using the fact that $\kappa \ll 1$ and $\beta \ll 1$, equation (9.2) reduces to

$$P_i^{(\text{IN})} \approx \underbrace{\mathbb{E}\{\|\sqrt{\rho_i} \mathbf{H}_{ii} \mathbf{e}_i^t\|^2\} + \beta \text{Diag}\{\mathbb{E}\{\|\sqrt{\rho_i} \mathbf{H}_{ii} \mathbf{x}_i\|^2\}\}}_{\text{distortion from the } i\text{-th transmitter}} + \underbrace{\mathbb{E}\{\|\sqrt{\eta_i} \mathbf{H}_{ij} \mathbf{e}_j^t\|^2\} + \beta \text{Diag}\{\mathbb{E}\{\|\sqrt{\eta_i} \mathbf{H}_{ij} \mathbf{x}_j\|^2\}\}}_{\text{SI from the } j\text{-th transmitter}}$$

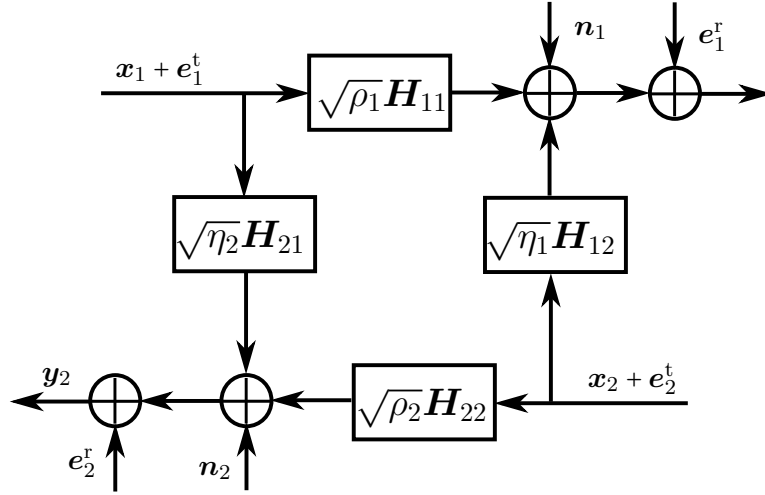


Figure 9.1: A MIMO point-to-point full-duplex system with insuppressible interference [DMBS12].

$$\underbrace{+ \beta \text{Diag}\{\mathbb{E}\{\|\mathbf{n}_i\|^2\}\} + \mathbb{E}\{\|\mathbf{n}_i\|^2\}}_{\text{enhanced noise}} \quad (9.3)$$

A detailed flow chart of the considered FD system is illustrated in Figure 9.1.

Due to the existence of insuppressible residual SI in (9.1), the sum rate achievable transmit strategies for HD systems, i.e., maximum power transmission for SISO, MRT for MISO, and WF for MIMO, are not necessarily optimal for our FD system. In fact the sum rate maximization problem of our system is non-convex and NP-hard [DMBS12]. Although in [DMBS12] a GP based algorithm is proposed to solve this problem, the algorithm is neither optimal nor computationally efficient. Thus, in our work we develop low complexity suboptimal transmit strategies to improve the performance of a FD system with insuppressible SI.

9.3 Signal to leakage plus noise ratio (SLNR) based precoder design

Clearly, the desired transmit techniques for our scenario must consider the trade-off between increasing the achievable rate and reducing the generated residual SI. Taking into account that in practice the desired channel is much weaker than the SI channel, i.e., $\rho_i \ll \eta_i$, we can conclude from equation (9.3) that the performance limitation of the system comes from the SI and the enhanced noise. Moreover, the SI has coupled the design of the two covariance

matrices which makes the optimization problem difficult to solve. Note that we are interested in developing efficient suboptimal precoding algorithms. To this end, we propose transmit strategies which maximize the so called SLNR for both MISO and MIMO setups. In this section we focus on precoding techniques and thus the SISO case will not be covered here, but in Section 9.4.

9.3.1 MISO

In the MISO case we have $M_t > M_r = 1$ and the vector channels $\{\mathbf{h}_{ii}, \mathbf{h}_{ij}\} \in \mathbb{C}^{M_t}$. The proposed transmit strategy which maximizes the SLNR is analogous to the concept of the SLNR based precoding design for a multi-user MIMO downlink system in [HMVS01] and [STS07]. Let us start by defining the leakage. The SI term in (9.3) is caused by the j -th transmitter and thus can be also treated as the signal leaked from the j -th transmitter to the i -th receiver. Let us define $\mathbf{Q}_i = \mathbf{w}_i \mathbf{w}_i^H$. Then the signal power leaked from the i -th transmitter is described by

$$P_i^{(L)} = \mathbb{E}\{\|\sqrt{\eta_j} \mathbf{h}_{ji}^T \mathbf{e}_i^t\|^2\} + \beta \text{Diag}\{\mathbb{E}\{\|\sqrt{\eta_j} \mathbf{h}_{ji}^T \mathbf{x}_i\|^2\}\} = \mathbf{w}_i^H \eta_j \kappa \text{Diag}\{\mathbf{h}_{ji}^* \mathbf{h}_{ji}^T\} \mathbf{w}_i + \mathbf{w}_i^H \beta \eta_j \mathbf{h}_{ji}^* \mathbf{h}_{ji}^T \mathbf{w}_i.$$

The effective signal from the i -th transmitter is given by

$$P_i^{(E)} = \mathbb{E}\{\|\sqrt{\rho_i} \mathbf{h}_{ii}^T \mathbf{x}_i\|^2\} = \mathbf{w}_i^H \rho_i \mathbf{h}_{ii}^* \mathbf{h}_{ii}^T \mathbf{w}_i$$

The SLNR maximization problem of the i -th transmitter is then formulated as

$$\begin{aligned} \max_{\mathbf{w}_i} \quad & \frac{P_i^{(E)}}{P_i^{(L)} + (\beta + 1)\sigma_n^2} \\ \text{s.t.} \quad & \mathbf{w}_i^H \mathbf{w}_i \leq P_{\max}, \end{aligned} \quad (9.4)$$

where the noise variance is the enhanced noise power in equation (9.3). Clearly, the constraint in (9.4) is satisfied with equality at the optimality. Inserting $\mathbf{w}_i^H \mathbf{w}_i = P_{\max}$ into the cost function of (9.4), it can be rewritten as the following unconstrained optimization problem

$$\max_{\|\mathbf{w}_i\|^2 = P_{\max}} \frac{\mathbf{w}_i^H \mathbf{A}_i \mathbf{w}_i}{\mathbf{w}_i^H \mathbf{B}_i \mathbf{w}_i}, \quad (9.5)$$

where $\mathbf{A}_i = \rho_i \mathbf{h}_{ii}^* \mathbf{h}_{ii}^T$ and $\mathbf{B}_i = \kappa \eta_j \text{Diag}\{\mathbf{h}_{ji}^* \mathbf{h}_{ji}^T\} + \beta \eta_j \mathbf{h}_{ji}^* \mathbf{h}_{ji}^T + \frac{(\beta+1)\sigma_n^2}{P_{\max}} \mathbf{I}_N$.

Problem (9.5) has the structure of a generalized Rayleigh quotient. Thus, the optimal value is the dominant eigenvalue of the matrix $\mathbf{B}_i^{-1} \mathbf{A}_i$ and the optimal $\mathbf{w}_{\text{opt},i}$ is a scaled version

of the corresponding eigenvector, i.e., $\mathbf{w}_{\text{opt},i} = \sqrt{P_{\text{max}}} \cdot \mathcal{P}(\mathbf{B}_i^{-1}\mathbf{A}_i)$, where $\mathcal{P}(\cdot)$ computes the dominant eigenvector of a Hermitain matrix.

Obviously, the SLNR based design avoids the joint optimization of the two beamforming vectors. Moreover, if the suppressible SI is supposed to be canceled at the transmitter instead of the receiver, the SLNR based design can be combined with a ZF schemes. By ZF we mean that the i -th transmitter uses the beamformer \mathbf{w}_i to transmit in the null space of the SI channel \mathbf{h}_{ji}^T . More specifically, we have

$$\mathbf{w}_i = \mathbf{\Pi}_{\mathbf{h}_{ji}^T}^\perp \bar{\mathbf{w}}_i, \quad (9.6)$$

where $\mathbf{\Pi}_{\mathbf{h}_{ji}^T}^\perp$ is the projection matrix which projects any vector onto the null space of \mathbf{h}_{ji}^T (which corresponds to the left null space of \mathbf{h}_{ji}). The orthogonal complement of the subspace spanned by \mathbf{h}_{ji}^T is a candidate of $\mathbf{\Pi}_{\mathbf{h}_{ji}^T}^\perp$ and is calculated by $\mathbf{\Pi}_{\mathbf{h}_{ji}^T}^\perp = \mathbf{I}_N - \frac{\mathbf{h}_{ji}^* \mathbf{h}_{ji}^T}{\|\mathbf{h}_{ji}\|^2}$.

The ZF design ensures that the suppressible interference in (9.1) vanishes, i.e., $\mathbf{h}_{ji}^T \mathbf{x}_i = 0$. Afterwards, we can insert (9.6) into (9.4). This does not change the problem and therefore a closed-form solution is still obtained. The drawback is that the ZF scheme sacrifices the degrees of freedom in the spatial domain. Therefore, if the number of antennas at the transmitter is not large enough, the performance degrades compared to the original SLNR based design.

9.3.2 MIMO

For the MIMO setup we consider the case where $M_r = M_t$. We again develop the transmit strategy which maximizes the ratio between the efficient signal power and the leakage plus noise. Unlike the MISO case, per-antenna signal leakage exists in the MIMO case. For simplicity, we choose the total SLNR as the design criterion. That is, we maximize the ratio between the sum of received signal power per-antenna and the sum of leakage plus noise power per antenna. Thereby, the total power leaked from the i -th transmitter to the j -th receiver is given by

$$\begin{aligned} P_i^{(L)} &= \mathbb{E}\{\|\sqrt{\eta_j} \mathbf{H}_{ji} \mathbf{e}_i^t\|^2\} + \beta \text{Diag}\{\mathbb{E}\{\|\sqrt{\eta_j} \mathbf{H}_{ji} \mathbf{x}_i\|^2\}\} \\ &= \text{Tr}\{\kappa \eta_j \mathbf{H}_{ji} \text{Diag}\{\mathbf{Q}_i\} \mathbf{H}_{ji}^H\} + \text{Tr}\{\beta \eta_j \text{Diag}\{\mathbf{H}_{ji} \mathbf{Q}_i \mathbf{H}_{ji}^H\}\}. \end{aligned} \quad (9.7)$$

The received signal power is computed as

$$P_i^{(E)} = \mathbb{E}\{\|\sqrt{\eta_j} \mathbf{H}_{ii} \mathbf{x}_i^t\|^2\} = \text{Tr}\{\rho_i \mathbf{H}_{ii} \mathbf{Q}_i \mathbf{H}_{ii}^H\}. \quad (9.8)$$

Our goal is to find optimal \mathbf{Q}_i such that the SLNR is maximized given the transmit power constraint. Mathematically, the optimization problem is formulated as

$$\begin{aligned} \max_{\mathbf{Q}_i} \quad & \frac{P_i^{(E)}}{P_i^{(L)} + (\beta + 1)M_r\sigma_n^2} \\ \text{s.t.} \quad & \text{Tr}\{\mathbf{Q}_i\} \leq P_{\max} \end{aligned} \quad (9.9)$$

To solve problem (9.9), further algebraic manipulation is required. Let us define the SVD of \mathbf{H}_{ji} as $\mathbf{H}_{ji} = \mathbf{U}_i\mathbf{T}_i\mathbf{V}_i^H$. Without loss of generality, we decompose the transmit covariance matrix $\mathbf{Q}_i \in \mathbb{C}^{M_t \times M_t}$ as

$$\mathbf{Q}_i = \mathbf{V}_i\boldsymbol{\Sigma}_i\boldsymbol{\Sigma}_i^H\mathbf{V}_i^H \quad (9.10)$$

where $\boldsymbol{\Sigma}_i \in \mathbb{C}^{M_t \times M_t}$ is a diagonal matrix and $\mathbf{W}_i = \mathbf{V}_i\boldsymbol{\Sigma}_i \in \mathbb{C}^{M_t \times M_t}$ is the precoding matrix applied at the i -th transmitter.

Using (9.10), equation (9.7) can be further expanded as

$$\begin{aligned} P_i^{(L)} &= \text{Tr}\{\beta\eta_j\text{Diag}\{\mathbf{H}_{ji}\mathbf{Q}_i\mathbf{H}_{ji}^H\}\} + \text{Tr}\{\kappa\eta_j\mathbf{H}_{ji}\text{Diag}\{\mathbf{Q}_i\}\mathbf{H}_{ji}^H\} \\ &= \boldsymbol{\sigma}_i^H\text{Diag}\{\beta\eta_j\mathbf{V}_i^H\mathbf{H}_{ji}^H\mathbf{H}_{ji}\mathbf{V}_i\}\boldsymbol{\sigma}_i + \boldsymbol{\sigma}_i^H\kappa\eta_j\text{Diag}\{\mathbf{1}^T \cdot (\mathbf{H}_{ji} \odot \mathbf{H}_{ji}^*) \cdot (\mathbf{V}_i \odot \mathbf{V}_i^*)\}\boldsymbol{\sigma}_i \\ &= \boldsymbol{\sigma}_i^H\left(\kappa\eta_j\text{Diag}\{\mathbf{1}^T \cdot (\mathbf{H}_{ji} \odot \mathbf{H}_{ji}^*) \cdot (\mathbf{V}_i \odot \mathbf{V}_i^*)\} + \text{Diag}\{\beta\eta_j\mathbf{V}_i^H\mathbf{H}_{ji}^H\mathbf{H}_{ji}\mathbf{V}_i\}\right)\boldsymbol{\sigma}_i \end{aligned} \quad (9.11)$$

where $\boldsymbol{\sigma}_i = \text{diag}\{\boldsymbol{\Sigma}_i\}$, and the facts that $\text{diag}\{\mathbf{X} \cdot \text{Diag}\{\mathbf{Y}\} \cdot \mathbf{X}^H\} = (\mathbf{X} \odot \mathbf{X}^*) \cdot \text{diag}\{\mathbf{Y}\}$ ¹ and $\mathbf{1}^T \cdot \text{diag}\{\mathbf{X}\} = \text{Tr}\{\mathbf{X}\}$ are used in the derivation.

Similarly, the received signal power $P_i^{(E)}$ is rewritten as

$$\begin{aligned} P_i^{(E)} &= \text{Tr}\{\rho_i\mathbf{H}_{ii}\mathbf{V}_i\boldsymbol{\Sigma}_i\boldsymbol{\Sigma}_i^H\mathbf{V}_i^H\mathbf{H}_{ii}^H\} = \text{Tr}\{\rho_i\boldsymbol{\Sigma}_i^H\mathbf{V}_i^H\mathbf{H}_{ii}^H\mathbf{H}_{ii}\mathbf{V}_i\boldsymbol{\Sigma}_i\} \\ &= \boldsymbol{\sigma}_i^H\text{Diag}\{\rho_i\mathbf{V}_i^H\mathbf{H}_{ii}^H\mathbf{H}_{ii}\mathbf{V}_i\}\boldsymbol{\sigma}_i. \end{aligned} \quad (9.12)$$

Applying (9.11) and (9.12), the original problem (9.9) is reformulated as

$$\begin{aligned} \max_{\boldsymbol{\sigma}_i} \quad & \frac{\boldsymbol{\sigma}_i^H\boldsymbol{\Gamma}_i\boldsymbol{\sigma}_i}{\boldsymbol{\sigma}_i^H\boldsymbol{\Theta}_i\boldsymbol{\sigma}_i + (\beta + 1)M_r\sigma_n^2} \\ \text{s.t.} \quad & \boldsymbol{\sigma}_i^H\boldsymbol{\sigma}_i \leq P_{\max} \end{aligned} \quad (9.13)$$

where $\boldsymbol{\Theta}_i = \kappa\eta_j\text{Diag}\{\mathbf{1}^T \cdot (\mathbf{H}_{ji} \odot \mathbf{H}_{ji}^*) \cdot (\mathbf{V}_i \odot \mathbf{V}_i^*)\} + \beta\eta_j\text{Diag}\{\mathbf{V}_i^H\mathbf{H}_{ji}^H\mathbf{H}_{ji}\mathbf{V}_i\}$ and we have $\boldsymbol{\Gamma}_i = \text{Diag}\{\rho_i\mathbf{V}_i^H\mathbf{H}_{ii}^H\mathbf{H}_{ii}\mathbf{V}_i\}$. Clearly, at the optimality of problem (9.13) the constraint has

¹It can be easily verified that: $[\text{diag}\{\mathbf{X} \cdot \text{Diag}\{\mathbf{Y}\} \cdot \mathbf{X}^H\}]_i = [(\mathbf{X} \odot \mathbf{X}^*) \cdot \text{diag}\{\mathbf{Y}\}]_i = \sum_{j=1}^{M_r} |[\mathbf{X}]_{i,j}|^2 \cdot [\mathbf{Y}]_{j,j}$.

to be satisfied with equality. Inserting $\boldsymbol{\sigma}_i^H \boldsymbol{\sigma}_i = P_{\max}$ into the objective function, we get the following unconstrained optimization problem

$$\max_{\|\boldsymbol{\sigma}_i\|^2=P_{\max}} \frac{\boldsymbol{\sigma}_i^H \boldsymbol{\Gamma}_i \boldsymbol{\sigma}_i}{\boldsymbol{\sigma}_i^H \left(\boldsymbol{\Theta}_i + \frac{(\beta+1)M_r \sigma_n^2}{P_{\max}} \mathbf{I}_N \right) \boldsymbol{\sigma}_i}. \quad (9.14)$$

Problem (9.14) is a generalized Rayleigh quotient problem. Therefore, the solution is given by

$$\boldsymbol{\sigma}_{\text{opt},i} = \sqrt{P_{\max}} \cdot \mathcal{P} \left(\left(\boldsymbol{\Theta}_i + \frac{(\beta+1)M_r \sigma_n^2}{P_{\max}} \mathbf{I}_N \right)^{-1} \boldsymbol{\Gamma}_i \right)$$

Finally, the optimal precoding matrix \mathbf{W}_i is obtained as $\mathbf{W}_i = \mathbf{V}_i \text{diag}\{\boldsymbol{\sigma}_{\text{opt},i}\}$.

9.4 Power adjustment for performance improvement

As an alternative to the precoding techniques in Section 9.3, one can always reduce the imposed SI at the receiver by correctly controlling the transmit power at the transmitter. In the following, we find the optimum power allocations that either maximize the system sum rate or maximize the minimum SINR at the two receivers, assuming that the transmit covariance matrices have been determined, e.g., using the results of Section 9.3.2.

9.4.1 SISO and MISO setting

Since the SISO and the MISO setup yield the same mathematical problem, we solve the MISO case in this part and the results can be directly applied to the SISO scenario. Given a fixed transmit covariance matrix, i.e., $\mathbf{Q}_i = P_i \mathbf{Q}_{i,\text{fix}}$, the sum rate maximization problem is formulated as

$$\max_{P_i, i \in \{1,2\}} R_{\text{sum}} = \sum_{i=1}^2 \log_2(1 + \text{SINR}_i), \quad \text{s.t.} \quad P_i \leq P_{\max}, \quad \forall i \in \{1,2\}, \quad (9.15)$$

where SINR_i is the SINR at the i -th receiver. Applying the fact that $\beta \ll 1$, the SINR_i is computed as

$$\text{SINR}_i = \frac{\mathbb{E}\{|\sqrt{\rho_i} \mathbf{h}_{ii}^T x_i|^2\}}{\mathbb{E}\{|\sqrt{\rho_i} \mathbf{h}_{ii}^T e_i^t|^2\} + \mathbb{E}\{|\sqrt{\eta_i} \mathbf{h}_{ij}^T e_j^t|^2\} + \mathbb{E}\{|e_i^r|^2\} + \sigma_n^2} \approx \frac{P_i a_i}{P_i b_i + P_j c_i + \sigma_n^2} \quad (9.16)$$

where a_i , b_i , and c_i are computed by $a_i = \rho_i \mathbf{h}_{ii}^T \mathbf{Q}_{i,\text{fix}} \mathbf{h}_{ii}^*$, $b_i = \kappa \rho_i \mathbf{h}_{ii}^T \text{Diag}\{\mathbf{Q}_{i,\text{fix}}\} \mathbf{h}_{ii}^* + \beta \rho_i \mathbf{h}_{ii}^T \mathbf{Q}_{i,\text{fix}} \mathbf{h}_{ii}^*$, and $c_i = \kappa \eta_i \mathbf{h}_{ij}^T \text{Diag}\{\mathbf{Q}_{j,\text{fix}}\} \mathbf{h}_{ij}^* + \beta \eta_i \mathbf{h}_{ij}^T \mathbf{Q}_{j,\text{fix}} \mathbf{h}_{ij}^*$.

Clearly, problem (9.15) is non-convex. To solve it, we notice that at least one of the constraints is satisfied with equality at the optimality, i.e., $P_1 = P_{\max}$ or $P_2 = P_{\max}$. Otherwise, we can always scale up P_1 and P_2 using the same scaling factor. This increases the optimal value of (9.15) and thus contradicts the optimality assumption. Exploiting this fact, we can relax problem (9.15) into two sub-problems: i) $P_2 = P_{\max}$, ii) $P_1 = P_{\max}$. Then we solve each sub-problem individually. Finally the optimal value is the largest optimal value of the sub-problems and the corresponding solution is the optimal solution. Since case i) and case ii) are symmetric, we take case i) as an example. The objective function of (9.15) is reformulated as:

$$R_{\text{sum}} = \log_2 \left(1 + \frac{P_1 a_1}{P_1 b_1 + P_{\max} c_1 + \sigma_n^2} \right) + \log_2 \left(1 + \frac{P_{\max} a_2}{P_{\max} b_2 + P_1 c_2 + \sigma_n^2} \right). \quad (9.17)$$

Equation (9.17) can be further simplified if we consider that in practice the SI channel is much stronger than the desired channel, i.e., $\rho_i \ll \eta_i$ and therefore $b_i \approx 0$, $\forall i$. Nevertheless, the resulting optimization problem is still non-convex. We calculate the first-order necessary condition for optimality of the resulting problem by taking the derivative with respect to P_1 and set it to zero. Then we get

$$\frac{\partial R_{\text{sum}}}{\partial P_1} = \frac{1}{\log_2} \left(\frac{f_2}{P_1 a_1 + f_2} \cdot \frac{a_1}{f_2} + \frac{\sigma_n^2 + P_1 c_2}{\sigma_n^2 + P_1 c_2 + f_1} \cdot \frac{-c_2 f_1}{(P_1 c_2 + (\beta + 1) \sigma_n^2)^2} \right) = 0.$$

where $f_1 = P_{\max} a_2$ and $f_2 = P_{\max} c_1 + \sigma_n^2$. After some algebraic manipulation, the following second-order polynomial function is obtained

$$P_1^2 k_1 + P_1 k_2 + k_3 = 0 \quad (9.18)$$

where $k_1 = a_1 c_2^2$, $k_2 = 2a_1 c_2 \sigma_n^2$, and $k_3 = a_1 \sigma_n^4 + a_1 f_1 \sigma_n^2 - f_1 f_2 c_2$.

In the following we show that regardless of the solution to equation (9.18) the optimal solution to problem (9.17) is either $P_1 = 0$ or $P_1 = P_{\max}$.

If the roots of equation (9.18) are complex, it is straightforward to conclude that the optimum P_1 must be at the boundary of the feasible region $[0, P_{\max}]$. If the roots of equation (9.18) are real, they are given by $P_{1,\text{root}} = \frac{-k_2 \pm \sqrt{k_2^2 - 4k_1 k_3}}{2k_1}$. Clearly, the negative root cannot be a valid solution. Moreover, the positive root is a minimum of the objective function (9.17). This conclusion is based on the following statements.

1. The cost function (9.17) is continuous. As $P_1 \rightarrow +\infty$, $R_{\text{sum}} \rightarrow +\infty$.
2. Function (9.18) has only two roots and one of them is negative. The feasible region of

our problem is $P_1 \in [0, P_{\max}]$.

Similar results can be derived for case ii). Thereby, the optimal solution of problem (9.15) should be chosen from the following three choices, i.e., i) $P_1 = 0, P_2 = P_{\max}$; ii) $P_1 = P_{\max}, P_2 = 0$; iii) $P_1 = P_2 = P_{\max}$.

9.4.2 MIMO setting

For the MIMO setup, we again follow the same target, i.e., adjusting the devices' transmit power so that a better system performance is obtained. To avoid dealing with the complicated logarithmic formulation of the channel capacity, we look for a solution which maximizes the sum of the total SINR of our system. Hence our initial problem is formulated as:

$$\max_{P_i, i \in \{1,2\}} \sum_{i=1}^2 \text{SINR}_i, \quad \text{s.t.} \quad P_i \leq P_{\max}, \quad \forall i \in \{1,2\}, \quad (9.19)$$

where SINR_i stands for the total SINR at the i -th receiver which is defined as ratio between the sum of the received signal power per antenna and the sum of the interference plus noise power per antenna. Similarly to the MISO case, we use the fact that $\beta \ll 1$. Furthermore, we define $\mathbf{Q}_i = P_i \mathbf{Q}_{i,\text{fix}}$ and define three auxiliary constants $a_i = \text{Tr}\{\rho_i \mathbf{H}_{ii} \mathbf{Q}_{i,\text{fix}} \mathbf{H}_{ii}^H\}$, $b_i = \text{Tr}\{\kappa \rho_i \mathbf{H}_{ii} \text{Diag}\{\mathbf{Q}_{i,\text{fix}}\} \mathbf{H}_{ii}^H + \beta \rho_i \mathbf{H}_{ii} \mathbf{Q}_{i,\text{fix}} \mathbf{H}_{ii}^H\}$, and $c_i = \text{Tr}\{\kappa \eta_i \mathbf{H}_{ij} \text{Diag}\{\mathbf{Q}_{j,\text{fix}}\} \mathbf{H}_{ij}^H + \beta \eta_i \mathbf{H}_{ij} \mathbf{Q}_{j,\text{fix}} \mathbf{H}_{ij}^H\}$. Then the sum of the total SINR of our system is expressed as

$$\sum_{i=1}^2 \text{SINR}_i \approx \frac{P_1 a_1}{P_1 b_1 + P_2 c_1 + \sigma_n^2} + \frac{P_2 a_2}{P_2 b_2 + P_1 c_2 + \sigma_n^2}. \quad (9.20)$$

Once again, we can conclude that at least one of the transmit powers has to be equal to P_{\max} at the optimality. Thereby, assuming that $P_1 = P_{\max}$, our original problem is reformulated into

$$\max_{P_2} \sum_{i=1}^2 \text{SINR}_i, \quad \text{s.t.} \quad P_2 \leq P_{\max}, \quad \forall i \in \{1,2\}. \quad (9.21)$$

Using the fact that $\rho_i \ll \eta_i$ and thus $b_i \approx 0$, the objective function now becomes

$$\sum_{i=1}^2 \text{SINR}_i \approx \frac{P_{\max} a_1}{P_2 c_1 + M_r \sigma_n^2} + \frac{P_2 c_2}{P_{\max} c_2 + M_r \sigma_n^2}. \quad (9.22)$$

By computing the first-order necessary condition for optimality we get

$$\frac{\partial \sum_{i=1}^2 \text{SINR}_i}{\partial P_2} = \frac{-c_1 a_1 P_{\max}}{(P_2 c_1 + M_r \sigma_n^2)^2} + \frac{c_2}{P_{\max} c_2 + M_r \sigma_n^2} = 0. \quad (9.23)$$

As for the MISO case, we can conclude that the solution of (9.23) is given by $P_2 = 0$ or P_{\max} if the roots of (9.23) are complex-valued. If the roots of (9.23) are real-valued, they are obtained as $P_{2,\text{root}} = \frac{-M_r\sigma_n^2 \pm \sqrt{\frac{k_4}{k_5}}}{c_1}$, where $k_4 = \frac{a_2}{P_{\max}c_2 + M_r\sigma_n^2}$ and $k_5 = P_{\max}a_1c_1$. Following the same arguments as in the MISO case, the optimal solution is one of the following possible solutions: i) $P_1 = 0, P_2 = P_{\max}$; ii) $P_1 = P_{\max}, P_2 = 0$; iii) $P_1 = P_2 = P_{\max}$.

9.4.3 Power adjustment for max-min fairness

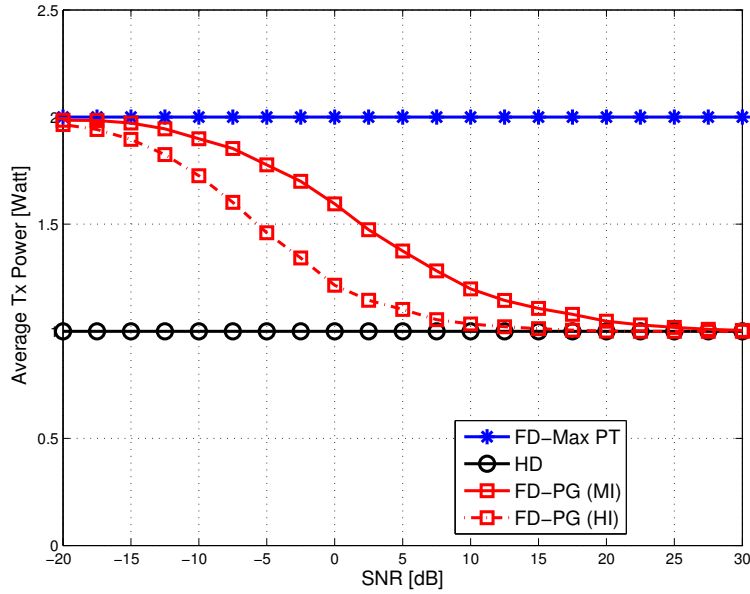


Figure 9.2: Average consumed power in a SISO FD system using power adjustment schemes in 9.4.1 and $P_{\max} = 1$ W. Max PT: full power transmission. MI: medium interference environment in Section 9.5. HI: high interference environment in Section 9.5.

Although the power adjustment schemes in Sections 9.4.1 and 9.4.2 maximize the achievable sum rate of the system, these are greedy algorithms which do not take into account the fairness between two transceivers. In fact, if the final solution in Sections 9.4.1 and 9.4.2 is given by the choice i) or ii), one of the receivers will have zero throughput and thus its QoS is not guaranteed. The simulation results in Figure 9.2 have also shown that this is likely to happen in the high SNR regime where the interference is dominant. Thus, instead of the sum rate criterion, one may consider the system design criterion which takes care of the QoS requirements. In the following, we develop such a power adjustment strategy which maximizes the minimum SINR

at the receiver. Utilizing the SINR definition for MISO and SISO setups in Section 9.4.1 and the total SINR for the MIMO setup in Section 9.4.2, we can develop a unified framework for achieving the max-min fairness.

Taking the MISO case as an example, we aim at solving the following max-min problem.

$$\max_{P_i, i \in \{1,2\}} \min_{P_i, i \in \{1,2\}} \text{SINR}_i, \quad \text{s.t.} \quad P_i \leq P_{\max}, \quad \forall i \in \{1,2\} \quad (9.24)$$

or equivalently

$$\max_{t, P_i, i \in \{1,2\}} t, \quad \text{s.t.} \quad \text{SINR}_i \geq t, \quad P_i \leq P_{\max}, \quad \forall i \in \{1,2\}. \quad (9.25)$$

To efficiently solve this problem, we need more insights. First, we find that $\text{SINR}_i = t, \forall i$ at the optimality. To see this, without loss of generality, we assume that $\text{SINR}_1 > \text{SINR}_2$ at the optimality. Then by decreasing P_1 we can decrease SINR_1 while SINR_2 increases. This will not violate the transmit power constraints. But it will increase the optimal value and thus contradicts the optimality. Second, at least one of the transmit power constraints is satisfied with equality at the optimality. Otherwise, we can still scale up P_1 and P_2 with the same scaling factor $\alpha > 1$. This will again increase the optimal value and thus contradicts the optimality. Finally, the optimization problem (9.25) can be split into the following sub-problems

1. $P_1 = P_{\max}, \text{SINR}_1 = \text{SINR}_2$
2. $P_2 = P_{\max}, \text{SINR}_1 = \text{SINR}_2$
3. $P_1 = P_2 = P_{\max}, \text{SINR}_1 = \text{SINR}_2$

The optimal solution will be the power pair (P_1, P_2) which is feasible and also provides the largest minimum SINR. When solving the three sub-problems, we find that the optimization problem can be further simplified. To illustrate this, we start by validating sub-problem 3. Inserting $P_1 = P_2 = P_{\max}$ into the SINR formulation (9.16), if $\text{SINR}_1 = \text{SINR}_2$, then $P_1 = P_2 = P_{\max}$ is the optimal solution. Otherwise, if $\text{SINR}_1 > \text{SINR}_2$, then the optimal solution is given by the solution of sub-problem 2. This is because decreasing P_1 while fixing $P_2 = P_{\max}$ will increase SINR_2 and also increase the optimal value. But decreasing P_2 while fixing $P_1 = P_{\max}$ will decrease SINR_2 and thus decrease the optimal value. Similarly, if $\text{SINR}_1 < \text{SINR}_2$, then the optimal solution is given by the solution of sub-problem 1.

Remark 12. The proposed power adjustment schemes can be combined with precoding techniques to further improve the system performance for MISO and MIMO setups. When SLNR

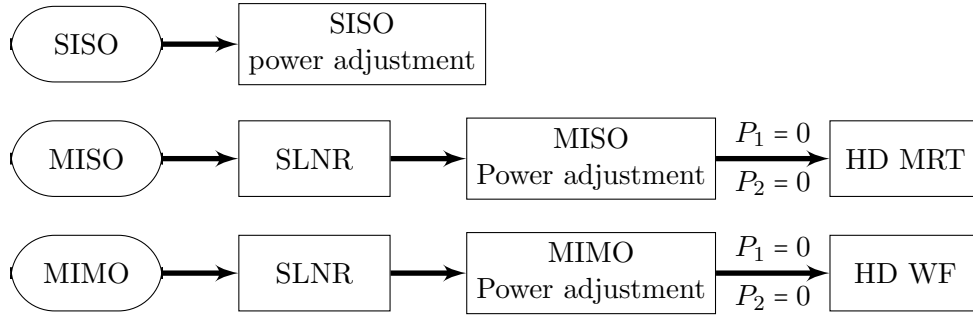


Figure 9.3: The proposed beamforming and power adjustment schemes selection procedure for achieving a higher sum rate.

transmit strategies are applied and $P_1 = 0$ or $P_2 = 0$ is obtained as the power adjustment solution to the sum rate maximization problem, the FD system reduces to a HD system. In such a situation the conventional HD transmit strategies together with the previous power adjustment solution will achieve a higher sum rate than the proposed SLNR techniques. The proposed beamforming and power adjustment selection procedures are shown in Figure 9.3.

9.5 Simulation results

In this section the proposed algorithms are verified using Monte Carlo simulations. The generated channels are uncorrelated Rayleigh flat fading channels and all the simulation results are averaged over 1000 channel realizations. The transmit power is set to unity and the SNR is given by $1/\sigma_n^2$. Moreover, we have the following parameter settings: i) $\rho_1 = 0$ dB, $\rho_2 = 0$ dB, $\eta_1 = 60$ dB, $\eta_2 = 60$ dB, $\beta = -65$ dB, $\kappa = -65$ dB, which represent an environment with less significant insuppressible SI (medium interference (MI) scenario). ii) $\rho_1 = 0$ dB, $\rho_2 = 0$ dB, $\eta_1 = 60$ dB, $\eta_2 = 60$ dB, $\beta = -60$ dB, $\kappa = -60$ dB, which represent an environment with intensive insuppressible SI (high interference (HI) scenario). We compare the performance of the proposed schemes with conventional capacity achieving HD transmit strategies where the residual interference is treated as noise. We also compare the system performance to the capacity of a HD baseline scenario where each transceiver has identical system settings as in our FD system but works in a TDD mode. “PG” denotes the power adjustment for sum rate maximization while “PF” denotes the power adjustment for max-min fairness. “Best Sel” denotes the best combination of the proposed power adjustment schemes and the beamforming techniques which achieves the highest sum rate.

Figure 9.4 shows how our power adjustment technique helps a SISO FD system to achieve

a higher system sum rate. Clearly, the proposed power adjustment technique has achieved a substantial gain over the traditional full power transmission scheme. Moreover, the proposed scheme is robust to the residual interference.

Figure 9.5 demonstrates the comparison of different algorithms in a MISO setup when $M_t = 4$. In both the MI and the HI scenario the proposed SLNR methods outperforms the classical transmit strategies such as ZF and MRT. When combining SLNR with the “PG” power adjustment technique, a larger gain can be obtained. Moreover, if the “PG” scheme is applied together with ZF and MRT schemes, a substantial gain is also obtained especially in the high SNR regime. When the residual interference is relatively high, the ZF scheme obtains the same performance as the SLNR method in the high SNR regime.

Figure 9.6 depicts the performance of the proposed techniques compared to the WF algorithm for a 2-by-2 MIMO FD system in the presence of high and medium residual interference. Similar results are observed as in the MISO case. The proposed SLNR method outperforms the WF method. When combining with the greedy power adjustment scheme “PG”, the proposed precoder selection scheme outperforms the HD baseline scenario, which makes a FD system more valuable. Furthermore, when applying the greedy power adjustment scheme to the WF method, a significant gain is obtained.

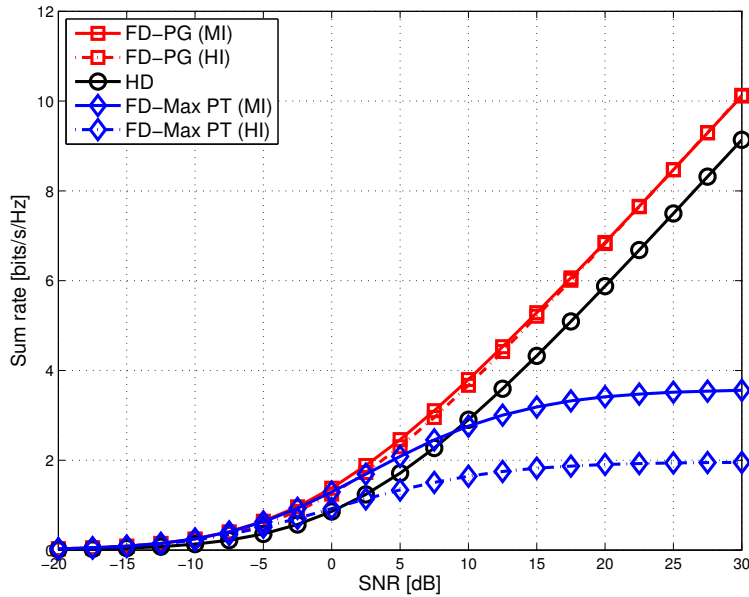


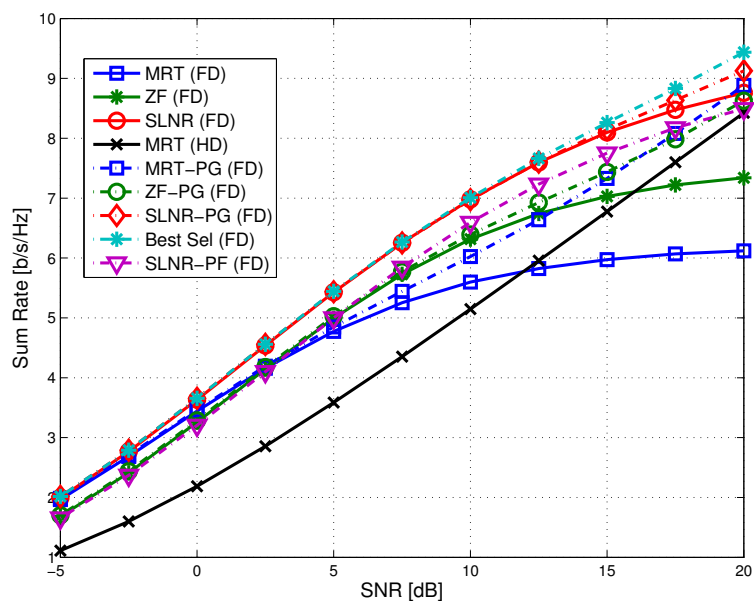
Figure 9.4: Comparison of different algorithms in a SISO setup. Max PT: full power transmission. MI: medium interference. HI: high interference.

9.6 Summary

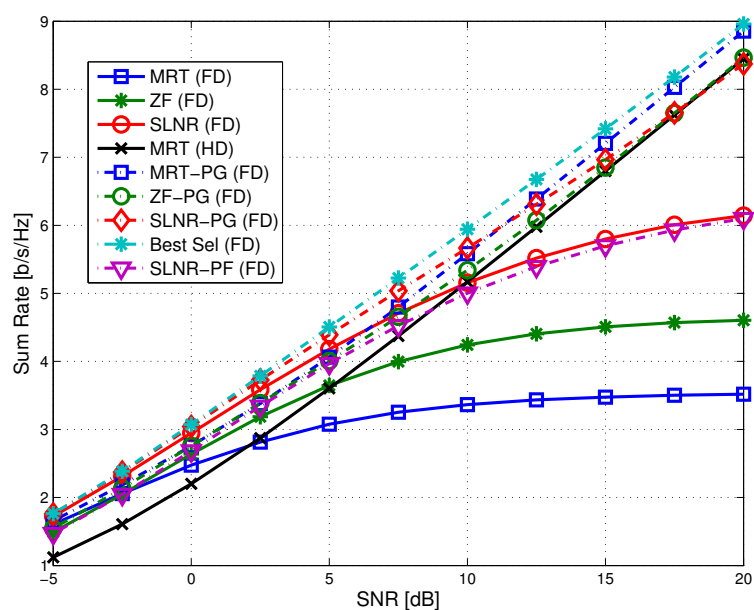
In this chapter we have studied a FD P2P system with imperfect RF chain. This residual SI dominates the system performance and prevents us from fully exploiting the advantage of a FD system. To combat the residual SI we have developed SLNR based precoding algorithms for MISO and MIMO setups. Moreover, noticing that power adjustment schemes can also be used to alleviate the effects of the residual interference, we have developed power adjustment schemes which maximize the system sum rate or maximize the minimum SINR in the system. The developed power adjustment schemes can also be combined with the SLNR based precoding algorithms to further improve the system performance.

Simulation results have demonstrated that

- The proposed transmit schemes have much better performance compared to the conventional HD transmit strategies when applied to FD systems.
- When the proposed SLNR beamforming is used, it outperforms the HD baseline scenario in the low to medium SNR regime. But it saturates in the high SNR regime due to the insuppressible SI. When combined with power adjustment schemes, which maximize the system sum rate, it always outperforms the HD baseline scenario. This is because the optimal power adjustment schemes switch a FD system to a HD system and thus the SI is avoided.

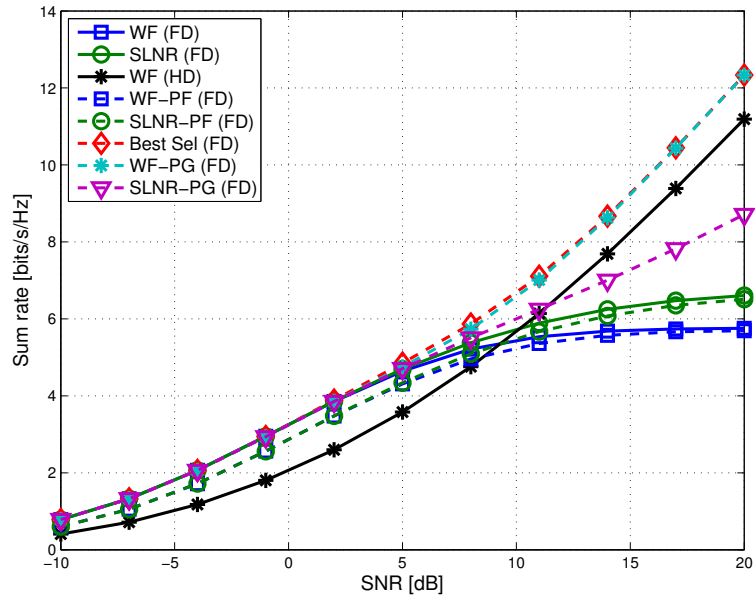


(a) MI: medium interference.

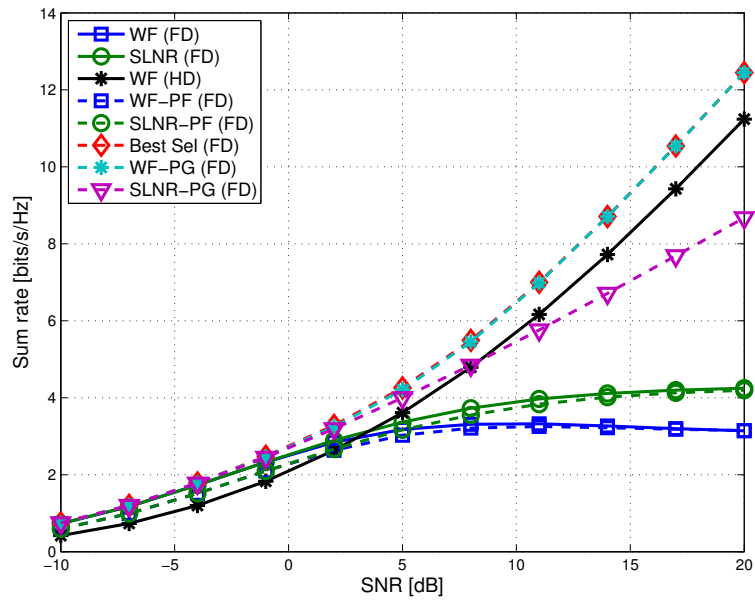


(b) HI: high interference.

Figure 9.5: Comparison of different algorithms in a MISO setup where $M_t = 4$. ZF: zero forcing technique



(a) MI: medium interference.



(b) HI: high interference.

Figure 9.6: Comparison of different algorithms in a MIMO setup where $M_r = M_t = 2$.

10 Summary of full-duplex wireless communication systems

10.1 Summary of contributions

This part of the thesis discusses transmit strategies for a MIMO FD P2P system with limited dynamic range. Our major contributions can be summarized as:

- The SI aware transmit strategies have been proposed [ZTLH12]. The SI aware transmit strategies can be combined with other-types of SI cancellation techniques to improve the reliability and the performance a FD system.
- Optimal SI aware transmit strategies, which maximizes the system sum rate of a MIMO FD P2P system, have been derived [ZTLH12]. When both the transmitter and the receiver have multiple antennas, i.e., the MIMO setup, the optimization problem is convex and thus a global optimal solution can be obtained. By analyzing whether the constraints are active at the optimality, a closed-form solution is obtained for the case of 2-by-2 MIMO. For MISO setup, the optimization problem is non-convex. However, the global optimal solution can still be obtained by using the SDR technique. Moreover, analytic solutions are derived.
- A robust transmit strategy has been developed to combat the imperfect CSI at the transmitter [ZTH13b]. The channel estimation errors are modeled as deterministic errors, which are bounded by ellipsoids. An optimization problem, which minimizes the total required transmit power of the system subject to total SINR constraints and SI power constraints, is formulated and solved. The same methodology can be used to develop robust transmit strategies subject to other system criteria of a FD system.
- Efficient transmit strategies for a FD system with imperfect RF chain have been developed [ZTH13c]. The SLNR based beamformer design for MISO and MIMO setup provides closed-form solutions, which can preserve a FD gain even when the residual SI is strong. When combined with power adjustment schemes and hybrid operation modes (switch between HD mode and FD mode), a FD gain (in terms of system sum rate) up to two-fold is always achieved regardless the strength of the residual SI.

More related contributions that are not explicitly discussed in this thesis but worth mentioning are:

- The SI aware transmit strategies are extended to the OWR system with a MIMO AF relay [ZTH13a] [TZH14]. Although analytic solutions cannot be obtained for such a scenario, convex optimization based techniques and gradient projection based techniques have been developed to exploit the advantages of a FD system.

10.2 Future work

The study of FD MIMO systems with limited dynamic range has opened up the following research areas.

- The fundamental limits of SI aware transmit strategies are worth investigating. Optimal SI aware transmit strategies for other system design criteria, e.g., max-min fairness, power minimization can be developed. In the MIMO case we consider only the average sum SI power constraint, which might be not practical since a per-antenna power constraint and instantaneous power constraints are more realistic. Moreover, receive-side beamforming assisted SI cancellation techniques or joint SI aware transmit and receive beamforming techniques are still not well studied. Furthermore, adaptive techniques should be developed for time-variant channels.
- Many SI cancellation techniques require channel knowledge of the SI channel. First, the characteristics of the SI channel is still unclear. Although the channel is more likely to be Rician fading channel or even line-of-sight (LOS) channel, it has to be investigated, e.g., via physical measurements and modeling. Second, the training phase, which is devoted to channel estimation, will also suffer from the SI. Therefore, efficient and/or optimal training protocols for FD systems should be studied. Moreover, it is interesting to know how to calibrate the RF chains of a FD system such that the reciprocity holds for the uplink and the downlink channel. Finally, robust transmit strategies subject to different system utility functions should be investigated.
- System level performance is always important for new physical layer techniques such as FD wireless communications. For example, in a MU-MIMO system, if the BS operates in a FD mode, it can serve the downlink users and the uplink users at the same time and on the same frequency. Precoding algorithms which can maximize the system throughput in such a scenario are worth investigating. Moreover, cross-layer designs, such as joint

user scheduling and precoder design, should be studied for a further improvement user experiences.

Part III

Conclusions and Outlook

11 Conclusions

In this thesis, we develop signal processing algorithms for two different class of wireless techniques, namely, two-way relaying (TWR) techniques and full-duplex (FD) techniques. The goal is to find the fundamental limits and to exploit the benefits of these two techniques for different wireless communication scenarios. As we show, optimal and suboptimal linear transmit strategies are developed subject to different system utility functions.

In the first part of the thesis we discuss multi-pair/multi-user TWR networks with AF relays. First, we have introduced the projection based separation of multiple operators (ProBaSeMO) scheme [ZRH12b] to accomplish the relay-assisted resource sharing in a multi-operator relaying network with a MIMO AF relay. Compared to a TDMA manner of the relay and the spectrum sharing, which is an orthogonal resource sharing schemes, the ProBaSeMO scheme is a non-orthogonal resource sharing scheme, where the interference-free transmission of different operators is achieved via orthogonal spatial domains. It is shown that the non-orthogonal resource sharing scheme is superior compared to the orthogonal one especially when there are many antennas at the relay and/or the noise power is weak. We also study the sum rate maximization problem of the considered scenario. Gradient based solutions have been developed regardless whether the user terminals (UTs) have single or multiple antennas. When each UT has a single antenna, a polynomial time solution, which is inspired by the polynomial-time DC (POTDC) algorithm, has been developed [ZVKH13], which performs close to the gradient based solution but yields a polynomial-time complexity. Since QoS criteria, such as minimizing the transmit power at the relay under guaranteed QoS or maximizing the minimum achievable SINR of each UT, are also important performance metrics for a modern wireless communication system. We have also developed optimal linear transmit strategies to achieve these goals [ZBR⁺12]. The derived strategies are based on the semidefinite relaxation (SDR) technique or the second-order cone programming (SOCP) technique. Furthermore, we have also developed optimal and suboptimal widely linear (WL) relay transmit strategies for such a multi-operator TWR network when non-circular signals are transmitted [ZH13]. Moreover, analytic results on the achievable WL gain are obtained for the WL dual channel matching (DCM) based scheme. After obtaining a comprehensive insight into the multi-operator TWR network, we shift our focus to a multi-pair TWR network with multiple single antenna AF relays. The relays in the network cooperate with each other to calculate their amplification coefficients. Again, we consider the sum rate maximization problem. We have shown that the

sum rate maximization problem can be formulated into a monotonic optimization problem, regardless whether the network has a total transmit power constraint [ZRH⁺12c] or each relay has its individual transmit power constraint [ZRH12a]. Thereby, a global optimal solution has been obtained by using the polyblock algorithm. Since in general the polyblock algorithm does not guarantee a polynomial-time complexity, we have derived low-complexity approximations of the optimal algorithm in the low SNR regime and the high SNR regime, respectively. The former solution is obtained by maximizing the total SINR while the latter one is obtained by applying the interference neutralization (IN) technique. Afterwards, we have studied a more general multi-pair TWR network, which consists of multiple cooperative smart multi-antenna AF relays and non-cooperative dumb repeaters. The interference in the network can be managed using the IN technique. Hence, we have derived necessary and sufficient conditions for neutralizing the interference in the network [ZHJH14a]. Moreover, a general framework to optimize different system utility functions in such a network with or without IN has been developed [ZHJH14c], [ZHJH14b]. Finally, a joint design of the precoder and the decoder at the BS and the relay amplification matrix at the relay has been studied for a TWR assisted relay broadcasting channel with a multi-antenna AF relay [ZRH11]. Three suboptimal solutions, which are based on the channel inversion criterion, the ProBaSeMO concept, or the zero-forcing dirty paper coding (ZFDPC) have been proposed.

In the second part of the thesis we investigate advanced transmit strategies for realizing a FD operation in wireless communication systems and especially a full-duplex (FD) MIMO point-to-point (P2P) system. The major challenge of realizing a FD operation is to suppress the overwhelming self-interference (SI). Although different RF domain or digital domain SI cancellation techniques are developed to solve this problem, they are far from perfect and thus cannot meet the requirements of real world applications [DMBS12]. By exploiting the MIMO techniques, we have proposed SI aware transmit strategies [ZTLH12]. They can be used to combine with current SI cancellation techniques to provide sufficient and/or reliable SI cancellation for real world applications. Moreover, they can be also adjusted such that the spatial multiplexing gain in a MIMO system is preserved. Optimal SI aware transmit strategies, which maximize the system sum rate in a FD MIMO system, have been developed using convex optimization. Specifically for the MISO case and the 2-by-2 MIMO case, closed-form solutions have been derived. The performance of the SI aware transmit strategies depends on the available channel state information (CSI) at the transmitter. If the CSI is imperfect, robust transmit strategies to combat the channel imperfections are desired. When the CSI errors are modeled deterministically and bounded by ellipsoids, a robust transmit strategy which can minimize the total required transmit power in the worst-case has been derived

[ZRH13]. Even though the SI can be estimated and subtracted at the digital baseband of the receiver side, the residual SI can still significantly affect the performance of the system due to the imperfect RF chain [DMBS12]. Hence, this motivates us to develop transmit strategies to suppress the residual SI so that the FD gain can still be exploited. For this purpose, we have developed signal to leakage plus noise ratio (SLNR) based beamforming strategies, which guarantee a FD gain especially when the residual SI is weak or in the low to medium SNR regime. When combined with the proposed power adjustment schemes, which automatically switch between the FD mode and the half-duplex (HD) mode, a FD gain is always achievable [ZTH13c].

Overall, the thesis demonstrates that many practical problems in TWR networks or FD wireless systems can efficiently be addressed using the developed signal processing algorithms. We benefit from these algorithms in multiple ways, e.g., a lower complexity (many suboptimal approaches presented in the context of TWR), enhanced flexibility (as for the ProBaSeMO scheme and the IN solution), or the possibility to provide benchmarks on the performance of the systems (as for the optimal solutions).

12 Future work

The thesis has addressed a broad spectrum of topics and, thereby, opened up many exciting directions for future research.

Regarding the first part on TWR with AF relays, many unanswered questions remain. One open research area is the analytical performance of the proposed algorithms. For example, computing the diversity order and multiplexing gain achieved by the ProBaSeMO scheme is a good starting point. Moreover, large-scale performance analysis is also desirable not only for the ProBaSeMO scheme but also for the IN solution and even optimal solutions.

An extension from single antenna UTs to multiple antenna UTs is also an important area. This opens up a challenging problem in relaying scenarios, i.e., the joint design of the UTs' transmit strategies and the relays' transmit strategies. However, one can also start from a simpler joint design problem, e.g., the joint optimization of the UTs' transmit power and the relays' transmit strategies.

Moreover, taking into account real-world conditions such as frequency-selective fading, imperfect synchronization, or reciprocity imbalance are of significant practical interest. Such considerations help to verify the robustness of the proposed algorithms and may lead to new ideas how to improve them further with respect to real-world conditions.

The knowledge we learn from optimal studies of TWR can also be extended by adopting other system utility functions, e.g., energy efficiency or by studying other relaying protocols and relaying strategies. For instance, one can consider applying the proposed algorithms to multi-way AF relaying or multi-pair DF relaying.

Finally, integrating the TWR protocol into a larger wireless communication system and performing system-level simulations to assess its performance is an important step towards the adaptation of our developed ideas into future mobile communication standards.

Concerning the second part on signal processing techniques for FD communications we would recommend to go two directions. The first direction is the continuous fundamental study. That is, we investigate how digital signal processing can help to suppress or cancel the SI, e.g., studying the joint design of transmitter-side and receiver-side SI cancellation techniques. Instead of using an ideal model, we take into account practical imperfections, e.g., time-invariant channels. Moreover, the SI cancellation technique for a multi-carrier system has to be addressed. The ultimate goal is to realize SI-free broadband MIMO FD communications for much wider applications. The second direction is to study the network aspects of FD

communications. For example, it is interesting to know how FD BSs improve the resource allocation and user scheduling in a MU-MIMO scenario.

Part IV
Appendices

Appendix A

Glossary of Acronyms, Symbols and Notation

A.1 Acronyms

1G	First Generation
2G	Second Generation
3G	Third Generation
4G	Fourth Generation
5G	Fifth Generation
AF	Amplify and Forward
ANC	Analog Network Coding
ANOMAX	Algebraic Norm Maximizing
BC	Broadcast Channel
BCD	Block Component Decomposition
BD	Block Diagonalization
BER	Bit Error Rate
BPSK	Binary Phase Shift Keying
BS	Base Station
CDF	Cumulative Density Function
CCDF	Complementary Cumulative Distribution Function
CI	Channel Inversion
CP	Cyclic Prefix
CrF	Compress and Forward
CSI	Channel State Information
CuF	Compute and Forward
DC	Difference of Convex Functions
DCM	Dual Channel Matching
DET	Dominant Eigenmode Transmission
DF	Decode and Forward
DPC	Dirty Paper Coding
eNB	Evolved Node B
EVD	EigenValue Decomposition
FD	Full-Duplex
FDD	Frequency Division Duplexing
FDMA	Frequency Division Multiple Access
GP	Gradient Projection
HD	Half-Duplex
IN	Interference Neutralization
LOS	Line Of Sight

LP	Linear Programming
LS	Least Squares
LTE	Long Term Evolution
LTI	Linear Time Invariant
M2M	Machine-to-Machine
MAC	Multiple Access Channel
MCS	Modulation and Coding Scheme
MIMO	Multiple Input Multiple Output
MISO	Multiple Input Single Output
MRC	Maximum Ratio Combining
MSE	Mean Squared Error
MMSE	Minimum Mean Squared Error
OFDM	Orthogonal Frequency Division Multiplexing
OFDMA	Orthogonal Frequency Division Multiple Access
OQAM	Offset Quadrature Amplitude Modulation
OWR	One-Way Relaying
POTDC	Polynomial time DC
P2P	Point to point
ProBaSeMO	Projection Based Separation of Multiple Operators
QAM	Quadrature Amplitude Modulation
QCQP	Quadratically Constrained Quadratic Programming
QoS	Quality of Service
RR-ANOMAX	Rank-Restored ANOMAX
RBD	Regularized Block Diagonalization
RF	Radio Frequency
RN	Relay Node
RS	Relay Station
SDMA	Space-Division Multiple Access
SDP	Semidefinite Programming
SDR	Semidefinite Relaxation
SI	Self-Interference
SIMO	Single Input Multiple Output
SISO	Single Input Single Output
SINR	Single to Interference Plus Noise Ratio
SLNR	Single to Leakage Plus Noise Ratio
SNR	Signal to Noise Ratio
SOCP	Second-Order Cone Programming
SVD	Singular Value Decomposition
TDD	Time Division Duplexing
TDMA	Time-Division Multiple Access
TWR	Two-Way Relaying
UE	User Equipment
UT	User Terminal
WF	Water Filling
WL	Widely Linear
ZF	Zero Forcing
ZFDPC	Zero Forcing Dirty Paper Coding
ZMCSG	Zero Mean Circularly Symmetric Complex Gaussian

A.2 Symbols and Notation

\mathbb{R}	Set of real numbers
\mathbb{R}_+	Set of non-negative real numbers
\mathbb{C}	Set of complex numbers
\mathcal{S}^n	Set of n -by- n Symmetric matrices
\mathcal{S}_+^n	Set of n -by- n Symmetric positive semidefinite matrices
\mathcal{S}_{++}^n	Set of n -by- n Symmetric positive definite matrices
\mathcal{H}^n	Set of n -by- n Hermitian matrices
\mathcal{H}_+^n	Set of n -by- n Hermitian positive semidefinite matrices
\mathcal{H}_{++}^n	Set of n -by- n Hermitian positive definite matrices
\mathbb{Z}	Set of integer numbers
e, π, j	Euler's number, π , and imaginary unit: $e^{j\pi} + 1 = 0$
a, b, c	Scalars
$\mathbf{a}, \mathbf{b}, \mathbf{c}$	Column vectors
$\mathbf{A}, \mathbf{B}, \mathbf{C}$	Matrices
$\operatorname{Re}\{x\}$	Real part of complex variable x
$\operatorname{Im}\{x\}$	Imaginary part of complex variable x
$\arg\{x\}$	Argument (phase) of complex variable x
x^*	Complex conjugate of x
\log	Natural logarithm
\log_2	Logarithm to the base 2
$\mathbf{0}_{M \times N}$	Matrix of zeros of size $M \times N$
$\mathbf{1}_{M \times N}$	Matrix of ones of size $M \times N$
\mathbf{I}_M	Identity matrix of size $M \times M$
$\mathbf{\Pi}_M$	Exchange of size $M \times M$ with ones on its anti-diagonal and zeros elsewhere
$\mathbf{Q} \geq \mathbf{0}$	\mathbf{Q} is a positive-semidefinite matrix
$\mathbf{Q} > \mathbf{0}$	\mathbf{Q} is a positive-definite matrix
$[\mathbf{A}]_{(i,j)}$	The (i, j) -element of the matrix \mathbf{A}
$[a_i]_{i=1,2,\dots,I}$	An $I \times 1$ column vector \mathbf{a} with i -th element a_i
$(\cdot)^T$	Matrix transpose
$(\cdot)^H$	Hermitian transpose
$\ \cdot\ _2$	Euclidean (two-) norm
$\ \cdot\ _F$	Frobenius norm

$\mathbf{A} \otimes \mathbf{B}$ Kronecker product between $\mathbf{A} \in \mathbb{C}^{M \times N}$ and $\mathbf{B} \in \mathbb{C}^{P \times Q}$ defined as

$$\mathbf{A} \otimes \mathbf{B} = \begin{bmatrix} a_{1,1} \cdot \mathbf{B} & a_{1,2} \cdot \mathbf{B} & \cdots & a_{1,N} \cdot \mathbf{B} \\ a_{2,1} \cdot \mathbf{B} & a_{2,2} \cdot \mathbf{B} & \cdots & a_{2,N} \cdot \mathbf{B} \\ \vdots & \vdots & \vdots & \vdots \\ a_{M,1} \cdot \mathbf{B} & a_{M,2} \cdot \mathbf{B} & \cdots & a_{M,N} \cdot \mathbf{B} \end{bmatrix}.$$

$\mathbf{A} \diamond \mathbf{B}$ Khatri-Rao (column-wise Kronecker) product between $\mathbf{A} \in \mathbb{C}^{M \times N}$ and $\mathbf{B} \in \mathbb{C}^{P \times N}$

$\mathbf{A} \odot \mathbf{B}$ Schur (element-wise) product between $\mathbf{A} \in \mathbb{C}^{M \times N}$ and $\mathbf{B} \in \mathbb{C}^{M \times N}$ and $\mathbf{B} \in \mathbb{C}^{M \times N}$

$\text{vec}\{\cdot\}$ Vec-operator: stack elements of a matrix/tensor into a column vector, begin with first (row) index, then proceed to second (column), third, etc.

$\text{unvec}_{I \times J}\{\cdot\}$ Inverse vec-operator: reshape elements of a vector back into a matrix/tensor of the indicated size

$\text{diag}\{\cdot\}$ Transform a vector into a square diagonal matrix or extract main diagonal of a square matrix and place elements into a vector

$\text{blkdiag}\{\mathbf{A}_n\}_{n=1}^N$ Transform matrices into a block diagonal matrix. The blkdiag operation on a sequence of matrices $\mathbf{A}_1, \dots, \mathbf{A}_N$ is defined as

$$\text{blkdiag}\{\mathbf{A}_n\}_{n=1}^N = \text{blkdiag}\{\mathbf{A}_1, \dots, \mathbf{A}_N\} = \begin{bmatrix} \mathbf{A}_1 & \cdots & \cdots \\ \vdots & \mathbf{A}_2 & \vdots \\ \vdots & \vdots & \vdots \\ \cdots & \cdots & \mathbf{A}_N \end{bmatrix}$$

$\text{Diag}\{\mathbf{B}\}$ Transform a square matrix $\mathbf{B} \in \mathbb{C}^{N \times N}$ into a square diagonal matrix by replacing all the off-diagonal elements with zeros

$\text{trace}\{\cdot\}$ Trace of a matrix (sum of diagonal elements = sum of eigenvalues)

$\text{det}\{\cdot\}$ Determinant of a matrix (product of eigenvalues)

$\text{rank}\{\cdot\}$ Rank of a matrix

$\lambda_{\max}\{\cdot\}$ Dominant eigenvalue of a matrix

$\mathcal{P}\{\cdot\}$ Dominant eigenvector of a square matrix

\mathbf{A}^+ Moore-Penrose pseudo inverse [Moo20, Pen55] of a matrix $\mathbf{A} \in \mathbb{C}^{M \times N}$, which we can compute via

- $\mathbf{A}^+ = \mathbf{V}_s \cdot \Sigma_s^{-1} \cdot \mathbf{U}_s^H$, where $\mathbf{A} = \mathbf{U}_s \cdot \Sigma_s \cdot \mathbf{V}_s^H$ represents the economy-size SVD of \mathbf{A} .

- $\mathbf{A}^+ = (\mathbf{A}^H \cdot \mathbf{A})^{-1} \cdot \mathbf{A}^H$ if $\text{rank}\{\mathbf{A}\} = N$ (full column rank)

- $\mathbf{A}^+ = \mathbf{A}^H \cdot (\mathbf{A} \cdot \mathbf{A}^H)^{-1}$ if $\text{rank}\{\mathbf{A}\} = M$ (full row rank).

$\mathbb{E}\{X\}$ Expectation operator, i.e., mean of the random variable X Note that

$\text{Med}\{X\} = \mathbb{E}\{X\}$ only if X has a symmetric distribution.

$\mathcal{N}(\mu, \sigma^2)$ Gaussian distribution with mean μ , variance σ^2

$\mathcal{CN}(\mu, \sigma^2)$ Circularly symmetric complex Gaussian distribution

Appendix B

Convex optimization background

In this chapter, we introduce the convexity theory, which is an important mathematical tool for signal processing in wireless communications. The convexity theory and convex optimization methods are also important for understanding the developed algorithms in this thesis. Specifically, the following two properties of convex sets and functions make them so attractive for our work:

- A convex function has no local minima that are not global.
- Convex problems can be solved efficiently using a generic polynomial-time algorithm, e.g., the interior-point algorithm [BV04].

The introduction is a summary of some important results from [BV04] (except Section B.3.5) and is organized in a compact way. For more details one can refer to [BV04] and [BNO03].

B.1 Convex sets and convex functions

B.1.1 Convex sets

Convex set: A set \mathcal{C} is *convex* if the line segment between any two points in \mathcal{C} lies in \mathcal{C} , i.e., if for any $\mathbf{X}_1, \mathbf{X}_2 \in \mathcal{C}$ and any $\mu \in [0, 1]$, we have

$$\mu \mathbf{X}_1 + (1 - \mu) \mathbf{X}_2 \in \mathcal{C}. \quad (\text{B.1})$$

Under the defining condition on μ , the linear sum in (B.1) is called a *convex combination* of \mathbf{X}_1 and \mathbf{X}_2 . If \mathbf{X}_1 and \mathbf{X}_2 are points in a real finite-dimensional Euclidean *vector space* \mathbb{R}^n or $\mathbb{R}^{m \times n}$, then (B.1) represents the closed line segment jointing them. Line segments are thereby convex sets [Dat05]. More specifically, such a set is *affine*.

Convex hull: The *convex hull* of a set \mathcal{C} , denoted $\text{conv}(\mathcal{C})$, is the set of all convex combinations of point in \mathcal{C} :

$$\text{conv}(\mathcal{C}) = \left\{ \mu_1 \mathbf{X}_1 + \dots + \mu_k \mathbf{X}_k \mid \mathbf{X}_i \in \mathcal{C}, \mu_i \geq 0, i = 1, \dots, k, \mu_1 + \dots + \mu_k = 1 \right\}. \quad (\text{B.2})$$

As the name suggests, the convex hull $\text{conv}(\mathcal{C})$ is always convex. It is the smallest convex set that contains \mathcal{C} .

Convex cone: A set \mathcal{C} is called a *cone*, or *nonnegative homogeneous*, if for every $\mathbf{X} \in \mathcal{C}$ and $\mu \geq 0$ we have $\mu\mathbf{X} \in \mathcal{C}$. A set \mathcal{C} is a *convex cone* if it is convex and a cone, which means that for any $\mathbf{X}_1, \mathbf{X}_2 \in \mathcal{C}$ and $\mu_1, \mu_2 \geq 0$, we have

$$\mu_1\mathbf{X}_1 + \mu_2\mathbf{X}_2 \in \mathcal{C}. \quad (\text{B.3})$$

Ellipsoids: An important family of convex sets is the *ellipsoids*, which have the form

$$\{\mathbf{x} \in \mathbb{R}^n \mid \|\mathbf{A}(\mathbf{x} - \mathbf{a})\|^2 = ((\mathbf{x} - \mathbf{a}))^T \mathbf{P}^{-1}((\mathbf{x} - \mathbf{a}))\} \quad (\text{B.4})$$

where $\mathbf{P} = \mathbf{P}^T > 0$, i.e., \mathbf{P} is symmetric and positive definite. The vector $\mathbf{a} \in \mathbb{R}^n$ is the center of the ellipsoid.

Norm ball & Norm cone: Suppose $\|\cdot\|$ is any norm on \mathbb{R}^n . From the general properties of norms it can be shown that a *norm ball* of radius r and center \mathbf{c} , given by $\{\mathbf{x} \in \mathbb{R}^n \mid \|\mathbf{x} - \mathbf{c}\| \leq r\}$ is convex. The *norm cone* associated with the norm $\|\cdot\|$ is the set $\{(\mathbf{x}, t) \in \mathbb{R}^n \times \mathbb{R} \mid \|\mathbf{x}\| \leq t\} \subset \mathbb{R}^{n+1}$. It is a convex cone.

Positive semidefinite cone: Let \mathcal{S}^n denote the set of symmetric $n \times n$ matrices,

$$\mathcal{S}^n = \{\mathbf{X} \in \mathbb{R}^{n \times n} \mid \mathbf{X} = \mathbf{X}^T\}, \quad (\text{B.5})$$

which is a vector space with dimension $n(n+1)/2$. Let \mathcal{S}_+^n and \mathcal{S}_{++}^n denote the set of symmetric positive semidefinite matrices

$$\mathcal{S}_+^n = \{\mathbf{X} \in \mathcal{S}^n \mid \mathbf{X} \geq 0\}, \quad (\text{B.6})$$

and the set of symmetric positive definite matrices

$$\mathcal{S}_{++}^n = \{\mathbf{X} \in \mathcal{S}^n \mid \mathbf{X} > 0\}, \quad (\text{B.7})$$

respectively. The set \mathcal{S}_+^n is a convex cone [BV04].

B.1.2 Convex functions

A function $f : \mathbb{R}^n \rightarrow \mathbb{R}$ is *convex* if its domain $\text{dom}\{f\}$ is a convex set and if for all $\mathbf{x}, \mathbf{y} \in \text{dom}\{f\}$, and $\mu \in [0, 1]$, we have

$$f(\mu\mathbf{x} + (1 - \mu)\mathbf{y}) \leq \mu f(\mathbf{x}) + (1 - \mu)f(\mathbf{y}). \quad (\text{B.8})$$

A function f is *strictly convex* if the strict inequality holds in (B.8) whenever $\mathbf{x} \neq \mathbf{y}$ and $\mu \in (0, 1)$. We say f is *concave* if $-f$ is convex, and *strictly concave* if $-f$ is strictly convex. For an affine function ¹, equation (B.8) is always satisfied with equality and thus all affine functions are both convex and concave. Conversely, any function that is convex and concave is affine.

B.1.2.1 First- and second-order conditions

Suppose f is differentiable (i.e., its gradient $\frac{\partial f(\mathbf{x})}{\partial \mathbf{x}}$ exists at each point in $\text{dom}\{f\}$, which is open). Then f is convex if and only if $\text{dom}\{f\}$ is convex and

$$f(\mathbf{y}) \geq f(\mathbf{x}) + \frac{\partial f(\mathbf{x})}{\partial \mathbf{x}}^\top (\mathbf{y} - \mathbf{x}) \quad (\text{B.9})$$

holds for all $\mathbf{x}, \mathbf{y} \in \text{dom}\{f\}$.

We now assume f is twice differentiable, that is, its Hessian or second derivative $\frac{\partial^2 f(\mathbf{x})}{\partial \mathbf{x}^2}$ exists at each point in $\text{dom}\{f\}$, which is open. Then f is convex if and only if $\text{dom}\{f\}$ is convex and its Hessian is positive semidefinite: for all $\mathbf{x} \in \text{dom}\{f\}$,

$$\frac{\partial^2 f(\mathbf{x})}{\partial \mathbf{x}^2} \geq 0. \quad (\text{B.10})$$

B.1.2.2 Composition of convex functions

Define functions $h : \mathbb{R}^k \rightarrow \mathbb{R}$ and $g_i : \mathbb{R}^n \rightarrow \mathbb{R}$, $i = 1, \dots, k$. In this section, we introduce the composition rules which guarantee the convexity or the concavity of the composed function $f = h \circ g : \mathbb{R}^n \rightarrow \mathbb{R}$, defined by

$$f(\mathbf{x}) = h(g(\mathbf{x})) = h(g_1(\mathbf{x}), \dots, g_k(\mathbf{x})). \quad (\text{B.11})$$

Depending on the convexity and concavity of h and g_i , $\forall i$, we can derive the following rules:

- f is convex if h is convex and nondecreasing in each argument, and the g_i are convex, $\forall i$,
- f is convex if h is convex and nonincreasing in each argument, and the g_i are concave, $\forall i$,

¹A function is affine if it is a sum of a linear function and a constant, e.g., $f(\mathbf{x}) = \mathbf{A}\mathbf{x} + \mathbf{b}$, where $\mathbf{A} \in \mathbb{R}^{m \times n}$ and $\mathbf{b} \in \mathbb{R}^m$ [BV04].

- f is concave if h is concave and nondecreasing in each argument, and the g_i are concave, $\forall i$,
- f is concave if h is concave and nonincreasing in each argument, and the g_i are convex, $\forall i$,

B.2 Convex optimization and duality theory

A general optimization problem of finding an \mathbf{x} that minimizes $f_0(\mathbf{x})$ among all \mathbf{x} that satisfy the conditions $f_i(\mathbf{x}) \leq 0$, $i = 1, \dots, m$, and $h_j(\mathbf{x}) = 0$, $j = 1, \dots, p$ is denoted as

$$\begin{aligned} \min_{\mathbf{x}} \quad & f_0(\mathbf{x}) \\ \text{subject to} \quad & f_i(\mathbf{x}) \leq 0, \quad i = 1, \dots, m \\ & h_j(\mathbf{x}) = 0, \quad j = 1, \dots, p. \end{aligned} \tag{B.12}$$

where $\mathbf{x} \in \mathbb{R}^n$ is called the *optimization variable* and the function f_0 is called the *objective function* or *cost function*. The inequalities $f_i(\mathbf{x}) \leq 0$ are called *inequality constraints*, and the equations $h_j(\mathbf{x}) = 0$ are called the equality constraints. If there are no constraints, we say the optimization problem is *unconstrained*. Moreover, we refer to (B.12) as an optimization problem in *standard form*.

A *convex optimization* problem is one of the form

$$\begin{aligned} \min_{\mathbf{x}} \quad & f_0(\mathbf{x}) \\ \text{subject to} \quad & f_i(\mathbf{x}) \leq 0, \quad i = 1, \dots, m \\ & \mathbf{a}_j^T \mathbf{x} = b_j, \quad j = 1, \dots, p. \end{aligned} \tag{B.13}$$

where f_0, \dots, f_m are convex functions. Compared to the general standard form problem (B.12), the convex problem has three additional requirements:

- the objective function must be convex,
- the inequality constraint functions must be convex,
- the equality constraint functions $h_j(\mathbf{x}) = \mathbf{a}_j^T \mathbf{x} - b_j$ must be affine.

If the optimization problem is convex, it can be solved efficiently using the interior-point algorithm in [BV04].

B.2.1 The Lagrangian dual problem

The Lagrangian dual problem provides a view of the optimization problem from the other angle and thus it plays an important role in optimization theory. In this section, we briefly introduce the Lagrangian dual function and the corresponding dual problem.

Lagrangian: Let $\boldsymbol{\lambda} = [\lambda_1, \dots, \lambda_m]^T$ and $\boldsymbol{\nu} = [\nu_1, \dots, \nu_p]^T$. The Lagrangian L associated with the problem (B.12) is given by

$$L(\mathbf{x}, \boldsymbol{\lambda}, \boldsymbol{\nu}) = f_0(\mathbf{x}) + \sum_{i=1}^m \lambda_i f_i(\mathbf{x}) + \sum_{j=1}^p \nu_j h_j(\mathbf{x}) \quad (\text{B.14})$$

where λ_i and ν_j are the Lagrangian multipliers that are associated with the inequality constraints $f_i(\mathbf{x}) \leq 0$ and the equality constraints $h_j(\mathbf{x}) = 0$, respectively.

Lagrangian dual function: For a fixed pair $(\boldsymbol{\lambda}, \boldsymbol{\nu})$, the Lagrangian dual function associated with the optimization problem (B.12) is defined as

$$g(\boldsymbol{\lambda}, \boldsymbol{\nu}) = \min_{\mathbf{x} \in \mathcal{D}} L(\mathbf{x}, \boldsymbol{\lambda}, \boldsymbol{\nu}) = \min_{\mathbf{x} \in \mathcal{D}} \left(f_0(\mathbf{x}) + \sum_{i=1}^m \lambda_i f_i(\mathbf{x}) + \sum_{j=1}^p \nu_j h_j(\mathbf{x}) \right) \quad (\text{B.15})$$

where \mathcal{D} is the domain of the optimization problem (B.12). The Lagrangian dual function is the pointwise minimum of a family of affine functions of $(\boldsymbol{\lambda}, \boldsymbol{\nu})$, it is always concave with respect to $\boldsymbol{\lambda}$ and $\boldsymbol{\nu}$ regardless of the convexity of the primal problem (B.12). For any dual feasible variables $\boldsymbol{\lambda}$ and $\boldsymbol{\nu}$, the Lagrangian dual function $g(\boldsymbol{\lambda}, \boldsymbol{\nu})$ gives a lower bound for the optimal values of the optimization problem (B.12), i.e., $g(\boldsymbol{\lambda}, \boldsymbol{\nu}) \leq f_0(\mathbf{x}^*)$ where \mathbf{x}^* represents the optimal point for the primal problem (B.12) [BV04].

Lagrangian dual problem: The Lagrangian dual problem is the problem of finding the tightest (i.e., the greatest) lower-bound for the optimal value of problem (B.12) using the Lagrangian dual function (B.15). The Lagrangian dual problem can be expressed as

$$\begin{aligned} & \max_{\boldsymbol{\lambda}, \boldsymbol{\nu}} && g(\boldsymbol{\lambda}, \boldsymbol{\nu}) \\ & \text{subject to} && \lambda_i \geq 0, \quad i = 1, \dots, m. \end{aligned} \quad (\text{B.16})$$

Since the Lagrangian dual function (B.15) is always concave, the Lagrangian dual problem (B.16) is always convex even if the primal problem (B.12) is not convex. Let $\boldsymbol{\lambda}^*$ and $\boldsymbol{\nu}^*$ denote the optimal points of the dual problem (B.16). Clearly, we always have $g(\boldsymbol{\lambda}^*, \boldsymbol{\nu}^*) \leq f_0(\mathbf{x}^*)$. This property is referred as the weak duality. The difference between the optimal values of the dual problem (B.16) and the primal problem (B.12) is called the duality gap.

The duality gap is in general nonzero. When the duality gap is zero, it is said that the strong duality holds. Convex optimization problems are optimization problems for which the strong duality holds under some mild conditions. More specifically, if the primal problem (B.12) is convex and it satisfies certain constraint qualifications, strong duality holds. One of the simplest constraint qualifications is the Slater's condition. Slater's condition holds if there exists a feasible point $\mathbf{x} \in \text{Int}\{\mathcal{D}\}$ for which all the inequalities $f_i(\mathbf{x}) < 0$, $i = 1, \dots, m$ hold true, where $\text{Int}\{\cdot\}$ denotes the interior of a set [BV04].

B.2.2 Necessary conditions for optimality

In this section, we discuss the Karush-Kuhn-Tucker (KKT) optimality conditions for problem (B.12). In general, for any optimization problem with differentiable objective f_0 and constraint functions $f_1, \dots, f_m, h_1, \dots, h_p$, for which strong duality holds, any pair of primal and dual optimal points, i.e., \mathbf{x}^* and $(\boldsymbol{\lambda}^*, \boldsymbol{\nu}^*)$, must satisfy the KKT conditions [BV04]. The KKT conditions are described with the following equations [BV04].

$$\begin{aligned}
 f_i(\mathbf{x}^*) &\leq 0, & , i = 1, \dots, m \\
 h_j(\mathbf{x}^*) &= 0, & , j = 1, \dots, p \\
 \lambda_i^* &\geq 0, & , i = 1, \dots, m \\
 \lambda_i^* f_i(\mathbf{x}^*) &= 0, & , i = 1, \dots, m \\
 \frac{\partial f_0(\mathbf{x})}{\partial \mathbf{x}} \Big|_{\mathbf{x}=\mathbf{x}^*} + \sum_{i=1}^m \lambda_i^* \frac{\partial f_i(\mathbf{x})}{\partial \mathbf{x}} \Big|_{\mathbf{x}=\mathbf{x}^*} + \sum_{j=1}^p \nu_j^* \frac{\partial h_j(\mathbf{x})}{\partial \mathbf{x}} \Big|_{\mathbf{x}=\mathbf{x}^*} &= 0
 \end{aligned} \tag{B.17}$$

The KKT conditions are also sufficient for the points to be primal and dual optimal if the primal problem is convex [BV04].

B.3 Convex optimization problems

In the following, we introduce several convex optimization problems which have also appeared in our derivations. Since in wireless communications and signal processing it is more common to have complex-valued signals, we will use notations from the complex domain, i.e., in Sections B.3.3, B.3.4, B.3.5. For complex variables, the convex optimization theory introduced in Sections B.1 and B.2 can be applied by representing the complex numbers using matrix representation, i.e., a complex number $x + jy$, where $\{x, y\} \in \mathbb{R}$, can be represented by a 2-by-2

real valued matrix in the following form

$$\begin{bmatrix} x & -y \\ y & x \end{bmatrix}. \quad (\text{B.18})$$

It is worth mentioning that when complex-domain notations are used all the functions have to be *real-valued* functions in the domain of the optimization problem. For optimization problems introduced in Sections B.3.1 and B.3.2, it is not common to define them in the complex domain and thus the real-domain notations will be preserved.

B.3.1 Linear programming (LP)

When the objective and constraint functions are all affine, the problem is called a *linear programming* (LP). A general linear programming has the form

$$\begin{aligned} \min_{\mathbf{x}} \quad & \mathbf{c}^T \mathbf{x} + d \\ \text{subject to} \quad & \mathbf{G}\mathbf{x} \leq \mathbf{h} \\ & \mathbf{A}\mathbf{x} = \mathbf{b}, \end{aligned} \quad (\text{B.19})$$

where $\mathbf{x} \in \mathbb{R}^n$, $\mathbf{G} \in \mathbb{R}^{m \times n}$ and $\mathbf{A} \in \mathbb{R}^{p \times n}$. Linear programmings are always convex optimization problems [BV04].

B.3.2 Second-order cone programming (SOCP)

The *second-order cone programming* (SOCP) is of the form

$$\begin{aligned} \min_{\mathbf{x}} \quad & \mathbf{f}^T \mathbf{x} \\ \text{subject to} \quad & \|\mathbf{A}_i \mathbf{x} + \mathbf{b}_i\|_2 \leq \mathbf{c}_i^T \mathbf{x} + d_i, \quad i = 1, \dots, m \\ & \mathbf{F}\mathbf{x} = \mathbf{g}, \end{aligned} \quad (\text{B.20})$$

where $\mathbf{A}_i \in \mathbb{R}^{n_i \times n}$ and $\mathbf{F} \in \mathbb{R}^{p \times n}$. The inequality constraint is called a *second-order cone constraint* since it is the same as requiring the affine function $(\mathbf{A}_i \mathbf{x} + \mathbf{b}_i, \mathbf{c}_i^T \mathbf{x} + d_i)$ to lie in the second-order cone in \mathbb{R}^{k+1} .

B.3.3 Quadratic programming (QP)

The convex optimization problem (B.13) is called a *quadratic programming* (QP) if the objective function is convex quadratic and the constraint functions are affine. A quadratic program can be expressed in the form

$$\begin{aligned} \min_{\mathbf{w}} \quad & (1/2)\mathbf{w}^H \mathbf{P} \mathbf{w} + \mathbf{q}^H \mathbf{w} + \mathbf{w}^H \mathbf{q} + r \\ \text{subject to} \quad & \mathbf{G} \mathbf{w} \leq \mathbf{h} \\ & \mathbf{A} \mathbf{w} = \mathbf{b}, \end{aligned} \tag{B.21}$$

where $\mathbf{w} \in \mathbb{C}^n$, $\mathbf{P} \in \mathcal{H}_+^n$, $\mathbf{G} \in \mathbb{C}^{m \times n}$, and $\mathbf{A} \in \mathbb{C}^{p \times n}$, where \mathcal{H}_+^n stands for the set of Hermitian positive semidefinite matrices. If the objective in (B.13) as well as the inequality constraint functions are convex quadratic as

$$\begin{aligned} \min_{\mathbf{w}} \quad & (1/2)\mathbf{w}^H \mathbf{P} \mathbf{w} + \mathbf{q}^H \mathbf{w} + \mathbf{w}^H \mathbf{q} + r \\ \text{subject to} \quad & (1/2)\mathbf{w}^H \mathbf{P}_i \mathbf{w} + \mathbf{q}_i^H \mathbf{w} + \mathbf{w}^H \mathbf{q}_i + r_i \leq 0, \quad i = 1, \dots, m \\ & \mathbf{A} \mathbf{w} = \mathbf{b}, \end{aligned} \tag{B.22}$$

where $\mathbf{P}_i \in \mathcal{H}_+^n$, $\forall i$, the problem is called a quadratically constrained quadratic program (QCQP).

B.3.4 Semidefinite programming (SDP)

A standard form *semidefinite programming* (SDP) has linear equality constraints, and a (matrix) nonnegativity constraint on the variable $\mathbf{X} \in \mathcal{H}^n$:

$$\begin{aligned} \min_{\mathbf{X}} \quad & \text{Tr}\{\mathbf{C} \mathbf{X}\} \\ \text{subject to} \quad & \text{Tr}\{\mathbf{A}_j \mathbf{X}\} = b_j, \quad j = 1, \dots, p \\ & \mathbf{X} \geq 0, \end{aligned} \tag{B.23}$$

where $\{\mathbf{C}, \mathbf{A}_1, \dots, \mathbf{A}_p\} \in \mathcal{H}^n$ and where \mathcal{H}^n denotes the set of Hermitian matrices.

B.3.5 Non-convex quadratic constrained quadratic programming (QCQP) problems via Semidefinite relaxation (SDR)

In wireless communications and signal processing, QCQP problems of the following homogeneous form often appear [HP10], [LMS⁺10], [GSS⁺10].

$$\begin{aligned}
 \min_{\mathbf{w}} \quad & \mathbf{w}^H \mathbf{A}_0 \mathbf{w} \\
 \text{subject to} \quad & \mathbf{w}^H \mathbf{A}_i \mathbf{w} \leq \alpha_i, \quad i = 1, \dots, m \\
 & \mathbf{w}^H \mathbf{B}_j \mathbf{w} = \beta_j, \quad j = 1, \dots, p,
 \end{aligned} \tag{B.24}$$

where A_i ($i = 0, \dots, m$) and \mathbf{B}_j , $\forall j$ are Hermitian matrices.

According to the definition of convex optimization in (B.13), (B.24) is a convex optimization problem unless there are only inequality constraints and the A_i are all positive semidefinite matrices. As a result, such QCQP problems are in general non-convex and difficult to deal with. This motivates researchers to develop generalized solutions [HP10], [LMS⁺10]. In the following, we introduce one general approach, namely, the semidefinite relaxation (SDR) technique. The principle of the SDR approach is to convexify the non-convex feasible region of the original QCQP problems. More specifically, the SDR technique enlarges the feasible region and thus an approximation technique is needed (in general), which can be used to obtain an approximate solution that is feasible for the original problem. In other words, the final solution of the SDR approach is not necessarily the optimal solution of the original problem [HP10].

By semidefinite relaxation, we mean that by introducing $\mathbf{X} = \mathbf{w}\mathbf{w}^H$ and using the property that $\text{Tr}\{\mathbf{\Gamma}\mathbf{X}\} = \mathbf{w}^H \mathbf{\Gamma} \mathbf{w}$ problem (B.24) can be rewritten as

$$\begin{aligned}
 \min_{\mathbf{X}} \quad & \text{Tr}\{\mathbf{A}_0 \mathbf{X}\} \\
 \text{subject to} \quad & \text{Tr}\{\mathbf{A}_i \mathbf{X}\} \leq \alpha_i, \quad i = 1, \dots, m \\
 & \text{Tr}\{\mathbf{B}_j \mathbf{X}\} = \beta_j, \quad j = 1, \dots, p \\
 & \mathbf{X} \geq 0, \quad \text{rank}\{\mathbf{X}\} = 1,
 \end{aligned} \tag{B.25}$$

where the only non-convex part is the rank-1 constraint while the other constraints are affine. If we drop the rank-1 constraint, a relaxed problem can be obtained

$$\begin{aligned}
 \min_{\mathbf{X}} \quad & \text{Tr}\{\mathbf{A}_0 \mathbf{X}\} \\
 \text{subject to} \quad & \text{Tr}\{\mathbf{A}_i \mathbf{X}\} \leq \alpha_i, \quad i = 1, \dots, m \\
 & \text{Tr}\{\mathbf{B}_j \mathbf{X}\} = \beta_j, \quad j = 1, \dots, p
 \end{aligned}$$

$$\mathbf{X} \geq 0. \tag{B.26}$$

Clearly, the new problem (B.26) is a convex SDP problem. It is always feasible and the optimal solution \mathbf{X}^* can have an arbitrary rank. In other words, the relaxed problem (B.26) is equivalent to the original problem (B.24) if and only if (B.26) has guaranteed rank-1 solutions [LMS⁺10]. There are some theoretical results on conditions under which rank-1 solutions are guaranteed for problem (B.26). For example, according to [HP10, Theorem 3.2 & Corollary 3.4], if there are no more than three constraints in (B.26), i.e., $m + p \leq 3$, a rank-1 optimal solution can be obtained. However, these conditions are not necessary conditions for the existence of rank-1 optimal solutions in general. In the following, we show how to compute an exact or approximate solution \mathbf{w}^* from the optimal solution \mathbf{X}^* .

If \mathbf{X}^* is rank-1, then \mathbf{w}^* is obtained as

$$\mathbf{w}^* = \sqrt{\lambda_{\max}\{\mathbf{X}^*\}} \cdot \mathcal{P}\{\mathbf{X}^*\} \tag{B.27}$$

where $\lambda_{\max}\{\mathbf{X}^*\}$ and $\mathcal{P}\{\mathbf{X}^*\}$ are the corresponding dominant eigenvalues and dominant eigenvectors of \mathbf{X}^* . If \mathbf{X}^* is not rank-1 and problem (B.26) does not satisfy [HP10, Theorem 3.2 & Corollary 3.4], a rank-1 approximation technique has to be applied to \mathbf{X}^* . In our work, the randomization technique, more specifically, the Gaussian randomization technique is applied. The randomization procedure is summarized in Algorithm 10. In practice 100 iterations, i.e., $N_{\text{ran}} = 100$, is sufficient to obtain a good approximate solution.

Algorithm 10 Gaussian randomization procedure

- 1: **Input:** SDR solution \mathbf{X}^* , and a number of randomizations N_{ran} .
 - 2: **Main step:**
 - 3: Calculate the eigen-decomposition of \mathbf{X} as $\mathbf{X} = \mathbf{U}\mathbf{\Sigma}\mathbf{U}^H$;
 - 4: **for** $n = 1$ to N_{ran} **do**
 - 5: Generate $\hat{\mathbf{w}}_n = \mathbf{U}\mathbf{\Sigma}^{1/2}\mathbf{z}_n$ where $\mathbf{z}_n \sim \mathcal{CN}(\mathbf{0}, \mathbf{I})$.
 - 6: Construct $\tilde{\mathbf{w}}_n = \gamma\hat{\mathbf{w}}_n$ which is feasible for the QCQP problem (B.24).
 - 7: Insert $\tilde{\mathbf{w}}_n$ into the cost function (B.24) to calculate the optimal value f_n^* .
 - 8: **if** $f_n^* < f_{n-1}^*$ **then**
 - 9: $\mathbf{w}^* = \tilde{\mathbf{w}}_n$.
 - 10: **end if**
 - 11: **end for**
-

Appendix C

Proofs and derivations for Part I

C.1 Derivation of RBD in the MAC Phase

In this section we derive the RBD solution is described in Section 3.3.2. Recall the cost function in (3.14), it can be further expanded as

$$\begin{aligned} \mathbf{G}_R &= \min_{\mathbf{G}_R} \mathbb{E} \left\{ \sum_{l=1}^L \left\| \mathbf{G}_R^{(\ell)} \tilde{\mathbf{H}}^{(l)} \tilde{\mathbf{x}}^{(\ell)} \right\|^2 + \sum_{l=1}^L \left\| \mathbf{G}_R^{(\ell)} \mathbf{n}_R \right\|^2 \right\} \\ &= \min_{\mathbf{G}_R} \mathbb{E} \left\{ \sum_{l=1}^L \left(\text{Tr} \left\{ \mathbf{G}_R^{(\ell)} \tilde{\mathbf{H}}^{(l)} \tilde{\mathbf{x}}^{(\ell)} \tilde{\mathbf{x}}^{(\ell)\text{H}} \tilde{\mathbf{H}}^{(l)\text{H}} \mathbf{G}_R^{(\ell)\text{H}} + \mathbf{G}_R^{(\ell)} \mathbf{n}_R \mathbf{n}_R^{\text{H}} \mathbf{G}_R^{(\ell)\text{H}} \right\} \right) \right\} \quad (\text{C.1}) \end{aligned}$$

Using $\mathbb{E} \{ \tilde{\mathbf{x}}^{(\ell)} \tilde{\mathbf{x}}^{(\ell)\text{H}} \} = P_k^{(\ell)} \mathbf{I}_{2(L-1)M_U}$, we obtain

$$\begin{aligned} & \min_{\mathbf{G}_R} \mathbb{E} \left\{ \sum_{l=1}^L \left(\text{Tr} \left\{ \mathbf{G}_R^{(\ell)} \tilde{\mathbf{H}}^{(l)} \tilde{\mathbf{x}}^{(\ell)} \tilde{\mathbf{x}}^{(\ell)\text{H}} \tilde{\mathbf{H}}^{(l)\text{H}} \mathbf{G}_R^{(\ell)\text{H}} + \mathbf{G}_R^{(\ell)} \mathbf{n}_R \mathbf{n}_R^{\text{H}} \mathbf{G}_R^{(\ell)\text{H}} \right\} \right) \right\} \\ &= \min_{\mathbf{G}_R} \left\{ \sum_{l=1}^L \left(\text{Tr} \left\{ \mathbf{G}_R^{(\ell)} \left(\frac{P_k^{(\ell)}}{M_U} \tilde{\mathbf{H}}^{(l)} \tilde{\mathbf{H}}^{(l)\text{H}} + \sigma_R^2 \mathbf{I}_{M_R} \right) \mathbf{G}_R^{(\ell)\text{H}} \right\} \right) \right\} \\ &= \min_{\mathbf{G}_R} \left\{ \sum_{l=1}^L \left(\text{Tr} \left\{ \mathbf{G}_R^{(\ell)} \tilde{\mathbf{U}}^{(\ell)} \left(\frac{P_k^{(\ell)}}{M_U} \tilde{\mathbf{\Sigma}}^{(\ell)} \tilde{\mathbf{\Sigma}}^{(\ell)\text{H}} + \sigma_R^2 \mathbf{I}_{M_R} \right) \tilde{\mathbf{U}}^{(\ell)\text{H}} \mathbf{G}_R^{(\ell)\text{H}} \right\} \right) \right\} \quad (\text{C.2}) \end{aligned}$$

According to [SH08], the expression in (C.2) is minimized by decomposing $\mathbf{G}_R^{(\ell)} = \mathbf{D}^{(\ell)} \mathbf{T}^{(\ell)}$. If we choose $\mathbf{T}^{(\ell)} = \tilde{\mathbf{U}}^{(\ell)\text{H}}$, then (C.2) reduces to

$$\min_{\mathbf{D}^{(\ell)}} \left\{ \sum_{l=1}^L \left(\text{Tr} \left\{ \left(\frac{P_k^{(\ell)}}{M_U} \tilde{\mathbf{\Sigma}}^{(\ell)} \tilde{\mathbf{\Sigma}}^{(\ell)\text{H}} + \sigma_R^2 \mathbf{I}_{M_R} \right) \mathbf{D}^{(\ell)^2} \right\} \right) \right\} \quad (\text{C.3})$$

where the matrices $\mathbf{D}^{(\ell)}$ have to be positive definite in order to find a nontrivial solution to (C.3) [SH08]. Using the results from [SH08], the final solution to (C.2) is given by

$$\mathbf{G}_R^{(\ell)} = \left(\frac{P_k^{(\ell)}}{M_U} \tilde{\Sigma}^{(\ell)} \tilde{\Sigma}^{(\ell)\text{H}} + \sigma_R^2 \mathbf{I}_{M_R} \right)^{-1/2} \tilde{\mathbf{U}}^{(\ell)\text{H}}. \quad (\text{C.4})$$

Note that an additional constraint $\mathbb{E}\{\|\mathbf{G}_R^{(\ell)} \mathbf{H}^{(\ell)} \mathbf{x}^{(\ell)}\|^2\} = 2P_u$ can be imposed on $\mathbf{G}_R^{(\ell)}$ so that after applying \mathbf{G}_R the level of the received signal power is normalized to the transmit power. However, since the AF relay does not decode the signal and the scaling with regard to the transmit power is handled via γ_0 we will not apply the normalization here.

C.2 Calculation of the precoding and decoding matrices in the presence of colored noise

The applied precoding and decoding matrices in Section 3.3.4 is derived here. Taking the first UT of the ℓ th operator as an example and recalling the signal model in (3.19), the received signal of the first UT after subtracting the self-interference is:

$$\tilde{\mathbf{y}}_1^{(\ell)} = \mathbf{H}_{1,2}^{(\ell)} \mathbf{x}_2^{(\ell)} + \tilde{\mathbf{n}}_1^{(\ell)}. \quad (\text{C.5})$$

Define the covariance matrix of the colored noise as $\mathbf{R}_{nn} = \mathbb{E}\{\tilde{\mathbf{n}}_1^{(\ell)} \tilde{\mathbf{n}}_1^{(\ell)\text{H}}\}$. To whiten the colored noise, we compute the EVD as $\mathbf{R}_{nn} = \mathbf{U}_n \Sigma_n \mathbf{U}_n^{\text{H}}$. Then the pre-whitening filter is chosen as:

$$\mathbf{R}_{\text{whiten}} = \Sigma_n^{-1/2} \mathbf{U}_n^{\text{H}}. \quad (\text{C.6})$$

Pre-multiplying equation (C.5) by $\mathbf{R}_{\text{whiten}}$, the SVD of the effective channel $\mathbf{H}_{1,2}^{(\text{eff})} = \mathbf{R}_{\text{whiten}} \mathbf{H}_{1,2}^{(\ell)}$ can be obtained by:

$$\mathbf{H}_{1,2}^{(\text{eff})} = \mathbf{U}_{1,2}^{(\text{eff})} \Sigma_{1,2}^{(\text{eff})} \mathbf{V}_{1,2}^{(\text{eff})\text{H}}. \quad (\text{C.7})$$

When DET is applied, the transmit beamforming vector $\mathbf{W}_2^{(\ell)} = \mathbf{w}_2^{(\ell)}$ and receive beamforming vector $\mathbf{F}_1^{(\ell)} = \mathbf{f}_1^{(\ell)}$ are selected as the first column of $\mathbf{V}_{1,2}^{(\text{eff})}$ and the conjugate transpose of the first column of $\mathbf{U}_{1,2}^{(\text{eff})}$, respectively.

When spatial multiplexing is applied, a new matrix $\Sigma_{1,2}^{(\text{wf})}$ is obtained by adjusting singular values in $\Sigma_{1,2}^{(\text{eff})}$ using the water-filling algorithm in [PNG03]. The transmit covariance matrix is given by:

$$\mathbf{R}_{\mathbf{x}_2^{(\ell)} \mathbf{x}_2^{(\ell)}} = \mathbf{V}_{1,2}^{(\text{eff})} \Sigma_{1,2}^{(\text{wf})} \mathbf{V}_{1,2}^{(\text{eff})\text{H}}. \quad (\text{C.8})$$

with $\mathbf{W}_2^{(\ell)} = \mathbf{V}_{1,2}^{(\text{eff})} \boldsymbol{\Sigma}_{1,2}^{(\text{wf})1/2}$. The decoding matrix can be chosen as $\mathbf{F}_1^{(\ell)} = \mathbf{U}_{1,2}^{(\text{eff})\text{H}} \mathbf{R}_{\text{whiten}}$.

C.3 Derivation of quadratic terms when each UT has a single antenna

The goal of this appendix is to arrive at quadratic formulas for the signal power, the interference power, and the noise power in Section 3.4.1. Using $\text{Tr}\{\mathbf{\Gamma}_1 \mathbf{\Gamma}_2\} = \text{Tr}\{\mathbf{\Gamma}_2 \mathbf{\Gamma}_1\}$ and $\text{vec}\{\mathbf{\Gamma}_1 \mathbf{X} \mathbf{\Gamma}_2\} = (\mathbf{\Gamma}_2^{\text{T}} \otimes \mathbf{\Gamma}_1) \text{vec}\{\mathbf{X}\}$, the numerator of equation (3.30), i.e., the signal power, is further expanded as

$$\begin{aligned} \mathbb{E} \left\{ \left| \mathbf{h}_k^{(\ell)\text{T}} \mathbf{G} \mathbf{h}_{3-k}^{(\ell)} x_{3-k}^{(\ell)} \right|^2 \right\} &= P_k^{(\ell)} \text{Tr} \left\{ \mathbf{h}_k^{(\ell)\text{T}} \mathbf{G} \mathbf{h}_{3-k}^{(\ell)} \left(\mathbf{h}_k^{(\ell)\text{T}} \mathbf{G} \mathbf{h}_{3-k}^{(\ell)} \right)^{\text{H}} \right\} \\ &= P_k^{(\ell)} \text{Tr} \left\{ \left(\mathbf{h}_{3-k}^{(\ell)\text{T}} \otimes \mathbf{h}_k^{(\ell)\text{T}} \right) \mathbf{g} \left(\mathbf{h}_{3-k}^{(\ell)\text{T}} \otimes \mathbf{h}_k^{(\ell)\text{T}} \right) \mathbf{g} \right\}^{\text{H}} \\ &= \mathbf{g}^{\text{H}} \underbrace{\left(P_k^{(\ell)} \left(\mathbf{h}_{3-k}^{(\ell)\text{T}} \otimes \mathbf{h}_k^{(\ell)\text{T}} \right)^{\text{H}} \left(\mathbf{h}_{3-k}^{(\ell)\text{T}} \otimes \mathbf{h}_k^{(\ell)\text{T}} \right) \right)}_{\mathbf{D}_k^{(\ell)}} \mathbf{g}. \end{aligned} \quad (\text{C.9})$$

Noticing that the interference term in (3.30) and the transmitted symbols are independently distributed with zero mean, the interference term can be calculated as

$$\mathbb{E} \left\{ \left| \sum_{\bar{k}, \bar{\ell} \neq \ell} \mathbf{h}_k^{(\ell)\text{T}} \mathbf{G} \mathbf{h}_{\bar{k}}^{(\bar{\ell})} x_{\bar{k}}^{(\bar{\ell})} \right|^2 \right\} = \mathbf{g}^{\text{H}} \left(\sum_{\bar{k}, \bar{\ell} \neq \ell} P_{\bar{k}}^{(\bar{\ell})} \left(\mathbf{h}_{\bar{k}}^{(\bar{\ell})\text{T}} \otimes \mathbf{h}_k^{(\ell)\text{T}} \right)^{\text{H}} \left(\mathbf{h}_{\bar{k}}^{(\bar{\ell})\text{T}} \otimes \mathbf{h}_k^{(\ell)\text{T}} \right) \right) \mathbf{g}$$

Finally, the forwarded noise term is calculated as

$$\begin{aligned} \mathbb{E} \left\{ \left| \mathbf{h}_k^{(\ell)\text{T}} \mathbf{G} \mathbf{n}_{\text{R}} \right|^2 \right\} &= \sigma_{\text{R}}^2 \mathbf{h}_k^{(\ell)\text{T}} \mathbf{G} \mathbf{G}^{\text{H}} \mathbf{h}_k^{(\ell)*} \\ &= \sigma_{\text{R}}^2 \text{vec}\{\mathbf{h}_k^{(\ell)\text{T}} \mathbf{G}\}^{\text{H}} \text{vec}\{\mathbf{h}_k^{(\ell)\text{T}} \mathbf{G}\} = \sigma_{\text{R}}^2 \left((\mathbf{I}_{M_{\text{R}}} \otimes \mathbf{h}_k^{(\ell)\text{T}}) \cdot \mathbf{g} \right)^{\text{H}} (\mathbf{I}_{M_{\text{R}}} \otimes \mathbf{h}_k^{(\ell)\text{T}}) \cdot \mathbf{g} \\ &= \mathbf{g}^{\text{H}} \left(\sigma_{\text{R}}^2 (\mathbf{I}_{M_{\text{R}}} \otimes (\mathbf{h}_k^{(\ell)} \mathbf{h}_k^{(\ell)\text{H}})^{\text{T}}) \right) \mathbf{g} \end{aligned}$$

C.4 Proof for Section 5.4.1 (feasibility of interference neutralization)

Since all the proofs for Section 5.4.1 are connected and are built on each other, we string them up in a series of subsections. First, we provide the proof of Theorem 5.4.1 in Appendix C.4.1. It consists of two parts. A pre-result (C.14) is shown in Appendix C.4.1 1), which is then

refined in Appendix C.4.1 2). Afterwards, the exact IN solution and its special cases are derived in Appendix C.4.2. Finally, the minimum required transmit power for IN is calculated in Appendix C.4.3.

C.4.1 Proof of Theorem 5.4.1

The IN condition is given by

$$\begin{cases} h_{2k-1,2\ell-1} + \mathbf{f}_{2k-1}^T \tilde{\mathbf{W}} \mathbf{f}_{2\ell-1} = 0 & \forall \ell, k, \ell \neq k \\ h_{2k-1,2\ell} + \mathbf{f}_{2k-1}^T \tilde{\mathbf{W}} \mathbf{g}_{2\ell} = 0 & \forall \ell, k, \ell \neq k \\ h_{2k,2\ell-1} + \mathbf{g}_{2k}^T \tilde{\mathbf{W}} \mathbf{f}_{2\ell-1} = 0 & \forall \ell, k, \ell \neq k \\ h_{2k,2\ell} + \mathbf{g}_{2k}^T \tilde{\mathbf{W}} \mathbf{g}_{2\ell} = 0 & \forall \ell, k, \ell \neq k \end{cases}, \quad (\text{C.10})$$

or equivalently

$$\begin{cases} h_{2k-1,2\ell-1} + \mathbf{h}_{2k-1,2\ell-1}^T \tilde{\mathbf{w}} = 0 & \forall \ell, k, \ell \neq k \\ h_{2k-1,2\ell} + \mathbf{h}_{2k-1,2\ell}^T \tilde{\mathbf{w}} = 0 & \forall \ell, k, \ell \neq k \\ h_{2k,2\ell-1} + \mathbf{h}_{2k,2\ell-1}^T \tilde{\mathbf{w}} = 0 & \forall \ell, k, \ell \neq k \\ h_{2k,2\ell} + \mathbf{h}_{2k,2\ell}^T \tilde{\mathbf{w}} = 0 & \forall \ell, k, \ell \neq k \end{cases}$$

Condition (C.10) can be rewritten as a linear system of equations (L. S. E.), which is expressed as

$$\mathbf{A}_1 \tilde{\mathbf{w}} = \mathbf{b}_1 \quad (\text{C.11})$$

where $\mathbf{A}_1 \in \mathbb{C}^{4K(K-1) \times NM_R^2}$ represents the effective channel which is defined as

$$\mathbf{A}_1 = \left[\mathbf{h}_{2k-1,2\ell-1} \quad \mathbf{h}_{2k-1,2\ell} \quad \mathbf{h}_{2k,2\ell-1} \quad \mathbf{h}_{2k,2\ell} \right]^T, \forall k, \ell,$$

and where $\mathbf{b}_1 \in \mathbb{C}^{4K(K-1)}$ is generated by

$$\mathbf{b}_1 = - \left[h_{2k-1,2\ell-1} \quad h_{2k-1,2\ell} \quad h_{2k,2\ell-1} \quad h_{2k,2\ell} \right]^T, \forall k, \ell.$$

Thereby, the feasibility problem of IN evolves to find solutions to a L. S. E.. Furthermore, the IN solution $\tilde{\mathbf{w}}$ has to fulfill the transmit power constraint at the relay, i.e.,

$$P_{R,\max} \geq \tilde{\mathbf{w}}^H \tilde{\mathbf{C}}_0^{(g)} \tilde{\mathbf{w}} \quad (\text{C.12})$$

when the total transmit power of the relays in the network is considered, or

$$P_{R,\max}^{(\text{Ind})} \geq \max_n \tilde{\mathbf{w}}^H \tilde{\mathbf{C}}_n^{(g)} \tilde{\mathbf{w}} \quad (\text{C.13})$$

when each relay has its own power constraint.

According to the Kronecker-Capelli Theorem [Mey04], a L. S. E. such as (C.11) has a solution if and only if (C.11) is consistent, where consistency is defined in the following lemma.

Lemma C.4.1. Consistency [Mey04]: *Each of the following is equivalent to saying that $[\mathbf{A}_1 \ \mathbf{b}_1]$ is consistent.*

1. *in row reducing $[\mathbf{A}_1 \ \mathbf{b}_1]$, a row of the following form never appears:*

$$\left[0 \ 0 \ \dots \ 0 \mid \alpha_1 \right], \alpha_1 \neq 0.$$

2. $\text{rank}\left\{[\mathbf{A}_1 \ \mathbf{b}_1]\right\} = \text{rank}\{\mathbf{A}_1\}$.

3. \mathbf{b}_1 is a combination of the basic columns in \mathbf{A}_1 .

Item 3 can be interpreted using the four fundamental subspaces of \mathbf{A}_1 . That is, the vector \mathbf{b}_1 has to be in the column space of \mathbf{A}_1 . Define the rank of \mathbf{A}_1 as r_A . Define the SVD of \mathbf{A}_1 as $\mathbf{A}_1 = [\mathbf{U}_{As} \ \mathbf{U}_{An}] \boldsymbol{\Sigma}_A \mathbf{V}_A^H$ where $\mathbf{U}_{As} \in \mathbb{C}^{4K(K-1) \times r_A}$ and $\mathbf{U}_{An} \in \mathbb{C}^{4K(K-1) \times (4K(K-1) - r_A)}$ are orthonormal bases of the column space of \mathbf{A}_1 and the left null space of \mathbf{A}_1 , respectively. Item 3 implies that equation (C.11) has a solution if and only if $\mathbf{U}_{An} \mathbf{U}_{An}^H \mathbf{b}_1 = \mathbf{0}$. Otherwise, the left null space component of \mathbf{b}_1 cannot be eliminated since $\mathbf{A}_1 \mathbf{x}$ is always a vector in the column space of \mathbf{A}_1 .

C.4.1.1 A general result

In our case \mathbf{A}_1 and \mathbf{b}_1 are generated from complex Gaussian distributions. Thus, \mathbf{A}_1 should have full rank in general, i.e., $\text{rank}\{\mathbf{A}_1\} = \min(4K(K-1), NM_R^2)$.¹ If \mathbf{A}_1 is a tall matrix, i.e., $4K(K-1) > NM_R^2$, equation (C.11) has no solution almost surely. In other words, (C.11) has a solution if and only if

$$NM_R^2 \geq 4K(K-1). \quad (\text{C.14})$$

In such a case, the solution to (C.11) is calculated using the pseudo inverse, i.e., $\tilde{\mathbf{w}} = \mathbf{A}_1^+ \mathbf{b}_1 + (\mathbf{I} - \mathbf{A}_1^+ \mathbf{A}_1) \tilde{\mathbf{w}}_n$ and $\mathbf{A}_1^+ = \mathbf{A}_1^H (\mathbf{A}_1 \mathbf{A}_1^H)^{-1}$. Notice that in practice \mathbf{A}_1 can be degenerated /

¹This is because the determinant of \mathbf{A}_1 is a multivariate polynomial in its entries. Since the entries are independent and from a continuous distribution, the probability to get a zero of the polynomial has measure zero [Mui82].

rank-deficient, e.g., in case of pure line of sight (LOS) channels. Nevertheless, this discussion is out of the scope of this thesis.

C.4.1.2 A specific result when the channel is reciprocal

Condition (C.14) reveals the dimensionality constraint in a general case, under which IN is feasible. For a special structure of the effective channel, i.e., the channel is reciprocal, the condition for IN can be relaxed. This is shown in the following. If $\tilde{\mathbf{w}}$ is designed such that

$$\begin{cases} \mathbf{f}_{2k-1}^T \tilde{\mathbf{W}} \mathbf{f}_{2\ell-1} = \mathbf{f}_{2\ell-1}^T \tilde{\mathbf{W}} \mathbf{f}_{2k-1} & \forall \ell, k, \ell \neq k \\ \mathbf{f}_{2k-1}^T \tilde{\mathbf{W}} \mathbf{g}_{2\ell} = \mathbf{f}_{2\ell}^T \tilde{\mathbf{W}} \mathbf{g}_{2k-1} & \forall \ell, k, \ell \neq k \\ \mathbf{g}_{2k}^T \tilde{\mathbf{W}} \mathbf{f}_{2\ell-1} = \mathbf{g}_{2\ell-1}^T \tilde{\mathbf{W}} \mathbf{f}_{2k} & \forall \ell, k, \ell \neq k \\ \mathbf{g}_{2k}^T \tilde{\mathbf{W}} \mathbf{g}_{2\ell} = \mathbf{g}_{2\ell}^T \tilde{\mathbf{W}} \mathbf{g}_{2k} & \forall \ell, k, \ell \neq k \end{cases}, \quad (\text{C.15})$$

there will be only $2K(K-1)$ equations in condition (C.10) while the other $2K(K-1)$ equations are duplicates and thus can be removed. Afterwards, we get a new L. S. E.

$$\mathbf{A} \tilde{\mathbf{w}} = \mathbf{b} \quad (\text{C.16})$$

where $\mathbf{A} \in \mathbb{C}^{2K(K-1) \times NM_{\text{R}}^2}$ is generated by

$$\mathbf{A} = \left[\mathbf{h}_{2\bar{i}-1, 2\bar{j}-1} \quad \mathbf{h}_{2\bar{i}-1, 2\bar{j}} \quad \mathbf{h}_{2\bar{i}, 2\bar{j}-1} \quad \mathbf{h}_{2\bar{i}, 2\bar{j}} \right]^T, \forall \bar{i}, \bar{j},$$

$\mathbf{b} \in \mathbb{C}^{2K(K-1)}$ is generated by

$$\mathbf{b} = - \left[\mathbf{h}_{2\bar{i}-1, 2\bar{j}-1} \quad \mathbf{h}_{2\bar{i}-1, 2\bar{j}} \quad \mathbf{h}_{2\bar{i}, 2\bar{j}-1} \quad \mathbf{h}_{2\bar{i}, 2\bar{j}} \right]^T, \forall \bar{i}, \bar{j},$$

and where $\bar{i} \in \{1, \dots, K\}$ and $\bar{j} \in \{\bar{i} + 1, \dots, K\}$. Moreover, condition (C.15) has to be satisfied for $2K(K-1)$ equations and via reformulation we get

$$\mathbf{A} \bar{\mathbf{K}} \tilde{\mathbf{w}} = \mathbf{0} \quad (\text{C.17})$$

where $\bar{\mathbf{K}} = \mathbf{I}_N \otimes (\mathbf{I}_{M_{\text{R}}^2} - \mathbf{K}_{M_{\text{R}}^2})$ and $\mathbf{K}_{M_{\text{R}}^2} \in \mathbb{C}^{M_{\text{R}}^2 \times M_{\text{R}}^2}$ is a commutation matrix, which is a unique permutation matrix such that $\mathbf{K}_{M_{\text{R}}^2} \text{vec}\{\mathbf{W}\} = \text{vec}\{\mathbf{W}^T\}$ [Lue96].

According to our previous discussion, equation (C.16) has a solution if and only if $2K(K-1) \leq NM_{\text{R}}^2$. However, the solution to (C.16) should be a feasible solution to (C.17) as well, and vice visa. That means, our new IN problem can be formulated as the following convex

feasibility problem

$$\begin{aligned} \text{find } & \tilde{\mathbf{w}} \\ \text{s.t. } & \mathbf{A}\tilde{\mathbf{w}} = \mathbf{b} \end{aligned} \quad (\text{C.18a})$$

$$\mathbf{A}\bar{\mathbf{K}}\tilde{\mathbf{w}} = \mathbf{0} \quad (\text{C.18b})$$

and $2K(K-1) \leq NM_{\text{R}}^2$ might be just an necessary condition such that problem (C.18) is feasible. Our task is to find necessary and sufficient conditions such that problem (C.18) is feasible. To this end, we find that it is useful to split the constraint (C.18b) into the following two cases, where the first one is given by

$$\bar{\mathbf{K}}\tilde{\mathbf{w}} = \mathbf{0} \quad (\text{C.19})$$

and the second one is

$$\left\{ \begin{array}{l} \mathbf{A}\bar{\mathbf{K}}\tilde{\mathbf{w}} = \mathbf{0} \\ \bar{\mathbf{K}}\tilde{\mathbf{w}} = \mathbf{c} \end{array} \right. \quad (\text{C.20a})$$

$$\left\{ \begin{array}{l} \bar{\mathbf{K}}\tilde{\mathbf{w}} = \mathbf{c} \end{array} \right. \quad (\text{C.20b})$$

where $\mathbf{c} \in \mathbb{C}^{NM_{\text{R}}^2}$ should have at least one non-zero element. The two cases can be interpreted using the four fundamental subspaces in linear algebra. That is, case (C.19) implies that $\tilde{\mathbf{w}}$ has to lie in the null space of $\bar{\mathbf{K}}$ while case (C.20) requires $\tilde{\mathbf{w}}$ to be in the intersection of the row space of $\bar{\mathbf{K}}$ and the null space of $\mathbf{A}\bar{\mathbf{K}}$. Since the null space and the row space of a matrix are orthogonal, case (C.19) and case (C.20) cannot be feasible at the same time. In the following, we discuss the solution to problem (C.18) under different cases.

Let us first consider case (C.19). Define the SVD $\bar{\mathbf{K}} = \mathbf{U}_1\boldsymbol{\Sigma}_1[\mathbf{V}_{\text{s},1} \ \mathbf{V}_{\text{n},1}]^{\text{H}}$ where $\mathbf{V}_{\text{n},1} \in \mathbb{C}^{NM_{\text{R}}^2 \times (NM_{\text{R}}^2 - r_1)}$ spans the null space of $\bar{\mathbf{K}}$ and r_1 is the rank of $\bar{\mathbf{K}}$. We have $r_1 = \frac{1}{2}NM_{\text{R}}(M_{\text{R}} - 1)$ based on the following two statements.

1. according to [Lue96, p. 116], the rank of $(\mathbf{I}_{M_{\text{R}}^2} - \mathbf{K}_{M_{\text{R}}^2})$ is equal to $\frac{1}{2}M_{\text{R}}(M_{\text{R}} - 1)$.
2. $\text{rank}\{\boldsymbol{\Gamma} \otimes \boldsymbol{\Omega}\} = \text{rank}\{\boldsymbol{\Gamma}\} \cdot \text{rank}\{\boldsymbol{\Omega}\}$ [Lue96, p. 20].

Without loss of generality, $\tilde{\mathbf{w}}$ which satisfies (C.19) can be expressed as

$$\tilde{\mathbf{w}} = \mathbf{V}_{\text{n},1}\hat{\mathbf{w}} \quad (\text{C.21})$$

where $\hat{\mathbf{w}} \in \mathbb{C}^{NM_{\text{R}}^2 - r_1}$. Inserting (C.21) into (C.18a), we get

$$\mathbf{A}\mathbf{V}_{\text{n},1}\hat{\mathbf{w}} = \mathbf{b}. \quad (\text{C.22})$$

Both \mathbf{A} and $\mathbf{V}_{n,1}$ have a full rank and thus the matrix product $\mathbf{A}\mathbf{V}_{n,1}$ has a full rank almost surely, i.e., the rank is given by $\min(2K(K-1), NM_R^2 - r_1)$. According to Lemma C.4.1, equation (C.22) has a solution if and only if

$$2K(K-1) \leq NM_R^2 - r_1 = \frac{1}{2}NM_R(M_R + 1). \quad (\text{C.23})$$

This condition means that

$$M_R \geq \left\lceil \frac{-1 + \sqrt{\frac{16K^2 - 16K}{N} + 1}}{2} \right\rceil. \quad (\text{C.24})$$

When case (C.20) is feasible, problem (C.18) be solved in a similar way. Nevertheless, the obtained solution is not useful for our purpose due to the following fact.

Lemma C.4.2. *If case (C.20) is feasible, the inequality $2K(K-1) \leq \frac{1}{2}NM_R(M_R - 1)$ has to hold.*

Proof. Please refer to Appendix C.5. □

Clearly, condition (C.35) is more stringent than (C.23). Therefore, assume that there is sufficient power at the relay. We can conclude that IN is feasible if and only if condition (C.23) is fulfilled.

C.4.2 Proof of Lemma 5.4.3 and Corollary 5.4.4

Define the SVD $\mathbf{A}\mathbf{V}_{n,1} = \mathbf{U}_2[\boldsymbol{\Sigma}_{s,2} \quad \mathbf{0}][\mathbf{V}_{s,2} \quad \mathbf{V}_{n,2}]^H$, where $\mathbf{V}_{s,2} \in \mathbb{C}^{\frac{1}{2}NM_R(M_R+1) \times r_2}$ and $\mathbf{V}_{n,2} \in \mathbb{C}^{\frac{1}{2}NM_R(M_R+1) \times (\frac{1}{2}NM_R(M_R+1) - r_2)}$ span the row space and the null space of $\mathbf{A}\mathbf{V}_{n,1}$, respectively. We have $\boldsymbol{\Sigma}_{s,2} \in \mathbb{C}^{r_2 \times r_2}$ and $r_2 = 2K(K-1)$. The IN solution of $\tilde{\mathbf{w}}$, which is also the solution to (C.22), is given by

$$\tilde{\mathbf{w}} = \mathbf{V}_{n,1}\boldsymbol{\Sigma}_{s,2}^{-1}\mathbf{U}_2^H\mathbf{b} + \mathbf{V}_{n,1}\mathbf{V}_{n,2}\hat{\mathbf{w}}_n, \quad (\text{C.25})$$

where $\hat{\mathbf{w}}_n \in \mathbb{C}^{\frac{1}{2}NM_R(M_R+1) - r_2}$. Using the orthogonal complement of $\mathbf{A}\mathbf{V}_{n,1}$, the IN solution can also be obtained as

$$\tilde{\mathbf{w}} = \mathbf{V}_{n,1} \left((\mathbf{A}\mathbf{V}_{n,1})^+\mathbf{b} + (\mathbf{I}_{\text{frac}12NM_R(M_R+1)} - (\mathbf{A}\mathbf{V}_{n,1})^+\mathbf{A}\mathbf{V}_{n,1})\mathbf{v} \right) \quad (\text{C.26})$$

where $\mathbf{v} \in \mathbb{C}^{\frac{1}{2}NM_R(M_R+1)}$. Although solution (C.25) and solution (C.26) provide the same number of signal dimensions, i.e., $\frac{1}{2}NM_R(M_R+1) - r_2$, optimizing \mathbf{v} yields a higher computational complexity since it has more elements than $\hat{\mathbf{w}}_n$. However, the computational complexity of

computing (C.26) is lower than computing (C.25). This is because the computational complexity of computing a pseudo inverse lies in the calculation of an inverse of a Hermitian positive definite matrix, which can be computed using the Cholesky decomposition. It is known that the Cholesky decomposition has a lower computational complexity compared to the SVD.

When $M_R = 1$, $N > 1$, and $N \geq 2K(K - 1)$, the IN solution is simplified to

$$\tilde{\mathbf{w}} = \mathbf{A}^+ \mathbf{b} + (\mathbf{I}_N - \mathbf{A}^+ \mathbf{A}) \mathbf{v}. \quad (\text{C.27})$$

Define the SVD $(\mathbf{I}_{M_R^2} - \mathbf{K}_{M_R^2}) = \mathbf{U}_3 \mathbf{\Sigma}_3 [\mathbf{V}_{s,3} \quad \mathbf{V}_{n,3}]^H$ where $\mathbf{V}_{n,3} \in \mathbb{C}^{M_R^2 \times (\frac{1}{2}M_R(M_R+1))}$ contains the last $(\frac{1}{2}M_R(M_R+1))$ columns. When $N = 1$, and $M_R \geq 2K - 2$, the IN solution is given by

$$\tilde{\mathbf{w}} = \mathbf{V}_{n,3} ((\mathbf{A}\mathbf{V}_{n,3})^+ \mathbf{b} + (\mathbf{I}_{\text{frac}12M_R(M_R+1)} - (\mathbf{A}\mathbf{V}_{n,3})^+ \mathbf{A}\mathbf{V}_{n,3}) \mathbf{v}). \quad (\text{C.28})$$

Without loss of generality, we can express the IN solutions (C.25), (C.26), (C.27) and (C.28) in the form of $\tilde{\mathbf{w}} = \mathbf{c} + \mathbf{B}\mathbf{v}$, where \mathbf{c} and \mathbf{B} are fixed and \mathbf{v} is a free parameter.

C.4.3 Proof of Corollary 5.4.5

Using the general IN solution $\tilde{\mathbf{w}} = \mathbf{c} + \mathbf{B}\mathbf{v}$ and the power constraints in (C.12) and (C.13), we compute the minimum required transmit power for IN and obtain the following lemma.

Lemma C.4.3.

Case 1 ($2K(K - 1) < \frac{1}{2}NM_R(M_R + 1)$). When a total transmit power of the relays in the network is considered, the minimum required transmit power $P_{R,\max}$ is

$$P_{R,\max} = \mathbf{c}^H \tilde{\mathbf{C}}_0^{(g)} \mathbf{c} - \mathbf{b}_p^H \mathbf{A}_p^+ \mathbf{b}_p \quad (\text{C.29})$$

where $\mathbf{A}_p = \mathbf{B}^H \tilde{\mathbf{C}}_0^{(g)} \mathbf{B}$ and $\mathbf{b}_p = \mathbf{B}^H \tilde{\mathbf{C}}_0^{(g)} \mathbf{c}$. When each relay has its own power constraint, the minimum required transmit power $P_{R,\max}^{(\text{Ind})}$ is calculated as

$$P_{R,\max}^{(\text{Ind})} = \max_n (\mathbf{c}^H \tilde{\mathbf{C}}_n^{(g)} \mathbf{c} - \mathbf{b}_{p,n}^H \mathbf{A}_{p,n}^+ \mathbf{b}_{p,n}) \quad (\text{C.30})$$

where $\mathbf{A}_{p,n} = \mathbf{B}^H \tilde{\mathbf{C}}_n^{(g)} \mathbf{B}$ and $\mathbf{b}_{p,n} = \mathbf{B}^H \tilde{\mathbf{C}}_n^{(g)} \mathbf{c}$.

Case 2 ($2K(K - 1) = \frac{1}{2}NM_R(M_R + 1)$). Under a total transmit power constraint, the minimum required transmit power $P_{R,\max}$ is

$$P_{R,\max} = \mathbf{c}^H \tilde{\mathbf{C}}_0^{(g)} \mathbf{c}. \quad (\text{C.31})$$

Under individual transmit power constraints, the minimum required transmit power $P_{R,\max}^{(\text{Ind})}$ is given by

$$P_{R,\max}^{(\text{Ind})} = \max_n \mathbf{c}^H \tilde{\mathbf{C}}_n^{(g)} \mathbf{c} \quad (\text{C.32})$$

Proof. When the total transmit power of the relays in the network is considered, the minimum required transmit power $P_{R,\max}$ is obtained by finding \mathbf{v} such that the following cost function is minimized

$$\begin{aligned} \mathcal{J}(\mathbf{v}) &= \tilde{\mathbf{w}}^H \tilde{\mathbf{C}}_0^{(g)} \tilde{\mathbf{w}} = (\mathbf{c} + \mathbf{B}\mathbf{v})^H \tilde{\mathbf{C}}_0^{(g)} (\mathbf{c} + \mathbf{B}\mathbf{v}) \\ &= \mathbf{c}^H \tilde{\mathbf{C}}_0^{(g)} \mathbf{c} + 2\text{Re}\{\mathbf{v}^H \mathbf{B}^H \tilde{\mathbf{C}}_0^{(g)} \mathbf{c}\} + \mathbf{v}^H \mathbf{B}^H \tilde{\mathbf{C}}_0^{(g)} \mathbf{B}\mathbf{v} \\ &= \mathbf{c}^H \tilde{\mathbf{C}}_0^{(g)} \mathbf{c} + 2\text{Re}\{\mathbf{v}^H \mathbf{b}_p\} + \mathbf{v}^H \mathbf{A}_p \mathbf{v} \end{aligned}$$

where $\text{Re}\{\cdot\}$ denotes the real part of a complex number. Clearly, we have $\mathbf{A}_p \geq 0$. Hence, $\mathcal{J}(\mathbf{v})$ is a convex function and it has a global minimum. To find the minimum value, we can take the derivative with respect to \mathbf{v}^* and set it to zero, i.e.,

$$\frac{\partial \mathcal{J}(\mathbf{v})}{\partial \mathbf{v}^*} = \mathbf{A}_p \mathbf{v} + \mathbf{b}_p = 0. \quad (\text{C.33})$$

Define the EVD $\mathbf{A}_p = [\mathbf{U}_{p,s} \ \mathbf{U}_{p,n}] \boldsymbol{\Sigma}_p [\mathbf{U}_{p,s} \ \mathbf{U}_{p,n}]^H$ where $\mathbf{U}_{p,n}$ contains the eigenvectors, which correspond to zero eigenvalues. Then $\mathbf{v} = -\mathbf{A}_p^+ \mathbf{b}_p + \mathbf{U}_{p,n} \mathbf{v}_{p,n}$, where $\mathbf{v}_{p,n}$ is a free variable, minimizes the function $\mathcal{J}(\mathbf{v})$. The minimum value of $\mathcal{J}(\mathbf{v})$ can be computed to be $\mathbf{c}^H \tilde{\mathbf{C}}_0^{(g)} \mathbf{c} - \mathbf{b}_p^H \mathbf{A}_p^+ \mathbf{b}_p$. Moreover, it is straightforward to get (C.30) when individual power constraints are considered.

The above derivation is based on the fact that \mathbf{A}_p is not a matrix with all zeros. However, this will happen under the condition that $2K(K-1) = \frac{1}{2}NM_R(M_R+1)$. In such a case, the matrix $\mathbf{A}\mathbf{V}_{n,1}$ becomes a full-rank square matrix. It does not possess a null space and thus the matrix \mathbf{B} is a zero matrix. Hence, the cost function $\mathcal{J}(\mathbf{v})$ becomes a constant. Conclusions (C.31) and (C.32) are obtained. □

Moreover, the minimum norm IN solution of $\tilde{\mathbf{w}}$ is given by $\tilde{\mathbf{w}} = \mathbf{c}$ since it minimizes $\|\tilde{\mathbf{w}}\|$.

In the following we discuss cases where IN is not feasible, i.e., the dimensionality requirement (C.23) or the minimum transmit power requirement (C.12) (or (C.13)) is violated. First, if only the dimensionality requirement (C.23) is violated, equation (C.22) has no solution almost surely since $\mathbf{A}\mathbf{V}_{n,1}$ will have a full column rank. But we can still obtain the least square solution $\tilde{\mathbf{w}} = \mathbf{V}_{n,1}(\mathbf{A}\mathbf{V}_{n,1})^+ \mathbf{b}$, i.e., $\tilde{\mathbf{w}} = \mathbf{c}$, which minimizes the least squares $\|\mathbf{A}\tilde{\mathbf{w}} - \mathbf{b}\|^2$.

It is straightforward to see that the least squares problem is equivalent to the interference minimization problem for our scenario. Thus, $\tilde{\mathbf{w}} = \mathbf{c}$ is also a solution to the total interference minimization problem:

$$\min_{\tilde{\mathbf{w}}} \sum_{k=1}^K \frac{1}{P_{2k-1}} P_{2k-1}^{(I)} + \frac{1}{P_{2k}} P_{2k}^{(I)}. \quad (\text{C.34})$$

When the minimum transmit power requirement (C.12) (or (C.13)) is violated, we can scale $\tilde{\mathbf{w}}$ such that the total interference is minimized. It is not difficult to see that the solution is given by

$$\tilde{\mathbf{w}} = \mathbf{c} \sqrt{\frac{P_{R,\max}}{\mathbf{c}^H \tilde{\mathbf{C}}_0^{(g)} \mathbf{c}}},$$

if a total transmit power constraint is considered, or

$$\tilde{\mathbf{w}} = \mathbf{c} \sqrt{\frac{P_{R,\max}^{(\text{Ind})}}{\max_n \mathbf{c}^H \tilde{\mathbf{C}}_n^{(g)} \mathbf{c}}},$$

if individual transmit power constraints are considered.

C.5 Proof to Lemma C.4.2

The proof to Lemma C.4.2 in Appendix C.4 is provided here. In general the matrix product $\mathbf{A}\bar{\mathbf{K}}$ has a full-rank which is equal to $\min(\text{rank}(\mathbf{A}), \text{rank}(\bar{\mathbf{K}})) = \min(2K(K-1), \frac{1}{2}NM_R(M_R-1))$. To see this, we define a change of basis matrix \mathbf{T} such that $\bar{\mathbf{K}} = \mathbf{T}[\bar{\mathbf{K}}' \ \mathbf{0}]\mathbf{T}^{-1}$, where $[\bar{\mathbf{K}}' \ \mathbf{0}]$ is the new basis and $\bar{\mathbf{K}}' \in \mathbb{C}^{NM_R^2 \times \frac{1}{2}N}$ [Mey04]. Then we have

$$\begin{aligned} \text{rank}(\mathbf{A}\bar{\mathbf{K}}) &= \text{rank}(\mathbf{A}\mathbf{T}[\bar{\mathbf{K}}' \ \mathbf{0}]\mathbf{T}^{-1}) = \text{rank}(\mathbf{A}\mathbf{T}[\bar{\mathbf{K}}' \ \mathbf{0}]) \\ &= \text{rank}(\mathbf{A}\mathbf{T}\bar{\mathbf{K}}'). \end{aligned}$$

Clearly, the matrix product $\mathbf{T}\bar{\mathbf{K}}'$ has a full rank. Thus, the matrix product $\mathbf{A}\bar{\mathbf{K}}$ has a full rank almost surely. According to [Mey04], this also implies that

$$\dim\{\mathcal{N}\{\mathbf{A}\} \cap \mathcal{S}\{\bar{\mathbf{K}}\}\} = 0$$

when $2K(K-1) > \frac{1}{2}NM_R(M_R-1)$. Or

$$\dim\{\mathcal{N}\{\bar{\mathbf{K}}^H\} \cap \mathcal{S}\{\mathbf{A}^H\}\} = 0$$

when $2K(K-1) \leq \frac{1}{2}NM_{\text{R}}(M_{\text{R}}-1)$ since the rank of a matrix product is obtained by

$$\begin{aligned} \text{rank}(\mathbf{A}\bar{\mathbf{K}}) &= \text{rank}(\mathbf{A}) - \dim\{\mathcal{N}\{\bar{\mathbf{K}}^{\text{H}}\} \cap \mathcal{S}\{\mathbf{A}^{\text{H}}\}\} \\ &= \text{rank}(\bar{\mathbf{K}}) - \dim\{\mathcal{N}\{\mathbf{A}\} \cap \mathcal{S}\{\bar{\mathbf{K}}\}\}. \end{aligned}$$

Moreover, case (C.20b) implies that the vector \mathbf{c} has to lie in the range of $\bar{\mathbf{K}}$. Inserting (C.20b) into (C.20a) shows that the vector \mathbf{c} has to lie in the null space of \mathbf{A} . In other words, the intersection of the subspace $\mathcal{S}\{\bar{\mathbf{K}}\}$ and the subspace $\mathcal{N}\{\mathbf{A}\}$ should not be empty. If the rank of the matrix $\mathbf{A}\bar{\mathbf{K}}$ is equal to $\frac{1}{2}NM_{\text{R}}(M_{\text{R}}-1)$, i.e., $2K(K-1) > \frac{1}{2}NM_{\text{R}}(M_{\text{R}}-1)$, there does not exist a vector \mathbf{c} which satisfies (C.20) since $\dim\{\mathcal{N}\{\mathbf{A}\} \cap \mathcal{S}\{\bar{\mathbf{K}}\}\} = 0$. If the rank of the matrix $\mathbf{A}\bar{\mathbf{K}}$ is equal to $2K(K-1)$, i.e., $2K(K-1) \leq \frac{1}{2}NM_{\text{R}}(M_{\text{R}}-1)$, there exists a nontrivial \mathbf{c} for (C.20). Hence, it is necessarily to have

$$2K(K-1) \leq \frac{1}{2}NM_{\text{R}}(M_{\text{R}}-1) \tag{C.35}$$

if case (C.20) is feasible.

C.6 Proof to Lemma 5.6.1

The optimality and the convergence behavior of the proposed DT algorithms in Section 5.6 are derived in this appendix. According to [LV12, Theorem 1.7.2], the set of all positive semidefinite matrices is closed. Moreover, given the two constraints in problem (5.31), the feasible region of problem (5.31) is closed under limits and thus it is compact. Then it is straightforward to apply Proposition 4.1 from [CFS85] and Theorem 2.1 from [CFS86], which state that problem (5.31) and its parametric representation (5.36) have the same set of optimal solutions if $f(\lambda) = 0$. Moreover, the generated sequences $\{\lambda^{(p)}\}$ converges at least linearly to λ_{opt} , and each convergent subsequences of $\{\mathbf{X}^{(p)}\}$ converges to an optimal solution of (5.31). Thus, the generalized Dinkelbach algorithm solves (5.31).

Next, we analyze the convergence behavior of the generalized Dinkelbach algorithm. Define $g_i(\mathbf{X}) = \text{Tr}\{\mathbf{F}_m\mathbf{X}^{(p)}\}$. According to [CFS85], if there is a single ratio in (5.31), a unique subgradient of $f(\lambda)$ is obtained and thus a superlinear convergence property of the Dinkelbach algorithm can be proven. When there are multiple ratios, the subgradient is not unique anymore. Instead, we have the following two relations.

Corollary C.6.1. [CFS85, Proposition 2.2] Assume that $\mathbf{X}^{(p)}$ is an optimal solution of (5.36)

at the (p) -th step. Then

$$\begin{cases} f(\lambda) \geq f(\lambda^{(p)}) - \underline{g}(\mathbf{X}^{(p)})(\lambda - \lambda^{(p)}) & \text{if } \lambda > \lambda^{(p)} \\ f(\lambda) \geq f(\lambda^{(p)}) - \bar{g}(\mathbf{X}^{(p)})(\lambda - \lambda^{(p)}) & \text{if } \lambda < \lambda^{(p)}. \end{cases} \quad (\text{C.36})$$

If DT-1 is applied, we have $\underline{g}(\mathbf{X}^{(p)}) = \min_m \text{Tr}\{\mathbf{F}_m \mathbf{X}^{(p)}\}$ and $\bar{g}(\mathbf{X}^{(p)}) = \max_m \text{Tr}\{\mathbf{F}_m \mathbf{X}^{(p)}\}$. If DT-2 is applied, we have $\underline{g}(\mathbf{X}^{(p)}) = \min_m (\text{Tr}\{\mathbf{F}_m \mathbf{X}^{(p)}\} / \text{Tr}\{\mathbf{F}_m \mathbf{X}^{(p-1)}\})$ and $\bar{g}(\mathbf{X}^{(p)}) = \max_m (\text{Tr}\{\mathbf{F}_m \mathbf{X}^{(p)}\} / \text{Tr}\{\mathbf{F}_m \mathbf{X}^{(p-1)}\})$. Using the inequalities in Corollary C.6.1, we derive the convergence speed of the proposed Dinkelbach-type algorithms. To this end, we apply the following fact, which can be proven in the same way as in [CFS85, Proposition 3.1],

$$\lambda^{(p+1)} \geq \lambda^{(p)} + f(\lambda^{(p)}) / \bar{g}(\mathbf{X}^{(p)}),$$

which is equivalent to

$$\lambda^{(p+1)} - \lambda_{\text{opt}} \geq \lambda^{(p)} - \lambda_{\text{opt}} + f(\lambda^{(p)}) / \bar{g}(\mathbf{X}^{(p)}). \quad (\text{C.37})$$

Furthermore, the first inequality in equation (C.36) implies that

$$f(\lambda^{(p)}) \geq f(\lambda_{\text{opt}}) + \underline{g}(\mathbf{X}_{\text{opt}})(\lambda_{\text{opt}} - \lambda^{(p)}) = \underline{g}(\mathbf{X}_{\text{opt}})(\lambda_{\text{opt}} - \lambda^{(p)}). \quad (\text{C.38})$$

Combining equations (C.37) and (C.38), we have

$$|\lambda^{(p+1)} - \lambda_{\text{opt}}| \leq |\lambda^{(p)} - \lambda_{\text{opt}}| (1 - \underline{g}(\mathbf{X}_{\text{opt}}) / \bar{g}(\mathbf{X}^{(p)})). \quad (\text{C.39})$$

Let $\delta_1 = \underline{g}(\mathbf{X}_{\text{opt}}) / \bar{g}(\mathbf{X}^{(p)})$. Clearly, in general $0 < \delta_1 < 1$ and thus the Dinkelbach algorithm has a linear convergence according to Definition 5.6.1. But if there is a single ratio, $\alpha_1 \rightarrow 1$ when $p \rightarrow \infty$, which implies a superlinear convergence. When there are multiple ratios and the DT-2 algorithm is applied, if the optimal solution is unique, i.e., $\mathbf{X}^{(p)}$ converges to \mathbf{X}_{opt} [CFS86], then

$$\underline{g}(\mathbf{X}_{\text{opt}}) = \min_m (\text{Tr}\{\mathbf{F}_m \mathbf{X}_{\text{opt}}\} / \text{Tr}\{\mathbf{F}_m \mathbf{X}^{(p-1)}\}) \xrightarrow{a.s.} 1 \quad (\text{C.40})$$

and

$$\bar{g}(\mathbf{X}^{(p)}) = \max_m (\text{Tr}\{\mathbf{F}_m \mathbf{X}^{(p)}\} / \text{Tr}\{\mathbf{F}_m \mathbf{X}^{(p-1)}\}) \xrightarrow{a.s.} 1. \quad (\text{C.41})$$

Again, a superlinear convergence will be obtained. Unfortunately, problem (5.31) does not have a unique solution because its denominator is not strictly convex [SS03]. Nevertheless, by using the convex analysis, an even higher convergence order might be obtained for the

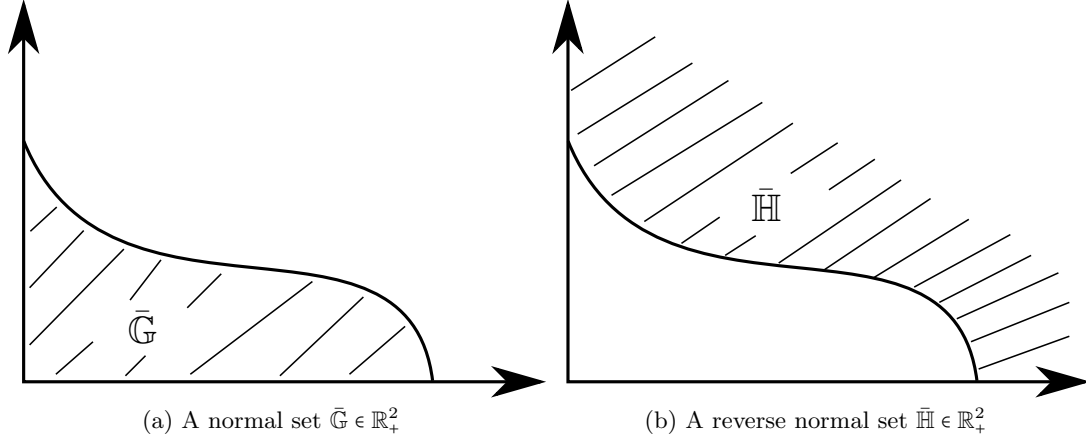


Figure C.1: An illustration of a normal set $\bar{\mathbb{G}} \in \mathbb{R}_+^2$ and a reverse normal set $\bar{\mathbb{H}} \in \mathbb{R}_+^2$.

DT-2 algorithm as in [BC87], which means a better than linear convergence speed in general. However, this is out of the scope of this thesis.

C.7 Monotonic optimization and the polyblock algorithm

This appendix devotes to the introduction of the monotonic optimization problem and its solution via polyblock algorithm, which are applied in Section 5.7.

C.7.1 Monotonic optimization

According to [Tuy00], a set $\bar{\mathbb{G}} \in \mathbb{R}_+^n$ is called *normal* if $\mathbf{y} \in \bar{\mathbb{G}}$ also implies that the hypercube $[\mathbf{0}, \mathbf{y}] \in \bar{\mathbb{G}}$, as depicted in Figure C.1a. A set $\bar{\mathbb{H}} \in \mathbb{R}_+^n$ is called *reverse normal* if $\mathbf{y} \in \bar{\mathbb{H}}$ and $\mathbf{y}' \geq \mathbf{y}$ also implies that $\mathbf{y}' \in \bar{\mathbb{H}}$, as depicted in Figure C.1b. A function $f : \mathbb{R}_+^n \rightarrow \mathbb{R}_+$ is an increasing function if $\mathbf{y}' \geq \mathbf{y}$ implies $f(\mathbf{y}') \geq f(\mathbf{y})$, $\forall \mathbf{y}'$.

Maximizing an increasing function over the intersection of a normal set and an inverse normal set, i.e.,

$$\max_{\mathbf{y}} f(\mathbf{y}), \quad \text{s. t. } \mathbf{y} \in \bar{\mathbb{G}} \cap \bar{\mathbb{H}}, \quad (\text{C.42})$$

is a monotonic optimization problem [Tuy00].

For problem (5.45), $y_m = \frac{\mathbf{w}^H \bar{\mathbf{E}}_m \mathbf{w}}{\mathbf{w}^H \mathbf{F}_m \mathbf{w}}$, $\forall m$ and $\mathbf{w} \in \mathbb{F}$, represents the Rayleigh quotient. Hence, it is bounded between $\min_m \lambda_{\min}\{\mathbf{F}_m^{-1} \bar{\mathbf{E}}_m\}$ and $\min_m \lambda_{\max}\{\mathbf{F}_m^{-1} \bar{\mathbf{E}}_m\}$ ². Thereby, the definitions of \mathbb{G} and \mathbb{L} satisfy the definitions of the normal set and the inverse normal set, respectively. It

² $y_m \geq 1$ because it is equal to $1 + \gamma_m$, $\forall m$.

is then straightforward to conclude that problem (5.45) is a monotonic optimization problem since its cost function $\Phi(\mathbf{y})$ is an increasing function.

C.7.2 Polyblock algorithm

The polyblock algorithm is a unified algorithm to solve the monotonic optimization problem [JL10], [Tuy00], [UB12]. A polyblock \mathbb{P} with vertex set $\mathbb{T} \in \mathbb{R}_+^n$ is simply a union of a finite number of hypercubes $[\mathbf{0}, \mathbf{z}]$, $\mathbf{z} \in \mathbb{T}$. A polyblock is dominated by its proper vertices, where a vertex $\mathbf{z} \in \mathbb{T}$ is proper if there is no $\mathbf{z}' \neq \mathbf{z}$ and $\mathbf{z}' \geq \mathbf{z}$, $\mathbf{z}' \in \mathbb{T}$. Since $\bar{\mathbb{G}}$ is a normal set there exists a polyblock $\mathbb{P}^{(1)}$ such that $\bar{\mathbb{G}} \subset \mathbb{P}^{(1)}$. Moreover, we can construct a nested sequence of polyblocks which approximate $\bar{\mathbb{G}}$ from above, i.e., an iteratively refined outer approximation of $\bar{\mathbb{G}}$ is created starting from $p = 1$

$$\mathbb{P}^{(1)} \supset \dots \supset \mathbb{P}^{(p)} \supseteq \bar{\mathbb{G}}.$$

If we replace $\bar{\mathbb{G}}$ by $\mathbb{P}^{(p)}$ in (C.42) and obtain

$$\max_{\mathbf{y}} f(\mathbf{y}), \quad \text{s. t.} \quad \mathbf{y} \in \mathbb{P}^{(p)} \cap \bar{\mathbb{H}}, \quad (\text{C.43})$$

then the maximizer $\mathbf{y}_{\text{opt}}^{(p)}$ to (C.43) should be attained at one proper vertex of the polyblock $\mathbb{P}^{(p)}$, say $\mathbf{z}_{\text{opt}}^{(p)}$, due to the monotonicity of f [Tuy00]. It will be also the global optimizer if $\mathbf{z}_{\text{opt}}^{(p)} \in \bar{\mathbb{G}}$. In other words, the global maximum of (C.42), if it exists, is attained on $\partial^+ \bar{\mathbb{G}}$, i.e., the upper boundary of $\bar{\mathbb{G}}$ [Tuy00]. However, in general, $\mathbf{z}_{\text{opt}}^{(p)}$ will lie outside of $\bar{\mathbb{G}}$ since the polyblock is just an outer approximation of $\bar{\mathbb{G}}$. In such a case, we need to create a new polyblock $\mathbb{P}^{(p+1)}$ which satisfies

$$\mathbb{P}^{(p+1)} \supset \mathbb{P}^{(p)} \supseteq \bar{\mathbb{G}}.$$

According to [Tuy00], this can be achieved using the following procedure. First, finding the unique intersection point $\hat{\mathbf{z}}^{(p)}$ between $\partial^+ \bar{\mathbb{G}}$ and the line segment connecting the origin and $\mathbf{z}_{\text{opt}}^{(p)}$ via

$$\hat{\mathbf{z}}^{(p)} = \mu^{(p)} \mathbf{z}_{\text{opt}}^{(p)}$$

with

$$\mu^{(p)} = \max_{\mu \in (0,1]} \mu, \quad \text{s. t.} \quad \mu \mathbf{z}_{\text{opt}}^{(p)} \in \bar{\mathbb{G}} \cap \bar{\mathbb{H}}. \quad (\text{C.44})$$

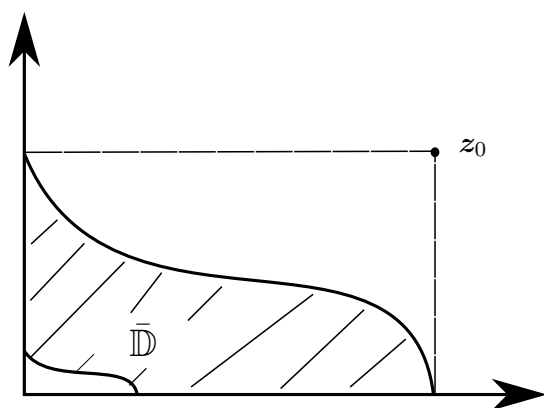
Then the current objective value is given by $f(\hat{\mathbf{z}}^{(p)})$ and the current best objective value is calculated as $f_{\text{opt}}^{(p)} = \max(f_{\text{opt}}^{(p-1)}, f(\hat{\mathbf{z}}^{(p)}))$. Second, let $\mathbb{T}^{(p)}$ be the proper vertices of $\mathbb{P}^{(p)}$ and

$\tilde{\mathbb{T}}^{(p)} \subset \mathbb{T}^{(p)}$ such that $\mathbf{z}_{\text{opt}}^{(p)} \in \tilde{\mathbb{T}}^{(p)} \subset \{\tilde{\mathbf{z}} \in \mathbb{T}^{(p)} \mid \tilde{\mathbf{z}} \succ \hat{\mathbf{z}}^{(p)}\}$. We replace all the $\mathbf{z} \in \tilde{\mathbb{T}}^{(p)}$ from $\mathbb{T}^{(p)}$ by points

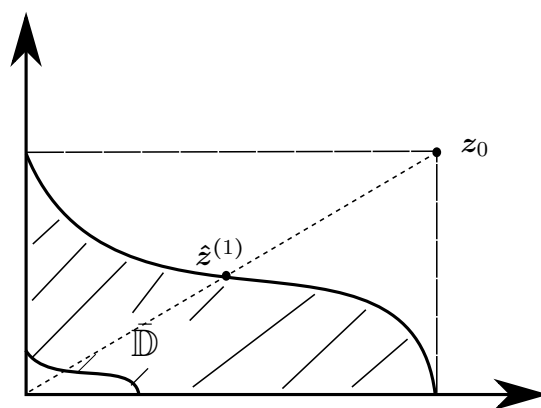
$$\bar{\mathbf{z}}_i = \mathbf{z} - (z_i - \hat{z}_i^{(p)})\mathbf{e}_i, \forall i \in \{1, \dots, n\}. \quad (\text{C.45})$$

Afterwards, we remove all improper elements as well as all points not belonging to $\bar{\mathbb{H}}$. Then the remaining vertex set is the proper vertex $\tilde{\mathbb{T}}^{(p+1)}$ for our new polyblock $\mathbb{P}^{(p+1)}$. This algorithm, which is referred to as the polyblock outer approximation algorithm in [Tuy00], runs iteratively until $\tilde{\mathbb{T}}^{(p+1)} = \emptyset$ or an ϵ -optimal solution is found. When the computational complexity is concerned, an ϵ -optimal solution is preferred. To this end, during the construction of $\tilde{\mathbb{T}}^{(p+1)}$, it is practical to discard vertices $\tilde{\mathbf{z}} \in \tilde{\mathbb{T}}^{(p+1)}$ and $f(\tilde{\mathbf{z}}) \leq (1 + \epsilon)f_{\text{opt}}^{(p)}$.

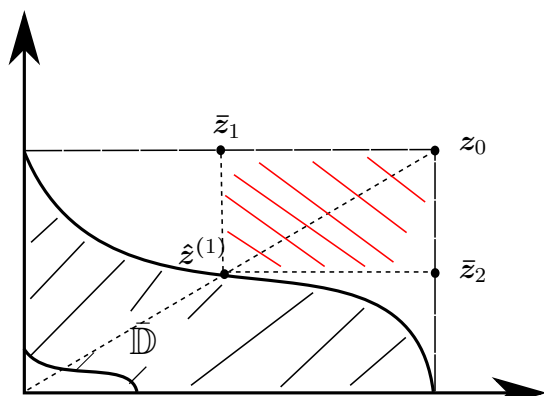
An example of the polyblock approach is shown in Figure C.2. The original feasible region is given by $\bar{\mathbb{D}} = \bar{\mathbb{G}} \cap \bar{\mathbb{H}} \in \mathbb{R}_+^2$ and an initial vertex set is $\mathbb{T}^{(1)} = \{\mathbf{z}_0\}$. As seen from Figure C.2a, the rectangular/polyblock defined by $[\mathbf{0}, \mathbf{z}_0]$ approximates $\bar{\mathbb{D}}$ from the outside. The maximizer $\mathbf{z}_{\text{opt}}^{(1)}$ from the current vertex set is \mathbf{z}_0 . Since $\mathbf{z}_{\text{opt}}^{(1)}$ does not lie on the boundary of $\bar{\mathbb{D}}$, in the second step (as depicted in Figure C.2b), the unique intersection $\hat{\mathbf{z}}^{(1)}$ between the boundary of $\bar{\mathbb{D}}$ and the line segment which connects the origin and $\mathbf{z}_{\text{opt}}^{(1)} = \mathbf{z}_0$ has to be computed. In the third step (as depicted in Figure C.2c), two new vertices $\bar{\mathbf{z}}_1$ and $\bar{\mathbf{z}}_2$ are computed using equation (C.45). The region, which are decided by the vectors $\hat{\mathbf{z}}^{(1)}$, \mathbf{z}_0 , $\bar{\mathbf{z}}_1$, and $\bar{\mathbf{z}}_2$, are marked red in Figure C.2c. It is infeasible for the original problem and thus should be discarded. Finally, the new vertex set $\tilde{\mathbb{T}}^{(2)} = \{\bar{\mathbf{z}}_1, \bar{\mathbf{z}}_2\}$ is decided as in Figure C.2d and thus a new polyblock is constructed. This approach continues until the global optimal is found.



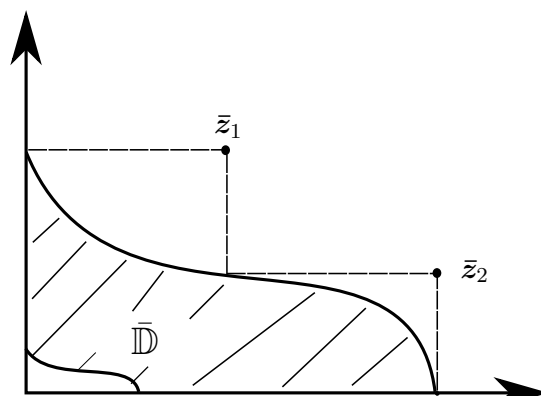
(a) Deciding the maximizer $z_{\text{opt}}^{(1)}$ from the current vertex set $\mathbb{T}^{(1)} = \{z_0\}$. Clearly, $z_{\text{opt}}^{(1)} = z_0$.



(b) Finding the unique intersection point $\hat{z}^{(1)}$.



(c) Replacing z_0 with new vertices \bar{z}_1 and \bar{z}_2 .



(d) Constructing the new vertex set $\hat{\mathbb{T}}^{(2)} = \{\bar{z}_1, \bar{z}_2\}$.

Figure C.2: An illustration of the polyblock approach for a feasible region of $\bar{\mathbb{D}} = \bar{\mathbb{G}} \cap \bar{\mathbb{H}} \in \mathbb{R}_+^2$. The initial vertex set is $\mathbb{T}^{(1)} = \{z_0\}$.

Appendix D

Proofs and derivations for Part II

D.1 Proof of Proposition 8.3.1

The statement i) of Proposition 8.3.1 is based on the following findings. First, at least one of the constraints has to be active at the optimality. Otherwise, the optimal solution $\mathbf{w}_{\text{opt},i}$ can be scaled up such that one of the constraints is satisfied with equality. The increasing of $\mathbf{w}_{\text{opt},i}$ will increase the objective value and thus contradicts the optimality. Second, at the optimality of problem (8.6), $\forall i$, it cannot happen that the SI power constraint is active and the transmit power constraint is inactive. This can be verified using proof by contradiction.

Define the orthogonal complement of $\mathbf{h}_{ji}^H \in \mathbb{C}^{M_t}$ as $\mathbf{\Pi}_{\mathbf{h}_{ji}^H}^\perp = \mathbf{I}_{M_t} - \frac{\mathbf{h}_{ji}^H \mathbf{h}_{ji}}{\|\mathbf{h}_{ji}\|^2} \in \mathbb{C}^{M_t \times M_t}$. Without loss of generality, we write the optimal $\mathbf{w}_{\text{opt},i}$ as

$$\mathbf{w}_{\text{opt},i} = \mathbf{h}_{ji}^H \cdot a_i + \mathbf{\Pi}_{\mathbf{h}_{ji}^H}^\perp \cdot \mathbf{b}_i \in \mathbb{C}^{M_t} \quad (\text{D.1})$$

where $a_i \in \mathbb{C}$ and $\mathbf{b}_i \in \mathbb{C}^{M_t}$. Assume that at the optimality of problem (8.6) the transmit power constraint is inactive and the SI power constraint is active. Inserting $\mathbf{w}_{\text{opt},i}$ into the two constraints and the objective function we get the following equations

$$\eta_i \mathbf{w}_{\text{opt},i}^H \mathbf{h}_{ji}^H \mathbf{h}_{ji} \mathbf{w}_{\text{opt},i} = \eta_i \cdot \|\mathbf{h}_{ji}\|^2 \cdot |a_i|^2 = P_i^{(\text{TH})}, \quad (\text{D.2})$$

$$\mathbf{w}_{\text{opt},i}^H \mathbf{w}_{\text{opt},i} = \|\mathbf{h}_{ji}\|^2 |a_i|^2 + \|\mathbf{b}_i\|^2 < \epsilon_i P_i^{(\text{TH})}, \quad (\text{D.3})$$

and

$$\mathbf{w}_{\text{opt},i}^H \mathbf{h}_{ii}^H \mathbf{h}_{ii} \mathbf{w}_{\text{opt},i} = |\mathbf{h}_{ii} \mathbf{h}_{ji}^H \cdot a_i + \mathbf{h}_{ii} \mathbf{\Pi}_{\mathbf{h}_{ji}^H}^\perp \cdot \mathbf{b}_i|^2 \leq \left(\left| \mathbf{h}_{ii} \mathbf{h}_{ji}^H \cdot a_i \right| + \left| \mathbf{h}_{ii} \mathbf{\Pi}_{\mathbf{h}_{ji}^H}^\perp \cdot \mathbf{b}_i \right| \right)^2. \quad (\text{D.4})$$

According to the triangular inequality, the maximum is obtained if the two complex numbers have the same phase, i.e., $\arg \{ \mathbf{h}_{ii} \mathbf{h}_{ji}^H \cdot a_i \} = \arg \{ \mathbf{h}_{ii} \mathbf{\Pi}_{\mathbf{h}_{ji}^H}^\perp \cdot \mathbf{b}_i \}$, where $\arg \{ \cdot \}$ obtains the angle of a complex number.

Since $|a_i|^2$ is fixed via the active transmit power constraint, it is straightforward to see that scaling up $\|\mathbf{b}_i\|$ will also increase the optimal value which contradicts the optimality. Therefore,

we conclude that the transmit power constraint has to be active if the SI power constraint is active.

The statement ii) of Proposition 8.3.1 comes directly from the fact that if the SI power constraint is inactive, problem (8.6) degenerates to a classical HD MISO setup.

D.2 Proof of Corollary 8.3.2

Using the definition of $\mathbf{w}_{\text{opt},i}$ from equation (D.1) and the fact that the SI constraint is satisfied with equality at the optimality, we conclude that the only uncertainty regarding a_i is its phase α_i , i.e.,

$$a_i = \sqrt{\frac{P_i^{(\text{TH})}}{\eta_i \cdot \|\mathbf{h}_{ji}\|^4}} e^{j\alpha_i}. \quad (\text{D.5})$$

Moreover, we conclude the optimization over $\mathbf{w}_{\text{opt},i}$ can be achieved by first optimizing \mathbf{b}_i and then α_i . Our conclusion is based on the following two statements:

1. The two active constraints do not depend on α_i .
2. The objective function of (8.6) satisfies the inequality (D.4). According to the triangular inequality, the maximum is obtained if $\arg\{\mathbf{h}_{ii}\mathbf{h}_{ji}^H \cdot a_i\} = \arg\{\mathbf{h}_{ii}\mathbf{\Pi}_{\mathbf{h}_{ji}^H}^\perp \cdot \mathbf{b}_i\}$. That is, if an optimal $\mathbf{b}_{\text{opt},i}$ is obtained, the optimal phase of a_i is computed as

$$\alpha_{\text{opt},i} = \arg\left\{ \frac{\mathbf{h}_{ii}\mathbf{\Pi}_{\mathbf{h}_{ji}^H}^\perp \cdot \mathbf{b}_{\text{opt},i}}{\mathbf{h}_{ii}\mathbf{h}_{ji}^H} \right\} \quad (\text{D.6})$$

Therefore, problem (8.6) with two active constraints can be decomposed into two equivalent problems, i.e., first finding optimal \mathbf{b}_i and then adjusting α_i . Without loss of generality, we set $\alpha_i = 0$. Thereby, problem (8.6) simplifies to the following optimization problem

$$\begin{aligned} \max_{\mathbf{b}_i} \quad & \mathbf{b}_i^H \mathbf{z}_{v,i}^H \mathbf{z}_{v,i} \mathbf{b}_i + z_{s,i}^* \mathbf{z}_{v,i} \mathbf{b}_i + \mathbf{b}_i^H \mathbf{z}_{v,i}^H z_{s,i} \\ \text{subject to} \quad & \mathbf{b}_i^H \mathbf{b}_i = \left(\epsilon_i - \frac{1}{\eta_i \|\mathbf{h}_{ji}\|^2} \right) P_i^{(\text{TH})} \end{aligned} \quad (\text{D.7})$$

where $\mathbf{z}_{v,i} = \mathbf{h}_{ii}\mathbf{\Pi}_{\mathbf{h}_{ji}^H}^\perp$ and $z_{s,i} = \frac{\mathbf{h}_{ii}\mathbf{h}_{ji}^H}{\|\mathbf{h}_{ji}\|^2} \sqrt{\frac{P_i^{(\text{TH})}}{\eta_i}}$.

Problem (D.7) can be solved using the Lagrangian multiplier method. The Lagrangian of problem (D.7) is expressed as

$$\mathcal{L}(\mathbf{b}_i, v_i) = \mathbf{b}_i^H \mathbf{z}_{v,i}^H \mathbf{z}_{v,i} \mathbf{b}_i + z_{s,i}^* \mathbf{z}_{v,i} \mathbf{b}_i + \mathbf{b}_i^H \mathbf{z}_{v,i}^H z_{s,i} - v_i \left(\mathbf{b}_i^H \mathbf{b}_i - \left(\epsilon_i - \frac{1}{\eta_i \|\mathbf{h}_{ji}\|^2} \right) P_i^{(\text{TH})} \right) \quad (\text{D.8})$$

where v_i represents the Lagrangian multiplier. Taking the first-order derivatives over \mathbf{b}_i^* and v_i and setting them to zero, we get

$$\mathbf{b}_i = (v_i \mathbf{I}_{M_t} - \mathbf{z}_{v,i}^H \mathbf{z}_{v,i})^{-1} \mathbf{z}_{v,i}^H z_{s,i} \quad (\text{D.9a})$$

$$\mathbf{b}_i^H \mathbf{b}_i = \left(\epsilon_i - \frac{1}{\eta_i \|\mathbf{h}_{ji}\|^2} \right) P_i^{(\text{TH})}. \quad (\text{D.9b})$$

Inserting (D.9a) into (D.9b), we have

$$\begin{aligned} \mathbf{b}_i^H \mathbf{b}_i &= \mathbf{z}_{v,i} z_{s,i}^* (v_i \mathbf{I}_{M_t} - \mathbf{z}_{v,i}^H \mathbf{z}_{v,i})^{-H} (v_i \mathbf{I}_{M_t} - \mathbf{z}_{v,i}^H \mathbf{z}_{v,i})^{-1} \mathbf{z}_{v,i}^H z_{s,i} \\ &= |z_{s,i}|^2 \text{Tr} \left\{ (v_i \mathbf{I}_{M_t} - \mathbf{z}_{v,i}^H \mathbf{z}_{v,i})^{-H} (v_i \mathbf{I}_{M_t} - \mathbf{z}_{v,i}^H \mathbf{z}_{v,i})^{-1} \mathbf{z}_{v,i}^H \mathbf{z}_{v,i} \right\} \\ &= |z_{s,i}|^2 \text{Tr} \left\{ (v_i \mathbf{I}_{M_t} - \mathbf{z}_{v,i}^H \mathbf{z}_{v,i})^{-2} \mathbf{z}_{v,i}^H \mathbf{z}_{v,i} \right\} \\ &= \frac{|z_{s,i}|^2 \|\mathbf{z}_{v,i}\|^2}{(v_i - \|\mathbf{z}_{v,i}\|^2)^2} = \left(\epsilon_i - \frac{1}{\eta_i \|\mathbf{h}_{ji}\|^2} \right) P_i^{(\text{TH})}. \end{aligned}$$

Although there are two roots in the above equation, the optimal v_i is given by

$$v_{\text{opt},i} = \|\mathbf{z}_{v,i}\|^2 - \frac{|z_{s,i}| \|\mathbf{z}_{v,i}\|}{\sqrt{\left(\epsilon_i - \frac{1}{\eta_i \|\mathbf{h}_{ji}\|^2} \right) P_i^{(\text{TH})}}} \quad (\text{D.10})$$

because the cost function in (D.7) has to be maximized. The optimal $\mathbf{b}_{\text{opt},i}$ is then calculated using (D.9a).

D.3 Proof of Proposition 8.3.4

In this appendix, we derive analytic solutions for a special case of the FD MIMO system, i.e., $M_r = M_t = 2$ and both the transmit power constraint and the SI constraint are satisfied with equality. Define $\mathbf{A}_{ii} = \mathbf{H}_{ii}^H \mathbf{H}_{ii} / \sigma_n^2$ and $\mathbf{B}_{ji} = \mathbf{H}_{ji}^H \mathbf{H}_{ji}$. Mathematically, for each $\{i, j\} \in \{1, 2\}$ and $i \neq j$, we solve the following optimization problem

$$\min_{\mathbf{Q}_i} -\log(|\mathbf{I}_M + \mathbf{A}_{ii} \mathbf{Q}_i|)$$

$$\begin{aligned} \text{s. t. } \mathbf{Q}_i &\geq 0, \quad \text{Tr}\{\mathbf{Q}_i\} = \epsilon_i P_i^{(\text{TH})} \\ \text{Tr}\{\eta_i \mathbf{B}_{ji} \mathbf{Q}_i\} &= P_i^{(\text{TH})}. \end{aligned} \quad (\text{D.11})$$

Problem (D.11) is convex with respect to \mathbf{Q}_i . The analytic solutions to problem (D.11) when $M_r = M_t = 2$ can be obtained using the Lagrangian multiplier method. The Lagrangian of problem (D.11) is given by

$$\mathcal{L}(\mathbf{Q}_i, \rho_i, v_i) = -\log(|\mathbf{I}_M + \mathbf{A}_{ii} \mathbf{Q}_i|) + \rho_i (\text{Tr}\{\mathbf{Q}_i\} - \epsilon_i P_i^{(\text{TH})}) + v_i (\text{Tr}\{\eta_i \mathbf{B}_{ji} \mathbf{Q}_i\} - P_i^{(\text{TH})}), \quad (\text{D.12})$$

where ρ_i and v_i denote the Lagrangian multipliers. To obtain the optimal solution for the original problem (D.11), an additional constraint on \mathbf{Q}_i has to be taken into account, i.e., \mathbf{Q}_i has to be Hermitian positive semidefinite. However, to make the Lagrangian method solvable, we propose to first relax \mathbf{Q}_i to be a Hermitian matrix, which is a larger set than the set of Hermitian positive semidefinite matrices. When $\mathbf{Q}_i = \mathbf{Q}_i^H$, the following rule from [Hj011] can be used, i.e.,

$$\frac{\partial \mathcal{L}}{\partial \mathbf{Q}_i^*} = \frac{\partial \mathcal{L}}{\partial \mathbf{Q}_i} + \left(\frac{\partial \mathcal{L}}{\partial \mathbf{Q}_i} \right)^T. \quad (\text{D.13})$$

Moreover, utilizing the fact that $d(\log|\mathbf{\Gamma}|) = \text{tr}\{\mathbf{\Gamma}^{-1}d\mathbf{\Gamma}\}$, $d\{\text{tr}\{\mathbf{\Gamma}\}\} = \text{tr}\{d\mathbf{\Gamma}\}$ [Hj011], the first-order derivative of the Lagrangian with respect to \mathbf{Q}_i^* is computed as

$$\left. \frac{\partial \mathcal{L}(\mathbf{Q}_i, \rho_i, v_i)}{\partial \mathbf{Q}_i^*} \right|_{\mathbf{Q}_i = \mathbf{Q}_i^H} = -(\mathbf{I}_{M_t} + \mathbf{A}_{ii} \mathbf{Q}_i)^{-1} \mathbf{A}_{ii} + \rho_i \mathbf{I}_{M_t} + v_i \eta_i \mathbf{B}_{ji}. \quad (\text{D.14})$$

Then by taking the first-order derivatives over \mathbf{Q}_i^* , ρ_i and v_i , respectively, and setting them to zero, we get

$$\mathbf{Q}_i = (\rho_i \mathbf{I}_{M_t} + v_i \eta_i \mathbf{B}_{ji})^{-1} - \mathbf{A}_{ii}^{-1} \quad (\text{D.15a})$$

$$\text{Tr}\{\mathbf{Q}_i\} = \epsilon_i P_i^{(\text{TH})} \quad (\text{D.15b})$$

$$\text{Tr}\{\eta_i \mathbf{B}_{ji} \mathbf{Q}_i\} = P_i^{(\text{TH})}. \quad (\text{D.15c})$$

Define the EVD of $\mathbf{A}_{ii} = \mathbf{U}_{ii} \cdot \text{diag}\{\boldsymbol{\lambda}_{ii}\} \mathbf{U}_{ii}^H$ and $\mathbf{B}_{ji} = \mathbf{U}_{ji} \cdot \text{diag}\{\boldsymbol{\lambda}_{ji}\} \mathbf{U}_{ji}^H$, where $\boldsymbol{\lambda}_{ii} = [\lambda_{ii,1}, \dots, \lambda_{ii,M_t}]^T$ and $\boldsymbol{\lambda}_{ji} = [\lambda_{ji,1}, \dots, \lambda_{ji,M_t}]^T$ are the corresponding eigenvalue profiles of \mathbf{A}_{ii} and \mathbf{B}_{ji} , respectively. Inserting (D.15a) into (D.15b), the following expressions are obtained

$$\text{Tr}\{(\rho_i \mathbf{I}_{M_t} + v_i \eta_i \mathbf{B}_{ji})^{-1} - \mathbf{A}_{ii}^{-1}\}$$

$$\begin{aligned}
 &= \text{Tr}\{(\rho_i \mathbf{I}_{M_t} + v_i \eta_i \mathbf{B}_{ji})^{-1}\} - \text{Tr}\{\mathbf{A}_{ii}^{-1}\} \\
 &= \text{Tr}\{\mathbf{U}_{ji}(\rho_i \mathbf{I}_{M_t} + v_i \eta_i \text{diag}\{\boldsymbol{\lambda}_{ji}\})^{-1} \mathbf{U}_{ji}^H\} - \text{Tr}\{\mathbf{U}_{ii} \text{diag}\{\boldsymbol{\lambda}_{ii}\}^{-1} \mathbf{U}_{ii}^H\} \\
 &= \sum_{m=1}^{M_t} \left((\rho_i + v_i \lambda_{ji,m})^{-1} - \lambda_{ii,m}^{-1} \right) = \epsilon_i P_i^{(\text{TH})}. \tag{D.16}
 \end{aligned}$$

Similarly, inserting (D.15a) into (D.15c), we obtain the following equation

$$\sum_{m=1}^{M_t} \left(\lambda_{ji,m} (\rho_i + v_i \lambda_{ji,m})^{-1} \right) - \text{Tr}\{\mathbf{B}_{ji} \mathbf{A}_{ii}^{-1}\} = P_i^{(\text{TH})} / \eta_i. \tag{D.17}$$

Equations (D.16) and (D.17) are polynomial equations with respect to ρ_i and v_i . They are solvable but closed-form expressions for the roots of the polynomial equations are available for specific polynomial order, e.g., the second order. Moreover, after obtaining ρ_i and v_i , equation (D.15a) has to be calculated. If the obtained \mathbf{Q}_i is positive semidefinite, the optimal solution to the original problem (D.11) is found. If the obtained \mathbf{Q}_i is not positive semidefinite, it implies that at least one of the eigenvalues of \mathbf{Q}_i is zero. A reformulation of the Lagrangian has to be done. Therefore, an analytic solution is in general difficult to obtain when both constraints are active. Nevertheless, in the following we derive analytical solutions for $M_r = M_t = 2$. When $M_t = 2$, by combining (D.16) and (D.17), ρ_i and v_i are computed by

$$\begin{aligned}
 \rho_i &= \frac{\lambda_{ji,1}}{\lambda_{ji,1} \tilde{z}_i - \bar{z}_i} + \frac{\lambda_{ji,2}}{\lambda_{ji,2} \tilde{z}_i - \bar{z}_i} \\
 v_i &= \frac{1}{\bar{z}_i - \lambda_{ji,1} \tilde{z}_i} + \frac{1}{\bar{z}_i - \lambda_{ji,2} \tilde{z}_i} \tag{D.18}
 \end{aligned}$$

where $\tilde{z}_i = \epsilon_i P_i^{(\text{TH})} + \sum_{m=1}^2 \lambda_{ii,m}^{-1}$ and $\bar{z}_i = P_i^{(\text{TH})} / \eta_i + \text{Tr}\{\mathbf{B}_{ji} \mathbf{A}_{ii}^{-1}\}$. If the obtained \mathbf{Q}_i is not positive semidefinite, one of its eigenvalues is zero, i.e., \mathbf{Q}_i is a rank-1 matrix. Without loss of generality, we define $\mathbf{Q}_i = \mathbf{w}_i \mathbf{w}_i^H$. Problem (D.11) can be reformulated into the following equivalent problem

$$\begin{aligned}
 \max_{\mathbf{w}_i} \quad & \mathbf{w}_i^H \mathbf{A}_{ii} \mathbf{w}_i \\
 \text{s. t.} \quad & \mathbf{w}_i^H \mathbf{w}_i = \epsilon_i P_i^{(\text{TH})}, \quad \eta_i \mathbf{w}_i^H \mathbf{B}_{ji} \mathbf{w}_i = P_i^{(\text{TH})}. \tag{D.19}
 \end{aligned}$$

The covariance matrix \mathbf{B}_{ji} is full rank and thus \mathbf{U}_{ji} is an orthonormal basis of the two-

dimensional space. Thereby, without loss of generality, we define

$$\mathbf{w}_i = \mathbf{U}_{ji} \mathbf{v}_i = \mathbf{U}_{ji} \begin{bmatrix} |v_{i,1}| & 0 \\ 0 & |v_{i,2}| \end{bmatrix} \begin{bmatrix} e^{j\alpha_i} \\ e^{j\beta_i} \end{bmatrix}, \quad (\text{D.20})$$

where $|v_{i,1}|$, $|v_{i,2}|$ and α_i , β_i , represent the corresponding amplitudes and phases of the elements of the vector $\mathbf{v}_i \in \mathbb{C}^2$. Inserting (D.20) into the two constraints of (D.19), we obtain

$$\begin{aligned} |v_{i,1}|^2 + |v_{i,2}|^2 &= \epsilon_i P_i^{(\text{TH})} \\ \lambda_{ji,1} |v_{i,1}|^2 + \lambda_{ji,2} |v_{i,2}|^2 &= P_i^{(\text{TH})} / \eta_i. \end{aligned} \quad (\text{D.21})$$

Thereby, the amplitudes of the elements of \mathbf{v}_i are decided by $|v_{i,1}| = \sqrt{\frac{P_i^{(\text{TH})} / \eta_i - \lambda_{ji,2} \epsilon_i P_i^{(\text{TH})}}{\lambda_{ji,1} - \lambda_{ji,2}}}$ and $|v_{i,2}| = \sqrt{\frac{\lambda_{ji,1} \epsilon_i P_i^{(\text{TH})} - P_i^{(\text{TH})} / \eta_i}{\lambda_{ji,1} - \lambda_{ji,2}}}$. Define $\mathbf{U}_{ji}^H \mathbf{A}_{ii} \mathbf{U}_{ji} = \begin{bmatrix} a_{11} & a_{12} \\ a_{12}^* & a_{22} \end{bmatrix}$ where $a_{11} \in \mathbb{R}$, $a_{22} \in \mathbb{R}$, and $a_{12} \in \mathbb{C}$. Inserting (D.20) into the objective function of (D.19), after some algebraic manipulation, we get

$$\mathbf{w}_i^H \mathbf{A}_{ii} \mathbf{w}_i = a_{11} |v_{i,1}|^2 + e^{j(\beta_i - \alpha_i)} \cdot |v_{i,1}| |v_{i,2}| a_{12} + e^{j(\alpha_i - \beta_i)} \cdot |v_{i,1}| |v_{i,2}| a_{12}^* + a_{22} |v_{i,2}|^2. \quad (\text{D.22})$$

Clearly, (D.22) is optimized if $\alpha_i - \beta_i = \arg \{a_{12}\}$. Hence, without loss of generality, we set $\beta_i = 0$ and thus $\alpha_i = \arg \{a_{12}\}$.

Bibliography

Publications and Technical Documents as Co- or First Author

- [ABZ⁺12] L. Anchora, L. Badia, H. Zhang, T. Fahldieck, J. Zhang, M. Szydelko, M. Schubert, and M. Haardt, "Resource allocation and management in multi-operator cellular networks with shared physical resources," in *Proc. Int. Symp. Wireless Communication Systems (ISWCS)*, Paris, France, Aug. 2012.
- [CLZ⁺12] Y. Cheng, S. Li, J. Zhang, F. Roemer, M. Haardt, Y. Zhou, and M. Dong, "Linear precoding-based geometric mean decomposition (LP-GMD) for multi-user MIMO systems," in *Proc. Int. Symp. Wireless Communication Systems (ISWCS)*, Paris, France, Aug. 2012.
- [CLZ⁺13] —, "An efficient and flexible transmission strategy for the multi-carrier multi-user MIMO downlink," *IEEE Trans. Veh. Technol.*, vol. 99, no. 9, Sep. 2013.
- [CZHH14] A. C. Cirik, J. Zhang, M. Haardt, and Y. Hua, "Sum-rate maximization for bi-directional full-duplex MIMO systems under multiple linear constraints," in *Proc. 15th Int. Workshop Signal Processing Advances in Wireless Communications (SPAWC 2014)*, Toronto, Canada, Jun. 2014.
- [DCL⁺13a] M. Dong, Y. Cheng, S. Li, F. Roemer, J. Zhang, B. Song, and M. Haardt, "Linear precoding method and device for communication system," Patent WO/2013/029 561, 03 07, 2013. [Online]. Available: <http://patentscope.wipo.int/search/en/WO2013029561>
- [DCL⁺13b] —, "Linear precoding method and device for multi-user multiple-input multiple-output systems," Patent WO/2013/034 088, 03 14, 2013. [Online]. Available: <http://patentscope.wipo.int/search/en/WO2013034088>
- [DCL⁺13c] —, "Method for SDMA transmission in multicarrier MU MIMO system and base station," Patent WO/2013/034 093, 03 14, 2013. [Online]. Available: <http://patentscope.wipo.int/search/en/WO2013034093>
- [GVJ⁺13a] J. Gao, S. A. Vorobyov, H. Jiang, J. Zhang, and M. Haardt, "Sum-rate maximization with minimum power consumption for MIMO DF two-way relaying: Part I-relay optimization," *IEEE Trans. Signal Process.*, vol. 61, no. 7, Jul. 2013.
- [GVJ⁺13b] —, "Sum-rate maximization with minimum power consumption for MIMO DF two-way relaying: Part II-network optimization," *IEEE Trans. Signal Process.*, vol. 61, no. 7, Jul. 2013.

- [GZV⁺12] J. Gao, J. Zhang, S. A. Vorobyov, H. Jiang, and M. Haardt, "Power allocation/beamforming for DF MIMO two-way relaying: Relay and network optimization," in *Proc. IEEE Global Communications Conf. (Globecom)*, Anaheim, CA, Dec. 2012.
- [LCZ⁺12] S. Li, Y. Cheng, J. Zhang, F. Roemer, B. Song, M. Haardt, Y. Zhou, and M. Dong, "Efficient spatial scheduling and precoding algorithms for MC MU MIMO system," in *Proc. Int. Symp. Wireless Communication Systems (ISWCS)*, Paris, France, Aug. 2012.
- [LZR⁺11] J. Li, J. Zhang, F. Roemer, M. Haardt, C. Scheunert, E. Jorswieck, M. Hekrdla, and J. Sykora, "Relay-assisted spectrum and infrastructure sharing between multiple operators," in *Proc. Future Network and Mobile Summit 2011*, Warsaw, Poland, Jun. 2011.
- [RZHJ10] F. Roemer, J. Zhang, M. Haardt, and E. Jorswieck, "Spectrum and infrastructure sharing in wireless networks: A case study with relay-assisted communications," in *Proc. Future Network and Mobile Summit 2010*, Florence, Italy, Jun. 2010.
- [TZH14] O. Taghizadeh, J. Zhang, and M. Haardt, "Transmit beamforming aided one-way MIMO full-duplex relaying systems with limited dynamic range," 2014, to be submitted to *IEEE Trans. Veh. Technol.*
- [ZBR⁺12] J. Zhang, N. Bornhorst, F. Roemer, M. Haardt, and M. Pesavento, "Optimal and suboptimal beamforming for multi-operator two-way relaying with a MIMO amplify-and-forward relay," in *Proc. 16th ITG Workshop on Smart Antennas (WSA)*, Dresden, Germany, Mar. 2012.
- [ZH13] J. Zhang and M. Haardt, "Widely linear signal processing for two-way relaying with MIMO amplify and forward relays," in *Proc. Int. Symp. Wireless Communication Systems (ISWCS)*, Ilmenau, Germany, Aug. 2013.
- [ZHJH14a] J. Zhang, Z. K. M. Ho, E. Jorswieck, and M. Haardt, "Interference neutralization for non-regenerative two-way relaying networks—Part I: feasibility," 2014, submitted to *IEEE Trans. Signal Process.*
- [ZHJH14b] —, "Interference neutralization for non-regenerative two-way relaying networks—Part II: optimization," 2014, submitted to *IEEE Trans. Signal Process.*
- [ZHJH14c] —, "SINR balancing for non-regenerative two-way relay networks with interference neutralization," in *Proc. IEEE Int. Conf. Acoustics, Speech, and Signal Processing (ICASSP)*, Florence, Italy, May 2014.
- [ZNH14] J. Zhang, K. Naskovska, and M. Haardt, "Tensor-based channel estimation for non-regenerative two-way relaying networks with multiple relays," in *Proc. 48th*

-
- Asilomar Conf. Signals, Systems, and Computers (Asilomar)*, Pacific Grove, CA, Nov. 2014.
- [ZRH11] J. Zhang, F. Roemer, and M. Haardt, “Beamforming design for multi-user two-way relaying with MIMO amplify and forward relays,” in *Proc. IEEE Int. Conf. Acoustics, Speech, and Signal Processing (ICASSP)*, Prague, Czech Republic, May 2011.
- [ZRH12a] —, “Distributed beamforming for two-way relaying networks with individual power constraints,” in *Proc. 46th Asilomar Conf. Signals, Systems, and Computers (Asilomar)*, Pacific Grove, CA, Nov. 2012.
- [ZRH12b] —, “Relay assisted physical resource sharing: Projection based separation of multiple operators (ProBaSeMO) for two-way relaying with MIMO amplify and forward relays,” *IEEE Trans. Signal Process.*, vol. 60, no. 9, Sep. 2012.
- [ZRH⁺12c] J. Zhang, F. Roemer, M. Haardt, A. Khabbazibasmenj, and S. A. Vorobyov, “Sum rate maximization for multi-pair two-way relaying with single-antenna amplify and forward relays,” in *Proc. IEEE Int. Conf. Acoustics, Speech, and Signal Processing (ICASSP)*, Kyoto, Japan, Mar. 2012.
- [ZRH13] J. Zhang, F. Roemer, and M. Haardt, “Robust design of block diagonalization using perturbation analysis,” in *Proc. IEEE Int. Conf. Acoustics, Speech, and Signal Processing (ICASSP)*, Vancouver, Canada, May 2013.
- [ZTH13a] J. Zhang, O. Taghizadeh, and M. Haardt, “Joint source and relay precoding design for one-way full-duplex MIMO relaying systems,” in *Proc. Int. Symp. Wireless Communication Systems (ISWCS)*, Ilmenau, Germany, Aug. 2013.
- [ZTH13b] —, “Robust transmit beamforming design for full-duplex point-to-point MIMO systems,” in *Proc. Int. Symp. Wireless Communication Systems (ISWCS)*, Ilmenau, Germany, Aug. 2013.
- [ZTH13c] —, “Transmit strategies for full-duplex point-to-point systems with residual self-interference,” in *Proc. 16th ITG Workshop Smart Antennas (WSA)*, Stuttgart, Germany, Mar. 2013.
- [ZTLH12] J. Zhang, O. Taghizadeh, J. Luo, and M. Haardt, “Full duplex wireless communications with partial interference cancellation,” in *Proc. 46th Asilomar Conf. Signals, Systems, and Computers (Asilomar)*, Pacific Grove, CA, Nov. 2012.
- [ZVKH13] J. Zhang, S. A. Vorobyov, A. Khabbazibasmenj, and M. Haardt, “Sum rate maximization in multi-operator two-way relay networks with a MIMO AF relay via POTDC,” in *Proc. 21st European Signal Processing Conference (EUSIPCO 2013)*, Marrakech, Morocco, Sep. 2013.

References by Other Authors

- [3GP08] 3GPP, “Universal terrestrial radio access (UTRA) repeater planning guidelines and system analysis,” 3rd Generation Partnership Project (3GPP), TR 25.956, Mar. 2008.
- [3GP10] —, “Further advancements for E-UTRA physical layer aspects,” 3rd Generation Partnership Project (3GPP), TR 36.814, v9.0.0, Mar. 2010.
- [3GP13] —, “Study on Mobile Relay for Evolved Universal Terrestrial Radio Access (E-UTRA),” 3rd Generation Partnership Project (3GPP), TR 36.836, v2.0.2, Jul. 2013.
- [4G 14] 4G Americas, “4G mobile broadband evolution,” 4G Americas, Tech. Rep., Feb. 2014.
- [5GN13] 5GNOW, “D2.1, 5G cellular communications scenarios and system requirements,” Mar. 2013.
- [AHV10] N. Aboutorab, W. Hardjawana, and B. Vucetic, “Interference cancellation in multi-user MIMO relay networks using beamforming and precoding,” in *IEEE Wireless Communications and Networking Conf. (WCNC)*, Mar. 2010.
- [AK10a] A. U. T. Amah and A. Klein, “Pair-aware transceive beamforming for non-regenerative multi-user two-way relaying,” in *Proc. IEEE Int. Conf. Acoustics, Speech, and Signal Processing (ICASSP)*, Dallas, TX, Mar. 2010.
- [AK10b] A. U. T. Amahl and A. Klein, “Beamforming-based physical layer network coding for non-regenerative multi-way relaying,” *EURASIP J Wirel Commun Netw*, 2010.
- [ASS11] T. Adali, P. J. Schreier, and L. L. Scharf, “Complex-valued signal processing: The proper way to deal with impropriety,” *IEEE Trans. Signal Process.*, Nov. 2011.
- [BBTT10] A. Beck, A. B.-Tal, and L. Tetrushvili, “A sequential parametric convex approximation method with applications to nonconvex truss topology design problems,” *J Global Optim*, vol. 47, no. 1, 2010.
- [BC87] J. Borde and J. P. Crouzeix, “Convergence of a Dinkelbach-type algorithm in generalized fractional programming,” *Zeitschrift fuer Operations Research*, vol. 31, no. 1, 1987.
- [Ber95] D. P. Bertsekas, *Nonlinear Programming*. Athena Scientific, 1995.

-
- [BJ13] E. Björnson and E. Jorswieck, *Optimal Resource Allocation in Coordinated Multi-Cell Systems*, ser. Foundations and Trends in Communications and Information Theory. Now Publishers, Jan. 2013, vol. 9, no. 2-3.
- [BNO03] D. P. Bertsekas, A. Nedic, and A. E. Ozdaglar, *Convex analysis and optimization*. Athena Scientific, 2003.
- [BPG12] N. Bornhorst, M. Pesavento, and A. B. Gershman, “Distributed beamforming for multi-group multicasting relay networks,” *IEEE Trans. Signal Process.*, vol. 60, pp. 221–232, Jan. 2012.
- [BSR⁺13] Ö. Bulakci, A. B. Saleh, S. Redana, B. Raaf, and J. Hämäläinen, “Resource sharing in LTE-advanced relay networks: uplink system performance analysis,” *Trans. Emerging Telecommun. Technologies*, vol. 24, pp. 32–48, Jan. 2013.
- [BUK⁺09] S. Berger, T. Unger, M. Kuhn, A. Klein, and A. Wittneben, “Recent advances in amplify-and-forward two-hop relaying,” *IEEE Commun. Mag.*, Jul. 2009.
- [BV04] S. Boyd and L. Vandenberghe, *Convex Optimization*. Cambridge, U.K., 2004.
- [BW05] S. Berger and A. Wittneben, “Cooperative distributed multiuser MMSE relaying in wireless Ad-Hoc networks,” in *Proc. 39th Asilomar Conf. Signals, Systems, and Computers (Asilomar)*, 2005, pp. 1072–1076.
- [CC62] A. Charnes and W. W. Cooper, “Programming with linear fractional functions,” *Naval Research Logistics Quarterly*, Sep. 1962.
- [CE79] T. M. Cover and A. El Gamal, “Capacity theorems for the relay channel,” *IEEE Trans. Inf. Theory*, vol. 25, no. 5, May 1979.
- [CF91] J.-P. Crouzeix and J. A. Ferland, “Algorithms for generalized fractional programming,” *Mathematical Programming*, vol. 52, 1991.
- [CFS85] J.-P. Crouzeix, J. A. Ferland, and S. Schaible, “An algorithm for generalized fractional programmes,” *J Optim Theory Appl*, vol. 47, 1985.
- [CFS86] ———, “A note on an algorithm for generalized fractional programs,” *J Optim Theory Appl*, vol. 50, 1986.
- [Cir14] A. C. Cirik, “On duality of MIMO relays and performance limits of full-duplex MIMO radios,” Ph.D. dissertation, University of California Riverside, 2014.
- [Cis14] Cisco, “Cisco visual networking index: global mobile data traffic forecast update, 2013-2018,” Cisco, Tech. Rep., Feb. 2014.
- [CJ09] V. R. Cadambe and S. A. Jafar, “Degrees of freedom of wireless networks with relays, feedback, co-operation and full duplex operation,” *IEEE Trans. Inf. Theory*, vol. 55, no. 5, pp. 2334–2344, May 2009.

- [CJLK10] J. I. Choi, M. Jain, K. S. P. Levis, and S. Katti, "Achieving single channel, full duplex wireless communication," in *Proc. 16th Annu. Int. Conf. Mobile Computing and Networking (Mobicom)*, Chicago, IL, Sep. 2010.
- [CT91] T. M. Cover and J. A. Thomas, *Elements of information theory*. John Wiley & Sons, Inc., 1991.
- [CTJC08] C.-B. Chae, T. Tang, R. W. H. Jr., and S. Cho, "MIMO relaying with linear processing for multiuser transmission in fixed relay networks," *IEEE Trans. Signal Process.*, Feb. 2008.
- [CVX12] CVX Research, Inc., "CVX: Matlab software for disciplined convex programming, version 2.0," <http://cvxr.com/cvx>, Aug. 2012.
- [CY09] M. Chen and A. Yener, "Multiuser two-way relaying: Detection and interference management strategies," *IEEE Trans. Wireless Commun.*, vol. 8, pp. 4296–4305, Aug. 2009.
- [Dat05] J. Dattorro, *Convex optimization and Euclidean distance geometry*. Meboo Publishing USA, 2005.
- [DDV00] L. De Lathauwer, B. De Moor, and J. Vanderwalle, "A multilinear singular value decomposition," *SIAM. J. Matrix Anal. & Appl.*, vol. 21, no. 4, 2000.
- [De 08] L. De Lathauwer, "Decompositions of a higher-order tensor in block terms - Part II: definitions and uniqueness," *SIAM. J. Matrix Anal. & Appl.*, vol. 30, Sep. 2008.
- [DGPV12] D. Darsena, G. Gelli, L. Paura, and F. Verde, "Widely-linear beamforming/combining techniques for MIMO wireless systems," in *Proc. 5th Int. Symp. Communications, Control and Signal Processing (ISCCSP)*, Rome, Italy, May 2012.
- [Din67] W. Dinkelbach, "On nonlinear fractional programming," *Management Science*, vol. 13, no. 7, 1967.
- [DKTL11] Z. Ding, I. Krikidis, J. Thompson, and K. K. Leung, "Physical layer network coding and precoding for the two-way relay channel in cellular systems," *IEEE Trans. Signal Process.*, vol. 59, Feb. 2011.
- [DMBS12] B. Day, A. Margetts, D. Bliss, and P. Schniter, "Full-duplex bidirectional MIMO: Achievable rates under limited dynamic range," *IEEE Trans. Signal Process.*, Jul. 2012.
- [DPS14] E. Dahlman, S. Parkvall, and J. Skoeld, *4G: LTE/LTE-advanced for mobile broadband*. Elsevier Ltd., 2014.

-
- [DS10] M. Dong and S. Shahbazpanahi, “Optimal spectrum sharing and power allocation for OFDM-based two-way relaying,” in *Proc. IEEE Int. Conf. Acoustics, Speech, and Signal Processing (ICASSP)*, Dallas, Texas, Mar. 2010.
- [EDDS11] E. Everett, M. Duarte, C. Dick, and A. Sabharwal, “Empowering full-duplex wireless communication by exploiting directional diversity,” in *Proc. 44th Asilomar Conf. Signals, Systems, and Computers (Asilomar)*, Pacific Grove, CA, Nov. 2011.
- [EH05] A. El Gamal and N. Hassanpour, “Relay-without-delay,” in *Proc. IEEE Int. Symp. Information Theory (ISIT)*, vol. 1, 2005, pp. 1078–1080.
- [EHM07] A. El Gamal, N. Hassanpour, and J. Mammen, “Relay networks with delays,” *IEEE Trans. Inf. Theory*, vol. 53, no. 10, pp. 3413–3431, Oct. 2007.
- [EK11] A. El Gamal and Y.-H. Kim, *Network Information Theory*. Cambridge University Press, 2011.
- [Eri13] Ericsson, “5G radio access: research and vision,” Ericsson, Tech. Rep., Jun. 2013.
- [EW08a] C. Esli and A. Wittneben, “Multiuser MIMO two-way relaying for cellular communications,” in *IEEE Int. Symp. Personal, Indoor and Mobile Radio Communications (PIMRC)*, New Orleans, LA, Sep. 2008.
- [EW08b] ———, “One- and two-way decode-and-forward relaying for wireless multiuser MIMO networks,” in *Proc. IEEE Global Communications Conf. (Globecom)*, New Orleans, LA, Nov. 2008.
- [Far11] B. Farhang-Boroujeny, “OFDM versus filter bank multicarrier,” *IEEE Signal Process. Mag.*, no. 5, 2011.
- [FDSG09] S. F.-Dehkordy, S. Shahbazpanahi, and S. Gazor, “Multiple peer-to-peer communications using a network of relays,” *IEEE Trans. Signal Process.*, vol. 57, pp. 3053–3062, Aug. 2009.
- [FWY13] Z. Fang, X. Wang, and X. Yuan, “Beamforming design for multiuser two-way relaying: a unified approach via max-min SINR,” *IEEE Trans. Signal Process.*, Dec. 2013.
- [GJ79] M. R. Garey and D. S. Johnson, *Computers and intractability: a guide to the theory of NP-completeness*. W. H. Freeman and Company, 1979.
- [GL96] G. H. Golub and C. F. V. Loan, *Matrix Computations*. The Johns Hopkins University Press, 1996.
- [GSL03] W. H. Gerstaecker, R. Schober, and A. Lampe, “Receivers with widely linear processing for frequency-selective channels,” *IEEE Trans. Commun.*, vol. 51, Sep. 2003.

- [GSM08] GSM, “Mobile infrastructure sharing,” GSM Association, Tech. Rep., Sep. 2008. [Online]. Available: <http://www.gsmworld.com/documents/gsma.pdf>
- [GSS⁺10] A. B. Gershman, N. D. Sidiropoulos, S. Shahbazpanahi, M. Bengtsson, and B. Ottersten, “Convex optimization based beamforming,” *IEEE Signal Process. Mag.*, May 2010.
- [GYGP09] D. Guenduez, A. Yener, A. Goldsmith, and H. V. Poor, “The multi-way relay channel,” in *Proc. IEEE Int. Symp. Information Theory (ISIT)*, Seoul, Korea, Jun. 2009.
- [HCM⁺12] C. Hoymann, W. Chen, J. Montojo, A. Golitschek, C. Koutsimanis, and X. Shen, “Relaying operations in 3GPP LTE: Challenges and solutions,” *IEEE Commun. Mag.*, Feb. 2012.
- [HDL11] M. Hajiaghayi, M. Dong, and B. Liang, “Jointly optimal channel pairing and power allocation for multichannel multihop relaying,” *IEEE Trans. Signal Process.*, vol. 59, Oct. 2011.
- [HJ12] Z. K. M. Ho and E. Jorswieck, “Instantaneous relaying: Interference neutralization and optimal strategies,” *IEEE Trans. Signal Process.*, vol. 60, no. 12, 2012.
- [HJG13a] Z. K. M. Ho, E. Jorswieck, and S. Gerbracht, “Efficient information leakage neutralization on a relay-assisted multi-carrier interference channel,” in *Proc. IEEE Int. Conf. Acoustics, Speech, and Signal Processing (ICASSP)*, 2013.
- [HJG13b] —, “Information leakage neutralization for the multi-antenna non-regenerative relay-assisted multi-carrier interference channel,” *IEEE J. Sel. Areas Commun.*, vol. 31, no. 9, 2013.
- [Hj011] A. Hjørungnes, *Complex-valued matrix derivatives with applications in signal processing and communications*. Cambridge University Press, 2011.
- [HLM⁺12] Y. Hua, P. Liang, Y. Ma, A. C. Cirik, and Q. Gao, “A method for broadband full-duplex MIMO radio,” *IEEE Signal Process. Letters*, vol. 19, Dec. 2012.
- [HMVS01] M. Haardt, C. F. Mecklenbraeuer, M. Vollmer, and P. Slanina, “Smart antennas for UTRA TDD,” *European Transactions on Telecommunications (ETT)*, vol. 12, Sep. 2001.
- [HNSG10] V. Havary-Nassab, S. Shahbazpanahi, and A. Grami, “Joint receive-transmit beamforming for multi-antenna relaying schemes,” *IEEE Trans. Signal Process.*, vol. 58, pp. 4966–4972, Sep. 2010.
- [HP10] Y. Huang and D. P. Palomar, “Rank-constrained separable semidefinite programming with applications to optimal beamforming,” *IEEE Trans. Signal Process.*, vol. 58, pp. 664–678, Feb. 2010.

-
- [IEE09] IEEE Std. 802.16j-2009, “IEEE standard for local and metropolitan area networks - Part 16: Air interface for fixed broadband wireless access systems - amendment 1: Multiple relay specification,” 2009.
- [ISRR07] T. Ihalainen, T. H. Stitz, M. Rinne, and M. Renfors, “Channel equalization in filter bank based multicarrier modulation for wireless communications,” *EURASIP J Adv Signal Process*, Jan. 2007.
- [ITN10] M. Iwamura, H. Takahashi, and S. Nagata, “Relay technology in LTE-advanced,” Radio access network development department, NTT DOCOMO, Tech. Rep., Dec. 2010.
- [JBF⁺10] E. Jorswieck, L. Badia, T. Fahldieck, D. Gesbert, S. Gustafsson, M. Haardt, K. Ho, E. Karipidis, A. Kortke, E. Larsson, H. Mark, M. Nawrocki, V. Palestini, R. Piesiewicz, P. Priotti, F. Roemer, M. Schubert, J. Sykora, P. Trossen, B. van den Ende, and M. Zorzi, “Resource sharing in wireless networks: The SAPHYRE approach,” in *Proc. Future Network and Mobile Summit 2010*, Florence, Italy, Jun. 2010.
- [JCK⁺11] M. Jain, J. I. Choi, T. Kim, D. Bharadia, K. Srinivasan, S. Seth, P. Levis, S. Katti, and P. Sinha, “Practical, real-time, full duplex wireless,” in *Proc. 17th Annu. Int. Conf. Mobile Computing and Networking (Mobicom)*, Las Vegas, NV, Sep. 2011.
- [JL10] E. A. Jorswieck and E. G. Larsson, “Monotonic optimization framework for the two-user MISO interference channel,” *IEEE Trans. Commun.*, vol. 58, Jul. 2010.
- [JS10] J. Joung and A. H. Sayed, “Multiuser two-way amplify-and-forward relay processing and power control methods for beamforming systems,” *IEEE Trans. Signal Process.*, vol. 58, pp. 1833–1846, Mar. 2010.
- [KGG05] G. Kramer, M. Gastpar, and P. Gupta, “Cooperative strategies and capacity theorems for relay networks,” *IEEE Trans. Inf. Theory*, vol. 51, no. 9, Sep. 2005.
- [Kha10] A. K. Khandani, “Methods for spatial multiplexing of wireless two-way channels,” Patent US 7817641 B1, 10 19, 2010. [Online]. Available: <http://www.google.ca/patents/US7817641>
- [Kra08] G. Kramer, *Foundations and Trends in Communications and Information Theory*. Now Publishers, 2008, vol. 4, ch. Topics in Multi-User Information Theory, pp. 265–444.
- [KRVH12] A. Khabbazibasmenj, F. Roemer, S. A. Vorobyov, and M. Haardt, “Sum-rate maximization in two-way AF MIMO relaying: Polynomial time solutions to a class of DC programming problems,” *IEEE Trans. Signal Process.*, Sep. 2012.

- [KSA⁺14] D. Korpi, V. Syrjälä, L. Anttila, M. Valkama, and R. Wichman, “Full-duplex transceiver system calculations: analysis of ADC and linearity challenges,” 2014, to appear in *IEEE Trans. Wireless Commun.*
- [KYA08] B. Khoshnevis, W. Yu, and R. Adve, “Grassmannian beamforming for MIMO amplify-and-forward relaying,” *IEEE J. Sel. Areas Commun.*, vol. 26, pp. 1397–1407, Oct. 2008.
- [Liu99] S. Liu, “Matrix results on the Khatri-Rao and Tracy-Singh products,” *Elsevier Linear Algebra and Its Applications*, vol. 289, no. 3, 1999.
- [LJ11] N. Lee and S. A. Jafar, “Aligned interference neutralization and the degrees of freedom of the 2 user interference channel with instantaneous relay,” *submitted to IEEE Trans. Inf. Theory*, available at <http://arxiv.org/abs/1102.3833>, pp. 1–17, 2011. [Online]. Available: <http://arxiv.org/abs/1102.3833>
- [LJ13] N. Lee and R. W. H. Jr., “Degrees of freedom for the two-cell two-hop MIMO interference channel: Interference-free relay transmission and spectrally efficient relaying protocol,” *IEEE Trans. Inf. Theory*, vol. 59, May 2013.
- [LJLM09] E. G. Larsson, E. A. Jorswieck, J. Lindblom, and R. Mochaourab, “Game theory and the flat-fading Gaussian interference channel,” *IEEE Signal Process. Mag.*, Sep. 2009.
- [LK10] P. Liu and I. M. Kim, “Performance analysis of bidirectional communication protocols based on decode-and-forward relaying,” *IEEE Trans. Commun.*, vol. 58, Sep. 2010.
- [LLL13] K. Lee, N. Lee, and I. Lee, “Achievable degrees of freedom on MIMO two-way relay interference channels,” *IEEE Trans. Wireless Commun.*, vol. 12, no. 4, 2013.
- [LLM10] J. Liu, X. Liu, and X. Ma, “First-order perturbation analysis of singular vectors in singular value decomposition,” *IEEE Trans. Signal Process.*, vol. 56, Nov. 2010.
- [LLSL09] K.-J. Lee, K. W. Lee, H. Sung, and I. Lee, “Sum-rate maximization for two-way mimo amplify-and-forward relaying systems,” in *Proc. IEEE Vehicular Technology Conf. (VTC)*, Barcelona, Spain, Apr. 2009.
- [LMS⁺10] Z.-Q. Luo, W.-K. Ma, A. M.-C. So, Y. Ye, and S. Zhang, “Semidefinite relaxation of quadratic optimization problems,” *IEEE Signal Process. Mag.*, May 2010.
- [LPP11] J. Li, A. P. Petropulu, and H. V. Poor, “Cooperative transmission for relay networks based on second-order statistics of channel state information,” *IEEE Trans. Signal Process.*, vol. 59, Mar. 2011.

-
- [LTV06] A. Lozano, A. M. Tulino, and S. Verdu, "Optimum power allocation for parallel Gaussian channels with arbitrary input distributions," *IEEE Trans. Inf. Theory*, vol. 52, Jul. 2006.
- [Lue96] H. Luetkepohl, *Handbook of matrices*. John Wiley & Sons Ltd, 1996.
- [LV08] P. Lioliou and M. Viberg, "Least-squares based channel estimation for MIMO relays," in *Proc. 11th Int. ITG Workshop Smart Antennas (WSA)*, Mar. 2008.
- [LV12] M. Laurent and F. Vallentin, "Semidefinite optimization," 2012, lecture notes.
- [LWZ11] G. Li, Y. Wang, and P. Zhang, "Optimal linear MMSE beamforming for two way multi-antenna relay systems," *IEEE Communications Letters*, vol. 15, pp. 533–535, May 2011.
- [LXDL10] T. C.-K. Liu, W. Xu, X. Dong, and W.-S. Lu, "Adaptive power allocation for bidirectional amplify-and-forward multiple-relay multiple-user networks," in *Proc. IEEE Global Communications Conf. (Globecom)*, Florida, LA, Dec. 2010.
- [LYC08] N. Lee, H. J. Yang, and J. Chun, "Achievable sum-rate maximizing AF relay beamforming scheme in two-way relay channels," in *Proc. IEEE Int. Conf. Communications (ICC)*, Beijing, China, May 2008.
- [MDFT08a] S. Mohajer, S. N. Diggavi, C. Fragouli, and D. Tse, "Transmission techniques for relay-interference networks," in *Proc. 46th Annu. Allerton Conf.*, UIUC, IL, Sep. 2008.
- [MDFT08b] S. Mohajer, S. N. Diggavi, C. Fragouli, and D. N. C. Tse, "Transmission techniques for relay-interference networks," in *Proc. 46th Annu. Allerton Conf. Communication, Control, and Computing*, Sep. 2008, pp. 467–474.
- [MDT09] S. Mohajer, S. N. Diggavi, and D. Tse, "Approximate capacity of a class of Gaussian relay-interference networks," in *Proc. IEEE Int. Symp. Information Theory (ISIT)*, 2009, pp. 31–35.
- [Mey04] C. D. Meyer, *Matrix analysis and applied linear algebra*. SIAM, 2004.
- [Moo20] E. H. Moore, "On the reciprocal of the general algebraic matrix," *Bulletin of the American Mathematical Society*, vol. 26, pp. 394–395, 1920.
- [MOS12] MOSEK ApS, Denmark, "The MOSEK optimization toolbox for MATLAB," <http://www.mosek.com>, Aug. 2012.
- [Mui82] R. J. Muirhead, *Aspects of multivariate statistical theory*. John Wiley & Sons Ltd, 1982.
- [NG11] B. Nazer and M. Gastpar, "Compute-and-forward: Harnessing interference through structured codes," *IEEE Trans. Inf. Theory*, vol. 57, Oct. 2011.

- [NW99] J. Nocedal and S. J. Wright, *Numerical Optimization*. Springer-Verlag New York, Inc., 1999.
- [OWB09] T. J. Oechtering, R. F. Wyrembelski, and H. Boche, “Multiantenna bidirectional broadcast channels’s optimal transmit strategies,” *IEEE Trans. Signal Process.*, vol. 57, May 2009.
- [Pen55] R. Penrose, “A generalized inverse for matrices,” *Proceedings of the Cambridge Philosophical Society*, vol. 51, pp. 406–413, 1955.
- [PK11] Z. Pi and F. Khan, “An introduction to millimeter-wave mobile broadband systems,” *IEEE Commun. Mag.*, Jun. 2011.
- [PNG03] A. Paulraj, R. Nabar, and D. Gore, *Introduction to Space-Time Wireless Communications*. Cambridge University Press, 2003.
- [PT03] N. T. H. Phuong and H. Tuy, “A unified monotonic approach to generalized linear fractional programming,” *J Global Optim.*, vol. 26, 2003.
- [QZH09] L. P. Qian, Y. J. Zhang, and J. Huang, “MAPEL: Achieving global optimality for a non-convex wireless power control problem,” *IEEE Trans. Wireless Commun.*, vol. 8, Mar. 2009.
- [RH09] F. Roemer and M. Haardt, “Algebraic norm-maximizing (ANOMAX) transmit strategy for two-way relaying with MIMO amplify and forward relays,” *IEEE Sig. Proc. Lett.*, vol. 16, Oct. 2009.
- [RH10a] —, “A low-complexity relay transmit strategy for two-way relaying with MIMO amplify and forward relays,” in *Proc. IEEE Int. Conf. Acoustics, Speech, and Signal Processing (ICASSP)*, Dallas, TX, Mar. 2010.
- [RH10b] —, “Tensor-based channel estimation (TENICE) and iterative refinements for two-way relaying with multiple antennas and spatial reuse,” *IEEE Trans. Signal Process.*, Dec. 2010.
- [RKX12] Y. Rong, M. R. A. Khandaker, and Y. Xiang, “Channel estimation of dual-hop MIMO relay system via parallel factor analysis,” *IEEE Trans. Wireless Commun.*, vol. 11, no. 6, 2012.
- [RTH09] Y. Rong, X. Tang, and Y. Hua, “A unified framework for optimization linear non-regenerative multicarrier MIMO relay communication systems,” *IEEE Trans. Signal Process.*, vol. 57, pp. 4837–4852, Dec. 2009.
- [RVW13] T. Riihonen, M. Vehkaperä, and R. Wichman, “Large-system analysis of rate regions in bidirectional full-duplex MIMO link: suppression versus cancellation,” in *Proc. 47th Annu. Conf. Information Sciences and Systems (CISS)*, Mar. 2013.

- [RW07] B. Rankov and A. Wittneben, "Spectral efficient protocols for half-duplex fading relay channels," *IEEE J. Sel. Areas Commun.*, vol. 25, pp. 379–389, Feb. 2007.
- [RWW11] T. Riihonen, S. Werner, and R. Wichman, "Mitigation of loopback self-interference in full-duplex MIMO relays," *IEEE Trans. Signal Process.*, vol. 59, Dec. 2011.
- [SAP10] SAPHYRE, "D3.3a, SAPHYRE reference scenarios and interference models," Dec. 2010.
- [Sei09] E. Seidel, "Initial thoughts on LTE advanced for 3GPP release 10," in *LTE World Summit, Berlin*, 2009.
- [Ser80] R. J. Serfling, *Approximation Theorems of mathematical statistics*. Hoboken, NJ: Wiley, 1980.
- [SGS11] A. Schad, A. B. Gershman, and S. Shahbazpanahi, "Capacity maximization for distributed beamforming in one- and bi-directional relay networks," in *Proc. IEEE Int. Conf. Acoustics, Speech, and Signal Processing (ICASSP)*, Prague, Czech Republic, May 2011.
- [SH08] V. Stankovic and M. Haardt, "Generalized design of multi-user MIMO precoding matrices," *IEEE Trans. Wireless Commun.*, vol. 7, pp. 953–961, Mar. 2008.
- [SH09] B. Song and M. Haardt, "Achievable throughput approximation for RBD precoding at high SNRs," in *Proc. IEEE Int. Conf. Acoustics, Speech, and Signal Processing (ICASSP)*, Taipei, Taiwan, Apr. 2009.
- [SH13] J. Steinwandt and M. Haardt, "Optimal widely-linear distributed beamforming for relay networks," in *Proc. IEEE Int. Conf. Acoustics, Speech, and Signal Processing (ICASSP)*, Vancouver, Canada, May 2013.
- [SMMVC10] S. Simoens, O. M.-Medina, J. Vidal, and A. D. Coso, "Compress-and-forward cooperative MIMO relaying with full channel state information," *IEEE Trans. Signal Process.*, vol. 58, Feb. 2010.
- [SPS11] A. Sahai, G. Patel, and A. Sabharwal, "Pushing the limits of full-duplex: Design and real-time implementation," Department of Electrical and Computer Engineering, Rice University, Tech. Rep., Jul. 2011.
- [SRH13] B. Song, F. Roemer, and M. Haardt, "Flexible coordinated beamforming (flex-cobf) for the downlink of multi-user mimo systems in single and clustered multiple cells," *Elsevier Signal Process.*, vol. 93, Sep. 2013.
- [SS03] S. Schaible and J. Shi, "Recent developments in fractional programming: Single ratio and max-min case," in *Proc. 3rd Int. Conf. non-linear analysis and convex analysis*, Tokyo, Japan, Aug. 2003.

- [SS10] P. J. Schreier and L. L. Scharf, *Statistical signal processing of complex-valued data: the theory of improper and noncircular signals*. Cambridge University Press, 2010.
- [SSH04] Q. H. Spencer, A. L. Swindlehurst, and M. Haardt, "Zero-forcing methods for downlink spatial multiplexing in multi-user MIMO channels," *IEEE Trans. Signal Process.*, vol. 52, pp. 461–471, Feb. 2004.
- [Ste07] F. Sterle, "Widely linear MMSE transceivers for MIMO channels," *IEEE Trans. Signal Process.*, Aug. 2007.
- [STS07] M. Sadek, A. Tarighat, and A. H. Sayed, "A leakage-based precoding scheme for downlink multi-user MIMO channels," *IEEE Trans. Wireless Commun.*, vol. 6, May 2007.
- [SVP⁺13] Y. Sui, J. Vihriaelae, A. Papadogiannis, M. Sternad, W. Yang, and T. Svensson, "Moving cells: a promising solution to boost performance for vehicular users," *IEEE Commun. Mag.*, Jun. 2013.
- [TCHC06] T. Tang, C.-B. Chae, R. W. Heath, and S. Cho, "On achievable sum rates of a multiuser MIMO relay channel," in *Proc. IEEE Int. Symp. Information Theory (ISIT)*, Seattle, USA, Jul. 2006.
- [TK12] T. Taleb and A. Kunz, "Machine type communications in 3GPP networks: Potential, challenges, and solutions," *IEEE Commun. Mag.*, Mar. 2012.
- [TS09] S. Toh and D. T. M. Slock, "A linear beamforming scheme for multi-user MIMO AF two-phase two-way relaying," in *IEEE Int. Symp. Personal, Indoor and Mobile Radio Communications (PIMRC)*, Sep. 2009.
- [Tuy00] H. Tuy, "Monotonic optimization: Problems and solution approaches," *SIAM J. Optim.*, vol. 11, 2000.
- [TW12] M. Tao and R. Wang, "Linear precoding for multi-pair two-way MIMO relay systems with max-min fairness," *IEEE Trans. Signal Process.*, vol. 60, Oct. 2012.
- [UB12] W. Utschick and J. Brehmer, "Monotonic optimization framework for coordinated beamforming in multicell networks," *IEEE Trans. Signal Process.*, vol. 60, Apr. 2012.
- [UK08] T. Unger and A. Klein, "Duplex schemes in multiple antenna two-hop relaying," *EURASIP J Adv Signal Process*, 2008.
- [VRWH11] R. Vaze and J. R. W. Heath, "On the capacity and diversity-multiplexing tradeoff of the two-way relay channel," *IEEE Trans. Inf. Theory*, vol. 57, pp. 4219–4234, Jul. 2011.

- [WCY⁺11] C. Wang, H. Chen, Q. Yin, A. Feng, and A. F. Molisch, “Multi-user two-way relay networks with distributed beamforming,” *IEEE Trans. Wireless Commun.*, vol. 10, Oct. 2011.
- [WIN06] WINNER II, “D3.5.1 v1.0, relaying concepts and supporting actions in the context of CGs,” Oct. 2006.
- [WM07] L. Weng and R. D. Murch, “Multi-user MIMO relay system with self-interference cancellation,” in *IEEE Wireless Communications and Networking Conf. (WCNC)*, Mar. 2007.
- [WP09] J. Wang and D. P. Palomar, “Worst-case robust MIMO transmission with imperfect channel knowledge,” *IEEE Trans. Signal Process.*, vol. 57, Aug. 2009.
- [YH10] Y. Yu and Y. Hua, “Power allocation for a MIMO relay system with multiple-antenna users,” *IEEE Trans. Signal Process.*, vol. 58, pp. 2823–2835, May 2010.
- [YHXM09] Y. Yang, H. Hu, J. Xu, and G. Mao, “Relay technologies for WiMAX and LTE-advanced mobile systems,” *IEEE Commun. Mag.*, Oct. 2009.
- [YZGK10] E. Yilmaz, R. Zakhour, D. Gesbert, and R. Knopp, “Multi-pair two-way relay channel with multiple antenna relay station,” in *Proc. IEEE Int. Conf. Communications (ICC)*, Cape Town, South Africa, May 2010.
- [YZWY10] G. Yuan, X. Zhang, W. Wang, and Y. Yang, “Carrier aggregation for LTE-advanced mobile communication systems,” *IEEE Commun. Mag.*, vol. 48, pp. 88–93, Feb. 2010.
- [ZLCC09] R. Zhang, Y. Liang, C. C. Chai, and S. Cui, “Optimal beamforming for two-way multi-antenna relay channel with analogue network coding,” *IEEE J. Sel. Areas Commun.*, vol. 27, pp. 699–712, Jun. 2009.

Erklärung

Ich versichere, dass ich die vorliegende Arbeit ohne unzulässige Hilfe Dritter und ohne Benutzung anderer als der angegebenen Hilfsmittel angefertigt habe. Die aus anderen Quellen direkt oder indirekt übernommenen Daten und Konzepte sind unter Angabe der Quelle gekennzeichnet.

Bei der Auswahl und Auswertung folgenden Materials haben mir die nachstehend aufgeführten Personen in der jeweils beschriebenen Weise entgeltlich/unentgeltlich geholfen:

1.
2.
3.

Weitere Personen waren an der inhaltlich-materiellen Erstellung der vorliegenden Arbeit nicht beteiligt. Insbesondere habe ich hierfür nicht die entgeltliche Hilfe von Vermittlungs- bzw. Beratungsdiensten (Promotionsberater oder anderer Personen) in Anspruch genommen. Niemand hat von mir unmittelbar oder mittelbar geldwerte Leistungen für Arbeiten erhalten, die im Zusammenhang mit dem Inhalte der vorgelegten Dissertation stehen.

Die Arbeit wurde bisher weder im In- noch im Ausland in gleicher oder ähnlicher Form einer Prüfungsbehörde vorgelegt.

Ich bin darauf hingewiesen worden, dass die Unrichtigkeit der vorstehenden Erklärung als Täuschungsversuch bewertet wird und gemäß §7 Abs. 10 der Promotionsordnung den Abbruch des Promotionsverfahrens zur Folge hat.

(Ort, Datum)

(Unterschrift)